Aus dem Institut für Virologie
Direktor: Prof. Dr. Stephan Becker
des Fachbereichs Medizin der Philipps-Universität Marburg

Phleboviruses versus the Type I/III Interferon Response: How Sandfly Fever Sicilian Virus NSs Tackles Interferon Induction and PKR-Mediated Restriction

Inaugural-Dissertation
zur Erlangung des Doktorgrades der Naturwissenschaften
(Dr. rer. nat.)

dem Fachbereich Medizin der Philipps-Universität Marburg
vorgelegt von

Jennifer Deborah Würth
aus Landau in der Pfalz

Marburg, 2022

Angenommen vom Fachbereich Medizin der Philipps-Universität Marburg am: 29.03.2022

Gedruckt mit Genehmigung des Fachbereichs Medizin

Dekanin: Frau Prof. Dr. D. Hilfiker-Kleiner

Referent: Herr Prof. Dr. F. Weber

1. Korreferent: Herr Prof. Dr. S. Bauer

Dedicated to

Grandpa – a scholar in his own right,

Mama – for everything,

and Amelie – a wonderful inspiration.

Table of Contents

Preface
Table of Contents 3
List of Publications and Manuscripts 4
Summary 5
Zusammenfassung 6
Abbreviations 7

1 Introduction 10
1.1 Phleboviruses and phenuiviruses 10
1.2 The type I and type III IFN systems in RNA virus infection 11
1.3 Phleboviruses and the type I and III IFN systems 12
1.4 The NSs protein – a highly diverse viral IFN antagonist 13
1.5 Objectives of the present thesis 14

2 Results 15
2.1 SFSV NSs targets IRF3 for inhibition of IFN induction 15
2.2 SFSV NSs fails to abrogate IFN signalling and ISG expression 17
2.3 SFSV NSs evades the PKR-mediated integrated stress response by targeting eIF2B 18

3 Discussion 21
3.1 SFSV and SFSV-like phleboviruses – emerging human pathogens 21
3.2 SFSV NSs, IRF3, and the interferon system 21
3.3 SFSV NSs, host gene expression, and the integrated stress response 22
3.4 Other candidate host interactors of SFSV NSs 24
3.5 PTV NSs combines inhibition of host transcription with targeting eIF2B 24
3.6 Correlation of NSs function and phenuivirus virulence? 25
3.7 Concluding remarks and future perspectives 28

4 Original peer-reviewed publications and manuscripts 29
4.1 Review article: *Phleboviruses and the Type I Interferon Response* 29
4.2 Research article: *NSs Protein of Sandfly Fever Sicilian Phlebovirus Counteracts Interferon (IFN) Induction by Masking the DNA-Binding Domain of IFN Regulatory Factor 3* 30
4.3 Research article: *NSs of the mildly virulent sandfly fever Sicilian virus is unable to inhibit interferon signaling and upregulation of interferon-stimulated genes* 31
4.4 Research article: *eIF2B as Target for Viral Evasion of PKR-Mediated Translation Inhibition* 32
4.5 Research article: *Viral Evasion of the Integrated Stress Response Through Antagonism of eIF2-P Binding to eIF2B* 33
4.6 News and Views: *Ferreting out viral pathogenesis* 34

5 References 35

Appendix 45
a Verzeichnis der Akademischen Lehrer 45
b Acknowledgement & Danksagung 46

List of Publications and Manuscripts

This thesis has been prepared in Prof. Friedemann Weber's laboratories at the Philipps-University Marburg and the Justus-Liebig University Gießen.

This is a cumulative thesis based on the following peer-reviewed publications and manuscripts:

1 **Wuerth JD** and Weber F.
Phleboviruses and the Type I Interferon Response.
Viruses **8**; 174 (2016)

2 **Wuerth JD**, Habjan M, Wulle J, Superti-Furga G, Pichlmair A, Weber F.
NSs Protein of Sandfly Fever Sicilian Phlebovirus Counteracts Interferon (IFN) Induction by Masking the DNA-Binding Domain of IFN Regulatory Factor 3.
Journal of Virology **92**; e01202-18 (2018)

3 **Wuerth JD** and Weber F.
NSs of the mildly virulent sandfly fever Sicilian virus is unable to inhibit interferon signaling and upregulation of interferon-stimulated genes.
Journal of General Virology **102**; 001676 (2021)

4 **Wuerth JD**, Habjan M, Kainulainen M, Berisha B, Bertheloot D, Superti-Furga G, Pichlmair A, Weber F.
eIF2B as Target for Viral Evasion of PKR-Mediated Translation Inhibition.
mBio **11**; e00976-20 (2020)

5 Schoof M[#], Wang L[#], Cogan Z, Lawrence R, Boone M, **Wuerth JD**, Frost A, Walter P.
Viral Evasion of the Integrated Stress Response Through Antagonism of eIF2-P Binding to eIF2B.
Manuscript accepted for publication at Nature Communications (2021)

6 **Wuerth JD** and Weber F.
Ferreting out viral pathogenesis.
Nature Microbiology **4**; 384-385 (2019)

See chapter 4 for personal contribution.

Summary

Phleboviruses (order *Bunyavirales*, family *Phenuiviridae*) are arthropod-borne viruses that are emerging globally due to the geographic expansion of long-known members and the identification of numerous novel ones. They span a wide spectrum of virulence, comprising clinically inapparent infection, febrile disease, encephalitis, up to severe haemorrhagic fever and multiorgan failure – with novel isolates including both highly virulent members and abundant others with as yet unknown disease potential. Rift Valley fever virus (RVFV), a long-known member, is highly pathogenic for humans and livestock. Thus, RVFV has been subject to extensive molecular characterization, which established the phleboviral non-structural protein NSs as antagonist of the antiviral interferon (IFN) system and main virulence factor in the mammalian host. Sandfly fever Sicilian virus (SFSV), on the other hand, was identified as causative agent of *'sandfly fever'*, a self-limited febrile disease, during World War II. Nowadays, SFSV is one of the geographically most widespread phleboviruses, causing disease mainly in immunologically naïve military troops and travellers. Although SFSV has been thoroughly characterized with regard to its clinical picture, its interaction with the mammalian host remained almost entirely elusive on the molecular level.

In this work, we thus elucidated the molecular mechanisms with which the NSs protein of SFSV counteracts the interferon system. We identified that SFSV NSs dampened the induction of both type I and III interferons by specifically masking the DNA-binding domain of the transcription factor interferon-regulatory factor 3 (IRF3). Despite IRF3 inhibition, however, SFSV did not fully abrogate IFN induction, leading to IFN-dependent upregulation of related transcription factor IRF7, which was not affected by SFSV NSs and fostered IFN induction. Additionally, SFSV NSs completely failed to impede IFN signalling, resulting in substantial expression of anti-phleboviral IFN-stimulated genes (ISGs). Thus, SFSV NSs appears to be a modulator rather than a full-blown antagonist of the IFN system.

Further, protein kinase R (PKR) possesses a strong restrictive activity towards phleboviruses due to the phosphorylation of its substrate eukaryotic elongation factor 2α (eIF2α) and the ensuing block of protein synthesis. Surprisingly, we found that the NSs protein of SFSV conferred PKR resistance and boosted translation without affecting the activation of PKR or the phosphorylation state of eIF2α. Instead, SFSV NSs targeted eIF2B, the central regulatory hub of the integrated stress response (ISR), further downstream. Of note, as previously characterized viral PKR antagonists all act at the levels of PKR activation and eIF2α phosphorylation, targeting of eIF2B by SFSV NSs represented a novel viral evasion strategy.

Interestingly, a common theme emerged during our studies: Highly virulent RVFV, on the one hand, utilizes its NSs to induce the degradation of target host factors via the proteasome, thereby acting in a catalytic mode. Furthermore, it establishes a global block of host gene expression to evade the IFN system. The NSs of mildly virulent SFSV, on the other hand, does not affect the expression levels of its host targets, but rather acts in a very specific and stoichiometric manner for both the inhibition of IFN induction and PKR evasion. Given its importance as exclusive phleboviral IFN antagonist, the NSs protein has been speculated to constitute a correlate of virulence. Our data on SFSV NSs support this hypothesis and argue for the characterization of the NSs proteins of novel phleboviruses with respect to their capacity to inhibit IFN induction, IFN signalling, and PKR activity in order to better estimate their potential to induce disease.

Zusammenfassung

Phleboviren (Ordnung *Bunyavirales*, Familie *Phenuiviridae*) sind Arboviren, die aufgrund der geographischen Expansion bekannter und der Identifizierung zahlreicher neuer Mitglieder global vermehrt auftreten. Sie umfassen ein breites Spektrum an Virulenz, darunter klinisch inapparente Infektionen, fiebrige Erkrankungen, Enzephalitis, bis hin zu hämorrhagischem Fieber und Multiorganversagen – wobei neue Isolate sowohl hochpathogene Mitglieder als auch zahllose andere mit soweit unbekanntem Krankheitspotential beinhalten. Das Rifttalfieber-Virus (RVFV), ein lange bekanntes Mitglied, ist hochpathogen für Mensch und Vieh. Daher wurde RVFV ausgiebig molekular charakterisiert, was das Nichtstrukturprotein NSs als Antagonist des antiviralen Interferon (IFN)-Systems und Hauptvirulenzfaktor im Säugetierwirt etabliert hat. Das sizilianische Sandfliegenfieber-Virus (SFSV) dagegen wurde während des Zweiten Weltkriegs als Erreger des „Sandfliegenfiebers", einer selbstlimitierten fiebrigen Erkrankung, identifiziert. Heute ist es bekannt als eines der Phleboviren mit der weitesten geographischen Verbreitung und verursacht Symptome hauptsächlich in immunologisch naiven Soldaten und Reisenden. Obwohl SFSV im Hinblick auf das klinische Bild ausführlich charakterisiert wurde, ist seine Interaktion mit dem Säugetierwirt auf der molekularen Ebene fast komplett unbekannt.

In dieser Arbeit haben wir daher die molekularen Mechanismen aufgeklärt, mit denen das NSs-Protein von SFSV dem IFN-System entgegenwirkt. Wir konnten zeigen, dass SFSV NSs die Induktion von Typ-I- und III IFN dämpft, indem es gezielt die DNA-Bindedomäne des Transkriptionsfaktors IRF3 verdeckt. Trotz der Inhibition von IRF3 unterband SFSV die IFN-Induktion dennoch nicht vollständig, was zu einer IFN-abhängigen Hochregulation des Transkriptionsfaktors IRF7 führt, der nicht von SFSV NSs beeinträchtigt wird und die IFN-Induktion fördert. Zusätzlich versagte SFSV NSs darin, die IFN-Signaltransduktion zu behindern, woraus eine erhebliche Expression anti-phleboviraler IFN-stimulierter Gene (ISGs) resultierte. Folglich scheint SFSV NSs eher ein Modulator als ein starker Antagonist des IFN-Systems zu sein.

Daneben besitzt die Proteinkinase R (PKR) aufgrund der Phosphorylierung des eukaryotischen Initiationsfaktors 2α (eIF2α), und der resultierenden Blockade der Proteinbiosynthese eine stark restriktive Aktivität gegenüber Phleboviren. Überraschenderweise fanden wir, dass das SFSV NSs eine PKR-Resistenz vermittelt und die Translation steigert, ohne jedoch die PKR-Aktivierung oder die eIF2α-Phosphorylierung zu beeinträchtigen. Vielmehr wirkt SFSV NSs auf den nachgeschalteten eIF2B-Komplex, den regulatorischen Knotenpunkt der integrierten Stressantwort. Bemerkenswerterweise hemmen alle bisher charakterisierten viralen PKR-Antagonisten die PKR-Aktivierung oder die eIF2α-Phosphorylierung, sodass die Manipulation von eIF2B durch SFSV NSs eine neue virale Evasionsstrategie darstellt.

Interessanterweise zeichnete sich bei unseren Untersuchungen ein gemeinsames Muster ab: Das hochvirulente RVFV setzt sein NSs-Protein für den proteasomalen Abbau seiner Zielfaktoren ein, agiert also sozusagen katalytisch. Daneben verursacht es eine globale Blockade der Genexpresssion des Wirtes, um dem IFN-System zu entgehen. Das NSs des weniger virulenten SFSV dagegen beeinträchtigt nicht die Expressionslevel von Zielfaktoren, sondern scheint sowohl die Hemmung der IFN-Induktion als auch die PKR-Evasion auf stöchiometrische Weise zu vermitteln. In Anbetracht seiner Bedeutung als alleiniger phleboviraler IFN-Antagonist wurde spekuliert, dass das NSs-Protein ein Korrelat für die Virulenz darstellt. Unsere Daten zu SFSV NSs unterstützen diese Hypothese und sprechen für die Charakterisierung der NSs-Proteine neuartiger Phleboviren bezüglich ihrer Fähigkeit, die IFN-Induktion, die IFN-Signaltransduktion und die PKR-Aktivität zu hemmen, um ihr Krankheitspotential besser einzuschätzen.

Abbreviations

4E-BP	eIF4E-binding protein
A	alanine
aa	amino acid(s)
ALEV	Alenquer virus
AP-1	activator protein 1
ATF4	activating transcription factor 4
BHAV	Bhanja virus
BVDV	bovine viral diarrhoea virus
CBP	CREB-binding protein
CHGV	Chagres virus
CHOP	C/EBP homologous protein
Clone 13	attenuated RVFV strain containing a large internal deletion within the NSs gene
D	aspartate
DASHV	Dashli virus
DBD	DNA-binding domain
DDIT3	DNA damage-inducible transcript 3, coding for CHOP (C/EBP homologous protein)
eGFP	enhanced green fluorescent protein
eIF	eukaryotic initiation factor
F	phenylalanine
Fig.	figure
Fig. S	supplementary/supporting figure
G	glycine
GADD34	growth arrest and DNA damage-inducible protein 34
GDP	guanosine diphosphate
GTP	guanosine triphosphate
GTV	Guertu virus
H	histidine
HA	hemagglutinin
HRTV	Heartland virus
HSV	herpes simplex virus
I	isoleucine
IFIT	IFN-induced protein with tetratricopeptide repeats
IFITM	IFN-induced transmembrane protein
IFN	interferon
IFNAR	interferon-alpha receptor
IFNB1, *Ifnb1*	human and murine genes coding for IFN-β, respectively
IFNL	human gene coding for IFN-λ
IKK	IκB kinase
IL	interleukin
IRES	internal ribosomal entry site

IRF	interferon-regulatory factor
IRF3(2A)	phospho- and dimerization-deficient IRF3 mutant
IRF3(5D)	constitutively active phosphomimetic IRF3 mutant
ISG	interferon-stimulated gene
ISGF3	interferon-stimulated gene factor 3
ISR	integrated stress response
ISRIB	ISR inhibitor
JAK	Janus kinase
K	lysine
KSHV	Kaposi sarcoma herpes virus
L	leucine
MAPK	mitogen-activated protein kinase
MAVS	mitochondrial antiviral signalling protein
MDA5	melanoma differentiation antigen 5
MP12	attenuated RVFV strain producing a functional NSs
mTORC1	mammalian target of rapamycin (mTOR) complex 1
MX1, *Mx1*	myxovirus resistance protein 1 genes coding for human MxA and murine Mx1, respectively
MxA	human myxovirus resistance protein A
MyD88	myeloid differentiation primary response protein 88
NES	nuclear export sequence
NF-κB	nuclear factor kappa-light-chain enhancer of activated B cells
NLS	nuclear localization sequence
NSm	non-structural protein coded on the M segment
NSs	non-structural protein coded on the S segment
OASL	2'-5'-oligoadenylate synthetase like protein
ORF	open reading frame
pDC	plasmacytoid dendritic cell
PARP12L	poly(ADP-ribose) polymerase family member 12, long isoform
PERK	PKR-like endoplasmic reticulum kinase
PI3K	phosphoinositide 3-kinase
PKR	protein kinase R
pLxIS	IRF-binding motif comprising a hydrophilic amino acid, followed by a leucine residue, any amino acid, an isoleucine residue, and a phosphorylatable serine residue
PPP1R15A	protein phosphatase 1 regulatory subunit 15A, coding for GADD34 (growth arrest and DNA damage-inducible protein 34)
PRD	positive regulatory domain
PTV-A	Punta Toro virus, Adames strain
PTV-B	Punta Toro virus, Balliet strain
R	asparagine
Ref.	reference

RIG-I	retinoic acid-inducible gene I
RVFV	Rift Valley fever virus
S	serine
S6K	S6 kinases
SFSV	sandfly fever Sicilian virus
SFTV	sandfly fever Turkey virus
SFTSV	severe fever with thrombocytopenia syndrome virus
siRNA	small interfering RNA
STAT	signal transducer and activator of transcription
STING	stimulator of IFN genes
SV40	simian virus 40
TBK1	TANK-binding kinase 1
TFIIH	transcription factor IIH
TLR	Toll-like receptor
TORV	Toros virus
TOSV	Toscana virus
TRAF	TNF receptor associated factor
TRIF	TIR-domain-containing adapter inducing interferon-β
TYK	tyrosin kinase
UUKV	Uukuniemi virus
vRNP	viral ribonucleoprotein
Y	tyrosine
ZH548	highly virulent RVFV strain

1 Introduction

1.1 Phleboviruses and phenuiviruses

Phleboviruses are globally emerging arthropod-borne viruses of significant public health impact and economic interest. While long-known members with characterized clinical symptoms (such as Rift Valley fever virus (RVFV), Toscana virus (TOSV), and sandfly fever Sicilian virus (SFSV)) are expanding geographically, numerous novel ones are identified continuously. The latter comprise both highly virulent members identified due to clinically apparent patients, but for the most part abundant others found in vector species and with yet unknown disease potential. Therefore, taxonomy is subject to frequent revisions [1, 2, 17, 24, 231]. Most recently, the order *Bunyavirales* (realm *Riboviria*, kingdom *Orthornavirae*, phylum *Negarnaviricota*, subphylum *Polyploviricotina*, class *Ellioviricetes*) was created and the members of the previous genus *Phlebovirus* reorganized into multiple distinct genera within the family *Phenuiviridae*, including, amongst others, the dipteran-borne phleboviruses and the tick-borne bandaviruses. Due to the cumulative nature of this thesis, both phlebo- and bandaviruses, as well as one uukuvirus will be discussed (collectively referred to as phenuiviruses) and the old nomenclature for individual virus species will be used.

Both phlebo- and bandaviruses cover a wide spectrum of virulence (**manuscript 1** and ref. 7, 55). Among dipteran-borne, that is to say sandfly- or mosquito-transmitted phleboviruses [212], RVFV is highly pathogenic in humans, causing mainly flu-like symptoms, but in some patients progresses to acute hepatitis, retinitis with persistent visual damage, delayed-onset encephalitis, or haemorrhagic fever [6, 84, 85]. Higher virulence is observed in ruminants, resulting in so-called abortion storms and high fatality in newborns [23, 46]. Due to the ensuing impact on public health and economic loss, as well as its spread throughout Africa and to the Arabian Peninsula [136], RVFV has been rated both as natural threat and potential bioterrorism agent [34, 44, 182, 188] and thus been subject to extensive research. TOSV, on the other hand, is endemic across the Mediterranean and causes fevers that can be complicated by meningitis or encephalitis [32]. SFSV was isolated from infected soldiers in Italy during the Second World War, due to an outbreak of so-called *'sandfly fever'*, *'three-day fever'*, *'Pappataci fever',* or *'dog disease'*, a self-limited but nonetheless incapacitating febrile disease with headaches, myalgia, and general malaise [19, 101, 184, 185]. Of note, SFSV is now one of the most widespread phleboviruses, with high seroprevalence levels in humans and domestic animals (up to 50% and almost 80%, respectively) reported from a geographic area ranging from Portugal to Bangladesh and the Northern Mediterranean to Somalia, affecting predominantly immunologically naïve soldiers and travellers [10, 11, 14, 20, 52-54, 56, 58, 64, 74, 115, 154, 155, 186, 187, 211, 227]. Further fever-inducing phleboviruses have been isolated also from sick patients in Central and Southern America, including Punta Toro (PTV), Chagres (CHGV), and Alenquer virus (ALEV) [76, 164, 208, 213]. In contrast, Drin, Hedi, Ntepes, and Wuxiang virus [22, 210, 218, 233] are only a few recent examples of novel phleboviruses with as-yet unknown disease potential.

Among tick-borne bandaviruses, severe fever with thrombocytopenia syndrome virus (SFTSV, previously also Henan or Hubei fever virus, recently reclassified and renamed as Dabie bandavirus) has been identified in rural China in 2009 due to cases of fever with thrombocytopenia, leukocytopenia, and multiple organ failure with a high fatality rate, and since been found also in other Asian countries [55, 181, 230, 240]. At the same time, similar symptoms led to the identification of Heartland virus (HRTV, now Heartland bandavirus) in Northern America [26, 141, 193], whereas closely related Guertu bandavirus (GTV) was

isolated from ticks only recently and its clinical picture remains elusive [203]. Furthermore, members of the Bhanja virus (BHAV) serogroup (now Bhanja bandavirus) are associated with febrile disease, and Uukuniemi virus (UUKV, now genus *Uukuvirus*) is considered to be apathogenic [50, 138, 163].

Molecularly, phenuiviruses viruses are spherical, enveloped particles of approximately 100 nm diameter that carry the tri-segmented negative- and ambisense single-stranded RNA genome (**manuscript 1, fig. 1**). The viral particle is covered by the transmembrane glycoproteins Gn and Gc, which are encoded on the medium (M) genome segment as precursor polyprotein that is co-translationally processed. The genomic RNA segments are encapsidated by the nucleoprotein N and associated with the viral RNA-dependent RNA polymerase L, which are coded on the small (S) and large (L) segments, respectively.

Following receptor-mediated endocytosis and the release of viral ribonucleoproteins (vRNPs) [83, 117, 134], viral replication occurs entirely in the cytoplasm of the infected host cell. There, the viral polymerase directly initiates primary transcription, using a cap-snatching mechanism to produce viral mRNA from incoming genomic segments [4, 61, 96, 123]. The synthesis of viral proteins then depends on the canonical host translation machinery. A subsequent switch to secondary transcription leads to primer-independent synthesis of full-length complementary antigenomic RNA and, subsequently, amplification of the genomic segments. Finally, assembly and budding take place at the Golgi apparatus [139].

In addition to the structural proteins described above, phleboviruses encode multiple non-structural accessory proteins, that are not required for replication per se, namely the NSm and 78-kDa proteins on the M [65, 225] and NSs on the S segment [68, 95, 215]. While NSm appears to be of importance predominantly in the dipteran vector of phleboviruses and is even absent in tick-borne bandaviruses, NSs is firmly established as the major virulence factor in the mammalian host of both phlebo- and bandaviruses (**manuscript 1** and ref. 42, 55, 135).

1.2 The type I and type III IFN systems in RNA virus infection

The interferon (IFN) system provides a potent and essential first host response to viral infection. Type I and III IFNs are rapidly secreted from most infected cell types to induce a transcriptional programme that culminates in the expression of hundreds of IFN-stimulated genes (ISGs). These establish an antiviral state that limits viral spread during the early stages of infection, thus allowing sufficient time for the generation of an adequate adaptive immune response that then, ideally, eliminates the virus.

Type I IFNs comprise a number of IFN-α subtypes, IFN-β, and other additional members [142, 145]. The main sensors of viral RNA in the cytoplasm for the induction of type I IFNs are the helicases RIG-I and MDA5 and their adaptor MAVS [94, 110, 111, 146, 194, 200, 232, 235, 239]. Additionally, endosomal double-stranded RNA can activate TLR3 and downstream adaptor TRIF [5, 234]. Both merge on the activation of the kinases TBK1 or IKKε, which in turn phosphorylate the transcription factor IRF3 [62, 201]. The latter then triggers the induction of IFNs and further genes together with NF-κB, AP-1, as well as transcriptional co-activators CBP and p300 [94, 219]. Activated IRF3 induces a first wave of IFN (comprising mostly IFN-β) that triggers the transcriptional and translational upregulation of IRF7 which is normally expressed in only low amounts or absent in most cell types [156]. IRF7 is then activated like IRF3 and induces a second, amplified wave of IFN that also includes a broad range of IFN-α subtypes [137, 191]. Besides, endosomal viral single-stranded RNA can activate TLR7/8, their adapter MyD88, and IRF7, resulting in the release of massive amounts of IFNs from plasmacytoid dendritic cells (pDCs), specialized

IFN-producers [39, 49, 88, 156, 206], and other specialized immune cells. Once secreted, type I IFNs signal in an auto- and paracrine manner through a ubiquitously expressed heterodimeric receptor, consisting of the IFNAR1 and IFNAR2 chains, and the kinases JAK1 and TYK2 which phosphorylate the transcription factors STAT1 and STAT2. Together with IRF9, the latter form the IFN-stimulated gene factor 3 (ISGF3) which then induces ISG expression. In addition, IFN signalling drives the induction of additional genes via other STAT combinations, and positively regulates MAPK and PI3K-mTOR signalling [142, 145].

Type III IFNs, on the other hand, comprise IFN-λ1 (also IL-29), IFN-λ2 (IL-28B), IFN-λ3 (IL-28A), and less understood IFN-λ4 [237]. They are induced in a similar manner as the type I IFNs, with *IFNL1* being expressed with similar kinetics as *IFNB1*, whereas *IFNL2* is more dependent on IRF7 and thus resembles *IFNA* genes [161, 162]. However, type III IFNs activate a distinct receptor consisting of the IFN-λR1 and IL10R2 chains. They also induce ISGs via ISGF3 and activate MAP kinases and PI3K, but receptor expression is restricted to a limited number of cell types, such as epithelial cells within mucosal barrier tissues and human hepatocytes [216, 237, 244].

ISGs exert their antiviral activity by interfering at multiple levels of the viral replication cycle, such as entry (IFITMs), viral transcription (MxA), and translation (PKR, IFITs) [195]. In addition, many pathogen sensors and transcription factors, such as RIG-I, IRF7 and STAT1, are themselves ISGs and engage in amplification loops [145]. Yet other ISGs mediate antiproliferative and immunomodulatory functions, thereby shaping the adaptive immune response.

Viruses, on the other hand, need to replicate considerably to ensure transmission to the next susceptible host and thus evolved diverse strategies to counteract the IFN system early on [81]. To this end, viral IFN antagonists are either expressed very early or already packaged into viral particles. They typically are multifunctional proteins that target several host functions within the infected cell, with molecular mechanisms ranging from a broad shutoff of gene expression to very precise targeting of specific host factors.

1.3 Phleboviruses and the type I and III IFN systems

The interaction of phenuiviruses and the IFN I and III systems has already been reviewed in **manuscript 1** and will thus be described only in an abbreviated form complemented by more recent advances.

The elevated susceptibility of IFN-signalling deficient mice, the protective effect of prophylactic or early therapeutic application of IFN or IFN inducers, as well as the association of an early onset of IFN production with survival in rodent and non-human primate models all demonstrate the importance of the IFN system during phleboviral infection [25, 51, 79, 112, 133, 144, 149, 150, 169, 205]. SFSV replication in particular can also be substantially reduced by the addition of ectopic IFN-α [43]. While a systematic analysis of ISGs for anti-phleboviral activity has not been reported yet, a few RVFV-restricting ISGs have been identified on occasion (**manuscript 1, table 1**), including IFITM-2 and -3 [151], MxA, which also restricts SFSV [63, 80, 189], and PKR [79, 97]. In addition, also IFITs, ISG15, OASL, and PARP12L appear to affect RVFV titres [13, 51, 172].

Both the genomic and antigenomic viral RNA segments contain 5'-triphosphorylated complementary ends that form short double-stranded *'pandhandle'* structures, which represent an optimal ligand for RIG-I [68, 77, 194, 222], such that already incoming vRNPs trigger RIG-I activation [221]. In agreement with this, the RIG-I-MAVS axis has been reported to constitute the predominant IFN-induction pathway for RVFV

in the mouse model, without detectable contribution from TLR7/8-MyD88 or TLR3-TRIF signalling [59]. Given the segmented genome structure and the resulting multiplication of RIG-I ligands, phenuiviruses thus require a potent IFN antagonist [222].

1.4 The NSs protein – a highly diverse viral IFN antagonist

The NSs protein is fascinating for several reasons: not only is NSs the sole phenuiviral gene encoded in ambisense orientation (**manuscript 1, fig. 1b**), but NSs proteins also display a high diversity with amino acid sequence identities in the range of only 7.5-28.6% amongst phleboviruses [68, 231]. More importantly, this diversity is reflected in distinct NSs sizes, subcellular localization patterns, targeted host factors, and molecular mechanisms to evade the IFN system (**manuscript 1, fig. 2 and table 2, 3**).

In brief, the NSs protein of RVFV allows for full RIG-I signalling up to the binding of transcription factors to their cognate promoter sites, but then blocks the induction of IFNs and other host-cell responses by establishing a general block of host cell transcription and mRNA export, and additionally recruits a transcriptional suppressor to the *IFNB1* promoter [21, 40, 103, 105, 125, 126]. Of note, RVFV NSs initiates the proteasomal degradation of both general transcription factor TFIIH subunit p62 and PKR by recruiting host E3 ubquitin ligases [103, 104, 152], implying that it acts rapidly and efficiently in a catalytic manner. Similarly, TOSV NSs employs proteasomal degradation of RIG-I and PKR but contains intrinsic E3 ubiquitin ligase activity and appears to be degraded along with its host targets [70-73, 107]. PTV NSs also seems to affect host-cell transcription to evade IFN induction but its potential to evade PKR remained unknown [127, 171].

Furthermore, highly pathogenic SFTSV (now Dabie bandavirus) spatially isolates several components of RIG-I signalling into granular NSs aggregates, while related HRTV and GTV NSs act on TBK1 [147, 156, 176, 180, 190, 228]. In contrast, apathogenic UUKV only weakly antagonizes IFN induction [179]. Strikingly, SFTSV, HRTV, and GTV NSs additionally affect IFN signalling by sequestering STAT2 (and STAT1) [33, 158, 180], implying that simultaneous inhibition of both IFN induction and signalling might be a common characteristic of highly virulent phenuiviruses.

In summary, the study of RVFV and a limited set of other family members indicated that the evasion of the IFN system is a common hallmark of human pathogenic phenuiviruses (**manuscript 1** and ref. 135). Curiously, distinct NSs proteins, however, display remarkably diverse strategies, both in terms of host targets and molecular mechanism, tempting speculation that the function of a given NSs protein might correlate with the virulence of the respective phlebovirus (**manuscript 1, 2** and ref. 179, 180).

1.5 Objectives of the present thesis

Despite detailed characterization of its clinical picture [19, 185], the molecular effects of SFSV infection have remained completely elusive for a long time. Renewed interest in SFSV, or more precisely its NSs protein, sparked upon the realization that the highly diverse NSs proteins might all act as IFN antagonists - but all by strikingly different mechanisms [220]. On the other hand, the still ongoing quest for a save and efficient RVFV vaccine led to the evaluation of recombinant RVFV viruses [128]. The study of chimeric viruses, in which the NSs gene of RVFV was substituted by the one of SFSV via reverse genetics, showed that the introduction of SFSV NSs rescued the IFN-antagonistic activity that was lost in NSs-deficient RVFV mutants [79, 127]. Notably, among a panel of chimeric viruses containing heterologous NSs genes, only the ones carrying SFSV NSs allowed enough viral replication for the induction of a protective adaptive immune response and simultaneously displayed sufficient attenuation in the mouse model [127, 159]. In line with this, SFSV NSs neither destroyed PKR, nor did it affect general host transcription [79, 107, 127], suggesting that SFSV NSs acts in a manner different from RVFV NSs and probably also by targeting different host factors. Indeed, determination of the interactomes of RVFV and SFSV NSs identified distinct, non-overlapping sets of candidate host interactors [173].

The objectives of this thesis therefore were to characterize the molecular function of SFSV NSs in the mammalian host cell, guided by the candidate host targets obtained from the aforementioned interactome dataset and with a focus on its interplay with the IFN system. First, it was to be tested whether the inhibitory activity observed with the recombinant chimeric viruses held true for parental SFSV. Then, the molecular mechanism used by SFSV NSs was to be determined. Second, SFSV and its NSs protein were to be tested for their ability to affect IFN signalling and ISG expression. Finally, it was to be investigated whether SFSV NSs also conferred resistance to the IFN-inducible restriction factor PKR, maintained translation, and how this was achieved.

To these ends, SFSV NSs was to be expressed either ectopically by transient transfection or studied under infection with the parental SFSV Sabin prototype strain or the abovementioned recombinant virus, that is to say a viral RVFV backbone containing the SFSV NSs gene [79]. Finally, the attenuated RVFV strains MP12 and partially NSs-deleted clone 13 [29, 98, 153] were to be used alongside parental SFSV, and the recombinant wild-type and NSs-deletion mutant of RVFV strain ZH548 [78, 79] alongside the recombinant chimeric virus, in order to derive conclusions for a possible correlation between NSs function and virulence of SFSV as compared to RVFV.

2 Results

2.1 SFSV NSs targets IRF3 for inhibition of IFN induction

Although SFSV NSs clearly inhibits IFN induction when expressed from a recombinant RVFV backbone [79, 127], it was not clear whether this was also the case for parental SFSV. Furthermore, while SFSV NSs acts in a way different from RVFV NSs, namely does not induce a general block of host gene expression [127], the molecular mechanism employed by SFSV NSs remained elusive.

Hence, we first infected A549 cells, a human lung carcinoma cell line that mounts a strong IFN response under RNA virus infection and is readily infected by phleboviruses. As expected, the MP12 and the NSs-deficient clone 13 strains of RVFV either faintly or strongly induced the expression of the *IFNB1* gene, respectively (**manuscript 2, fig. 1A**). In comparison, SFSV induced only low levels of *IFNB1* (**manuscript 2, fig. 1A**). Neither a natural NSs-deficient strain nor a reverse genetic system is available for SFSV yet. To mimic NSs deficiency under SFSV infection, we thus designed a pool of small interfering RNAs (siRNA), which we validated by concomitant transfection with an expression construct for SFSV NSs (**manuscript 2, fig. 1B**). siRNA treatment also significantly reduced the levels of NSs-containing RNA species and at the same time enhanced *IFNB1* induction under infection with SFSV, but not MP12, clone 13, highly related SFTV, or TOSV; neither did it possess an intrinsic IFN-inducing activity (**manuscript 2, fig. 1C, D** and data not shown). Of note, the knockdown of NSs also resulted in lower levels of the viral L segment (**manuscript 2, fig. 1E**), which is not targeted by the siRNA pool and thus serves as proxy for viral replication. In contrast to IFN-competent A549 cells, such a reduction was not observed in IFN-incompetent Vero B4 cells (data not shown). Taken together, the loss of NSs resulted in simultaneous attenuation of IFN antagonism and viral replication in IFN-competent cells, reminiscent of the behaviour of NSs-deleted phleboviruses [21, 25, 27, 95, 153, 171].

As both RVFV and TOSV use the host ubiquitin-proteasome system to deplete target host factors [73, 79, 97, 103, 104], we wondered whether SFSV NSs used a similar strategy. However, neither a chimeric SFSV NSs-expressing virus nor parental SFSV reduced the levels of RIG-I, MAVS, TBK1, IRF3, or RVFV targets PKR or p62 (**manuscript 2, fig. 2**).

To narrow down the molecular mechanism of SFSV NSs, we performed reporter assays with ectopically expressed NSs. In agreement with our infection experiments, SFSV NSs inhibited *Ifnb1* reporter activity induced by viral RNA or overexpression of MAVS in a dose-dependent manner (**manuscript 2, fig. 3A** and data not shown). Next, we dissected the contribution of different *Ifnb1* promoter elements, the so-called positive regulatory domains (PRDs) [94]. SFSV NSs reduced the activity of the IRF-responsive PRDI reporter with similar strength as the full *Ifnb1* promoter, whereas the NF-κB-activated PRDII reporter was only weakly affected (**manuscript 2, fig. 3B, C**). Moreover, SFSV NSs also diminished both *Ifnb1* and PRDI reporter activity when TBK1 or TRIF overexpression was used as stimulus (data not shown). In conclusion, SFSV NSs inhibited IFN induction via the TBK1-IRF3 axis.

Compatibly, IRF3 was among the candidate host targets of SFSV NSs in the previously conducted interactome study [173]. We extensively confirmed the interaction by co-immunoprecipitation (**manuscript 2, fig. 4** and data not shown). As also IRF7 plays a major role in IFN induction [92, 137, 156, 191] and other IRFs have been implicated in one way or other in the regulation of IFN induction or signalling [93], we thus tested whether SFSV NSs displayed a more promiscuous IRF-binding activity.

However, it interacted neither with most closely related IRF7, nor with IRF2, IRF5, or IRF9 (**manuscript 2, fig. 5A, B**) but exclusively targeted IRF3.

IRF3 resides predominantly in the cytoplasm due to a strong nuclear export sequence (NES) [122]. Upon viral infection, IRF3 activation comprises the following steps: phosphorylation by TBK1 or IKKε at the surface of adapters MAVS, TRIF, or STING, dimerization, and finally accumulation in the nucleus, where it binds to responsive promoter elements and engages the transcriptional co-factors CBP and p300 [129, 219, 238]. Ectopically expressed NSs, on the other hand, localized to both the cytoplasm and nucleoplasm in several cell lines (data not shown) and could thus interfere at any step of IRF3 activation and function.

The recruitment of IRF3 to upstream adaptors MAVS, TRIF, and STING depends both on a conserved pLxIS motif within the adaptor (in which p denotes a hydrophilic residue, L leucine, x any amino acid, I isoleucine, and S serine) and the phosphorylation of the final serine residue upon immune activation [132]. Curiously, SFSV NSs possesses a similar, pLxIS-like motif (RLGLS, aa 176-180), suggestive of molecular mimicry. To test whether the latter played a role in IRF3 targeting, we generated the corresponding phosphomimetic and phosphodeficient NSs mutants. While both were identical to wild-type NSs in expression and subcellular localization, the phosphodeficient S180A mutant lost the ability to bind IRF3 and inhibit *Ifnb1* reporter activity (data not shown). We further generated chimeric mutants of SFSV and PTV-B NSs, in which the RLGLS motif of SFSV and the corresponding amino acid stretch of PTV-B NSs were swapped. However, neither did the loss of the RLGLS motif abrogate IRF3-binding by SFSV NSs, nor did its acquisition confer the ability to bind IRF3 to PTV-B NSs (data not shown). Thus, IRF3 binding was not mediated by the RLGLS motif and, while phosphorylation of S180 appeared to be required, it might have a structural and/or regulatory role rather than directly contribute to the binding interface.

Surprisingly, when we then assessed the classical hallmarks of IRF3 activation – that is phosphorylation, dimerization, and nuclear accumulation – under SFSV infection, we found none of them affected (**manuscript 2, fig. 6**). In accordance, SFSV NSs also bound the constitutively active phosphomimetic mutant IRF3(5D) and inhibited *Ifnb1* and PRDI reporter activity induced by IRF3(5D) overexpression, whereas it did not affect the latter's dimerization state (**manuscript 2, fig. 7A-C** and data not shown). Similarly, SFSV NSs interacted with dimerization-deficient mutant IRF3(2A) and further derivatives with additional mutations within the dimerization interface (**manuscript 2, fig. 7D** and data not shown). Thus, the IRF3-NSs interaction neither depended on nor affected the dimerization state of IRF3, indicating that SFSV NSs exerted its inhibitory function downstream of IRF3 activation and targeted a region of IRF3 that is accessible independent of its activation state.

IRF3 can be subdivided into distinct domains, comprising an N-terminal DNA-binding domain (DBD, aa 1-113) that also harbours a bipartite nuclear localization sequence (NLS, K77/R78 and R86/K87), a nuclear export sequence (NES, aa 139-150), a proline-rich domain (aa 150-190), an IRF-association domain (aa 190-384), and, finally, a serine-rich domain (aa 384-427) that is phosphorylated during IRF3 activation [60, 122, 130, 238, 245] (**manuscript 2, fig. 8A**). Domain mapping of IRF3 revealed that the isolated DBD of IRF3 was sufficient for binding, whereas the one of IRF7 was not bound (**manuscript 2, fig. 8B, C** and data not shown). While further truncation of the DBD according to secondary structure elements was unfortunately inconclusive, a truncated IRF3 mutant lacking the far N-terminus (aa 1-57) interacted with SFSV NSs as efficiently as full-length IRF3 (data not shown). Together, this indicated that the binding interface on IRF3 is located within amino acids 58-113.

Intriguingly, this very region contains secondary structure elements that intimately interact with the *IFNB1* promoter [60, 166, 167]. It therefore suggested itself that NSs might interfere with the promoter-binding activity of IRF3. To test this hypothesis, we set up a promoter-binding assay, in which the *IFNB1* promoter was used to pull down activated IRF3. Indeed, SFSV NSs dose-dependently decreased the association of activated IRF3 with the *IFNB1* promoter without binding to the promoter itself (**manuscript 2, fig. 9**). Thus, in summary, SFSV NSs allows for IRF3 activation but then highly specifically obstructs the latter's DBD and thus inhibits *IFNB1* promoter binding and transactivation.

2.2 SFSV NSs fails to abrogate IFN signalling and ISG expression

While the previous study elucidated that SFSV NSs can mask the DNA-binding domain of IRF3 and thus negatively regulate IRF3-dependent IFN induction, it did not fully assess the efficiency of this evasion mechanism, nor did it address whether SFSV was capable of interfering with IFN signalling, ISG induction, and thus the establishment of an antiviral state.

Actually, when we analysed the expression levels of selected host factors under infection (**manuscript 2, fig. 2**), we did observe an upregulation of IFN-inducible RIG-I not only under infection with NSs-deleted viruses, but also under infection with the recombinant SFSV NSs-expressing virus and parental SFSV. We thus wondered whether this was specific to RIG-I or also the case for other ISGs. We selected IRF3- and IFN-inducible *ISG15* as well as strictly IFN-dependent *MX1* (MxA) for further analysis as these ISGs display anti-phleboviral activity [63, 75, 80, 91, 189]. Indeed, besides *DDX58* (RIG-I) also *ISG15* and *MX1* were induced by SFSV infection on the transcript and protein levels, although *IFNB1* levels were only mildly elevated compared to positive control clone 13 across a range of MOIs (**manuscript 3, fig. 1** and data not shown). Simultaneously, both STAT1 and STAT2 were phosphorylated (**manuscript 3, fig. 1a, S1b**), indicative of active IFN signalling under SFSV infection. Furthermore, also STAT1 and STAT2, both ISGs as well [195], were elevated on the protein and mRNA levels (**manuscript 3, fig. 1a, S1** and data not shown). Interestingly, treatment of cells with IFN-α prior to infection did not significantly enhance STAT phosphorylation or ISG expression (**manuscript 3, fig. S2** and data not shown), suggesting that SFSV infection on its own triggers maximal ISG expression.

To exclude that IFN signalling and ISG induction was due to the presence of IFNs in viral stocks (as observed for certain hantaviruses [175]), we performed virus inactivation experiments. When virus was inactivated with β-propiolactone, neither viral replication nor IFN signalling and ISG induction were observed (**manuscript 3, fig. S3**). In contrast, ultrafiltration of the virus stocks (expected to remove IFNs from virus particles), did not alter IFN signalling (data not shown), suggesting that SFSV infection itself stimulates IFN signalling and ISG expression despite modulation of IFN induction.

We therefore compared the ability of ectopically expressed SFSV NSs to counteract IFN induction and IFN signalling. As before, SFSV NSs strongly inhibited IFN induction (**manuscript 3, fig. 2a**). In contrast, indirect IFN signalling (IFN-dependent *MX1* induction in response to overexpression of MAVS as IFN-inducing stimulus) was only weakly reduced, and direct IFN signalling (*MX1* induction upon stimulation with IFN-β) remained entirely unaffected (**manuscript 3, fig. 2b, c** and data not shown). Taken together with the observed STAT phosphorylation, the inability of SFSV NSs to bind STAT1 and STAT2 (data not shown), and the absence of IFN signalling factors from the NSs interactome (**manuscript 4, fig. S3** and ref. 173), SFSV NSs is not able to counteract IFN signalling or the induction of antiviral ISGs.

Similar to *IFNB1* also type III IFNs *IFNL1* and *IFNL2/3* were induced only weakly due to the action of SFSV NSs and the amounts of secreted IFN-λ1/3 lower in response to infection with SFSV as compared to clone 13 (**manuscript 3, fig. 3**), suggesting that low amounts of type I and type III IFNs secreted from SFSV-infected cells are already sufficient to induce maximal ISG levels.

In fact, given the stoichiometric and highly specific evasion strategy of SFSV NSs, we had already speculated that it was a mild modulator rather than a strong antagonist of IFN induction. To establish whether IFN induction was due to incomplete inhibition of IRF3 by SFSV NSs, its inability to target IRF7, or a combination thereof, we performed knockdown experiments targeting *IRF3*, *IRF7*, or both simultaneously (**manuscript 3, fig. 4**). First, the single knockdown of *IRF3* resulted in a partial reduction of all analysed IFN subtypes under infection with SFSV, indicative of incomplete IRF3 inhibition by SFSV NSs. Second, the single knockdown of *IRF7*, although less efficient than the knockdown of *IRF3*, had an even stronger reducing effect across all IFN subtypes for SFSV but not the positive control virus clone 13. Thus, IFN induction appears to rely more strongly on IRF7 under SFSV infection. Finally, the double knockdown of *IRF3* and *IRF7* further reduced the transcript levels of all tested IFNs. In contrast, knockdown of *IRF5* alone or in combination with other *IRFs* did not further affect IFN induction under SFSV infection (data not shown). In short, IFN induction under SFSV infection appeared to be partially due to incomplete inhibition of IRF3 by NSs, but predominantly driven by IRF7.

IRF7 is expressed only at very low levels or absent in most cell types and needs to be upregulated by IFNs before it can contribute to IFN induction [137, 156, 191]. To dissect whether IFN induction was due to this IFN-dependent amplification loop, we repeated the infection under treatment with JAK inhibitor ruxolitinib (**manuscript 3, fig. 5** and data not shown). While ruxolitinib did not affect *IRF3* levels, it abrogated the upregulation of both *IRF7* and strictly IFN-dependent *MX1*, as expected. Similarly, ruxolitinib dramatically reduced (but did not completely blunt) the induction of all tested IFN subtypes under SFSV infection, confirming the IRF7-mediated positive feedback loop as essential and dominant driver of IFN and ISG induction under SFSV infection.

In summary, this suggests that SFSV NSs is not able to sufficiently sequester IRF3 – probably due to an excess of IRF3 over SFSV NSs early in infection – resulting in the secretion of low amounts of IFNs. Unaffected by NSs, these then induce the upregulation of IRF7 which, not being targeted by NSs either, drives the induction of second-wave IFNs and ISGs even if by now sufficient NSs has been produced to sequester the entire cellular IRF3 pool. All taken together, we observed that SFSV NSs is a modulator rather than a potent antagonist of IFN induction, resulting in IFN signalling and extensive ISG induction.

2.3 SFSV NSs evades the PKR-mediated integrated stress response by targeting eIF2B

All viruses depend on the host translation machinery for the synthesis of their proteins [209]. The restrictive power of the IFN-upregulated serine-threonine kinase PKR therefore lies in its ability to rapidly shut off host translation in response to viral RNA [140]. Phleboviruses are highly susceptible to restriction by this PKR-mediated translation block (**manuscript 1, 4** and ref. 106, 135). Thus, they must efficiently counteract PKR signalling to allow for the synthesis of viral proteins. RVFV and TOSV NSs utilize the ubiquitin-proteasome system of the host to destroy PKR and thereby maintain translation (**manuscript 4, fig. 7b** and ref. 104, 107, 152). In contrast, recombinant chimeric viruses in which the NSs gene of RVFV was substituted by the ones of SFSV or PTV failed to degrade PKR [79, 127].

To first explore the potential of SFVS and PTV NSs to evade restriction by PKR, recombinant chimeric viruses carrying SFSV, PTV-A, or PTV-B NSs were screened for their replicative capacity under PKR knockdown and inducible PKR overexpression (**manuscript 4, fig. 1a**). In line with previous studies, the recombinant RVFV wild-type replicated to equal titres in all cell lines, while NSs-deleted viruses were attenuated in PKR-overexpressing cells and their titres rescued by PKR knockdown (**manuscript 4, fig. 1b, c**). Interestingly, also the chimeric viruses containing SFSV and PTV-A NSs replicated to similar titres under PKR knockdown and overexpression, indicating that SFSV and PTV-A NSs conferred PKR resistance.

Double-stranded RNA sensing by PKR results in its auto-phosphorylation and activation. PKR then phosphorylates downstream substrates, most prominently the eukaryotic initiation factor eIF2 on serine 51 of its α subunit (**manuscript 4, fig. 7a**). Normally, eIF2 forms a ternary complex together with GTP and the starter methionine-tRNA (tRNAi-Met), providing the latter for translation initiation [99, 168, 207]. After start codon recognition and GTP consumption, eIF2-GDP is released and recycled to eIF2-GTP by its guanine-nucleotide exchange factor eIF2B. Upon phosphorylation of eIF2α by kinases of the integrated stress response (ISR) such as PKR, however, its binding mode to eIF2B is dramatically altered, leading to tight, non-productive binding and thereby allosteric inhibition of eIF2B [3, 69, 108, 113, 120, 165, 168]. Consequently, the cellular pool of active eIF2 and thus translation initiation declines (**manuscript 4, fig. 7a**). Furthermore, eIF2 is expressed in excess over eIF2B, such that already partial phosphorylation of the cellular eIF2 pool is sufficient to fully sequester eIF2B and induce a general shutoff of translation [209]. Unsurprisingly, known viral PKR antagonists affect PKR levels, PKR activation, or eIF2α phosphorylation (**manuscript 4, fig. 7b** and ref. 28, 31, 47, 66, 86, 100, 197, 209). However, the chimeric viruses containing SFSV or PTV-A NSs, as well as parental SFSV induced strong PKR activation and eIF2α phosphorylation (**manuscript 4, fig. 2, S1**). Hence, SFSV and PTV-A NSs both confer PKR resistance but - in contrast to the other viral PKR antagonists - affected neither PKR activation nor eIF2α phosphorylation.

Using a bicistronic reporter transcript, we found that SFSV NSs specifically boosted canonical eIF2-dependent translation, whereas eIF2-independent translation driven by an internal ribosomal entry site (IRES) [224] remained unaffected (**manuscript 4, fig. 3a, b**). Similarly, mRNA translation was maintained under SFSV infection, whereas it was blunted by the PKR-restricted control virus clone 13 (**manuscript 4, fig. 3d**). Finally, activation of the ISR by PKR and other eIF2α kinases not only results in a block of general translation but also simultaneously favours the production of activating transcription factor 4 (ATF4), which then acts as transcription factor for ISR target genes, such as *DDIT3* (coding for CHOP) and *PPP1R15A* (GADD34) [165]. Both *DDIT3* and *PPP1R15A* were induced in a PKR-dependent manner in cells infected with positive control clone 13, but not by SFSV (data not shown). Thus, while SFSV NSs allowed PKR activation and eIF2α phosphorylation, it nonetheless maintained mRNA translation and viral replication. In other words, it decoupled the activating arm of the ISR (eIF2α phosphorylation) from its effector arm (translational control).

Strikingly, the interactome of SFSV NSs contained all five subunits of eIF2B (eIF2Bα-ε), the eIF2 recycling factor and central hub of the ISR, as highest scoring interactors (**manuscript 4, fig. S3** and ref. 173). We validated this interaction by co-immunoprecipitation of all five eIF2B subunits with SFSV NSs for both overexpressed and endogenous eIF2B (**manuscript 4, fig. 4a, b and S4a**). Curiously, both eIF2B binding and the amplification of cap-dependent translation were lost when SFSV NSs was equipped with an N-

terminal tag (**manuscript 4, fig. 3a, b and 4c, d**), although IFN suppression was unaffected (**manuscript 4, S2**). This strongly indicated that the effect of SFSV NSs on eIF2-dependent host translation was mediated by its interaction with eIF2B.

Besides the fact that it is inhibited by phosphorylated eIF2, the regulation of eIF2B is only partially understood and currently a highly dynamic research field [41, 168]. eIF2B is known for some time though to be upregulated in certain cancer types to satisfy their increased demand for protein synthesis [16]. The phosphorylation of S539 of the catalytic eIF2Bε subunit, in contrast, reduces its activity [226]. Finally, eIF2B has recently been reported to possess higher activity when forming a decamer, a configuration that is stabilized by the synthetic small molecule ISRIB [199, 204, 214, 247]. However, neither ectopic NSs expression, nor virus infection affected eIF2B expression, eIF2Bε(S539) phosphorylation, or eIF2B decamerisation (**manuscript 4, fig. 5** and data not shown).

Determination of the eIF2B subunit(s) targeted by SFSV NSs proved to be difficult: as eIF2B is highly conserved among eukaryotic organisms, direct binding assays need to be performed with highly purified proteins or in a prokaryotic expression system. Unfortunately, SFSV NSs lost its eIF2B-binding activity when produced in *E. coli* (data not shown), precluding binding studies with dual combinations of bacterially expressed eIF2B subunits. Subsequent analysis by Far Western blotting [229], using lysates of NSs-expressing cells as bait and bacterially expressed single eIF2B subunits as prey, yielded no binding (data not shown), suggesting that SFSV NSs, like eIF2, may be using a composite binding site. In fact, recent structural data revealed that eIF2 even uses two different binding sites on eIF2B - depending on the phosphorylation state of eIF2α [3, 69, 108, 113]. Non-phosphorylated eIF2 contacts eIF2B in a way that is optimal for its enzymatic activity (productive binding). In contrast, phosphorylation induces a conformational change in eIF2α that forces the association at another site on eIF2B (non-productive binding). SFSV NSs could be envisioned to use the same or a similar, overlapping binding site as phosphorylated eIF2, thereby blocking non-productive binding and shielding eIF2B from phosphorylated eIF2. However, phosphorylated eIF2α specifically co-precipitated with eIF2B, unperturbed by the presence of SFSV NSs and, *vice versa*, equal amounts of SFSV NSs co-precipitated with eIF2B, unaffected by the presence of phosphorylated eIF2α (**manuscript 4, fig. 6b**). Similarly, phosphorylated eIF2α was recovered by specific pulldown of the NSs-eIF2B complex (**manuscript 4, fig. 6c**). Finally, phosphorylated eIF2α co-sedimented exclusively with endogenous eIF2B rather than shifting to eIF2B-free fractions even under extensive overexpression of SFSV NSs (**manuscript 4, fig. 6a and S5**). Thus, SFSV NSs does not compete with phosphorylated eIF2α from a common binding site on eIF2B in our cellular assays.

All taken together, SFSV NSs conferred PKR resistance - that is to say facilitated ongoing protein synthesis and viral replication even under PKR overexpression and activation. In contrast to previously characterized PKR antagonists, however, SFSV NSs did so not by affecting PKR activation or eIF2α phosphorylation, but instead uncoupled the activating arm from the effector arm of the ISR by binding remarkably strongly to eIF2B, the central hub of the ISR, and rendered it resistant to the inhibitory effect of phosphorylated eIF2α by a yet-to-be elucidated mechanism (**manuscript 4, fig. 7c**).

3 Discussion

3.1 SFSV and SFSV-like phleboviruses – emerging human pathogens

SFSV is one of the most widespread phenuiviruses and, as the geographic range of sandfly-borne phleboviruses is closely linked to the distribution of its respective phlebotomine vector [212], further expansion of both the vector habitat and the virus are expected due to climate change [143, 148]. Originally identified as pathogen of military importance in the 1940s, SFSV continues to cause outbreaks among deployed military personnel and additionally gained relevance in travel medicine. Similarly, several novel SFSV-like viruses have been described recently, including sandfly fever Turkey (SFTV), Dashli (DASHV) and Toros (TORV) viruses, with SFTV displaying increased virulence and causing seasonal strain on the public health system in endemic areas [8, 9, 30, 57]. Additionally, the recent Syrian refugee crisis has been accompanied by a large outbreak of leishmaniasis, an infectious disease transmitted by the same insect vector [148], suggesting that SFSV might also be relevant in the context of economically or politically motivated population movements. Furthermore, sandfly-borne phleboviruses might be delivered to the host together with leishmania parasites. In fact, recent studies even reported an exacerbation of leishamiasis under co-infection with mildly pathogenic phleboviruses, including SFSV, TOSV, and Icoaraci virus (ICOV) [89, 178, 183]. While IFN induction and PKR activation might play a causative role, the mutual modulation within this *ménage à trois* of phlebovirus, leishmania parasite, and host remains to be characterized in more detail.

3.2 SFSV NSs, IRF3, and the interferon system

Similar to its activity when expressed from a recombinant RVFV backbone [79, 127], the NSs protein of SFSV also interferes with IFN induction in the parental virus context or when expressed ectopically. Like RVFV NSs, SFSV NSs allows for the activation of IRF3, namely phosphorylation, dimerization, and nuclear accumulation, but then specifically inhibits IRF3-driven gene expression instead of general host transcription.

SFSV NSs binds IRF3 independent of its activation state by targeting its DNA-binding domain (DBD), thus interfering with promoter binding and *trans*-activation. The DBD of IRF3 itself possesses a conserved architecture consisting of three alpha helices (α1-α3), four beta sheets (β1-β4), and three loops (L1-L3) [167]. Although our attempts to further narrow down the binding interface on IRF3 to secondary structure elements experimentally remained inconclusive, an educated guess can be made: since SFSV NSs interacted with IRF3 but not other IRF family members, it probably targets IRF3 residues within aa 58-113 that are in contact with DNA but are not conserved in other IRFs. Prime candidates include R78 and R86 but these are also part of the NLS and, as nuclear import was not affected, less likely targets. This leaves strands β3 and β4, as well as loops L2 and L3 as the most probable candidate regions. Determination of the binding interface on SFSV NSs by truncation analysis was unfortunately inconclusive. This is not surprising, though, as even small deletions within RVFV NSs result in misfolding, mislocalisation, and loss of function, implying that the structural conformation of NSs proteins rather than linear sequence motifs contribute to the binding of host interactors [87]. Structural analysis of the complex of SFSV NSs and the IRF3 DBD is currently ongoing to characterize the binding interface in more detail.

Constitutively expressed IRF3 is crucial for the induction of first wave IFNs, as illustrated by the increased susceptibility of *Irf3*-deficient mice to viral infection [192, 236]. Besides, several viral IFN antagonists

across taxonomically distinct RNA and DNA viruses target IRF3, affecting IRF3 phosphorylation, dimerization, nuclear accumulation, or inducing its degradation [18, 198, 202]. Bovine viral diarrhoea virus (BVDV) NPro has been reported to inhibit IRF3 promoter binding prior to its degradation, but a direct interaction between NPro and IRF3 could not be demonstrated [15, 90]. Kaposi's sarcoma-associated herpes virus (KSHV) K-bZIP and LANA-1 also interfere with the promoter binding of IRF3, but do so by sequestering the promoter from activated IRF3, not the other way round [38, 124]. Only the DNA viruses human bocavirus and herpes simplex virus 2 (HSV-2) use a mechanism similar to SFSV NSs [242, 243]. Hence, to our knowledge, SFSV NSs is the only known IFN antagonist from an RNA virus that directly interferes with the promoter-binding activity of IRF3. A possible explanation might be the limited efficiency of this evasion strategy: although SFSV NSs can target IRF3 regardless of its activation state, masking an interaction interface requires high levels of NSs to bind off the cellular pool of IRF3. Given that NSs is thought to be absent from viral particles and thus needs to be freshly produced upon infection, it is probably outnumbered by constitutively expressed IRF3 during the early phase. Furthermore, SFSV NSs fails to target IRF7, the 'master regulator of innate immunity' [92], and thus IFN induction in cells with high levels of IRF7, obtained either due to high basic levels (as observed in specialized cell types such as monocytes and pDCs [156]) or previous stimulation by IFN. In other words, the stoichiometric and IRF3-limited strategy of SFSV NSs makes it a modulator rather than a full-blown antagonist of IFN induction.

In line with this, we observed significant expression of the anti-phleboviral ISGs *ISG15* and *MX1*, *DDX58* (RIG-I) and *STAT1* despite simultaneous modulatory activity of SFSV NSs on type I and III IFN induction. While both IRF3 and IRF7 were involved in the induction of type I and III IFNs, IRF7 and the IFN-dependent positive feedback loop appeared to be the main drivers of IFN induction. Finally, neither SFSV infection nor ectopically expressed NSs inhibited type I IFN signalling, resulting in additional upregulation of RIG-I, STAT1, and STAT2, which can contribute to further amplification of the IFN response.

In summary, we propose the following model for IFN induction and signalling under SFSV infection: given the stoichiometric nature of IRF3 inhibition, the need to freshly synthesize NSs, and the activation of RIG-I by incoming viral ribonucleoproteins, the race between IRF3 activation and NSs accumulation within the infected host cell will determine whether IFN is produced in the early stage of infection. Consequently, two scenarios can be envisioned for SFSV-infected cells: if IRF3 activation outruns NSs-mediated inhibition, already small amounts of secreted first-wave IFN can signal back in an autocrine manner – unhindered by NSs – and IRF7 production is active before NSs has reached sufficient levels to control IRF3. IRF7 can then take over and induce an amplified second wave of IFNs, leaving NSs powerless to IFN induction and IFN signalling. This is even more facilitated in cells with constitutively high IRF7 expression. In contrast, cell types in which NSs production successfully outruns IRF3 activation do not secrete IFNs themselves but can be activated in a paracrine manner to commit to full ISG upregulation. In the end, both scenarios result in a strong IFN and ISG response and we speculate that the self-limited nature of SFSV infection is, at least partially, due to its failure to sufficiently interfere with the IFN system and the ensuing rapid establishment of a systemic antiviral state, in line with its sensitivity to IFN-mediated restriction [43].

3.3 SFSV NSs, host gene expression, and the integrated stress response

PKR represents an especially powerful anti-phleboviral ISG due its ability to shut down cap-dependent translation. While RVFV and TOSV directly blunt PKR activity by rapidly inducing its degradation, SFSV

and PTV NSs did not show such a destructive activity, nor did they affect PKR activation or eIF2α phosphorylation. In contrast, both SFSV NSs and PTV-A NSs (data not shown) targeted eIF2B further downstream, thereby rescuing cap-dependent translation and viral replication.

eIF2B stands out from guanine-nucleotide exchange factors due to its remarkably complex architecture and, despite tremendous recent progress, the intricacies of its regulation are still only partially understood [41, 168]. While we robustly confirmed the interaction between SFSV NSs and eIF2B, none of the mechanism of upregulating eIF2B activity described at the time of our study (elevated expression levels, eIF2Bε(S539) de-phosphorylation, and increased eIF2B decamerisation) appeared applicable to SFSV NSs. Additionally, we did not find evidence for binding competition of SFSV NSs with phosphorylated eIF2α. We thus speculated that SFSV NSs might induce structural changes within the complex of eIF2B with phosphorylated eIF2 such that a second, non-phosphorylated eIF2 moiety can be recycled, or nucleotide exchange would be facilitated on phosphorylated eIF2α itself. Further, numerous residues of eIF2B subunits besides eIF2Bε(S539) are subject to post-translational modifications and might have been involved in NSs-mediated regulation of eIF2B activity. Finally, while its binding sites for eIF2 and GDP/ GTP have been identified, additional surface area on eIF2B remains uncharacterized and offers potential for the interaction with as-yet elusive regulatory host factors [214, 247]. SFSV NSs could act as adapter to facilitate the recruitment of such factors. Exploration of these possibilities depended on advanced structural approaches (due to the complexity of eIF2B) or further progress in the characterization of eIF2B regulation.

In fact, more recent studies on eIF2B regulation [196, 248] indicate that the binding of phosphorylated eIF2 switches eIF2B from a catalytically active conformation (*'A state'*) into an inactive, inhibited conformation (*'I state'*) that displays altered substrate-binding interfaces and reduced enzymatic activity. Two follow-up studies on SFSV NSs (**manuscript 5** and ref. 109) now confirm tight eIF2B binding and ISR evasion by SFSV NSs, demonstrate a rescue of enzymatic eIF2B activity in the presence of phosphorylated eIF2, and finally reveal the molecular mechanism employed by SFSV NSs. Using cryo-EM, both studies agree on direct binding competition of SFSV NSs with phosphorylated eIF2α within the cleft between the eIF2Bα and δ subunits. However, in contrast to phosphorylated eIF2α, SFSV NSs does not induce the inhibitory *'I state'* but maintains eIF2B in the productive *'A state'* by contacting eIF2B in a manner distinct to phosphorylated eIF2α. More precisely, five aromatic residues (or *'aromatic fingers'*) within the N-terminus of SFSV NSs (comprising Y5, F7, F33, Y79, and F80) tightly grab helices α3 and α4 of eIF2Bα, aided by additional contact between NSs H36 and D37 and eIF2Bδ. This mode of binding explains some of our previous observations, including the lack of NSs binding to isolated eIF2B subunits, the tight binding to the fully assembled eIF2B complex even under high-salt conditions, and the loss of eIF2B binding by N-terminally tagged NSs. However, an obvious disagreement exists with regard to the binding competition between SFSV NSs and phosphorylated eIF2α. Then again, different experimental systems were used: while *in vitro* binding assays with purified proteins allow for the determination of binding kinetics and saturating protein concentrations, our previous experiments relied on transient transfection or infection. Consequently, it is conceivable that NSs levels in our cellular assays might have simply been insufficient to fully compete out phosphorylated eIF2 from both binding sites on the eIF2B decamer and observe binding competition in co-immunoprecipitation and co-sedimentation assays.

By successfully uncoupling the ISR at the level of eIF2B, SFSV can evade also the PERK-eIF2 axis of ER stress (**manuscript 5** and ref. 109). Further experiments are required to determine whether ER stress is

activated by phleboviruses and/or plays a restrictive role. Nonetheless, given the identification of eIF2B as viral target for the NSs proteins of SFSV and PTV-A, that is to say both an Old World and a New World phlebovirus, we suggest that targeting eIF2B is a more common viral strategy of ISR evasion that has been underappreciated so far. Indeed, Rabouw *et al.* recently reported that also accessory protein AcP10 of beluga whale coronavirus SW10 and AiVL protein of Aichivirus evade the ISR by targeting eIF2B and competing with p-eIF2α for eIF2B binding [177].

On the other hand, translation under viral infection is a double-edged sword: while viruses require access to the host translation machinery for the synthesis of viral proteins, they simultaneously need to prevent the production of antiviral effector proteins such as IFNs, ISGs, and other immune mediators. One efficient strategy is to shut off canonical host translation (for example by allowing or fostering eIF2α phosphorylation) and produce viral proteins via alternative mechanisms (such as the recruitment of translation factors by IRESs) [209]. *Vice versa*, some lytic viruses, such as RVFV maintain canonical translation and instead cut off the supply of host mRNA by blocking transcription and/or nuclear export. In both cases, the production of antiviral effectors by the host is abrogated, while the virus gains unhindered access to translation factors, tRNA, and ribosomes. Given the lack of a negative effect on mRNA synthesis [127], readily observable co-expression of reporter genes or tagged host factors driven by diverse promoters (including SV40, CMV, and NF-κB-responsive PRDII), and its failure to efficiently prevent the upregulation of ISGs, it can be assumed that SFSV does not interfere with the synthesis or nuclear export of host mRNA. Thus, the maintenance of cap-dependent translation comes at an additional cost for SFSV: while it ensures viral protein production, it also promotes the expression of IFNs, ISGs and other immune mediators, which then counteract viral replication and contribute to limiting viral infection. Hence, the PKR evasion strategy of SFSV NSs might finally contribute to its failure of sufficiently antagonizing the IFN system and overcoming the host immune response.

3.4 Other candidate host interactors of SFSV NSs

Besides IRF3 and eIF2B, another candidate host interactor of SFSV NSs attracted our attention: TRAF6 is involved in numerous host processes, including multiple signalling pathways of the innate immune response, and is targeted by virulence factors of both RNA and DNA viruses [217]. Although ectopically expressed SFSV NSs readily and robustly bound endogenous TRAF6, we could not observe any inhibitory effect of SFSV NSs in MAVS-mediated NF-κB activation (**manuscript 2, fig. 3C**), most probably due to the redundancy of TRAF6 with TRAF2 and TRAF5 in this pathway [131]. In contrast, SFSV NSs dose-dependently decreased NF-κB-dependent luciferase reporter activity in response to IL-1β, the TLR7 ligand R848, and overexpression of the adapter MyD88, but not downstream kinase IKKα (data not shown), consistent with interference at the level of TRAF6. However, SFSV infection did not affect the upregulation of IL-1β target genes upon cytokine super-stimulation (data not shown). Thus, a possible role of TRAF6 targeting by SFSV NSs in MyD88-dependent IL-1 and/or TLR signalling awaits further clarification.

3.5 PTV NSs combines inhibition of host transcription with targeting eIF2B

Similar to SFSV, also Punta Toro virus (PTV) is a long-known agent of febrile disease [76, 164] but remains only rudimentarily characterized on the molecular level. Of note, two strains of PTV with different degrees of virulence in the rodent model have been isolated, namely the highly pathogenic Adames (PTV-A) and

weakly pathogenic Balliet (PTV-B) strains [12], which possess NSs proteins that are strong or weak IFN antagonists, respectively [171].

We included both NSs proteins in our experiments and, in agreement with other studies [127], found that, like RVFV NSs, PTV-A NSs interfered with gene expression independently of the promoter used in our reporter assays (**manuscript 2, fig. 3, 7A, B** and data not shown), whereas PTV-B NSs had only negligible effects. In contrast to RVFV NSs, neither PTV-A nor PTV-B NSs induced the degradation of PKR (**manuscript 2, fig. 2A** and data not shown). Rather, like SFSV NSs, PTV-A NSs also conferred PKR resistance without affecting PKR activation and eIF2α phosphorylation, but targeted eIF2B instead (**manuscript 4, fig. 1, 2a** and data not shown). Taken together, PTV-A NSs appears to blunt the antiviral IFN response by a general block of host transcription (like RVFV NSs) and maintains host translation to allow for viral protein production (like SFSV NSs). This combination of activities is potentially more potent at suppressing the IFN and ISG response than the strategy employed by SFSV NSs.

3.6 Correlation of NSs function and phenuivirus virulence?

Dipteran-borne phleboviruses and tick-borne bandaviruses can be ranked from high to low virulence levels in humans, resulting in the rankings RVFV > TOSV > PTV-A > SFSV and SFTSV > HRTV > BHAV, respectively. Given its status as predominant virulence factor of these viruses and its high diversity in sequence, localization, and host interactome, the NSs protein, or rather its mode of action, has been suggested to correlate with the virulence of the respective phenuivirus (**manuscripts 1-3** and ref. 179, 180). So, what are commonalities and differences between the NSs proteins of these phenuiviruses and how can their molecular functions explain distinct degrees of virulence?

Highly pathogenic RVFV NSs and intermediately pathogenic TOSV NSs both make use of the ubiquitin-proteasome system of the host [71-73, 79, 97, 103-107], thus entirely eliminating host factors and signalling

Virulence levels and NSs functions of currently characterized phenuiviruses | Virus species are grouped into dipteran-borne phleboviruses (top) and tick-borne banda- and uukuviruses (bottom). Colour scale indicates virulence spectra from high (red) to apathogenic (green), or unknown virulence for GTV (grey).

Virus	Virulence	NSs activity		References
		IFN induction and signalling antagonism	PKR evasion	
RVFV		General transcription and mRNA export block (degradation and sequestration of host factors)	PKR degradation	21, 40, 79, 97, 103-106, 125-126, 152
TOSV		Inhibits IFN induction by RIG-I degradation, antagonism of IFN signalling unclear	PKR degradation	70-73, 107
PTV-A		General transcription block	eIF2B binding	127, 171, **manuscripts 2,4**
SFSV		Modulates IFN induction by binding IRF3, no antagonism of IFN signalling	eIF2B binding	**manuscripts 2-5**
PTV-B		No effective antagonism	Negligible activity	171, **manuscripts 2,4**
SFTSV		Sequestration of multiple RIG-I signalling factors and STAT2 into viral inclusion bodies	Unknown	33, 157-158, 176, 180, 190, 228
HRTV		Inhibits IFN induction and signalling by targeting TBK1 and STAT2	Unknown	180
BHAV		Unclear	Unknown	
UUKV		No effective antagonism	Unknown	179-180
GTV		Inhibits IFN induction and signalling by targeting TBK1 and STAT2	Unknown	147

pathway activation in a catalytic manner. However, TOSV NSs appears to get degraded along with at least one of its target factors [72, 73], thus somewhat reducing its efficiency. Besides, RVFV NSs abrogates host gene expression as a whole to evade IFN induction, whereas TOSV NSs only blunts RIG-I-dependent expression programs [21, 40, 71-73, 103-106, 125]. Thus, host target degradation would appear to be common to highly pathogenic phleboviruses, whereas the limited range of TOSV NSs-targeted transcriptional programs coincides with its decreased virulence as compared to RVFV. However, proteasomal degradation of host factors is not observed in highly virulent tick-borne bandaviruses, such as SFTSV (now Dabie bandavirus) [114, 241]. Instead, the latter sequesters numerous target host factors into NSs aggregates, with slightly less virulent HRTV sequestering an overlapping set of host factors, but without their spatial re-distribution. More importantly, SFTSV, HRTV, and GTV NSs specifically address also IFN type I and III signalling by sequestering STAT2. While it is currently unknown whether TOSV also interferes with IFN signalling and ISG expression, this is self-evident for RVFV NSs (as it causes a pronounced host-cell shutoff) and, taken together with bandavirus NSs activities, suggests that an effective evasion of the IFN response at both the induction and signalling levels is required for high virulence.

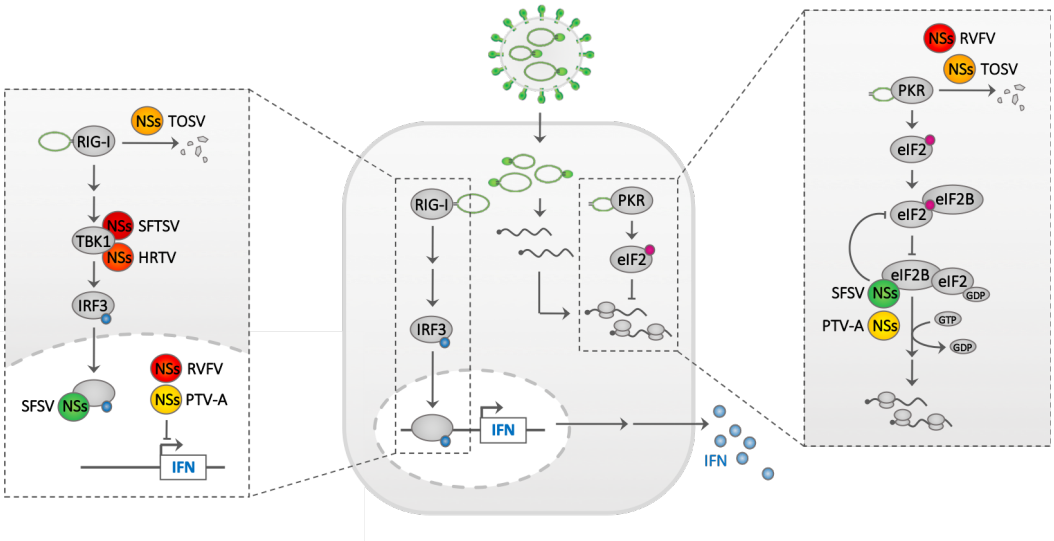

Interference of NSs proteins with IFN induction and PKR signalling | RNA from incoming phenuivirus particles and replication activates both RIG-I-driven type I and III IFN induction via the transcription factor IRF3, as well as PKR-mediated phosphorylation of eIF2α and, consequently, suppression of cap-dependent translation and inhibition of viral protein production (middle panel). These host responses are counteracted by the highly diverse NSs proteins of phlebo- and bandaviruses at multiple levels and via multiple distinct mechanisms, including proteasomal degradation, sequestration, binding competition, or other means of inhibition (outer panels). NSs proteins are coloured according to the virulence of the corresponding phenuivirus with virulence ranging from high (dark red) to mild (green).

How does SFSV fit in this picture? By exclusively targeting IRF3, it obviously exhibits both the weakest and most limited strategy for hampering with IFN induction so far. Similarly, SFSV NSs specifically compensates for the translation-regulatory arm of PKR by targeting eIF2B, thus potentially leaving further PKR functions such as the regulation of NF-κB and apoptosis [66] unaffected. Furthermore, the underlying stoichiometric nature requires higher levels of NSs to accumulate within an infected cell. Given that NSs is thought not to be packaged into viral particles, this puts it at a more pronounced kinetic disadvantage in the race between NSs synthesis, on the one hand, and IFN induction and ISR activation, on the other hand,

the race between NSs synthesis, on the one hand, and IFN induction and ISR activation, on the other hand, as compared to other 'catalytically' functioning NSs proteins. Finally, it completely fails to counteract IFN signalling and the transcriptional upregulation of ISGs – and may even boost IFN and ISG production at the translational level, thus probably resulting overall in a strong IFN response. Thus, while SFSV NSs may modulate the IFN response to a certain degree, the latter rapidly takes over and restricts the number of cells susceptible to replication, paving the way for rapid clearance of infection by the adaptive immune response. This actually fits quite well with the self-limited course of disease: after a short incubation period, febrile and other flu-like symptoms set on suddenly with a slight delay compared to viremia, last only for a short duration (typically 2-4 days), and are followed by long-term immunity [19, 185]. Furthermore, while SFSV does not induce apparent symptoms in rodents or non-human primates [185], a RVFV chimera containing SFSV NSs is dramatically attenuated in outbred mouse models [159]. Hence, the mild and limited host antagonism of SFSV NSs coupled with its comparatively low virulence supports the aforementioned correlation hypothesis.

Eventually, the outcome of infection is highly dependent on the initial race between viral propagation, on the one hand, and mounting a strong antiviral immune response, on the other hand. Besides its ability to delay the IFN and adaptive immune responses, further virus-inherent characteristics (such as replication efficiency and tissue tropism) come into play and require to be taken into consideration. One example is the curious case of PTV-A: while it is capable of blunting host transcription and evading PKR, it has been associated only with febrile disease in humans. In contrast, both PTV-A and chimeric viruses containing PTV-A NSs are highly lethal in rodents, suggesting that species-specific differences in pro- or antiviral host components, such as host factors required for attachment or entry, could play a decisive role in this case. Moreover, external factors, such as vector-mediated manipulation of the inflammatory milieu at the bite site during the blood meal, can modulate the capacity of the transmitted pathogen for propagation and spread [48, 170, 174].

Nonetheless, a common picture remains, in which the efficiency of inhibition of both branches of the IFN system (induction and signalling) exhibited by a given NSs protein significantly contributes to the virulence of the respective phenuivirus. Directly, a number of obvious questions are coming up for future research, such as: is TOSV NSs able to counteract IFN signalling? What are the host factors targeted by PTV NSs for IFN antagonism and how does PTV NSs operate? What are determinants of species-specific differences in PTV-mediated virulence? What is the full repertoire of anti-phleboviral and anti-bandaviral ISGs? Do bandaviruses evade PKR and, if yes, how? And finally, does the molecular characterization of further as-yet uncharacterized NSs proteins support a correlation between NSs function and virulence?

Of note, striking similarities exist between phenuiviruses and influenza A viruses with regards to the activation and evasion of the innate immune response: influenza A viruses also possess a segmented negative-strand RNA genome that forms RIG-I-activating '*panhandle*' structures, initiate viral mRNA synthesis by cap snatching, and, consequently, are in principle susceptible to restriction by PKR [45, 119, 222]. In the case of influenza viruses, innate immune evasion is predominantly (but not exclusively) mediated by the non-structural NS1 protein which uses a multitude of mechanisms to interfere with the recognition of viral RNA, subsequent IFN induction and signalling, as well as PKR activation [82, 121, 160]. More importantly, although the virulence of influenza A viruses is considered a multigenic trait and multiple other viral proteins contribute to immune evasion [223], correlations between the efficiency of

immune evasion by NS1 and virulence of the corresponding virus have been described for multiple influenza virus strains. For example, the presence of a serine residue at position 42 of the NS1 proteins of avian H5N1 influenza viruses has been linked to both increased IFN antagonism and lethality in a mouse model [102]. Similarly, also the NS1 protein of the particularly virulent 1918 pandemic H1N1 strain displays enhanced suppression of the IFN and ISG responses [67, 116, 118].

All taken together, we suggest to include the systematic analysis of the IFN-antagonistic function of the NSs protein into the characterization of novel phenuiviruses in order to estimate their virulence potential.

3.7 Concluding remarks and future perspectives

Phenuiviruses are globally emerging viruses that affect human health – directly or also indirectly by exacerbating the pathogenesis of simultaneous parasite infection – and impose significant economic burden. While some novel phenuiviruses are identified in clinically apparent cases, the major share of novel isolates is discovered by surveillance of vector species and their potential to cause disease unknown. The phenuiviral NSs protein is firmly established as dominant virulence factor in the mammalian host and antagonist of the IFN system, supported by the characterization of a growing number of NSs proteins of distinct phenuiviruses. So far, the characterization of NSs proteins has often been limited to whether and how they affect the induction of type I IFN. Only with the identification of SFTSV and HRTV (now Dabie and Heartland bandavirus) was the analysis expanded to also include IFN signalling [33, 158, 180]. In the light of the data on intermediately virulent SFSV presented here, we propose to systematically analyse NSs proteins for their inhibitory capacity towards both IFN induction and signalling. Likewise, it appears imperative for even mildly virulent phenuiviruses to override the translation-inhibitory effect of PKR. Thus, PKR sensitivity and/or PKR antagonistic activity should also feature in such a systematic analysis.

Furthermore, in addition to its IFN-antagonistic activities, the NSs of SFTSV (now Dabie bandavirus) actively triggers both the expression of the anti-inflammatory cytokine IL-10 (ref. 35 and **manuscript 6**) and immune-regulatory Nrf2 signalling [36], besides other emerging activities [114]. It might thus be time to consider NSs proteins as truly multifunctional (immune) regulatory proteins and explore other, unsuspected functions beyond IFN-antagonism. This endeavour will certainly be benefited by the rapid progress of unbiased *-omics* techniques and eventually expand our understanding of the diversity of NSs proteins and their contribution to virulence, provide novel targets for the development of host-directed antiviral therapy, and inform the design of novel attenuated and/or chimeric vaccine candidates.

Finally, solving the structure of the eIF2B-NSs complex and thus the molecular mechanism of ISR evasion by SFSV NSs not only informed the intricacies of this virus-host interaction, but additionally revealed a novel regulatory interaction site on eIF2B that is potentially druggable. Given the promising results of allosteric modulation of eIF2B by the small molecule ISRIB and its derivatives in models of traumatic brain injury, Down syndrome, and other brain dysfunctions [37, 41, 246] and the high efficiency of NSs over ISRIB in enzymatic activity assays, targeting the NSs interaction site on eIF2B might lead to improved therapeutic approaches for neuropathologic conditions. Thus, the comprehensive study of NSs functions holds the promise of not only identifying further as-yet elusive virulence mechanisms, but may also provide novel targets for rational drug design and targeted therapeutic interventions beyond infectious diseases.

4 Original peer-reviewed publications and manuscripts

4.1 Review article:

Phleboviruses and the Type I Interferon Response

Own contribution:

I contributed to writing and illustrating the manuscript.

_____

Jennifer Würth

viruses

MDPI

Review

Phleboviruses and the Type I Interferon Response

Jennifer Deborah Wuerth and Friedemann Weber *

Institute for Virology, FB10-Veterinary Medicine, Justus-Liebig University, Giessen 35392, Germany; wuerthje@staff.uni-marburg.de

* Correspondence: friedemann.weber@vetmed.uni-giessen.de; Tel.: +49-641-99-383-50

Academic Editors: Jane Tao and Pierre-Yves Lozach

Received: 8 May 2016; Accepted: 20 June 2016; Published: 22 June 2016

Abstract: The genus *Phlebovirus* of the family *Bunyaviridae* contains a number of emerging virus species which pose a threat to both human and animal health. Most prominent members include Rift Valley fever virus (RVFV), sandfly fever Naples virus (SFNV), sandfly fever Sicilian virus (SFSV), Toscana virus (TOSV), Punta Toro virus (PTV), and the two new members severe fever with thrombocytopenia syndrome virus (SFTSV) and Heartland virus (HRTV). The nonstructural protein NSs is well established as the main phleboviral virulence factor in the mammalian host. NSs acts as antagonist of the antiviral type I interferon (IFN) system. Recent progress in the elucidation of the molecular functions of a growing list of NSs proteins highlights the astonishing variety of strategies employed by phleboviruses to evade the IFN system.

Keywords: phlebovirus; NSs protein; interferon; RIG-I; PKR

1. Introduction

The family *Bunyaviridae* contains five genera, among which the *Orthobunyavirus*, *Phlebovirus*, *Nairovirus*, and *Hantavirus* all contain species that are pathogenic to humans and animals, while the genus *Tospovirus* contains plant-infecting viruses [1]. According to the International Committee on Taxonomy of Viruses (ICTV), the genus *Phlebovirus* comprises more than 70 accepted members that are grouped into ten species complexes, namely Bujaru virus (BUJV), Candiru virus (CDUV), Chilibre virus (CHIV), Frijoles virus (FRIV), Punta Toro virus (PTV), Rift Valley fever virus (RVFV), Salehabad virus (SALV), sandfly fever Naples virus (SFNV), severe fever with thrombocytopenia syndrome virus (SFTSV), and Uukuniemi virus (UUKV), as well as unassigned viruses [2]. Phleboviruses were traditionally classified by serologic methods, but recently extensive efforts were undertaken to refine phlebovirus taxonomy by genome sequencing [3–21].

Phleboviruses can cause a wide spectrum of symptoms, ranging from mild febrile disease up to hemorrhagic fever and death [22,23]. RVFV, for example, causes disease in cattle, sheep, and other ruminants, with symptoms including hepatitis, hemorrhage, and abortion [24]. Humans exposed to RVFV can present febrile illness, but in 1% to 2% of the cases it can progress to retinitis with persisting visual impairment, meningoencephalitis or hemorrhagic fever, resulting in mortality of up to 20% in hospitalized patients [25]. Since its original description during an outbreak of RVFV in ruminants in Kenya in 1931 [26], periodic outbreaks have been observed throughout the African continent, accompanied by so-called 'abortion storms' in livestock populations and simultaneously occurring illness in humans. Notably, RVFV has spread to the Arabian Peninsula in 2000 [27].

Sandfly fever Sicilian virus (SFSV) and SFNV were isolated from foreign soldiers stationed in Italy during 1943 and 1944. In spite of a full recovery after the so-called 'three-day' or 'Pappataci fever', the febrile illness provoked by SFSV and SFNV can be incapacitating due to headaches, myalgia, and general malaise [22]. The strongly neurotropic Toscana virus (TOSV) was also isolated in Italy first. It is the predominant cause of meningitis or meningoencephalitis during the summer season in countries

bordering the Mediterranean Sea [28]. Similarly to SFSV and SFNV, several phleboviruses in Central America have been isolated from febrile soldiers or patients, such as PTV, Chagres virus (CHGV), and Alenquer virus (ALEV) [17,29,30].

Despite their obvious capacity for causing human and veterinary disease, as well as potential associated economic losses, only few phleboviruses are adequately characterized in terms of their interaction with the mammalian host organism. In this review, we will attempt to provide an overview spanning both the current knowledge about the activation of the type I interferon (IFN) system by phleboviruses, as well as the broadening spectrum of their IFN-antagonistic strategies.

2. Phleboviruses—An Emerging Group of Arthropod-Transmitted Pathogens

Phleboviruses are arboviruses that are taxonomically divided into dipteran- and tick-borne viruses. Dipteran-borne phleboviruses are generally found in eponymous *Phlebotomus* sandflies [22,31], with RVFV representing an outlier that is associated with *Aedes* and *Culex* mosquitoes, and more promiscuous in its vector range. The specific vector species are thought to be predominantly responsible for the maintenance of the viruses by vertical (transovarial) transmission, the geographic distribution of the virus and the spatial and temporal occurrence of the specific disease. Given the increasing spread of competent vector species, concerns have been raised about the potential introduction of RVFV into new areas with both susceptible vectors and hosts, and potential consequences for the human population and massive economic loss caused among affected livestock [32,33].

The epidemiological potential of the phleboviruses has been underscored by the recent identification of two new members as the causative agents of severe human disease [23]. In rural regions of China, cumulative cases of a febrile illness accompanied by thrombocytopenia, leukocytopenia, multiple organ dysfunction, and a high case-fatality rate led to the discovery of a novel phlebovirus, SFTSV, transmitted by *Haemaphysalis longicornis* ticks [34–38]. Since its discovery, SFTSV and associated cases have also been reported from Japan and Korea [39–41]. In North America, nearly simultaneously-occurring cases of a similar set of symptoms were shown to be caused by a related, tick-transmitted phlebovirus termed Heartland virus (HRTV) [42,43]. Thus, while tick-borne phleboviruses were long thought to be negligible with respect to public health, the emergence of SFTSV and HRTV suggested that this perception needed reevaluation. As one result, the genome sequences of members of the Bhanja virus (BHAV) serogroup, which has been associated with febrile illness, were determined and re-classified into the tick-borne phlebovirus group [10,44].

Accumulating reports indicate novel associations of diseases with phleboviruses in the Mediterranean area, such as sandfly fever Turkey virus (SFTV) [45–47] and Adria virus (ADRV) [48], or describe still more novel phleboviruses, such as Granada virus (GRV) [49], Adana virus (ADAV) [3] and Medjerda Valley virus (MVV) [7], to name only a few examples.

3. Viral Replication in the Mammalian Host

Phleboviruses have spherical particles of approximately 100 nm diameter [23,50,51]. They are enveloped by a host-derived lipid membrane with the two viral glycoproteins Gn and Gc decorating the surface of the virus particle, and contain three distinct single-stranded RNA genome segments which are packaged into ribonucleoprotein particles (RNPs) by the nucleocapsid protein N and associated with the RNA-dependent RNA polymerase (RdRp) L (Figure 1A). The tripartite genome consists of the large (L), medium (M), and small (S) segments. The L and M segments are of negative polarity and code for the polymerase L and a polyprotein precursor spanning the two glycoproteins and the nonstructural protein NSm, respectively (Figure 1B). The S segment uses an ambisense coding strategy, *i.e.,* it contains two genes with opposite polarities. The nucleocapsid protein N is thereby translated from a mRNA that is directly transcribed from the genomic S segment, whereas the nonstructural protein NSs mRNA is transcribed from the antigenomic S segment. Gene expression from the ambisense segments is regulated by an intergenic region (IGR), a sequence stretch that is proposed to form an irregular double-stranded RNA (dsRNA) structure [24], and

by pentanucleotide transcription termination motifs [52–54]. The genome segments further contain conserved complementary oligonucleotide sequences at their 5′- and 3′-ends, allowing the formation of "panhandle" structures and the pseudocircularization of the RNPs [55].

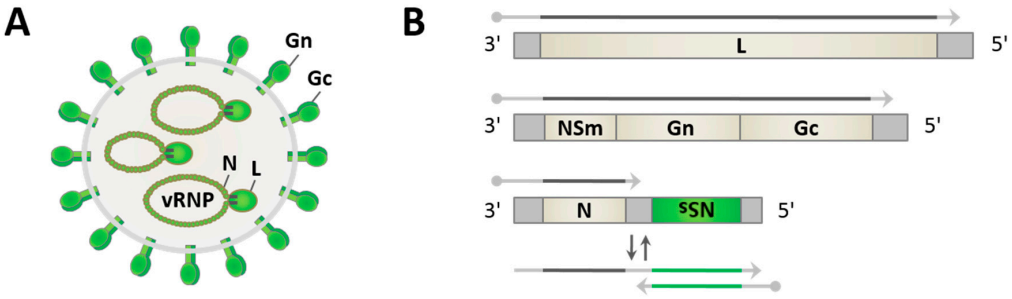

Figure 1. Prototypic phlebovirus virion and genome organization. (**A**) Virus particles contain the pseudocircularized tripartite single-stranded RNA genome, packaged into virus-sense RNPs (vRNPs) by nucleocapsid protein N and associated with the viral RNA-dependent RNA polymerase (RdRp) L, within a lipid envelope covered by heterodimers of glycoproteins Gn and Gc; and (**B**) the three viral genome segments large (L), medium (M) (both being purely negative-sense), and small (S) (ambisense) code for the structural proteins L, the Gn and Gc, and N, respectively. Viral mRNAs contain a 5′-cap (dot) and short heterogenous host-derived sequences. mRNAs transcribed from genomic RNAs are shown as grey arrows. The nonstructural protein NSs mRNA (green arrow) is synthesized from antigenomic RNA (two-colored arrow). Dipteran-borne phleboviruses also encode a nonstructural protein on the M segment (NSm).

Viral replication occurs entirely in the cytoplasm of infected mammalian host cells. Central features of the transmission from vector to host and the entry of phlebo- and other bunyaviruses has recently been reviewed elsewhere [56]. In short, after attachment of virus particles, uncoating is mediated by the fusion of the viral envelope with host membranes in the acidified compartments of the endocytic system [57,58]. Incoming RNPs then first serve as templates for primary transcription. To this end, the endonuclease domain [59,60] within the L protein cleaves host mRNAs 10–20 nucleotides downstream of the 5′-cap to use the resulting short fragments as primers for the synthesis of viral transcripts (cap snatching). Primary transcription is terminated prior to the segment termini via a specific sequence motif [52–54]. Phleboviral transcripts thus contain a 5′-cap and a short stretch of a heterogenous, host-derived sequence, but no poly(A) tail. Translation of viral proteins in the cytoplasm and at the endoplasmic reticulum (ER) is accompanied by cleavage of the polyprotein encoded by the M segment into Gn and Gc (and depending on the virus species, some other proteins e.g., NSm), heterodimerization of Gn and Gc, and their transport to the Golgi apparatus. For replication of the viral genome, the viral polymerase switches to primer-independent synthesis of full-length antigenomic RNA, which then, in turn, serves as a template for the synthesis of progeny genomic RNA. In a process called secondary transcription, these newly-generated genomes then produce even more viral mRNAs. Both the genomic and antigenomic RNA segments carry a 5′-triphosphate moiety and are packaged into RNPs. Assembly and budding finally take places at membranes of the Golgi apparatus, followed by release of virions via the secretory pathway.

The nonstructural proteins NSm and NSs are dispensable for viral replication [61–64]. sandfly-borne phleboviruses encode an NSm protein which may have a role in the regulation of apoptosis (as shown for RVFV [65]). The NSs protein is remarkable in its low conservation across the *Phlebovirus* genus compared to other viral proteins, with sequence similarities ranging only from approximately 10% to 30% [7,37]. As will be outlined below, the NSs protein is an important virulence determinant, acting as an inhibitor of the antiviral type I IFN system of the mammalian host [24,66,67].

4. The Type I Interferon System in RNA Virus Infection

Type I IFNs are cytokines that are produced by virus-infected cells [68]. In humans, there are thirteen IFN-α subtypes, a single IFN-β, and the less well-characterized IFN-ε, -τ, -κ, -ω, -δ, which activate the

transcription of hundreds of IFN-stimulated genes (ISGs) [68,69]. Characterization of an ever-increasing number of ISGs shows that many of their products not only exert antiviral activity at every step of the viral replication cycle, but also possess antiproliferative and immunomodulatory functions.

The production of type I IFN is induced in response to conserved pathogen-associated molecular patterns (PAMPs), which are sensed by germline-encoded, so-called pattern-recognition receptors (PRRs). As PRRs of the cytoplasm, the RNA helicases retinoic acid-inducible gene 1 (RIG-I) and melanoma differentiation-associated protein 5 (MDA5) react to infection by distinct sets of RNA viruses [70]. RIG-I and MDA5 primarily recognize short 5′-triphosphate dsRNA, or long (preferentially of higher-order structure) dsRNA and its analogue polyinosinic:polycytidylic acid (poly(I:C)), respectively [71–73]. The prototypical RIG-I possesses two N-terminal caspase recruitment domains (CARDs), a central helicase domain and a C-terminal domain, and is kept in an auto-inhibited conformation by intramolecular interactions involving the CARDs and the helicase domains. Ligand binding by the helicase and C-terminal domains induces both ATP-dependent RIG-I oligomerization and a conformational switch, resulting in the exposure of the CARDs [73,74]. The latter then engage in K63-polyubiquitin-mediated homotypic CARD-CARD interaction with the adaptor mitochondrial antiviral signaling (MAVS) which in turn assembles prion-like fibrillary aggregates that are sufficient and necessary for the recruitment of tumor necrosis factor (TNF) receptor associated factor (TRAF) 2, 5, and 6 for downstream signaling [75,76]. The kinases TRAF family member-associated nuclear factor kappa-light-chain-enhancer of activated B cells (NF-κB) activator (TANK)-binding kinase 1 (TBK1) and inhibitor of kappa B kinase epsilon (IKKε) subsequently activate the transcription factor IFN regulatory factor 3 (IRF3) by phosphorylation, followed by its dimerization and nuclear accumulation, where it activates the production of type I IFN expression together with the transcription factors nuclear factor kappa-light-chain-enhancer of activated B cells (NF-κB) and activator protein (AP-1) [73].

Within the endosomal compartments, Toll-like receptor 3 (TLR3) recognizes viral dsRNA and poly(I:C), and signals via the adaptor Toll-interleukin 1 receptor (TIR) domain-containing adapter-inducing IFN-β (TRIF) to activate IRF3, NF-κB, and AP-1, and consequently induce the production of type I IFNs as well as inflammatory cytokines [77]. Further, recognition of single-stranded RNA by TLR7/8 and subsequent signaling via the adaptor myeloid differentiation primary response gene 88 (MyD88) results in the secretion of IFN-α, particularly by specialized plasmacytoid dendritic cells [78].

IFN-α/β bind to a common heterodimeric receptor, consisting of the subunits interferon-α/β receptor IFNAR1 and IFNAR2, on both infected and uninfected bystander cells. Signaling via the receptor-associated tyrosine kinases Janus kinase 1 (JAK1) and tyrosine kinase 2 (TYK2) leads to phosphorylation of Signal Transducer and Activator of Transcription 1 (STAT1) and STAT2, which then undergo heterodimerization and translocation to the nucleus. There, in a complex with IRF9, they bind to IFN-stimulated response elements (ISRE) within ISG promoters, finally resulting in the transcription of ISGs [68,69].

As the functions of the well characterized ISGs have been reviewed extensively elsewhere [68,79], only a few examples of antiviral ISGs will be described here. IFN-inducible transmembrane (IFITM) proteins interfere with fusion of the viral envelope at the plasma membrane (IFITM1) or in the endosomal pathway (IFITM2, 3) and, thus, the release of viral RNPs into the cytoplasm of infected cells [80]. The family of dynamin-like Mx GTPases are capable of restricting a wide range of viruses, presumably via trapping and missorting of incoming viral RNPs [81]. In contrast to other ISGs, Mx proteins are not expressed at low constitutive levels or in response to virus infection, but depend entirely on IFN signaling, rendering the abrogation of IFN induction and signaling an effective means of evading Mx activity. Protein kinase R (PKR) is expressed at low levels in an inactive form [82]. Binding of dsRNA results in PKR activation, leading to phosphorylation of its target eukaryotic initiation factor 2α (eIF2α) and, in consequence, the inhibition of the translation of both viral and cellular mRNA. PKR has also been implicated in NF-κB activation and the induction of apoptosis [83]. Interferon-induced protein with tetratricopeptide repeats (IFIT) proteins IFIT1, 2 and 3 are involved in

translation inhibition and innate recognition of RNAs that lack proper 2′-*O* methylation or contain a 5′ ppp end [80,84].

Expression of the transcription factor IRF7 is also enhanced by IFN signaling. While the aforementioned activation of IRF3 leads to an initial wave of type I IFN secretion, including IFN-β and (in mice) IFN-α4, enhanced IRF7 expression and activation generates a second wave of type I IFN production which involves additional IFN-α subtypes [85].

In addition to direct antiviral effects of ISGs and the positive feedback loop via IRF7, type I IFN signaling also induces the production of a range of cytokines and chemokines, pro- and antiapoptotic factors, and affects multiple other signaling pathways. Through modulation of the differentiation and function of dendritic cells, T cells, natural killer (NK) cells, and B cells, type I IFNs shape the antiviral immune response beyond the initial innate immune response [68,79,86].

5. Activation of the Interferon System by Phleboviruses

Like other negative-strand RNA viruses, phleboviruses do not produce substantial amounts of dsRNA during infection [87,88]. As shown for RVFV, their naked virion RNA is, nonetheless, a strong activator of RIG-I due to the presence of the 5′-triphosphorylated dsRNA panhandle formed by the genome ends [89]. Moreover, also when packaged into RNPs, the RNA of RVFV particles can activate the RIG-I signaling pathway [90]. In fact, incoming RNPs already trigger RIG-I conformational switching and oligomerization, as well as IRF3 activation. Additionally, in vivo, the cytoplasmic RNA helicase/MAVS axis was demonstrated to be the primary IFN induction pathway for RVFV [91]. The *in vivo* role of TLRs, by contrast, is less clear. While Ermler et al. found for RVFV that neither the TLR7/8-MyD88 nor the TLR3-TRIF pathway play a significant role in IFN induction [91], Gowen *et al*. showed for PTV that TLR3 was activated and contributed to increased liver damage and mortality [92]. It remains to future studies to reveal whether these discrepancies are due to different experimental conditions or a differential ability of distinct phleboviruses to activate or inhibit TLR3.

Studies in a range of animal models suggested a protective effect of type I IFN in phleboviral infection. Treatment with synthetic type I IFN inducers, such as poly(I:C) or polyinosinic-polycytidylic acid, poly-L-lysine and carboxymethylcellulose (poly(ICLC)) in a prophylactic or therapeutic regimen was reported to protect mice and hamsters from lethal RVFV infection [93–95]. Similarly, administration of poly(I:C), poly(ICLC), or of IFN itself protect against PTV-induced liver damage and mortality in a mouse model [96–98], whereas treatment with IFN-neutralizing antibodies rendered otherwise resistant mice susceptible to PTV-associated death [99]. Several in vivo studies correlated the onset of type I IFN synthesis with increased survival after lethal RVFV challenge [100,101]. Lastly, mice deficient in IFN signaling are more prone to infections with RVFV and PTV [102,103]. Thus, induction of sufficient amounts of type I IFNs at an early point during infection is crucial for protective effects.

It is known that different viruses are targeted by distinct sets of ISGs [104,105]. Additionally, for phleboviruses, a number of inhibitory ISG products have been described (Table 1). Mx proteins drastically inhibit the replication of several phleboviruses, including RVFV, TOSV, and SFSV [106,107]. For human MxA it was shown that it sequesters RVFV N into large perinuclear complexes, thereby inhibiting primary and secondary transcription [108,109]. Replication of RVFV is also affected by IFITM2 and IFITM3, but not IFITM1, in accordance with their localization in the endocytic pathway and at the plasma membrane, respectively [110]. PKR is activated during phleboviral infection and can act as potent restriction factor [93,111]. Therefore, it is not surprising that PKR is targeted by different phleboviruses, as discussed below. Furthermore, IFIT proteins (mostly IFIT1 and IFIT2), long isoform of poly(ADP-ribose) polymerase 12 (PARP12L), 2'-5' oligoadenylate synthetase-like 2 (OASL2), and ISG15 influence the replication of RVFV [100,112,113]. The latter two ISGs are not upregulated in embryonic fibroblasts derived from a mouse strain with increased susceptibility to RVFV (MBT/Pas) and a generally decreased and delayed ISG response, compared to BALB/cByJ, C57BL/6J and 129/Sv/Pas mice. Small interfering RNA (siRNA)-mediated reduction of Oasl2 and ISG15, however, resulted in only slightly increased titers of recombinant NSs-deficient RVFV [100].

Table 1. Interferon (IFN)-induced proteins acting as restriction factors for phleboviruses.

ISG	Affected Step in Replication	Affected Phleboviruses (Strains)	References
IFITM2, 3	uncoating	RVFV (ZH501, MP12)	[110]
Mx	primary and secondary transcription	RVFV (MP12, Clone 13), TOSV, SFSV	[106–108]
OASL2	?	RVFV (rZH548ΔNSs)	[100]
PKR	viral protein translation	NSs-deficient RVFV mutants (e.g., Clone 13)	[93,111]
IFIT1-3	viral protein translation	RVFV (Clone 13)	[113]
mPARP12	?	RVFV (MP12)	[112]
ISG15	?	RVFV (rZH548ΔNSs)	[100]

ISG: IFN-stimulated genes; IFITM: IFN-inducible transmembrane; OASL2: 2′-5′ oligoadenylate synthetase-like 2; PKR: protein kinase R; IFIT: interferon-induced protein with tetratricopeptide repeats; mPARP12: murine poly(ADP-ribose) polymerase 12; RVFV: Rift Valley fever virus; TOSV: Toscana virus; SFSV: sandfly fever Sicilian virus.

6. Viral Countermeasures

As described above, phleboviruses are sensitive to IFN and an early induction of type I IFN seems to be a determinant of disease outcome in animal models. Furthermore, given the segmented nature of their genome, phleboviruses carry at least three RIG-I-activating moieties (5′ppp-dsRNA panhandle) per virus particle. Thus, in order to compensate for their stimulatory potential and to prevent or sufficiently delay a type I IFN response, they require highly efficient counterstrategies (Figure 2, Tables 2 and 3).

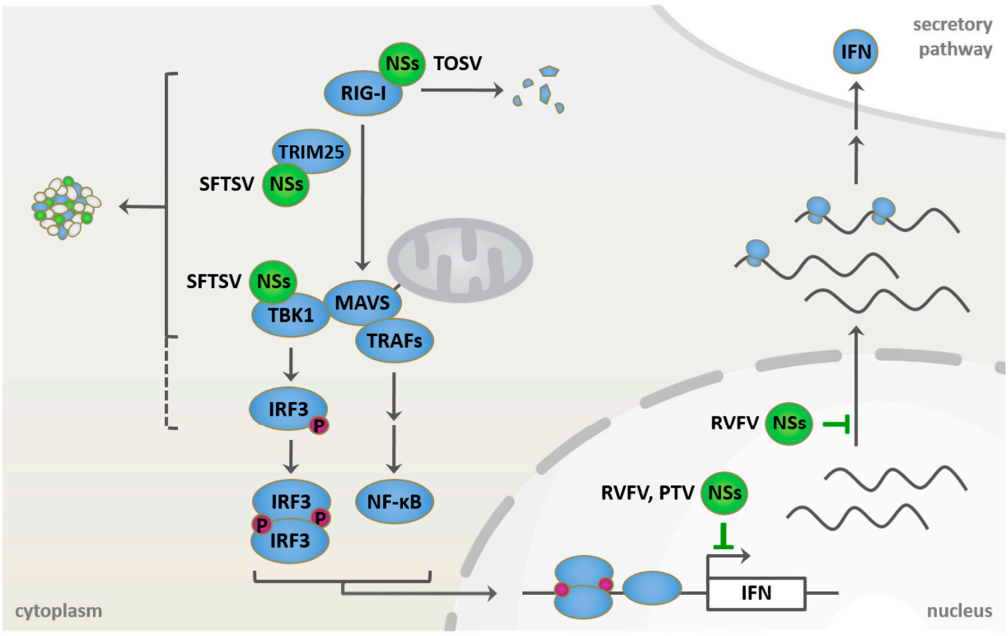

Figure 2. Known host targets of phleboviral NSs proteins in retinoic acid-inducible gene 1 (RIG-I) signaling and type I IFN induction. Incoming phleboviral RNPs are sensed by RIG-I, potentially leading to interferon induction via mitochondrial antiviral signaling (MAVS)-mediated activation of the transcription factors interferon regulatory factor 3 (IRF3) and nuclear factor kappa-light-chain-enhancer of activated B cells (NF-κB). NSs proteins, however, mediate the escape from the induction and the antiviral effects of the IFN system. Rift Valley fever virus (RVFV) NSs acts in the nucleus, where it blocks both the transcription and the export of host mRNAs. Toscana virus (TOSV) NSs localizes to the cytoplasm, where it interacts with and induces proteasomal degradation of RIG-I. Characteristic cytoplasmic structures are formed by severe fever with thrombocytopenia syndrome virus (SFTSV) NSs and serve as site of sequestration for several signaling factors of the RIG-I pathway. Punta Toro virus (PTV) NSs also inhibits host transcription.

The NSs protein of RVFV was the first to be identified as an IFN antagonist and still remains the most extensively studied phleboviral virulence factor. Comparative studies using the naturally-attenuated strain Clone 13 and the virulent RVFV isolate ZH548, as well as reassortants between these two viruses, showed that the S segment carries the determinant for attenuation and interference with IFN-α/β production in a murine model [102,114]. Since the S segment encodes the NSs and Clone 13 is a natural NSs deletion mutant, it was concluded that NSs confers an anti-IFN activity.

Although phleboviruses replicate exclusively in the cytoplasm, RVFV NSs is localized in the nucleus, forming characteristic filaments [115,116]. In contrast, Clone 13 contains a large in-frame deletion within the NSs open reading frame, resulting in a loss of 69% of the ORF [117]. Hence, Clone 13 NSs does not form nuclear filaments but instead is rapidly degraded [114]. The NSs of the RVFV wild-type strain ZH548 alone was then shown to almost completely block IFN-β promoter activation in response to poly(I:C), while Clone 13 NSs had no inhibitory effect [118]. Further, ZH548 did not affect IRF3 dimerization or nuclear accumulation, yet impaired IFN-β, NF-κB-driven, AP-1-driven, and even SV40 promoter activity, suggesting that RVFV NSs broadly inhibits both inducible and constitutive host cell transcription. Indeed, RVFV NSs targets the host mRNA synthesis machinery to induce a general cellular shutoff, including sequestration of general transcription factor II H (TFIIH) subunit p44 and, thus, prevention of TFIIH assembly [119]. In addition, NSs triggers the rapid proteasomal degradation of the TFIIH subunit p62 early in infection [120]. Proteomic analyses led to the identification of the F-box protein FBXO3 as host cell interactor of RVFV NSs [121]. F-box proteins are the substrate recognition component of modular E3 ubiquitin ligases of the Skp1, Cullin1, F-box (SCF) protein type [122], and FBXO3 was shown to be recruited by NSs to achieve TFIIH-p62 degradation [123]. The interaction with TFIIH-p62 thereby depends on a ΩXaV motif (where Ω: aromatic, X: any, a: acidic, V: valine) located in the C-terminal region of RVFV NSs [124]. Moreover, a nuclear mRNA export block was observed in RVFV NSs-expressing cells [125]. In contrast to these broadly-acting host cell shutoff mechanisms, RVFV NSs was also reported to specifically inhibit IFN induction by recruiting a transcriptional suppressor complex containing Sin3A associated protein 30 (SAP30) to the IFN-β promoter [126].

If not counteracted by viral measures, PKR has a strong restrictive effect on the replication of phleboviruses [93,111]. RVFV solves this problem by proteasomal degradation of PKR, thereby avoiding eIF2α phosphorylation and inhibition of translation [93,111]. Recent studies revealed that RVFV NSs recruits the F-box proteins FBXW11 and FBXW1 (also called beta-transducin repeat containing protein 1 (β-TRCP1)) as specific adaptors to mediate PKR degradation [127,128]. NSs thereby directly interacts with FBXW11/β-TRCP1 through a "degron" sequence [128]. Remarkably, this degron motif (DDGFVE) overlaps with the aforementioned ΩXaV motif (FVEV) necessary for TFIIH-p62 degradation, suggesting that RVFV NSs utilizes the very C-terminal part of the protein for the degradation of multiple host target factors, each time recruiting specific F-box proteins.

Infection of hamsters and mice with the PTV strain Adames is lethal, whereas PTV strain Balliet produces beneficial outcomes [103,129]. Reassortants between these two strains again identified the S segment genotype and NSs expression as correlates for lethality and suppression of type I IFN production [130]. Similar to RVFV, the NSs of PTV Adames has also been found to inhibit host transcription [131]. In contrast to RVFV NSs, however, PTV NSs does not form nuclear filaments or share the C-terminal ΩXaV motif of RVFV NSs [124]. A further difference between RVFV and PTV NSs is that the latter does not affect the levels of PKR [131,132].

In contrast to RVFV NSs, TOSV NSs localizes exclusively to the cytoplasm and does not affect cellular transcription [132,133], but inhibits IFN induction [134]. Instead, it has been shown to interact with RIG-I and trigger its proteasomal degradation [135]. Interestingly, binding of RIG-I and proteasomal degradation appear to be mediated by different regions of the NSs protein [136]. Also contrary to RVFV NSs, levels of TOSV NSs were found to be increased under MG132 treatment [132,135]. In line with this, C-terminally-truncated TOSV NSs mutants that were incapable

of degrading RIG-I, but still able to bind RIG-I, were also detected at higher levels than the full-length protein [136], allowing speculations that TOSV NSs might be degraded along with its host target.

Peculiarly, while TOSV NSs efficiently inhibited IRF3 activation and IFN induction when expressed via transfection or from a recombinant RVFV, infection with the parental Italian TOSV isolate resulted in IRF3 activation, IFN-β induction and Mx expression [134]. A Spanish isolate, by contrast, was a potent IFN suppressor as expected from NSs action [137]. This discrepancy might be attributable to strain-specific differences in the kinetics of NSs accumulation.

Like RVFV NSs, TOSV NSs has also been observed to induce degradation of PKR in a proteasome-dependent manner [131,132].

Additionally, the NSs protein of the intermediately-pathogenic sandfly-borne SFSV possesses the capacity for inhibiting type I IFN induction [93,131]. The levels of PKR, however, are not affected [93,131,132].

The recent identification of tick-borne SFTSV as human pathogenic phlebovirus was quickly followed by a number of reports concerning the anti-IFN mechanism employed by its NSs protein. Type I IFN and ISGs were only moderately induced in SFTSV-infected cells, as observed by microarray analysis [138]. Indeed, SFTSV NSs was identified by several groups as inhibitor of IFN-β promoter activity, presumably acting at the level of TBK1 and IKKε [138–141].

SFTSV NSs neither forms nuclear filaments, nor is it diffusely distributed in the cytoplasm as described for the NSs proteins of sandfly-borne phleboviruses. Instead, it is concentrated in unprecedented cytoplasmic structures of granular appearance after both infection and transfection of a wide range of cell lines. Although these 'viral inclusion bodies' or 'viroplasm-like structures' seem to be subject to dynamic fission and fusion [139] and were found to be positive for the autophagosome marker microtubule-associated protein 1A/1B-light chain 3 (LC3), their formation was independent of autophagy-related protein 7 (Atg7), suggesting that they are not classical autophagosomes [140]. The early endosome RAS-associated protein Rab5 showed co-localization, but neither its presence nor canonical function were required for the formation of NSs inclusion bodies. Further analysis ruled out an association with ER, Golgi, mitochondria, peroxisomes, EDEMosomes, lysosomes and late endosomes, as well as aggresomes [139,140]. Furthermore, the inclusion bodies appeared to co-localize with lipid droplets and their formation associated with fatty acid synthesis [142].

Despite the open questions concerning biochemical composition and compartmental identity of the SFTSV NSs inclusions, it has become clear that they represent a site of sequestration and spatial isolation of multiple components of the RIG-I signaling pathway [139–141]. While all studies agree on TBK1 (and IKKε, where tested) as host interactors of SFTSV NSs, individual studies reported additional interactions with tripartite motif-containing protein 25 (TRIM25) (an E3 ubiquitin ligase involved in RIG-I signaling [143]), RIG-I [140], and IRF3 [139,141]. Remarkably, SFTSV NSs also sequesters transcription factors STAT1 and STAT2 into the inclusion bodies and inhibits STAT2 phosphorylation, thus interfering with their nuclear translocation, the stimulation of the interferon-stimulated response element (ISRE) promoter and, consequently, the induction of ISGs [144].

The non-pathogenic UUKV is the prototype of tick-borne phleboviruses. Its NSs is distributed throughout the cytoplasm [145] and has only a weak IFN-antagonistic effect [146]. Currently, there are no reports concerning the IFN-inhibitory capacity or action of the NSs proteins of HRTV and BHAV, despite their association with human illness.

Given the ambisense coding strategy of the S segment, the NSs would be expected to be expressed only late, after production of viral antigenomic RNA. This would represent a considerable disadvantage for the virus and is contradictory to the NSs-mediated effects that occur early after infection. This contradiction is resolved by the observation that antigenomic RNA segments are packaged into virions in both dipteran-borne RVFV and tick-borne UUKV [145,147,148]. Thus, the respective NSs proteins are directly produced during primary transcription, despite being encoded on the antigenomic RNA.

Table 2. IFN-related host pathways targeted by diptera-borne phleboviruses.

Phlebovirus	Host Target	Mechanism	References
RVFV	TFIIH p44, XPB	sequestration	[119]
	TFIIH p62	proteasomal degradation by recruitment of a SKP1-FBXO3 E3-ubiquitin ligase complex	[120,123,124]
	SAP30	recruitment of suppressors to the IFN promoter	[126]
	mRNA export	unknown	[125]
	PKR	proteasomal degradation by recruitment of a SKP1-CUL1-FBXW11 E3 ligase complex	[93,111,127,128]
TOSV	RIG-I	proteasomal degradation	[134–136]
	PKR	proteasomal degradation	[132]
PTV	IFN induction	unknown	[131]
SFSV	IFN induction	unknown	[93,131]

PTV: Punta Toro virus; TFIIH: transcription factor II H; XPB: *xeroderma pigmentosum* type B; SAP30: Sin3A associated protein 30; RIG-I: retinoic acid-inducible gene 1.

Table 3. IFN-related host pathways targeted by tick-borne phleboviruses.

Phlebovirus	Host Target	Mechanism	References
SFTSV	RIG-I, TRIM25, TBK1/IKKε, IRF3	sequestration into cytoplasmic inclusion bodies	[138–141]
	STAT1, STAT2	sequestration into cytoplasmic inclusion bodies	[144]
UUKV	unknown	unknown	[146]

SFTSV: severe fever with thrombocytopenia syndrome virus; UUKV: Uukuniemi virus; TRIM: tripartite motif-containing protein; TBK1: (TANK)-binding kinase 1; IKKε: inhibitor of kappa B kinase epsilon; STAT: Signal Transducer and Activator of Transcription.

7. Conclusions and Future Directions

Phleboviruses are emerging arboviruses, causing human diseases ranging from mild febrile illness to severe cases of hemorrhagic fever or multiple organ dysfunction and death. Further, RVFV is associated with livestock epidemics and substantial economic losses. Within the genus *Phlebovirus*, the NSs protein is only weakly conserved in terms of its amino acid sequences or subcellular localization. Nevertheless, NSs proteins are highly conserved in their function as IFN antagonist, with their variety in sequence and localization being mirrored by a plethora of different molecular strategies. The diversity of IFN-antagonistic mechanisms of distinct phleboviruses tempts one to speculate whether a correlation between the NSs action and the degree of virulence exists.

Among sandfly-borne viruses, a common strategy of the more pathogenic members, such as RVFV and TOSV, seems the proteasomal degradation of host target factors that are involved in IFN induction or antiviral effector functions. Interestingly, while the NSs of the highly-virulent RVFV is not negatively affected, the NSs of intermediately pathogenic TOSV NSs seems to be susceptible to the proteasomal degradation machinery as well. For the highly pathogenic tick-borne virus SFTSV, the NSs protein sequesters a major fraction of the host factors involved in the RIG-I signaling pathway, as well as IFN signaling factors, into characteristic granular structures in the cytoplasm. This might suggest that broader action on multiple host cell functions, such as the general transcription block caused by RVFV or the deactivation of entire signaling chains, as seen for SFTSV, might be a correlate of increased phleboviral virulence.

Much of our current understanding of the functioning of the NSs protein has been achieved employing reverse genetics, such as the rMP12 and rZH548 rescue systems for the dipteran-borne RVFV [63,149–151], allowing the study of NSs-deficient mutants or chimeric viruses. Recently, reverse genetic systems were also established for the tick-borne phleboviruses UUKV and SFTSV [146,147].

It remains to future studies to further expand and specify the molecular characterization of the NSs proteins of both familiar and newly-emerging phleboviruses.

Acknowledgments: Our work is kindly supported by the SFB 1021 of the Deutsche Forschungsgemeinschaft (DFG) and by the Infect-ERA grant "ESCential" by the Bundesministerium für Bildung und Forschung (BMBF).

Conflicts of Interest: The authors declare no conflict of interest.

References

1. Walter, C.T.; Barr, J.N. Recent advances in the molecular and cellular biology of bunyaviruses. *J. Gen. Virol.* **2011**, *92*, 2467–2484. [CrossRef] [PubMed]
2. International Committee on Taxonomy of Viruses. Phleboviruses. Available online: http://ictvonline.org/virusTaxonomy.asp?version=2012 (accessed on 15 July 2012).
3. Alkan, C.; Alwassouf, S.; Piorkowski, G.; Bichaud, L.; Tezcan, S.; Dincer, E.; Ergunay, K.; Ozbel, Y.; Alten, B.; de Lamballerie, X.; *et al.* Isolation, genetic characterization, and seroprevalence of Adana virus, a novel phlebovirus belonging to the Salehabad virus complex, in Turkey. *J. Virol.* **2015**, *89*, 4080–4091. [CrossRef] [PubMed]
4. Alkan, C.; Kasap, O.E.; Alten, B.; de Lamballerie, X.; Charrel, R.N. Sandfly-borne phlebovirus isolations from Turkey: New insight into the sandfly fever Sicilian and sandfly fever Naples species. *PLoS Negl. Trop. Dis.* **2016**, *10*, e0004519. [CrossRef] [PubMed]
5. Amaro, F.; Hanke, D.; Ze-Ze, L.; Alves, M.J.; Becker, S.C.; Hoper, D. Genetic characterization of Arrabida virus, a novel phlebovirus isolated in South Portugal. *Virus Res.* **2016**, *214*, 19–25. [CrossRef] [PubMed]
6. Amaro, F.; Ze-Ze, L.; Alves, M.J.; Borstler, J.; Clos, J.; Lorenzen, S.; Becker, S.C.; Schmidt-Chanasit, J.; Cadar, D. Co-circulation of a novel phlebovirus and Massilia virus in sandflies, Portugal. *Virol. J.* **2015**, *12*, 174. [CrossRef] [PubMed]
7. Bichaud, L.; Dachraoui, K.; Alwassouf, S.; Alkan, C.; Mensi, M.; Piorkowski, G.; Sakhria, S.; Seston, M.; Fares, W.; de Lamballerie, X.; *et al.* Isolation, full genomic characterization and neutralization-based human seroprevalence of Medjerda Valley virus, a novel sandfly-borne phlebovirus belonging to the Salehabad virus complex in northern Tunisia. *J. Gen. Virol.* **2016**, *97*, 602–610. [CrossRef] [PubMed]
8. Charrel, R.N.; Moureau, G.; Temmam, S.; Izri, A.; Marty, P.; Parola, P.; da Rosa, A.T.; Tesh, R.B.; de Lamballerie, X. Massilia virus, a novel *Phlebovirus* (Bunyaviridae) isolated from sandflies in the Mediterranean. *Vector Borne Zoonotic Dis.* **2009**, *9*, 519–530. [CrossRef] [PubMed]
9. Dachraoui, K.; Fares, W.; Bichaud, L.; Barhoumi, W.; Beier, J.C.; Derbali, M.; Cherni, S.; Lamballerie, X.; Chelbi, I.; Charrel, R.N.; *et al.* Phleboviruses associated with sand flies in arid bio-geographical areas of Central Tunisia. *Acta Trop.* **2016**, *158*, 13–19. [CrossRef] [PubMed]
10. Matsuno, K.; Weisend, C.; Travassos da Rosa, A.P.; Anzick, S.L.; Dahlstrom, E.; Porcella, S.F.; Dorward, D.W.; Yu, X.J.; Tesh, R.B.; Ebihara, H. Characterization of the Bhanja serogroup viruses (Bunyaviridae): A novel species of the genus *Phlebovirus* and its relationship with other emerging tick-borne phleboviruses. *J. Virol.* **2013**, *87*, 3719–3728. [CrossRef] [PubMed]
11. Matsuno, K.; Weisend, C.; Kajihara, M.; Matysiak, C.; Williamson, B.N.; Simuunza, M.; Mweene, A.S.; Takada, A.; Tesh, R.B.; Ebihara, H. Comprehensive molecular detection of tick-borne phleboviruses leads to the retrospective identification of taxonomically unassigned bunyaviruses and the discovery of a novel member of the genus phlebovirus. *J. Virol.* **2015**, *89*, 594–604. [CrossRef] [PubMed]
12. Palacios, G.; da Rosa, A.T.; Savji, N.; Sze, W.; Wick, I.; Guzman, H.; Hutchison, S.; Tesh, R.; Lipkin, W.I. Aguacate virus, a new antigenic complex of the genus *Phlebovirus* (family Bunyaviridae). *J. Gen. Virol.* **2011**, *92*, 1445–1453. [CrossRef] [PubMed]
13. Palacios, G.; Tesh, R.; Travassos da Rosa, A.; Savji, N.; Sze, W.; Jain, K.; Serge, R.; Guzman, H.; Guevara, C.; Nunes, M.R.; *et al.* Characterization of the Candiru antigenic complex (Bunyaviridae: *Phlebovirus*), a highly diverse and reassorting group of viruses affecting humans in tropical America. *J. Virol.* **2011**, *85*, 3811–3820. [CrossRef] [PubMed]
14. Palacios, G.; Savji, N.; Travassos da Rosa, A.; Desai, A.; Sanchez-Seco, M.P.; Guzman, H.; Lipkin, W.I.; Tesh, R. Characterization of the Salehabad virus species complex of the genus *Phlebovirus* (Bunyaviridae). *J. Gen. Virol.* **2013**, *94*, 837–842. [CrossRef] [PubMed]

15. Palacios, G.; Savji, N.; Travassos da Rosa, A.; Guzman, H.; Yu, X.; Desai, A.; Rosen, G.E.; Hutchison, S.; Lipkin, W.I.; *et al.* Characterization of the Uukuniemi virus group (*Phlebovirus*: Bunyaviridae): Evidence for seven distinct species. *J. Virol.* **2013**, *87*, 3187–3195. [CrossRef] [PubMed]
16. Palacios, G.; Tesh, R.B.; Savji, N.; Travassos da Rosa, A.P.; Guzman, H.; Bussetti, A.V.; Desai, A.; Ladner, J.; Sanchez-Seco, M.; Lipkin, W.I. Characterization of the sandfly fever Naples species complex and description of a new Karimabad species complex (genus *Phlebovirus*, family Bunyaviridae). *J. Gen. Virol.* **2014**, *95*, 292–300. [CrossRef] [PubMed]
17. Palacios, G.; Wiley, M.R.; Travassos da Rosa, A.P.; Guzman, H.; Quiroz, E.; Savji, N.; Carrera, J.P.; Bussetti, A.V.; Ladner, J.T.; Lipkin, W.I.; *et al.* Characterization of the Punta Toro species complex (genus *Phlebovirus*, family Bunyaviridae). *J. Gen. Virol.* **2015**, *96*, 2079–2085. [CrossRef] [PubMed]
18. Remoli, M.E.; Fortuna, C.; Marchi, A.; Bucci, P.; Argentini, C.; Bongiorno, G.; Maroli, M.; Gradoni, L.; Gramiccia, M.; Ciufolini, M.G. Viral isolates of a novel putative phlebovirus in the Marche Region of Italy. *Am. J. Trop. Med. Hyg.* **2014**, *90*, 760–763. [CrossRef] [PubMed]
19. Xu, F.; Chen, H.; Travassos, A.P.; Tesh, R.B.; Xiao, S.Y. Phylogenetic relationships among sandfly fever group viruses (*Phlebovirus*: Bunyaviridae) based on the small genome segment. *J. Gen. Virol.* **2007**, *88*, 2312–2319. [CrossRef] [PubMed]
20. Zhao, G.Y.; Krishnamurthy, S.; Cai, Z.Q.; Popov, V.L.; da Rosa, A.P.T.; Guzman, H.; Cao, S.; Virgin, H.W.; Tesh, R.B.; Wang, D. Identification of novel viruses using VirusHunter—An automated data analysis pipeline. *PLoS ONE* **2013**, *8*, e78470. [CrossRef] [PubMed]
21. Zhioua, E.; Moureau, G.; Chelbi, I.; Ninove, L.; Bichaud, L.; Derbali, M.; Champs, M.; Cherni, S.; Salez, N.; Cook, S.; *et al.* Punique virus, a novel phlebovirus, related to sandfly fever Naples virus, isolated from sandflies collected in Tunisia. *J. Gen. Virol.* **2010**, *91*, 1275–1283. [CrossRef] [PubMed]
22. Alkan, C.; Bichaud, L.; de Lamballerie, X.; Alten, B.; Gould, E.A.; Charrel, R.N. Sandfly-borne phleboviruses of Eurasia and Africa: Epidemiology, genetic diversity, geographic range, control measures. *Antivir. Res.* **2013**, *100*, 54–74. [CrossRef] [PubMed]
23. Elliott, R.M.; Brennan, B. Emerging phleboviruses. *Curr. Opin. Virol.* **2014**, *5*, 50–57. [CrossRef] [PubMed]
24. Boshra, H.; Lorenzo, G.; Busquets, N.; Brun, A. Rift Valley fever: Recent insights into pathogenesis and prevention. *J. Virol.* **2011**, *85*, 6098–6105. [CrossRef] [PubMed]
25. Bird, B.H.; Ksiazek, T.G.; Nichol, S.T.; Maclachlan, N.J. Rift Valley fever virus. *J. Am. Vet. Med. Assoc.* **2009**, *234*, 883–893. [CrossRef] [PubMed]
26. Daubney, R.; Hudson, J.R.; Garnham, P.C. Enzootic hepatitis or Rift Valley fever. An undescribed virus disease of sheep cattle and man from East Africa. *J. Pathol. Bacteriol.* **1931**, *34*, 545–579. [CrossRef]
27. Arishi, H.; Ageel, A.; Rahman, M.A.; Hazmi, A.A.; Arishi, A.R.; Ayoola, B.; Menon, C.; Ashraf, J.; Frogusin, O.; Sawwan, F.; *et al.* Outbreak of Rift Valley fever—Saudi Arabia, August-October, 2000. *MMMW Rep.* **2000**, *49*, 905–908.
28. Charrel, R.N.; Bichaud, L.; de Lamballerie, X. Emergence of Toscana virus in the mediterranean area. *World J. Virol.* **2012**, *1*, 135–141. [CrossRef] [PubMed]
29. Srihongse, S.; Johnson, C.M. Human infections with Chagres virus in Panama. *Am. J. Trop. Med. Hyg.* **1974**, *23*, 690–693. [PubMed]
30. Travassos da Rosa, A.P.; Tesh, R.B.; Pinheiro, F.P.; Travassos da Rosa, J.F.; Peterson, N.E. Characterization of eight new phlebotomus fever serogroup arboviruses (Bunyaviridae: *Phlebovirus*) from the Amazon region of Brazil. *Am. J. Trop. Med. Hyg.* **1983**, *32*, 1164–1171. [PubMed]
31. Tesh, R.B. The genus Phlebovirus and its vectors. *Annu. Rev. Entomol.* **1988**, *33*, 169–181. [CrossRef] [PubMed]
32. Rolin, A.I.; Berrang-Ford, L.; Kulkarni, M.A. The risk of Rift Valley fever virus introduction and establishment in the United States and European Union. *Emerg. Microbes Infect.* **2013**, *2*, e81. [CrossRef] [PubMed]
33. Salman, M. Is the United States really at risk for introduction of Rift Valley fever virus? *J. Am. Vet. Med. Assoc.* **2013**, *242*, 606–608. [CrossRef] [PubMed]
34. Huang, X.; Liu, L.; Du, Y.; Ma, H.; Mu, Y.; Tang, X.; Wang, H.; Kang, K.; Zhang, S.; Wu, W.; *et al.* Detection of a novel bunyavirus associated with fever, thrombocytopenia and leukopenia syndrome in Henan Province, China, using real-time reverse transcription PCR. *J. Med. Microbiol.* **2013**, *62*, 1060–1064. [CrossRef] [PubMed]

35. Luo, L.M.; Zhao, L.; Wen, H.L.; Zhang, Z.T.; Liu, J.W.; Fang, L.Z.; Xue, Z.F.; Ma, D.Q.; Zhang, X.S.; Ding, S.J.; *et al.* Haemaphysalis longicornis ticks as reservoir and vector of severe fever with thrombocytopenia syndrome virus in China. *Emerg. Infect. Dis.* **2015**, *21*, 1770–1776. [CrossRef] [PubMed]
36. Xu, B.; Liu, L.; Huang, X.; Ma, H.; Zhang, Y.; Du, Y.; Wang, P.; Tang, X.; Wang, H.; Kang, K.; *et al.* Metagenomic analysis of fever, thrombocytopenia and leukopenia syndrome (FTLS) in Henan Province, China: Discovery of a new bunyavirus. *PLoS Pathog.* **2011**, *7*, e1002369. [CrossRef] [PubMed]
37. Yu, X.J.; Liang, M.F.; Zhang, S.Y.; Liu, Y.; Li, J.D.; Sun, Y.L.; Zhang, L.; Zhang, Q.F.; Popov, V.L.; Li, C.; *et al.* Fever with thrombocytopenia associated with a novel bunyavirus in China. *N. Engl. J. Med.* **2011**, *364*, 1523–1532. [CrossRef] [PubMed]
38. Zhang, Y.Z.; Zhou, D.J.; Qin, X.C.; Tian, J.H.; Xiong, Y.; Wang, J.B.; Chen, X.P.; Gao, D.Y.; He, Y.W.; Jin, D.; *et al.* The ecology, genetic diversity, and phylogeny of Huaiyangshan virus in China. *J. Virol.* **2012**, *86*, 2864–2868. [CrossRef] [PubMed]
39. Kim, K.H.; Yi, J.; Kim, G.; Choi, S.J.; Jun, K.I.; Kim, N.H.; Choe, P.G.; Kim, N.J.; Lee, J.K.; Oh, M.D. Severe fever with thrombocytopenia syndrome, South Korea, 2012. *Emerg. Infect. Dis.* **2013**, *19*, 1892–1894. [CrossRef] [PubMed]
40. Park, S.W.; Han, M.G.; Yun, S.M.; Park, C.; Lee, W.J.; Ryou, J. Severe Fever with thrombocytopenia syndrome virus, South Korea, 2013. *Emerg. Infect. Dis.* **2014**, *20*, 1880–1882. [CrossRef] [PubMed]
41. Takahashi, T.; Maeda, K.; Suzuki, T.; Ishido, A.; Shigeoka, T.; Tominaga, T.; Kamei, T.; Honda, M.; Ninomiya, D.; Sakai, T.; *et al.* The First Identification and retrospective study of severe fever with thrombocytopenia syndrome in Japan. *J. Infect. Dis.* **2014**, *209*, 816–827. [CrossRef] [PubMed]
42. McMullan, L.K.; Folk, S.M.; Kelly, A.J.; MacNeil, A.; Goldsmith, C.S.; Metcalfe, M.G.; Batten, B.C.; Albarino, C.G.; Zaki, S.R.; Rollin, P.E.; *et al.* A New phlebovirus associated with severe febrile illness in Missouri. *N. Engl. J. Med.* **2012**, *367*, 834–841. [CrossRef] [PubMed]
43. Savage, H.M.; Godsey, M.S.; Lambert, A.; Panella, N.A.; Burkhalter, K.L.; Harmon, J.R.; Lash, R.R.; Ashley, D.C.; Nicholson, W.L. First detection of Heartland virus (Bunyaviridae: *Phlebovirus*) from ffield collected arthropods. *Am. J. Trop. Med. Hyg.* **2013**, *89*, 445–452. [CrossRef] [PubMed]
44. Dilcher, M.; Alves, M.J.; Finkeisen, D.; Hufert, F.; Weidmann, M. Genetic characterization of Bhanja virus and Palma virus, two tick-borne phleboviruses. *Virus Genes* **2012**, *45*, 311–315. [CrossRef] [PubMed]
45. Carhan, A.; Uyar, Y.; Ozkaya, E.; Ertek, M.; Dobler, G.; Dilcher, M.; Wang, Y.; Spiegel, M.; Hufert, F.; Weidmann, M. Characterization of a sandfly fever Sicilian virus isolated during a sandfly fever epidemic in Turkey. *J. Clin. Virol. Off. Publ. Pan Am. Soc. Clin. Virol.* **2010**, *48*, 264–269. [CrossRef] [PubMed]
46. Ergunay, K.; Ismayilova, V.; Colpak, I.A.; Kansu, T.; Us, D. A case of central nervous system infection due to a novel sandfly fever virus (SFV) variant: Sandfly fever Turkey virus (SFTV). *J. Clin. Virol.* **2012**, *54*, 79–82. [CrossRef] [PubMed]
47. Kocak Tufan, Z.; Weidmann, M.; Bulut, C.; Kinikli, S.; Hufert, F.T.; Dobler, G.; Demiroz, A.P. Clinical and laboratory findings of a sandfly fever Turkey virus outbreak in Ankara. *J. Infect.* **2011**, *63*, 375–381. [CrossRef] [PubMed]
48. Anagnostou, V.; Pardalos, G.; Athanasiou-Metaxa, M.; Papa, A. Novel phlebovirus in febrile child, Greece. *Emerg. Infect. Dis.* **2011**, *17*, 940–941. [CrossRef] [PubMed]
49. Collao, X.; Palacios, G.; de Ory, F.; Sanbonmatsu, S.; Perez-Ruiz, M.; Navarro, J.M.; Molina, R.; Hutchison, S.K.; Lipkin, W.I.; Tenorio, A.; *et al.* Granada Virus: A natural phlebovirus reassortant of the sandfly fever Naples serocomplex with low seroprevalence in humans. *Am. J. Trop. Med. Hyg.* **2010**, *83*, 760–765. [CrossRef] [PubMed]
50. Huiskonen, J.T.; Overby, A.K.; Weber, F.; Grunewald, K. Electron cryo-microscopy and single-particle averaging of Rift Valley fever virus: Evidence for Gn-Gc glycoprotein heterodimers. *J. Virol.* **2009**, *83*, 3762–3769. [CrossRef] [PubMed]
51. Overby, A.K.; Pettersson, R.F.; Grunewald, K.; Huiskonen, J.T. Insights into bunyavirus architecture from electron cryotomography of Uukuniemi virus. *Proc. Natl. Acad. Sci. USA* **2008**, *105*, 2375–2379. [CrossRef] [PubMed]
52. Albarino, C.G.; Bird, B.H.; Nichol, S.T. A shared transcription termination signal on negative and ambisense RNA genome segments of Rift Valley fever, sandfly fever Sicilian, and Toscana viruses. *J. Virol.* **2007**, *81*, 5246–5256. [CrossRef] [PubMed]

53. Ikegami, T.; Won, S.; Peters, C.J.; Makino, S. Characterization of Rift Valley fever virus transcriptional terminations. *J. Virol.* **2007**, *81*, 8421–8438. [CrossRef] [PubMed]
54. Lara, E.; Billecocq, A.; Leger, P.; Bouloy, M. Characterization of wild-type and alternate transcription termination signals in the Rift Valley fever virus genome. *J. Virol.* **2011**, *85*, 12134–12145. [CrossRef] [PubMed]
55. Hewlett, M.J.; Pettersson, R.F.; Baltimore, D. Circular forms of Uukuniemi virion RNA: an electron microscopic study. *J. Virol.* **1977**, *21*, 1085–1093. [PubMed]
56. Leger, P.; Lozach, P.Y. Bunyaviruses: From transmission by arthropods to virus entry into the mammalian host first-target cells. *Future Virol.* **2015**, *10*, 859–881. [CrossRef]
57. Lozach, P.Y.; Mancini, R.; Bitto, D.; Meier, R.; Oestereich, L.; Overby, A.K.; Pettersson, R.F.; Helenius, A. Entry of bunyaviruses into mammalian cells. *Cell Host Microbe* **2010**, *7*, 488–499. [CrossRef] [PubMed]
58. Lozach, P.Y.; Kuhbacher, A.; Meier, R.; Mancini, R.; Bitto, D.; Bouloy, M.; Helenius, A. DC-SIGN as a receptor for phleboviruses. *Cell Host Microbe* **2011**, *10*, 75–88. [CrossRef] [PubMed]
59. Klemm, C.; Reguera, J.; Cusack, S.; Zielecki, F.; Kochs, G.; Weber, F. Systems To establish bunyavirus genome replication in the absence of transcription. *J. Virol.* **2013**, *87*, 8205–8212. [CrossRef] [PubMed]
60. Morin, B.; Coutard, B.; Lelke, M.; Ferron, F.; Kerber, R.; Jamal, S.; Frangeul, A.; Baronti, C.; Charrel, R.; de Lamballerie, X.; *et al.* The N-terminal domain of the Arenavirus L protein is an RNA endonuclease essential in mRNA transcription. *PLoS Pathog.* **2010**, *6*, 8990–8995. [CrossRef] [PubMed]
61. Bird, B.H.; Albarino, C.G.; Hartman, A.L.; Erickson, B.R.; Ksiazek, T.G.; Nichol, S.T. Rift Valley fever virus lacking the NSs and NSm genes is highly attenuated, confers protective immunity from virulent virus challenge, and allows for differential identification of infected and vaccinated animals. *J. Virol.* **2008**, *82*, 2681–2691. [CrossRef] [PubMed]
62. Bird, B.H.; Maartens, L.H.; Campbell, S.; Erasmus, B.J.; Erickson, B.R.; Dodd, K.A.; Spiropoulou, C.F.; Cannon, D.; Drew, C.P.; Knust, B.; *et al.* Rift Valley fever virus vaccine lacking the NSs and NSm genes is safe, nonteratogenic, and confers protection from viremia, pyrexia, and abortion following challenge in adult and pregnant sheep. *J. Virol.* **2011**, *85*, 12901–12909. [CrossRef] [PubMed]
63. Gerrard, S.R.; Bird, B.H.; Albarino, C.G.; Nichol, S.T. The NSm proteins of Rift Valley fever virus are dispensable for maturation, replication and infection. *Virology* **2007**, *359*, 459–465. [CrossRef] [PubMed]
64. Won, S.; Ikegami, T.; Peters, C.J.; Makino, S. NSm and 78-kilodalton proteins of Rift Valley fever virus are nonessential for viral replication in cell culture. *J. Virol.* **2006**, *80*, 8274–8278. [CrossRef] [PubMed]
65. Won, S.Y.; Ikegami, T.; Peters, C.J.; Makino, S. NSm protein of Rift Valley fever virus suppresses virus-induced apoptosis. *J. Virol.* **2007**, *81*, 13335–13345. [CrossRef] [PubMed]
66. Weber, M.; Weber, F. Segmented negative-strand RNA viruses and RIG-I: Divide (your genome) and rule. *Curr. Opin. Microbiol.* **2014**, *20*, 96–102. [CrossRef] [PubMed]
67. Weber, M.; Weber, F. RIG-I-like receptors and negative-strand RNA viruses: RLRly bird catches some worms. *Cytokine Growth Factor Rev.* **2014**, *25*, 621–628. [CrossRef] [PubMed]
68. Schneider, W.M.; Chevillotte, M.D.; Rice, C.M. Interferon-stimulated genes: A complex web of host defenses. *Annu. Rev. Immunol.* **2014**, *32*, 513–545. [CrossRef] [PubMed]
69. Ng, C.T.; Mendoza, J.L.; Garcia, K.C.; Oldstone, M.B. Alpha and beta type 1 interferon signaling: Passage for diverse biologic outcomes. *Cell* **2016**, *164*, 349–352. [CrossRef] [PubMed]
70. Kato, H.; Takeuchi, O.; Sato, S.; Yoneyama, M.; Yamamoto, M.; Matsui, K.; Uematsu, S.; Jung, A.; Kawai, T.; Ishii, K.J.; *et al.* Differential roles of MDA5 and RIG-I helicases in the recognition of RNA viruses. *Nature* **2006**, *441*, 101–105. [CrossRef] [PubMed]
71. Pichlmair, A.; Schulz, O.; Tan, C.P.; Rehwinkel, J.; Kato, H.; Takeuchi, O.; Akira, S.; Way, M.; Schiavo, G.; Sousa, C.R.E. Activation of MDA5 requires higher-order RNA structures generated during virus infection. *J. Virol.* **2009**, *83*, 10761–10769. [CrossRef] [PubMed]
72. Schlee, M. Master sensors of pathogenic RNA—RIG-I like receptors. *Immunobiology* **2013**, *218*, 1322–1335. [CrossRef] [PubMed]
73. Yoneyama, M.; Onomoto, K.; Jogi, M.; Akaboshi, T.; Fujita, T. Viral RNA detection by RIG-I-like receptors. *Curr. Opin. Immunol.* **2015**, *32*, 48–53. [CrossRef] [PubMed]
74. Sparrer, K.M.; Gack, M.U. Intracellular detection of viral nucleic acids. *Curr. Opin. Microbiol.* **2015**, *26*, 1–9. [CrossRef] [PubMed]

75. Davis, M.E.; Gack, M.U. Ubiquitination in the antiviral immune response. *Virology* **2015**, *479–480*, 52–65. [CrossRef] [PubMed]
76. Liu, S.; Chen, J.; Cai, X.; Wu, J.; Chen, X.; Wu, Y.T.; Sun, L.; Chen, Z.J. MAVS recruits multiple ubiquitin E3 ligases to activate antiviral signaling cascades. *eLife* **2013**, *2*, e00785. [CrossRef] [PubMed]
77. Mogensen, T.H. Pathogen recognition and inflammatory signaling in innate immune defenses. *Clin. Microbiol. Rev.* **2009**, *22*, 240–273. [CrossRef] [PubMed]
78. Goubau, D.; Deddouche, S.; Sousa, C.R.E. Cytosolic Sensing of Viruses. *Immunity* **2013**, *38*, 855–869. [CrossRef] [PubMed]
79. MacMicking, J.D. Interferon-inducible effector mechanisms in cell-autonomous immunity. *Nat. Rev. Immunol.* **2012**, *12*, 367–82. [CrossRef] [PubMed]
80. Diamond, M.S.; Farzan, M. The broad-spectrum antiviral functions of IFIT and IFITM proteins. *Nat. Rev. Immunol.* **2013**, *13*, 46–57. [CrossRef] [PubMed]
81. Haller, O.; Staeheli, P.; Schwemmle, M.; Kochs, G. Mx GTPases: Dynamin-like antiviral machines of innate immunity. *Trends Microbiol.* **2015**, *23*, 154–163. [CrossRef] [PubMed]
82. Garcia, M.A.; Gil, J.; Ventoso, I.; Guerra, S.; Domingo, E.; Rivas, C.; Esteban, M. Impact of protein kinase PKR in cell biology: From antiviral to antiproliferative action. *Microbiol. Mol. Biol. Rev. MMBR* **2006**, *70*, 1032–1060. [CrossRef] [PubMed]
83. Gil, J.; Garcia, M.A.; Gomez-Puertas, P.; Guerra, S.; Rullas, J.; Nakano, H.; Alcami, J.; Esteban, M. TRAF family proteins link PKR with NF-kappa B activation. *Mol. Cell. Biol.* **2004**, *24*, 4502–4512. [CrossRef] [PubMed]
84. Fensterl, V.; Sen, G.C. Interferon-induced IFIT Proteins: Their role in viral pathogenesis. *J. Virol.* **2015**, *89*, 2462–2468. [CrossRef] [PubMed]
85. Levy, D.E.; Marie, I.; Smith, E.; Prakash, A. Enhancement and diversification of IFN induction by IRF-7-mediated positive feedback. *J. Interferon Cytokine Res.* **2002**, *22*, 87–93. [CrossRef] [PubMed]
86. McNab, F.; Mayer-Barber, K.; Sher, A.; Wack, A.; O'Garra, A. Type I interferons in infectious disease. *Nat. Rev. Immunol.* **2015**, *15*, 87–103. [CrossRef] [PubMed]
87. Weber, F.; Wagner, V.; Rasmussen, S.B.; Hartmann, R.; Paludan, S.R. Double-stranded RNA is produced by positive-strand RNA viruses and DNA viruses but not in detectable amounts by negative-strand RNA viruses. *J. Virol.* **2006**, *80*, 5059–5064. [CrossRef] [PubMed]
88. Zielecki, F.; Weber, M.; Eickmann, M.; Spiegelberg, L.; Zaki, A.M.; Matrosovich, M.; Becker, S.; Weber, F. Human cell tropism and innate immune system interactions of human respiratory coronavirus EMC compared to those of severe acute respiratory syndrome coronavirus. *J. Virol.* **2013**, *87*, 5300–5304. [CrossRef] [PubMed]
89. Habjan, M.; Andersson, I.; Klingstrom, J.; Schumann, M.; Martin, A.; Zimmermann, P.; Wagner, V.; Pichlmair, A.; Schneider, U.; Muhlberger, E.; *et al.* Processing of genome 5′ termini as a strategy of negative-strand RNA viruses to avoid RIG-I-dependent interferon induction. *PLoS ONE* **2008**, *3*, e2032. [CrossRef] [PubMed]
90. Weber, M.; Gawanbacht, A.; Habjan, M.; Rang, A.; Bomer, C.; Schmidt, A.M.; Veitinger, S.; Jacob, R.; Devignot, S.; Kochs, G.; *et al.* Incoming RNA virus nucleocapsids containing a 5′-triphosphorylated genome activate RIG-I and antiviral signaling. *Cell Host Microbe* **2013**, *13*, 336–346. [CrossRef] [PubMed]
91. Ermler, M.E.; Yerukhim, E.; Schriewer, J.; Schattgen, S.; Traylor, Z.; Wespiser, A.R.; Caffrey, D.R.; Chen, Z.J.J.; King, C.H.; Gale, M.; *et al.* RNA helicase signaling is critical for type I interferon production and protection against Rift Valley fever virus during mucosal challenge. *J. Virol.* **2013**, *87*, 4846–4860. [CrossRef] [PubMed]
92. Gowen, B.B.; Hoopes, J.D.; Wong, M.H.; Jung, K.H.; Isakson, K.C.; Alexopoulou, L.; Flavell, R.A.; Sidwell, R.W. TLR3 deletion limits mortality and disease severity due to phlebovirus infection. *J. Immunol.* **2006**, *177*, 6301–6307. [CrossRef] [PubMed]
93. Habjan, M.; Pichlmair, A.; Elliott, R.M.; Overby, A.K.; Glatter, T.; Gstaiger, M.; Superti-Furga, G.; Unger, H.; Weber, F. NSs protein of Rift Valley fever virus induces the specific degradation of the double-stranded RNA-dependent protein kinase. *J. Virol.* **2009**, *83*, 4365–4375. [CrossRef] [PubMed]
94. Kende, M. Prophylactic and therapeutic efficacy of poly(I,C)-LC against Rift-Valley fever virus-infection in Mice. *J. Biol. Response Modif.* **1985**, *4*, 503–511.

95. Peters, C.J.; Reynolds, J.A.; Slone, T.W.; Jones, D.E.; Stephen, E.L. Prophylaxis of Rift Valley fever with antiviral drugs, immune serum, an interferon inducer, and a macrophage activator. *Antivir. Res.* **1986**, *6*, 285–297. [CrossRef]
96. Gowen, B.B.; Wong, M.H.; Jung, K.H.; Sanders, A.B.; Mitchell, W.M.; Alexopoulou, L.; Flavell, R.A.; Sidwell, R.W. TLR3 is essential for the induction of protective immunity against Punta Toro virus infection by the double-stranded RNA (dsRNA), poly(I:C12U), but not poly(I:C): Differential, recognition of synthetic dsRNA molecules. *J. Immunol.* **2007**, *178*, 5200–5208. [CrossRef] [PubMed]
97. Sidwell, R.W.; Huffman, J.H.; Smee, D.F.; Gilbert, J.; Gessaman, A.; Pease, A.; Warren, R.P.; Huggins, J.; Kende, M. Potential role of immunomodulators for treatment of phlebovirus infections of animals. *Ann. N. Y. Acad. Sci.* **1992**, *653*, 344–355. [CrossRef] [PubMed]
98. Sidwell, R.W.; Huffman, J.H.; Barnard, D.L.; Smee, D.F.; Warren, R.P.; Chirigos, M.A.; Kende, M.; Huggins, J. Antiviral and immunomodulating inhibitors of experimentally-induced Punta Toro virus infections. *Antivir. Res.* **1994**, *25*, 105–122. [CrossRef]
99. Pifat, D.Y.; Smith, J.F. Punta Toro virus infection of C57BL/6J mice—A model for phlebovirus-induced disease. *Microb Pathog.* **1987**, *3*, 409–422. [CrossRef]
100. Do Valle, T.Z.; Billecocq, A.; Guillemot, L.; Alberts, R.; Gommet, C.; Geffers, R.; Calabrese, K.; Schughart, K.; Bouloy, M.; Montagutelli, X.; *et al.* A new mouse model reveals a critical role for host innate immunity in resistance to Rift Valley fever. *J. Immunol.* **2010**, *185*, 6146–6156. [CrossRef] [PubMed]
101. Morrill, J.C.; Jennings, G.B.; Johnson, A.J.; Cosgriff, T.M.; Gibbs, P.H.; Peters, C.J. Pathogenesis of Rift Valley fever in Rhesus monkeys—Role of interferon response. *Arch. Virol.* **1990**, *110*, 195–212. [CrossRef] [PubMed]
102. Bouloy, M.; Janzen, C.; Vialat, P.; Khun, H.; Pavlovic, J.; Huerre, M.; Haller, O. Genetic evidence for an interferon-antagonistic function of Rift Valley fever virus nonstructural protein NSs. *J. Virol.* **2001**, *75*, 1371–1377. [CrossRef] [PubMed]
103. Mendenhall, M.; Wong, M.H.; Skirpstunas, R.; Morrey, J.D.; Gowen, B.B. Punta Toro virus (Bunyaviridae, *Phlebovirus*) infection in mice: Strain differences in pathogenesis and host interferon response. *Virology* **2009**, *395*, 143–151. [CrossRef] [PubMed]
104. Schoggins, J.W.; Wilson, S.J.; Panis, M.; Murphy, M.Y.; Jones, C.T.; Bieniasz, P.; Rice, C.M. A diverse range of gene products are effectors of the type I interferon antiviral response. *Nature* **2011**, *472*, 481–485. [CrossRef] [PubMed]
105. Schoggins, J.W.; MacDuff, D.A.; Imanaka, N.; Gainey, M.D.; Shrestha, B.; Eitson, J.L.; Mar, K.B.; Richardson, R.B.; Ratushny, A.V.; Litvak, V.; *et al.* Pan-viral specificity of IFN-induced genes reveals new roles for cGAS in innate immunity. *Nature* **2014**, *505*, 691–695. [CrossRef] [PubMed]
106. Frese, M.; Kochs, G.; Feldmann, H.; Hertkorn, C.; Haller, O. Inhibition of bunyaviruses, phleboviruses, and hantaviruses by human MxA protein. *J. Virol.* **1996**, *70*, 915–923. [PubMed]
107. Sandrock, M.; Frese, M.; Haller, O.; Kochs, G. Interferon-induced rat Mx proteins confer resistance to Rift Valley fever virus and other arthropod-borne viruses. *J. Interferon Cytokine Res.* **2001**, *21*, 663–668. [CrossRef] [PubMed]
108. Habjan, M.; Penski, N.; Wagner, V.; Spiegel, M.; Overby, A.K.; Kochs, G.; Huiskonen, J.T.; Weber, F. Efficient production of Rift Valley fever virus-like particles: The antiviral protein MxA can inhibit primary transcription of bunyaviruses. *Virology* **2009**, *385*, 400–408. [CrossRef] [PubMed]
109. Kochs, G.; Janzen, C.; Hohenberg, H.; Haller, O. Antivirally active MxA protein sequesters La Crosse virus nucleocapsid protein into perinuclear complexes. *Proc. Natl. Acad. Sci. USA* **2002**, *99*, 3153–3158. [CrossRef] [PubMed]
110. Mudhasani, R.; Tran, J.P.; Retterer, C.; Radoshitzky, S.R.; Kota, K.P.; Altamura, L.A.; Smith, J.M.; Packard, B.Z.; Kuhn, J.H.; Costantino, J.; *et al.* IFITM-2 and IFITM-3 but not IFITM-1 restrict Rift Valley fever virus. *J. Virol.* **2013**, *87*, 8451–8464. [CrossRef] [PubMed]
111. Ikegami, T.; Narayanan, K.; Won, S.; Kamitani, W.; Peters, C.J.; Makino, S. Rift Valley fever virus NSs protein promotes post-transcriptional downregulation of protein kinase PKR and inhibits eIF2alpha phosphorylation. *PLoS Pathog.* **2009**, *5*, e1000287. [CrossRef] [PubMed]
112. Atasheva, S.; Akhrymuk, M.; Frolova, E.I.; Frolov, I. New PARP gene with an anti-alphavirus function. *J. Virol.* **2012**, *86*, 8147–8160. [CrossRef] [PubMed]

113. Pichlmair, A.; Lassnig, C.; Eberle, C.A.; Gorna, M.W.; Baumann, C.L.; Burkard, T.R.; Burckstummer, T.; Stefanovic, A.; Krieger, S.; Bennett, K.L.; *et al.* IFIT1 is an antiviral protein that recognizes 5′-triphosphate RNA. *Nat. Immunol.* **2011**, *12*, 624–630. [CrossRef] [PubMed]
114. Vialat, P.; Billecocq, A.; Kohl, A.; Bouloy, M. The S segment of Rift Valley fever phlebovirus (Bunyaviridae) carries determinants for attenuation and virulence in mice. *J. Virol.* **2000**, *74*, 1538–1543. [CrossRef] [PubMed]
115. Struthers, J.K.; Swanepoel, R. Identification of a major non-structural protein in the nuclei of Rift Valley fever virus-infected cells. *J. Gen. Virol.* **1982**, *60*, 381–384. [CrossRef] [PubMed]
116. Yadani, F.Z.; Kohl, A.; Prehaud, C.; Billecocq, A.; Bouloy, M. The carboxy-terminal acidic domain of Rift Valley fever virus NSs protein is essential for the formation of filamentous structures but not for the nuclear localization of the protein. *J. Virol.* **1999**, *73*, 5018–5025. [PubMed]
117. Muller, R.; Saluzzo, J.F.; Lopez, N.; Dreier, T.; Turell, M.; Smith, J.; Bouloy, M. Characterization of Clone-13, a naturally attenuated avirulent isolate of Rift Valley fever virus, which is altered in the small segment. *Am. J. Trop. Med. Hyg.* **1995**, *53*, 405–411. [PubMed]
118. Billecocq, A.; Spiegel, M.; Vialat, P.; Kohl, A.; Weber, F.; Bouloy, M.; Haller, O. NSs protein of Rift Valley fever virus blocks interferon production by inhibiting host gene transcription. *J. Virol.* **2004**, *78*, 9798–9806. [CrossRef] [PubMed]
119. Le May, N.; Dubaele, S.; Proietti De Santis, L.; Billecocq, A.; Bouloy, M.; Egly, J.M. TFIIH transcription factor, a target for the Rift Valley hemorrhagic fever virus. *Cell* **2004**, *116*, 541–550. [CrossRef]
120. Kalveram, B.; Lihoradova, O.; Ikegami, T. NSs protein of Rift Valley fever virus promotes posttranslational downregulation of the TFIIH subunit p62. *J. Virol.* **2011**, *85*, 6234–6243. [CrossRef] [PubMed]
121. Pichlmair, A.; Kandasamy, K.; Alvisi, G.; Mulhern, O.; Sacco, R.; Habjan, M.; Binder, M.; Stefanovic, A.; Eberle, C.A.; Goncalves, A.; *et al.* Viral immune modulators perturb the human molecular network by common and unique strategies. *Nature* **2012**, *487*, 486–490. [CrossRef] [PubMed]
122. Hermand, D. F-box proteins: More than baits for the SCF? *Cell Div.* **2006**, *1*, 30. [CrossRef] [PubMed]
123. Kainulainen, M.; Habjan, M.; Hubel, P.; Busch, L.; Lau, S.; Colinge, J.; Superti-Furga, G.; Pichlmair, A.; Weber, F. Virulence factor NSs of Rift Valley fever virus recruits the F-box protein FBXO3 to degrade subunit p62 of general transcription factor TFIIH. *J. Virol.* **2014**, *88*, 3464–3473. [CrossRef] [PubMed]
124. Cyr, N.; de la Fuente, C.; Lecoq, L.; Guendel, I.; Chabot, P.R.; Kehn-Hall, K.; Omichinski, J.G. A Omega XaV motif in the Rift Valley fever virus NSs protein is essential for degrading p62, forming nuclear filaments and virulence. *Proc. Natl. Acad. Sci. USA* **2015**, *112*, 6021–6026. [CrossRef] [PubMed]
125. Copeland, A.M.; van Deusen, N.M.; Schmaljohn, C.S. Rift Valley fever virus NSs gene expression correlates with a defect in nuclear mRNA export. *Virology* **2015**, *486*, 88–93. [CrossRef] [PubMed]
126. Le May, N.; Mansuroglu, Z.; Leger, P.; Josse, T.; Blot, G.; Billecocq, A.; Flick, R.; Jacob, Y.; Bonnefoy, E.; Bouloy, M. A SAP30 complex inhibits IFN-beta expression in Rift valley fever virus infected cells. *PLoS Pathog.* **2008**, *4*, e13. [CrossRef] [PubMed]
127. Kainulainen, M.; Lau, S.; Samuel, C.E.; Hornung, V.; Weber, F. NSs virulence factor of Rift Valley fever virus engages the F-box proteins FBXW11 and beta-TRCP1 to degrade the antiviral protein kinase PKR. *J. Virol.* **2016**, *90*, 6140–6147. [CrossRef] [PubMed]
128. Mudhasani, R.; Tran, J.P.; Retterer, C.; Kota, K.P.; Whitehouse, C.A.; Bavari, S. Protein kinase R degradation is essential for Rift Valley fever virus infection and is regulated by SKP1-CUL1-F-box (SCF)FBXW11-NSs E3 Ligase. *PLoS Pathog.* **2016**, *12*, e1005437. [CrossRef] [PubMed]
129. Anderson, G.W., Jr.; Slayter, M.V.; Hall, W.; Peters, C.J. Pathogenesis of a phleboviral infection (Punta Toro virus) in golden Syrian hamsters. *Arch. Virol.* **1990**, *114*, 203–212. [CrossRef] [PubMed]
130. Perrone, L.A.; Narayanan, K.; Worthy, M.; Peters, C.J. The S segment of Punta Toro virus (Bunyaviridae, *Phlebovirus*) is a major determinant of lethality in the Syrian hamster and codes for a type I interferon antagonist. *J. Virol.* **2007**, *81*, 884–892. [CrossRef] [PubMed]
131. Lihoradova, O.A.; Indran, S.V.; Kalveram, B.; Lokugamage, N.; Head, J.A.; Gong, B.; Tigabu, B.; Juelich, T.L.; Freiberg, A.N.; Ikegami, T. Characterization of Rift Valley fever virus MP-12 strain encoding NSs of Punta Toro virus or sandfly fever Sicilian virus. *PLoS Negl. Trop. Dis.* **2013**, *7*, e2181. [CrossRef] [PubMed]
132. Kalveram, B.; Ikegami, T. Toscana virus NSs protein promotes degradation of double-stranded RNA-dependent protein kinase. *J. Virol.* **2013**, *87*, 3710–3718. [CrossRef] [PubMed]
133. Di Bonito, P.; Nicoletti, L.; Mochi, S.; Accardi, L.; Marchi, A.; Giorgi, C. Immunological characterization of Toscana virus proteins. *Arch. Virol.* **1999**, *144*, 1947–1960. [CrossRef] [PubMed]

134. Savellini, G.G.; Weber, F.; Terrosi, C.; Habjan, M.; Martorelli, B.; Cusi, M.G. Toscana virus induces interferon although its NSs protein reveals antagonistic activity. *J. Gen. Virol.* **2011**, *92*, 71–79. [CrossRef] [PubMed]
135. Gori-Savellini, G.; Valentini, M.; Cusi, M.G. Toscana Virus NSs Protein Inhibits the Induction of Type I Interferon by Interacting with RIG-I. *J. Virol.* **2013**, *87*, 6660–6667. [CrossRef] [PubMed]
136. Savellini, G.G.; Gandolfo, C.; Cusi, M.G. Truncation of the C-terminal region of Toscana Virus NSs protein is critical for interferon-beta antagonism and protein stability. *Virology* **2015**, *486*, 255–262. [CrossRef] [PubMed]
137. Brisbarre, N.M.; Plumet, S.; de Micco, P.; Leparc-Goffart, I.; Emonet, S.F. Toscana virus inhibits the interferon beta response in cell cultures. *Virology* **2013**, *442*, 189–194. [CrossRef] [PubMed]
138. Qu, B.; Qi, X.; Wu, X.; Liang, M.; Li, C.; Cardona, C.J.; Xu, W.; Tang, F.; Li, Z.; Wu, B.; *et al.* Suppression of the interferon and NF-kappaB responses by severe fever with thrombocytopenia syndrome virus. *J. Virol.* **2012**, *86*, 8388–8401. [CrossRef] [PubMed]
139. Ning, Y.J.; Wang, M.; Deng, M.; Shen, S.; Liu, W.; Cao, W.C.; Deng, F.; Wang, Y.Y.; Hu, Z.; Wang, H. Viral suppression of innate immunity via spatial isolation of TBK1/IKKepsilon from mitochondrial antiviral platform. *J. Mol. Cell Biol.* **2014**, *6*, 324–337. [CrossRef] [PubMed]
140. Santiago, F.W.; Covaleda, L.M.; Sanchez-Aparicio, M.T.; Silvas, J.A.; Diaz-Vizarreta, A.C.; Patel, J.R.; Popov, V.; Yu, X.J.; Garcia-Sastre, A.; Aguilar, P.V. Hijacking of RIG-I signaling proteins into virus-induced cytoplasmic structures correlates with the inhibition of type I interferon responses. *J. Virol.* **2014**, *88*, 4572–4585. [CrossRef] [PubMed]
141. Wu, X.D.; Qi, X.; Qu, B.Q.; Zhang, Z.R.; Liang, M.F.; Li, C.; Cardona, C.J.; Li, D.X.; Xing, Z. Evasion of antiviral immunity through sequestering of TBK1/IKK epsilon/IRF3 into viral inclusion bodies. *J. Virol.* **2014**, *88*, 3067–3076. [CrossRef] [PubMed]
142. Wu, X.D.; Qi, X.; Liang, M.F.; Li, C.; Cardona, C.J.; Li, D.X.; Xing, Z. Roles of viroplasm-like structures formed by nonstructural protein NSs in infection with severe fever with thrombocytopenia syndrome virus. *Faseb J. Off. Publ. Fed. Am. Soc. Exp. Biol.* **2014**, *28*, 2504–2516. [CrossRef] [PubMed]
143. Gack, M.U.; Shin, Y.C.; Joo, C.H.; Urano, T.; Liang, C.; Sun, L.J.; Takeuchi, O.; Akira, S.; Chen, Z.J.; Inoue, S.S.; *et al.* TRIM25 RING-finger E3 ubiquitin ligase is essential for RIG-I-mediated antiviral activity. *Nature* **2007**, *446*, 916–920. [CrossRef] [PubMed]
144. Ning, Y.J.; Feng, K.; Min, Y.Q.; Cao, W.C.; Wang, M.; Deng, F.; Hu, Z.; Wang, H. Disruption of type I interferon signaling by the nonstructural protein of severe fever with thrombocytopenia syndrome virus via the hijacking of STAT2 and STAT1 into inclusion bodies. *J. Virol.* **2015**, *89*, 4227–4236. [CrossRef] [PubMed]
145. Simons, J.F.; Hellman, U.; Pettersson, R.F. Uukuniemi virus S RNA Segment—Ambisense coding strategy, packaging of complementary strands into virions, and homology to members of the genus *Phlebovirus*. *J. Virol.* **1990**, *64*, 247–255. [PubMed]
146. Rezelj, V.V.; Overby, A.K.; Elliott, R.M. Generation of mutant Uukuniemi viruses lacking the nonstructural protein NSs by reverse genetics indicates that NSs is a weak interferon antagonist. *J. Virol.* **2015**, *89*, 4849–4856. [CrossRef] [PubMed]
147. Brennan, B.; Li, P.; Zhang, S.; Li, A.; Liang, M.; Li, D.; Elliott, R.M. Reverse genetics system for severe fever with thrombocytopenia syndrome virus. *J. Virol.* **2015**, *89*, 3026–3037. [CrossRef] [PubMed]
148. Ikegami, T.; Won, S.; Peters, C.J.; Makino, S. Rift Valley fever virus NSs mRNA is transcribed from an incoming anti-viral-sense S RNA segment. *J. Virol.* **2005**, *79*, 12106–12111. [CrossRef] [PubMed]
149. Billecocq, A.; Gauliard, N.; le May, N.; Elliott, R.M.; Flick, R.; Bouloy, M. RNA polymerase I-mediated expression of viral RNA for the rescue of infectious virulent and avirulent Rift Valley fever viruses. *Virology* **2008**, *378*, 377–384. [CrossRef] [PubMed]
150. Habjan, M.; Penski, N.; Spiegel, M.; Weber, F. T7 RNA polymerase-dependent and -independent systems for cDNA-based rescue of Rift Valley fever virus. *J. Gen. Virol.* **2008**, *89*, 2157–2166. [CrossRef] [PubMed]
151. Ikegami, T.; Won, S.; Peters, C.J.; Makino, S. Rescue of infectious Rift Valley fever virus entirely from cDNA, analysis of virus lacking the NSs gene, and expression of a foreign gene. *J. Virol.* **2006**, *80*, 2933–2940. [CrossRef] [PubMed]

4.2 Research article:

NSs Protein of Sandfly Fever Sicilian Phlebovirus Counteracts Interferon (IFN) Induction by Masking the DNA-Binding Domain of IFN Regulatory Factor 3

Own contribution:
I performed all experiments presented in the figures and contributed to the design of the study and writing the manuscript.

Recombinant viruses were generated by Matthias Habjan, and interactome data was generated by Matthias Habjan and Andreas Pichlmair. Julia Wulle generated expression plasmids for truncated NSs mutants (data not shown).

_____

Jennifer Würth

AMERICAN SOCIETY FOR MICROBIOLOGY | Journal of Virology®

VIRUS-CELL INTERACTIONS

NSs Protein of Sandfly Fever Sicilian Phlebovirus Counteracts Interferon (IFN) Induction by Masking the DNA-Binding Domain of IFN Regulatory Factor 3

Jennifer Deborah Wuerth,[a,b] Matthias Habjan,[c] Julia Wulle,[a,b] Giulio Superti-Furga,[d,e] Andreas Pichlmair,[d,e,f,g] Friedemann Weber[a,b]

[a]Institute for Virology, Philipps-University Marburg, Marburg, Germany
[b]Institute for Virology, FB10-Veterinary Medicine, Justus-Liebig University, Giessen, Germany
[c]Innate Immunity Laboratory, Max Planck Institute of Biochemistry, Munich, Germany
[d]CeMM Research Center for Molecular Medicine, Austrian Academy of Sciences, Vienna, Austria
[e]Center for Physiology and Pharmacology, Medical University of Vienna, Vienna, Austria
[f]Institute of Virology, School of Medicine, Technical University of Munich, Munich, Germany
[g]Munich Partner Site, German Center for Infection Research (DZIF), Munich, Germany

ABSTRACT Sandfly fever Sicilian virus (SFSV) is one of the most widespread and frequently identified members of the genus *Phlebovirus* (order *Bunyavirales*, family *Phenuiviridae*) infecting humans. Being transmitted by *Phlebotomus* sandflies, SFSV causes a self-limiting, acute, often incapacitating febrile disease ("sandfly fever," "Pappataci fever," or "dog disease") that has been known since at least the beginning of the 20th century. We show that, similarly to other pathogenic phleboviruses, SFSV suppresses the induction of the antiviral type I interferon (IFN) system in an NSs-dependent manner. SFSV NSs interfered with the TBK1-interferon regulatory factor 3 (IRF3) branch of the RIG-I signaling pathway but not with NF-κB activation. Consistently, we identified IRF3 as a host interactor of SFSV NSs. In contrast to IRF3, neither the IFN master regulator IRF7 nor any of the related transcription factors IRF2, IRF5, and IRF9 were bound by SFSV NSs. In spite of this specificity for IRF3, NSs did not inhibit its phosphorylation, dimerization, or nuclear accumulation, and the interaction was independent of the IRF3 activation or multimerization state. In further studies, we identified the DNA-binding domain of IRF3 (amino acids 1 to 113) as sufficient for NSs binding and found that SFSV NSs prevented the association of activated IRF3 with the IFN-β promoter. Thus, unlike highly virulent phleboviruses, which either destroy antiviral host factors or sequester whole signaling chains into inactive aggregates, SFSV modulates type I IFN induction by directly masking the DNA-binding domain of IRF3.

IMPORTANCE Phleboviruses are receiving increased attention due to the constant discovery of new species and the ongoing spread of long-known members of the genus. Outbreaks of sandfly fever were reported in the 19th century, during World War I, and during World War II. Currently, SFSV is recognized as one of the most widespread phleboviruses, exhibiting high seroprevalence rates in humans and domestic animals and causing a self-limiting but incapacitating disease predominantly in immunologically naive troops and travelers. We show how the nonstructural NSs protein of SFSV counteracts the upregulation of the antiviral interferon (IFN) system. SFSV NSs specifically inhibits promoter binding by IFN transcription factor 3 (IRF3), a molecular strategy which is unique among phleboviruses and, to our knowledge, among human pathogenic RNA viruses in general. This IRF3-specific and stoichiometric mechanism, greatly distinct from the ones exhibited by the highly virulent phleboviruses, correlates with the intermediate level of pathogenicity of SFSV.

Received 10 July 2018 **Accepted** 13 September 2018

Accepted manuscript posted online 19 September 2018

Citation Wuerth JD, Habjan M, Wulle J, Superti-Furga G, Pichlmair A, Weber F. 2018. NSs protein of sandfly fever sicilian phlebovirus counteracts interferon (IFN) induction by masking the DNA-binding domain of IFN regulatory factor 3. J Virol 92:e01202-18. https://doi.org/10.1128/JVI.01202-18.

Editor Adolfo García-Sastre, Icahn School of Medicine at Mount Sinai

Address correspondence to Friedemann Weber, friedemann.weber@vetmed.uni-giessen.de.

KEYWORDS DNA-binding domain, IRF3, NSs, sandfly fever Sicilian virus, interferon beta promoter, interferon induction

Members of the genus phlebovirus (order Bunyavirales, family *Phenuiviridae*) are present worldwide and gain increasing attention as vector-borne agents of disease (1). In addition to prominent, recently emerged phleboviruses such as severe fever with thrombocytopenia syndrome virus (SFTSV) in Asia and Heartland virus (HRTV) in North America (2), there are long-known members, such as Rift Valley fever virus (RVFV), Punta Toro virus (PTV), Toscana virus (TOSV), and sandfly fever Sicilian virus (SFSV), that are often reemerging or spreading into new geographical areas (3). In addition to these highly virulent (SFTSV, HRTV, and RVFV) and intermediately virulent (TOSV and SFSV) human pathogens, rapid progress in high-throughput sequencing enabled the identification of novel phleboviruses for which the disease potential is either recognized (e.g., sandfly fever Turkey virus [4] and Adria virus [5]) or not yet clarified (e.g., Massilia virus [6], Aguacate virus [7], and Dashli virus [8]).

Infection by SFSV and related sandfly fever viruses, all transmitted by phlebotomine sandflies, typically presents as an acute febrile disease with abrupt onset, often developing into incapacitating myalgia, headaches, malaise, leukocytopenia, or ocular or gastrointestinal symptoms (9, 10). An outbreak of this so-called "sandfly fever," "Pappataci fever," or "dog disease" during the Sicilian campaign of World War II in 1943 enabled Albert Sabin to isolate SFSV from infected soldiers (11). SFSV later proved to be one of the most widespread phleboviruses; it is present across the entire Mediterranean basin, in Portugal, in the Middle East inclusive of the Arabian peninsula, in Sudan, in Ethiopia, and in Somalia and in locations as distant as India and Bangladesh (12–18). In regions of endemicity, seroprevalence can reach levels of up to 50% in humans and close to 80% in dogs and other domestic animals, including cattle (12, 14, 19, 20). Hence, sandfly fever viruses are recognized as a significant public health threat, predominantly for immunologically naive groups such as soldiers or travelers (21–24). Nonetheless, little is known about the molecular interplay of SFSV and SFSV-like viruses with the host organism.

Like all phleboviruses, SFSV contains a tripartite single-stranded RNA genome (1, 3). While the large (L) genome segment and the medium (M) genome segment encode the viral polymerase (Pol) L and the glycoproteins, respectively, in a negative orientation, the small (S) segment codes for the nucleocapsid protein N and the nonstructural protein NSs in an ambisense manner. The genomic RNA segments are packaged into ribonucleoproteins (RNPs) by the nucleocapsid N protein and the L polymerase and are transcribed and replicated in the cytoplasm (25).

Due to complementarity of the 5′ and 3′ termini, the three RNP-packaged genome segments have the capacity to anneal to a so-called "panhandle." This RNA structure, with its short double-stranded region and 5′-triphosphate moiety, is an activator of the cytoplasmic RNA helicase RIG-I, an important virus sensor of the antiviral type I interferon (IFN) system (26). Ligand-bound RIG-I signals via the adaptor mitochondrial antiviral-signaling protein (MAVS) and the kinases TBK1/IκB kinase ε (IKKε) to eventually activate the ubiquitously expressed transcription factor interferon regulatory factor 3 (IRF3) (27). The latter thereby becomes phosphorylated, dimerizes, and accumulates in the nucleus, where, together with NF-κB and ATF-2/c-Jun, it transactivates the IFN-β promoter to kick off a first wave of IFN secretion (28). Autocrine and paracrine action of IFN-β then triggers the upregulation of IRF7, which amplifies and diversifies the initial IRF3-driven IFN response by inducing both the *IFNB* gene and multiple *IFNA* genes (29–31). Simultaneously, it induces the transcription of IFN-stimulated genes (ISGs), several of them with demonstrated antiphleboviral activity (3).

Phleboviruses counteract the induction of the IFN response by means of their NSs protein (3, 32). The best-characterized NSs, namely, that of RVFV, allows the full RIG-I signaling cascade to reach the point of IRF3 binding to the IFN-β promoter but then abrogates host gene expression by targeted sequestration and deletion of general

transcription factors, as well as by the recruitment of corepressors and induction of an mRNA export block (33–38). In the case of TOSV, in contrast, the NSs protein causes proteasomal degradation of RIG-I (39), and for SFTSV, the NSs sequesters multiple factors of the signaling cascade into cytoplasmic aggregates (40–43). For many phleboviruses, including the sandfly-borne SFSV, however, the mechanism of NSs action is unclear.

We and others previously found that the NSs of SFSV, expressed by a recombinant RVFV, was able to block transcription of the *IFNB* gene (44, 45). Here, we investigated the molecular mechanism and identified IRF3 as a functional target.

RESULTS

SFSV NSs inhibits IFN induction. SFSV NSs expressed by recombinant RVFV was previously shown to inhibit the upregulation of the *IFNB* gene (44, 45). Accordingly, infection with parental SFSV strain Sabin resulted in only limited upregulation of IFN-β mRNA, as measured by reverse transcriptase quantitative PCR (RT-qPCR) (Fig. 1A). As controls, we used RVFV strain MP12 (expressing a functional RVFV NSs) and clone 13 (expressing an internally deleted RVFV NSs) in parallel (33), which suppressed and activated IFN induction, respectively, in the expected manner.

Unlike RVFV, neither a natural nor a recombinant NSs-deficient strain is available for SFSV. In order to abort NSs function, we designed a pool of four small interfering RNAs (siRNAs) that specifically target the NSs gene sequence. The efficiency of the siRNAs was tested by cotransfection of an expression plasmid for 3×FLAG-tagged SFSV NSs and either the NSs-targeting siRNA pool or a control siRNA. The specific siRNAs caused a significant reduction of SFSV NSs RNA levels in RT-PCR and a complete loss of the FLAG signal in immunoblot analysis, while the control siRNA had no effect (Fig. 1B). In contrast, RNA and protein levels of the 3×FLAG-tagged NSs of PTV-A were not affected, confirming the specificity of the siRNA pool for SFSV NSs.

We then combined transfection of the NSs-specific siRNA pool with infection by either SFSV or RVFV MP-12, followed by RT-qPCR analysis. Of note, in infected cells the siRNA pool as well as the PCR primers can target not only the NSs transcript but also the entire S genome segment. Therefore, we could not determine whether only the NSs mRNA was affected by the siRNAs or whether the viral genome was also affected. However, due to encapsidation of the genome, we expect a certain level of protection, which in turn would result in an underestimation of siRNA effects on NSs transcripts. In any case, a substantial depletion of NSs sequence-containing RNA species (fold reduction, 3.3 ± 0.3) was observed (Fig. 1C). Moreover, in the presence of the NSs-specific siRNAs, SFSV infection upregulated the amounts of IFN-β transcripts (fold increase, 5.1 ± 2.6) (Fig. 1D), despite the fact that virus replication (measured via analysis of L segment levels) was diminished (fold reduction, 2.0 ± 0.42) (Fig. 1E). For RVFV MP12, in contrast, the SFSV NSs-specific siRNAs affected neither the IFN-β mRNA levels (Fig. 1C) nor the accumulation of its S segment (Fig. 1F). The same applied to clone 13, TOSV, and the closely related sandfly fever Turkey virus (data not shown), demonstrating both the specificity of the siRNA pool and its effect on the induction of IFN-β by SFSV. Furthermore, no intrinsic IFN-stimulatory activity of the siRNA pool was observed in the mock samples (Fig. 1C). Taking into consideration the opposing effects of the siRNA on *IFNB* induction and on SFSV replication, a normalized fold induction of 9.8 ± 3.7 was calculated for *IFNB*, compared to 1.0 ± 0.4 for RVFV (Fig. 1G, right column).

Of note, the impairment of SFSV replication by the NSs-specific siRNA was far less pronounced in IFN-incompetent Vero B4 cells (data now shown), indicating that it was largely mediated by the antiviral IFN system rather than by interference with the integrity of the genomic S segment. In summary, siRNA knockdown of SFSV NSs resulted in simultaneous upregulation of IFN induction and downregulation of SFSV replication in IFN-competent cells, reminiscent of the behavior of NSs-deficient phleboviruses. Together with the data from recombinant NSs-expressing RVFV (44, 45), this validates the identification of SFSV NSs as an IFN induction antagonist.

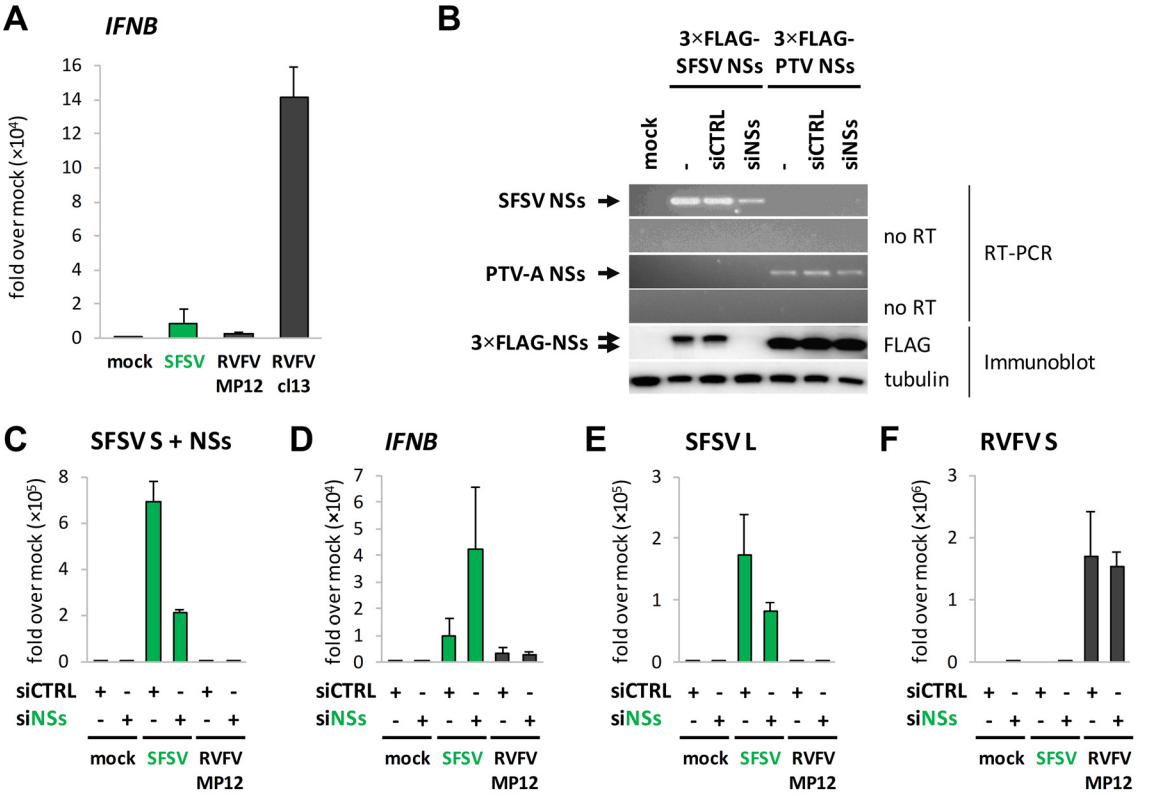

G

Virus	siRNA	Fold induction over mock/siCTRL				Fold increase *IFNB* (siNSs over siCTRL) over viral burden
		SFSV S + NSs	*IFNB*	SVSV L	RVFV S	
mock	siCTRL	1.0 ± 0.0	1.0 ± 0.00	1.0 ± 0.0	1.0 ± 0.0	n.a.
	siNSs	3.7 ± 4.6	2.4 ± 0.92	1.2 ± 0.2	3.1 ± 3.7	
SFSV	siCTRL	$6.9\times10^5 \pm 8.9\times10^4$	$9.7\times10^3 \pm 6.6\times10^3$	$1.7\times10^5 \pm 6.5\times10^4$	1.2 ± 0.1	9.8 ± 3.7
	siNSs	$2.1\times10^5 \pm 1.4\times10^4$	$4.2\times10^4 \pm 2.3\times10^4$	$8.3\times10^4 \pm 1.4\times10^4$	1.4 ± 0.3	
RVFV MP12	siCTRL	2.4 ± 2.2	$3.6\times10^3 \pm 1.9\times10^3$	2.2 ± 0.8	$1.7\times10^6 \pm 7.4\times10^5$	1.0 ± 0.4
	siNSs	1.6 ± 0.7	$2.9\times10^3 \pm 9.9\times10^2$	1.4 ± 0.3	$1.5\times10^6 \pm 2.3\times10^5$	

FIG 1 SFSV NSs and *IFNB* induction. (A) A549 cells were infected with SFSV, RVFV MP12, or clone 13 (Cl13) at an MOI of 1, harvested 12 hpi, and analyzed by RT-qPCR analysis for *IFNB* ($n = 4$; mean ± SD). (B) A549 cells were cotransfected with expression constructs for 3×FLAG-tagged SFSV or PTV-A NSs and nontargeting control siRNA or SFSV NSs-specific siRNA. Samples were subjected to RT-PCR analysis (upper panels) and immunoblotting using anti-FLAG and anti-tubulin antibodies (lower panel) 24 h after transfection. To exclude amplification of NSs sequences from plasmid DNA, a duplicate set of reactions was performed without the reverse transcription step (no RT). (C to F) A549 cells were pretransfected with control or SFSV NSs-targeting siRNA and infected with SFSV or RVFV MP12 at an MOI of 1. RNA was isolated 12 hpi for RT-qPCR analysis for NSs-containing RNA (C), *IFNB* (D), the L segment of SFSV (E), and the S segment of RVFV MP12 ($n = 3$; means ± SD) (F). (G) Summary of the relative fold induction data depicted in panels C to F, normalized to the mock sample pretreated with control siRNA as well as the fold induction of *IFNB* in siNSs-treated cells over siCTRL-treated cells that occurred in a manner independent of the viral burden (means ± SD). n.a., not applicable.

SFSV NSs acts in a nondegradative manner. Many pathogenic phleboviruses are known to counteract the IFN response by diminishing the levels of key host factors (3). The NSs of RVFV induces proteasomal degradation of cellular proteins such as TFIIH-p62 (to block IFN induction) and protein kinase R (PKR) (to prevent the antiviral action of IFN) (35, 44, 46–48). The NSs of TOSV was also shown to cause PKR degradation and to block IFN induction by decreasing RIG-I levels (39, 49). We investigated whether the NSs protein of SFSV might execute a similar form of degradative activity on host proteins. As controls, we employed TOSV NSs and RVFV NSs, and we also included the so far

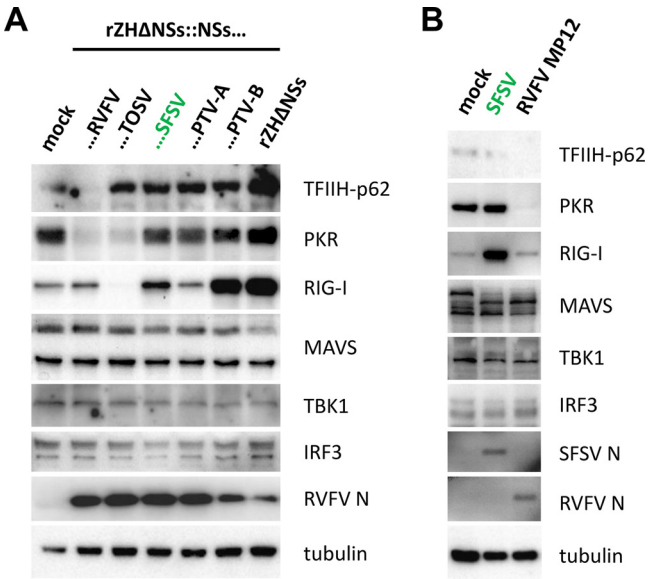

FIG 2 Effect of selected NSs proteins on phlebovirus host targets and central RIG-I signaling components. (A) A549 cells were infected at an MOI of 1 with recombinant RVFV expressing the NSs of RVFV, TOSV, SFSV, PTV-A, or PTV-B or entirely lacking an NSs-coding sequence. Cells were harvested 8 hpi for immunoblot analysis. (B) A549 cells were infected with SFSV or RVFV MP12 at an MOI of 1 and harvested 12 hpi for SDS-PAGE and Western blot analysis.

little-investigated PTV NSs, which is known to inhibit host cell transcription (45). For PTV, there are two distinct strains, namely, Adames (PTV-A) and Balliett (PTV-B), which strongly and weakly suppress IFN induction, respectively (45, 50). To directly compare the degradative capacities of the NSs proteins of RVFV, TOSV, SFSV, PTV-A, and PTV-B, we infected A549 cells with recombinant RVFV encoding the respective NSs genes and monitored the intracellular levels of the known phleboviral targets TFIIH-p62, PKR, and RIG-I, as well as of the central RIG-I signaling factors MAVS, TBK1, and IRF3. As shown in Fig 2A, levels of TFIIH-p62 were reduced only by RVFV NSs. Moreover, and in agreement with previous studies (44, 45, 49), PKR levels were decreased upon expression of the NSs of RVFV and TOSV but not by those of SFSV and PTV. RIG-I levels were left unchanged by the NSs of RVFV or PTV-A, strongly decreased by the NSs of TOSV, and upregulated after infection with the recombinant RVFV expressing NSs of SFSV (weakly) or PTV-B (strongly). In fact, in the presence of PTV-B NSs the upregulation of RIG-I was indistinguishable from the level seen with the NSs-deficient control virus rZHΔNSs. The levels of MAVS, TBK1, and IRF3 were not affected by any of the NSs proteins. These results were confirmed in cells infected with the parental SFSV strain Sabin (Fig. 2B). Thus, the NSs proteins of SFSV and PTV do not degrade the host targets of other phleboviruses.

SFSV NSs inhibits the IRF branch of IFN induction. For our further investigations, we focused on the NSs of SFSV but also included those of RVFV (as a well-characterized control) and PTV. To interrogate their activity on IFN induction, we performed luciferase reporter assays. Human HEK293 cells were transfected with increasing amounts of expression plasmids encoding the respective NSs proteins, along with a reporter construct harboring the firefly luciferase (FF-Luc) gene under the control of the IFN-β promoter and a constitutively expressing *Renilla* luciferase (R-Luc) plasmid for normalization. Activation of the IFN-β promoter was stimulated by cotransfection of a MAVS cDNA plasmid. As expected, overexpression of MAVS strongly activated the IFN-β promoter, which was undisturbed by increasing doses of the N terminus of the human MxA protein (ΔMx [35]) which was used as a negative control (Fig. 3A). Expression of the NSs proteins of RVFV, SFSV, and PTV-A, in contrast, suppressed the promoter in a dose-dependent manner. PTV-B NSs showed only a partial effect in response to large plasmid amounts, in line with previous observations (50).

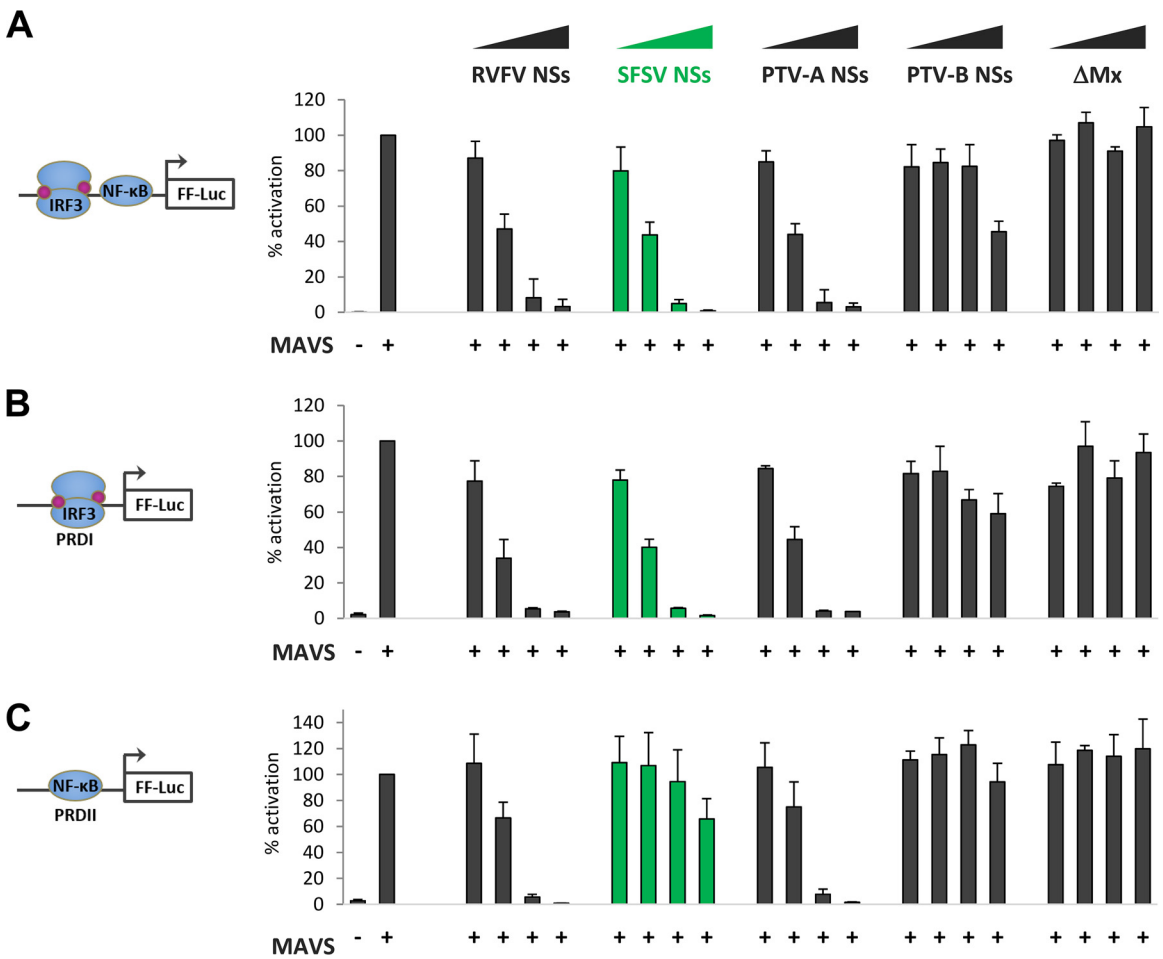

FIG 3 Influence of phlebovirus NSs proteins on *IFNB* promoter elements. HEK293 cells were transfected with expression plasmids for MAVS; NSs of RVFV, SFSV, PTV-A, or PTV-B; or inactive control ΔMx (0.1 ng, 1 ng, or 10 ng), as well as stimulation-dependent firefly luciferase (FF-Luc) and constitutively active *Renilla* luciferase reporters. Firefly luciferase was under the control of (A) the entire IFN-β promoter ($n = 3$; means ± SD), (B) IRF-driven PRDI ($n = 3$; means ±SD), or (C) NF-κB-driven PRDII ($n = 3$; means ± SD). Cell lysates were harvested 24 h after transfection for dual-luciferase assays. Firefly reporter activities were normalized to the *Renilla* reporter activities, and the positive controls were set to 100% prior to calculating means and SD across biological replicates.

The IFN-β promoter contains several positive regulatory domains (PRDs), among which PRDI binds transcription factors of the interferon regulatory factor (IRF) family and PRDII binds NF-κB (51, 52). Reporter assays showed that the inhibitory effect of SFSV NSs on the PRDI promoter element was comparable to that seen with the full IFN-β promoter but that PRDII activity was inhibited only weakly (Fig. 3B and C). This is in contrast to the NSs of PTV-A, which, like the RVFV NSs, inhibited the two PRD reporters indiscriminately. As similar results were obtained when TBK1 was used for stimulation instead of MAVS (data not shown), we concluded that SFSV NSs specifically targets the IRF branch of IFN induction at the level of TBK1 or further downstream, whereas PTV-A NSs blocks IFN induction in a broad manner, as shown previously (45).

SFSV NSs interacts with IRF3 in a highly specific manner. Previously, we took part in a large proteomics screen to identify host cell interactors of viral IFN antagonists that included SFSV NSs (53). The SFSV NSs cDNA, equipped with the sequence for a C-terminal tandem affinity purification (TAP) tag, was inserted into recombinant RVFV to replace the RVFV NSs gene (rRVFVΔNSs::NSs_{SFSV}-CTAP). 293T cells were infected with this recombinant virus, tandem affinity purification was performed, and protein complexes were analyzed by liquid chromatography-mass spectrometry (LC-MS). Strikingly, IRF3 was among the host cell interactors of SFSV NSs, which is compatible with the results of our reporter assays. In order to test the data obtained by mass spectrometry,

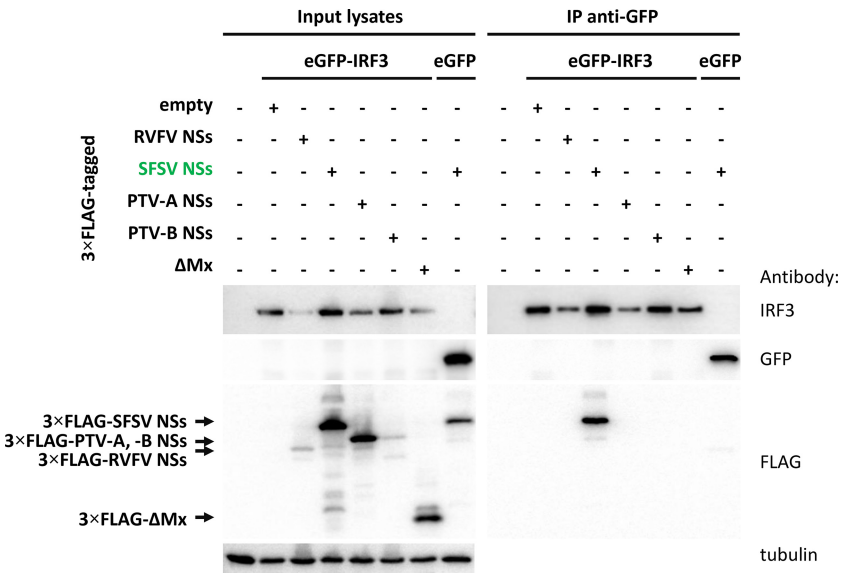

FIG 4 Coimmunoprecipitation of NSs proteins with eGFP-IRF3. Selected 3×FLAG-tagged NSs proteins were coexpressed with eGFP-IRF3 in HEK293 cells. eGFP and ΔMx served as negative controls for eGFP-IRF3 and the NSs proteins, respectively. Cell lysates were subjected to immunoprecipitation via a GFP-binding nanobody immobilized on the bottom of a 96-well plate. Input samples and bound proteins were analyzed via immunoblotting ($n = 3$).

we performed pulldown analyses. An enhanced green fluorescent protein (eGFP)-IRF3 fusion protein was coexpressed with the recombinant 3×FLAG-tagged NSs of SFSV, RVFV, PTV-A, or PTV-B or with the negative-control ΔMx. Cell lysates were then subjected to immunoprecipitation using a plate coated with a nanobody directed against GFP. The NSs proteins of RVFV and PTV-A negatively affected the coexpression of eGFP-IRF3 (Fig. 4 and data not shown), but eGFP-IRF3 was enriched in all GFP precipitates nonetheless. SFSV NSs clearly coprecipitated with eGFP-IRF3 but not with eGFP alone. In contrast, neither of the other phleboviral NSs proteins interacted with eGFP-IRF3. Similar results were also observed in an inverse setting; i.e., SFSV NSs was able to pull down eGFP-IRF3 (or hemagglutinin-IRF3 [HA-IRF3]), while PTV-A and ΔMx were not (data not shown). This confirms our earlier mass spectrometry data (53) and demonstrates that SFSV NSs is unique among the tested phleboviral proteins in its interaction with IRF3.

We extended our assays to include other members of the IRF family. IRF7 is the family member most closely related to IRF3 in both sequence and function (31). However, SFSV NSs did not coprecipitate with eGFP-IRF7 (Fig. 5A). Likewise, eGFP-IRF2, eGFP-IRF5, and eGFP-IRF9 did not interact with SFSV NSs (Fig. 5B). Hence, we conclude that SFSV NSs selectively targets the immediate early-acting IFN transcription factor IRF3.

SFSV NSs does not inhibit IRF3 activation. In uninfected cells, IRF3 localizes predominantly to the cytoplasm. Upon activation, IRF3 becomes phosphorylated by TBK1/IKKε, dimerizes, and accumulates in the nucleus, where it associates with the transcriptional cofactors CBP and p300 (52, 54–57). Transiently expressed SFSV NSs, on the other hand, localized diffusely to both the cytoplasm and the nucleoplasm (data not shown), suggesting that it could interfere with IRF3 activation or function at any level. We thus simultaneously investigated the three classic hallmarks of IRF3 activation in SFSV-infected cells. First, immunoblot analysis showed that IRF3 phosphorylation was affected neither in SFSV-infected cells (Fig. 6A) nor in cells infected with a recombinant RVFV expressing SFSV NSs (Fig. 6B). The latter experiment also demonstrated that PTV NSs was acting downstream of IRF3 phosphorylation. Also, IRF3 dimerization (Fig. 6C) and virus-triggered accumulation in the nucleus (Fig. 6D) were not impaired by SFSV

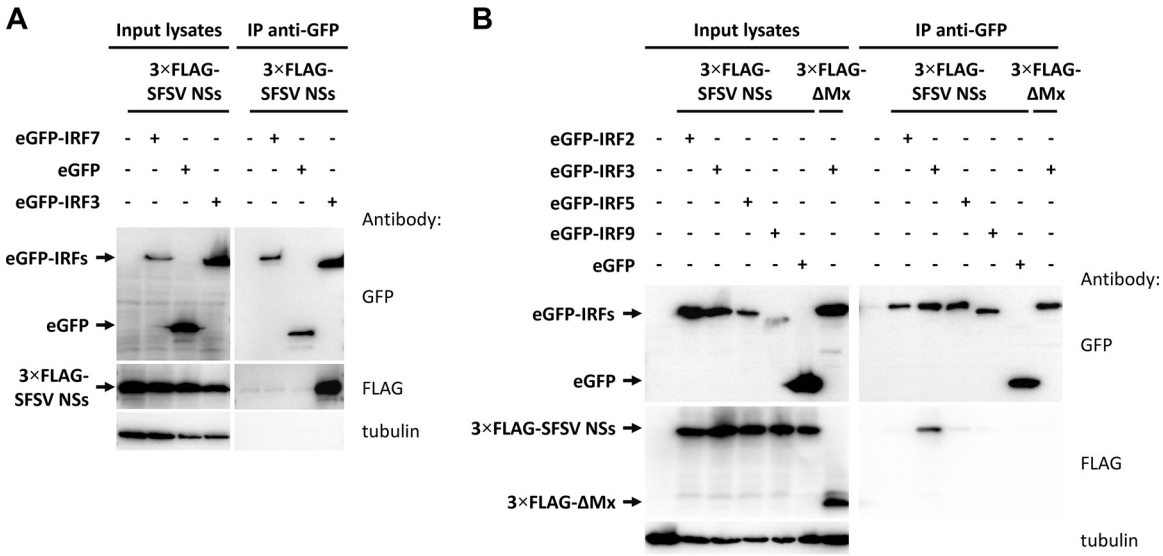

FIG 5 Coimmunoprecipitation of SFSV NSs with IRF proteins. 3×FLAG-tagged SFSV NSs plasmids were transfected into HEK293 cells together with eGFP-fused IRF7 (A) or IRF2, IRF5, or IRF9 (B). eGFP-IRF3 and eGFP were included as positive and negative controls, respectively. Cells were lysed, immunoprecipitation (IP) was performed via the use of GFP, and input lysates and immunoprecipitates were subjected to immunoblotting.

infection. Thus, SFSV—like RVFV, which was used as a control (33)—was not preventing phosphorylation, dimerization, or nuclear localization of IRF3.

We tested the impact of SFSV NSs on specific IRF3 mutants. IRF3(5D) is constitutively active and dimerized due to phosphomimetic aspartate residues that replace five serine and threonine phosphorylation sites in the region from amino acid (aa) 395 to aa 407 (54, 55). SFSV NSs was able to inhibit both IFN induction and PRD I activation by IRF3(5D) (Fig. 7A and B), just like the NSs of PTV-A, which was used in parallel. SFSV NSs, however, was additionally able to pull down IRF3(5D) (Fig. 7C). SFSV NSs also interacted with IRF3 mutants that are deficient in dimerization, namely, IRF3(S385A/S386A) (58) (Fig. 7D) as well as IRF3(S385A/S386A-R211A/R213A) and IRF3(S385A/S386A-R285A/H288A/H290A), further derivatives with additional mutations of essential arginine and histidine residues within the dimerization interface (data not shown).

In summary, these experiments demonstrated that SFSV NSs inhibits a molecular step that takes place after the nuclear importation of activated IRF3 but prior to IRF3-driven transcription and that the interaction interface on IRF3 is accessible in both the inactive and the active states.

SFSV NSs interacts with the DNA-binding domain of IRF3. IRF3 possesses an N-terminal DNA-binding domain (DBD; aa 1 to 113) (59) which also contains the bipartite nuclear localization signal (NLS; K77/R78 and R86/K87) (60, 61), followed by an activation domain comprising the nuclear export signal (NES; aa 139 to 150) (52, 60), a proline-rich domain (Pro; aa 150 to 190), an IRF association domain (IAD; aa 190 to 384) (62), and a serine-rich domain (SR; aa 384 to 427) that is phosphorylated upon activation (63) (Fig. 8A). Crystal structures of the C-terminal portion of IRF3 (aa 173/175 to 427) indicate that IRF3 phosphorylation induces a marked conformational change in the IAD, resulting in the exposure of residues that facilitate dimerization and the interaction with CBP/p300 (58, 64, 65). We employed systematic deletion analysis to map the IRF3 domain that is bound by SFSV NSs. As a first step, we cut GFP-tagged IRF3 into two halves at position 190. As shown in Fig. 8B, only the N-terminal part, ranging from aa 1 to 190, was able to pull down NSs. We then removed the remaining domains from this fragment one by one in the C- to N-terminal direction. In this way, we found that the N-terminal DBD alone (aa 1 to 113) was sufficient for binding SFSV NSs (Fig. 8C). Unfortunately, fine mapping by further C-terminal deletions was inconclusive, as were

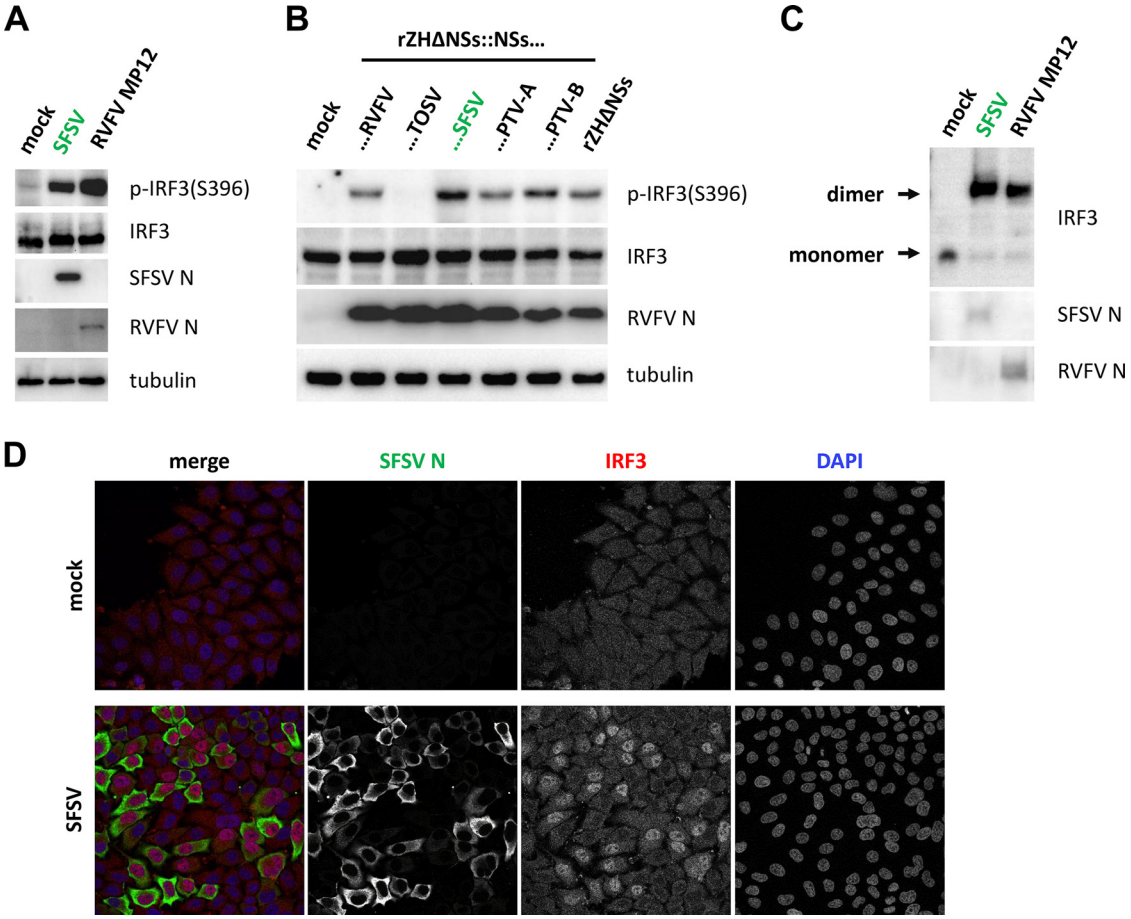

FIG 6 Markers of IRF3 activation under conditions of SFSV infection. (A to C) IRF3 phosphorylation and dimerization. A549 cells were infected with the indicated viruses at an MOI of 1, harvested 12 hpi (A) and 8 hpi (B), and analyzed by immunoblotting for IRF3 phosphorylation and viral nucleocapsid proteins. (C) Samples from the experiment described for panel A were additionally subjected to native PAGE, followed by immunoblotting. (D) Nuclear importation of IRF3. A549 cells seeded onto glass coverslips were infected at an MOI of 1, fixed 12 hpi with paraformaldehyde, and subsequently stained for IRF3 and the SFSV nucleocapsid protein N.

our attempts to map the corresponding IRF3-interacting region within SFSV NSs (data not shown).

SFSV NSs prevents IRF3 from binding to the IFN promoter. We hypothesized that SFSV NSs might interfere with the promoter-binding activity of IRF3. To investigate this, we established an assay in which we used biotinylated IFN-β promoter oligonucleotides to pull down MAVS-activated IRF3 via the use of streptavidin-coated magnetic beads. eGFP-IRF3 and MAVS were coexpressed in HEK293 cells either on their own or together with increasing doses of 3×FLAG-tagged SFSV NSs or the negative-control ΔMx. As observable in the input samples, overexpressed MAVS induced the phosphorylation and dimerization of eGFP-IRF3, as expected (Fig. 9, left panels, and data not shown). The presence of SFSV NSs did not affect IRF3 activation, confirming our observations of SFSV-infected cells. Analyzing the precipitated proteins (Fig. 9, right panels), we detected activated eGFP-IRF3 but not eGFP, indicating specific binding to the IFN-β promoter oligonucleotide. Furthermore, no protein precipitation was observed when empty beads without the biotinylated oligonucleotide were used (data not shown). The sequence specificity of eGFP-IRF3 binding was confirmed by the addition of an excess of nonbiotinylated IFN-β promoter oligonucleotide, which strongly diminished eGFP-IRF3 binding, whereas a scrambled control oligonucleotide had no such effect. Importantly, coexpression of SFSV NSs reduced the amount of promoter-bound eGFP-IRF3 in a dose-dependent manner, but the control protein ΔMx had no influence. Of note, SFSV NSs did not coprecipitate with the promoter oligonu-

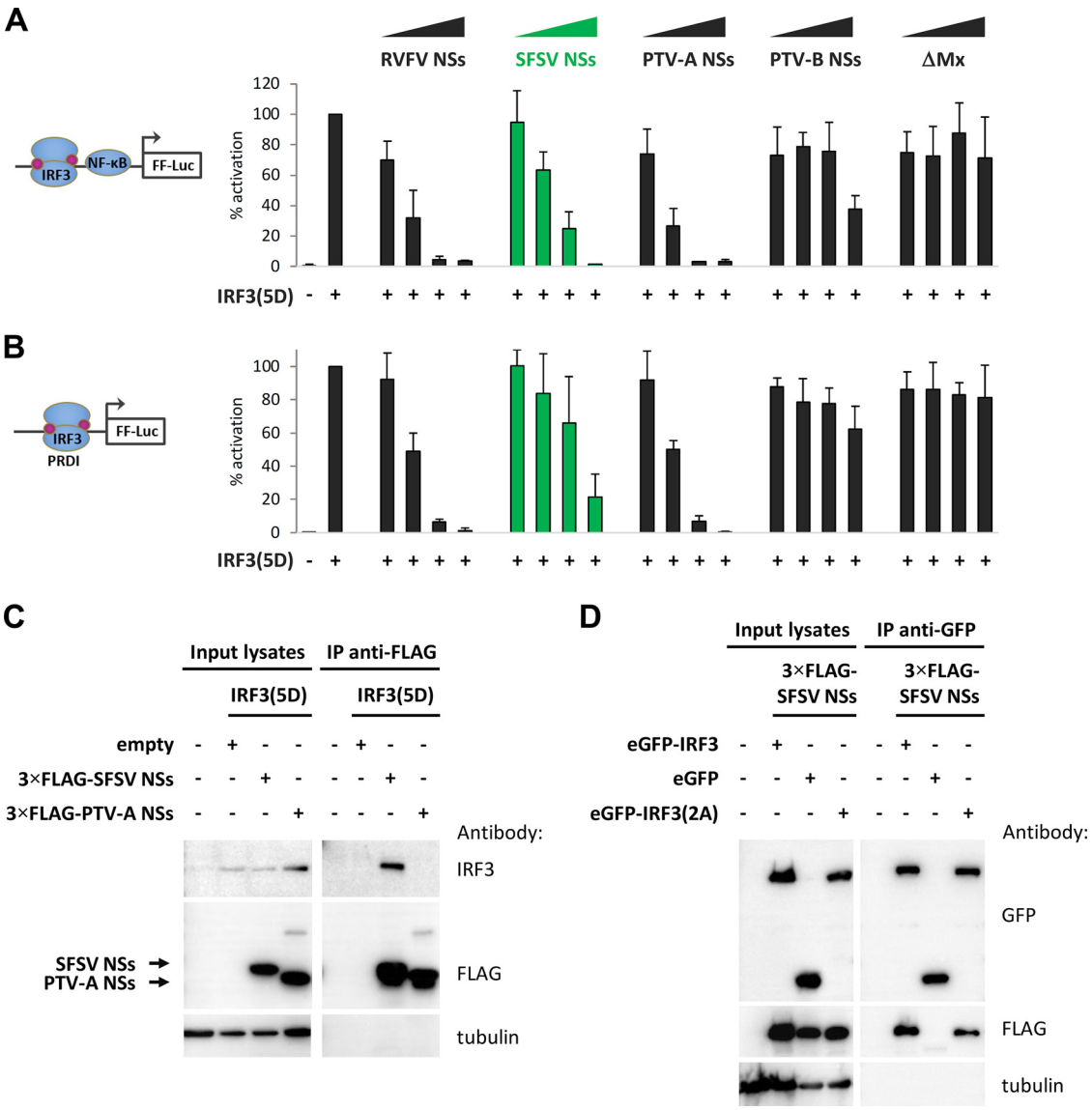

FIG 7 Phosphomimetic and dimerization-deficient IRF3 mutants. (A and B) Promoter reporter assays were performed under conditions of stimulation with a phosphomimetic, constitutively active IRF3(5D). (A) HEK293 cells were transfected with expression plasmids for NSs of RVFV, SFSV, PTV-A, or PTV-B or inactive control ΔMx, as well as firefly and *Renilla* luciferase reporters, under the control of the IFN-β and constitutively active simian virus 40 (SV40) promoters, respectively. IFN-β induction was stimulated by overexpression of IRF3(5D) and total plasmid adjusted to equal levels with empty vector. Firefly activities were normalized to those of *Renilla*, and the stimulation control was set to 100% ($n = 3$; means ± SD). (B) A dual-luciferase assay was performed in parallel with a PRDI-responsive firefly luciferase reporter ($n = 3$; means ± SD). (C and D) Interaction with IRF3 mutants. (C) 3×FLAG-tagged SFSV NSs or PTV-A NSs was coexpressed with IRF3(5D) in HEK293 cells. Cell lysates were then subjected to immunoprecipitation using an antibody against FLAG that was covalently coupled to magnetic beads beforehand. (D) GFP-IRF3(S385/386A), eGFP-IRF3, or eGFP, as well as 3×FLAG-tagged SFSV NSs, was obtained by transient transfection of HEK293 cells. Immunoprecipitation was performed via the use of GFP.

cleotide, indicating the absence of intrinsic or indirect DNA-binding activity. Thus, we conclude that SFSV NSs stoichiometrically impairs the binding of IRF3 to the IFN-β promoter by covering essential amino acid residues within the DBD.

DISCUSSION

SFSV, first isolated in 1943 (11), is one of the geographically most widespread members of the genus phlebovirus, with high seroprevalence rates in regions of endemicity (12–20). Despite the long-standing association with an acute incapacitating disease, little is known about the interaction of SFSV with the host cell. Also, there is no

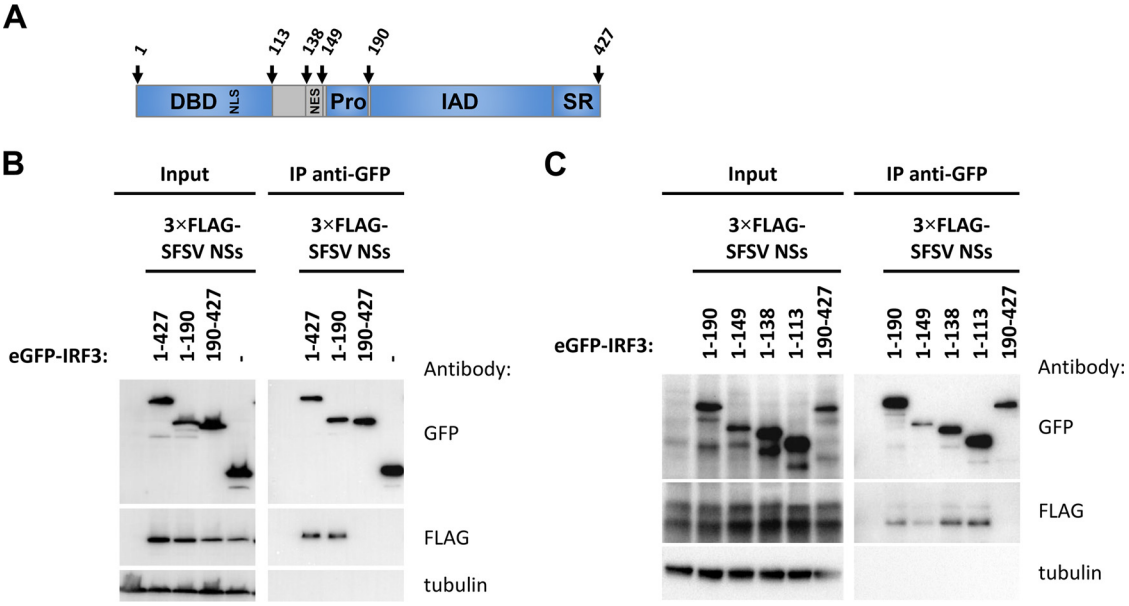

FIG 8 FIG 8 Domain mapping of binding region within IRF3. (A) Schematic representation of the IRF3 domain structure. IRF3 contains a DNA-binding domain (DBD, aa 1 to 113) with an embedded bipartite nuclear localization signal(s) (NLS; K77/R78 and R86/K87), a nuclear export signal (NES; aa 139 to 150), and a proline-rich region (Pro;aa 150 to 190) directly followed by the IRF association domain (IAD; aa 190 to 384) and a serine-rich region (SR; aa 384 to 427) at the C terminus. (B) eGFP-fused full-length IRF3, its N-terminal portion (1–190) or C-terminal portion (190–427), or eGFP alone was expressed together with 3×FLAG-tagged SFSV NSs in HEK293 cells, followed by immunoprecipitation via the use of GFP and immunoblotting. (C) A series of successively truncated eGFP-IRF3 mutants were produced from DNA templates by coupled *in vitro* transcription-translation and added to lysates of HEK293 cells expressing 3×FLAG-tagged SFSV NSs for subsequent immunoprecipitation via the use of GFP.

established animal model (11, 24), prompting earlier researchers to fall back on experiments with human volunteers (9).

We found that the induction of IFN-β in SFSV-infected cells is inhibited by NSs, although SFSV does not destroy any of the key antiviral host factors that other dipteran-borne phleboviruses attack. Rather, SFSV NSs binds to the DBD of IRF3, thus prohibiting IFN-β promoter activation. Curiously, none of the other IRF family members, including the master regulator IRF7 (66), are targeted, indicating high specificity. Although a significant role in the generation of a full IFN response has been attributed to the IFN-inducible IRF7 (66), the constitutively expressed IRF3 is indispensable for the induction of a first wave of IFN-β expression from virus-infected cells and the subsequent upregulation of IRF7 expression (30, 31). Hence, *Irf3* knockout mice exhibit substantially increased susceptibility to viral infection (31, 67). IRF3 activation is the target of a number of virulence factors (28), e.g., human papillomavirus 16 (HPV16) E6 (68), the V protein of paramyxoviruses (69), herpes simplex virus 1 (HSV-1) VP16 (70), and rotavirus NSP1 (71). However, in contrast to SFSV NSs, these virulence factors affect phosphorylation, dimerization, nuclear accumulation, or the expression level of IRF3. SFSV NSs interacted with nonactivated and constitutively active (and dimerized) as well as dimerization-incompetent IRF3, suggesting an ability to target IRF3 both before and after it becomes activated. Moreover, this interaction pattern pointed to a region of IRF3 that is accessible independently of its activation and dimerization state. Domain mapping consistently revealed that the N-terminal DBD alone was sufficient for binding of SFSV NSs. Taking the data together, including the interference with SFSV NSs at a late stage in the signaling pathway on the one hand and the domain mapping on the other hand, a mechanism involving the sequestration of the DBD by SFSV NSs from the IFN-β promoter was strongly implied, and its presence was confirmed by a promoter binding assay.

The N-terminal DNA-binding domain of interferon regulatory factors is about 120 amino acid residues long and displays a conserved architecture consisting of three α

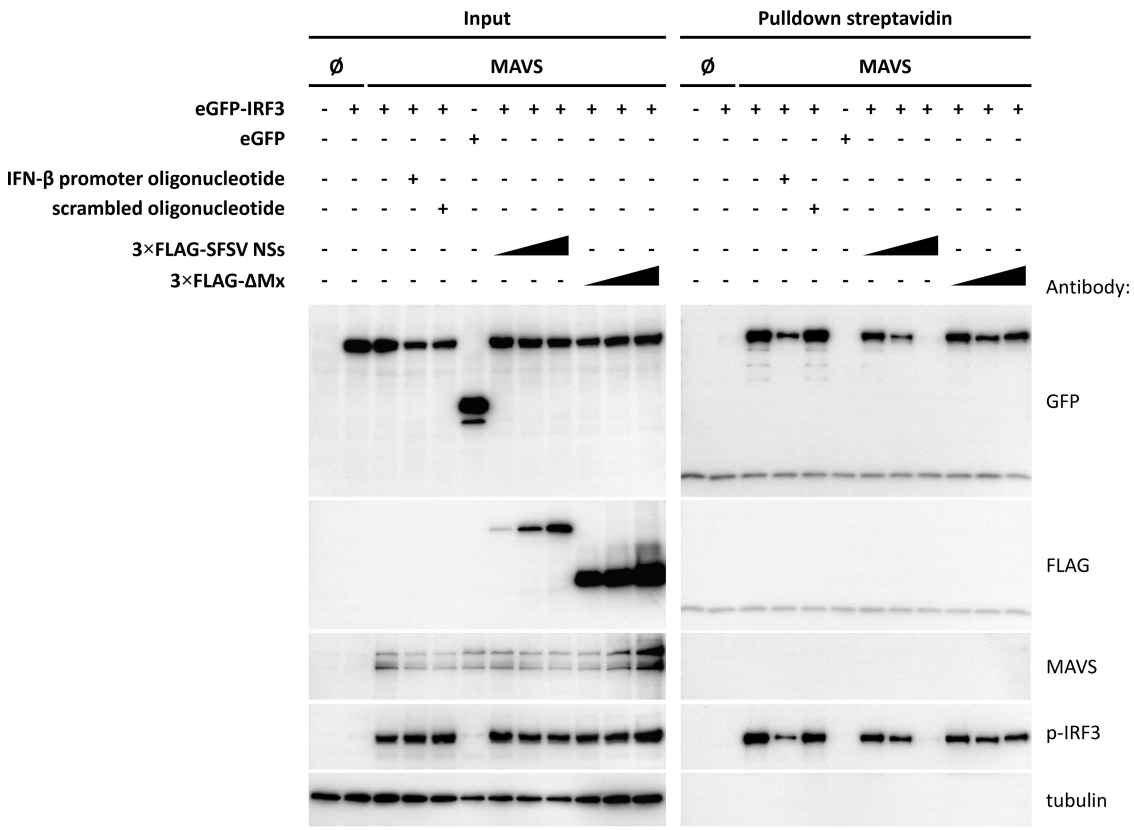

FIG 9 IFN-β promoter binding assay. HEK293 cells were cotransfected with plasmids encoding eGFP-IRF3 or eGFP or MAVS, as well as with increasing amounts of plasmids encoding 3×FLAG-tagged SFSV NSs, or the 3×FLAG-tagged control protein ΔMx, as indicated. Cell lysates were then incubated with an unlabeled, double-stranded DNA oligonucleotide comprising the IFN-β promoter or with a scrambled control oligonucleotide or were left untreated. Next, streptavidin-coated magnetic beads covered with biotinylated IFN-β promoter oligonucleotide were used to pull down activated IRF3. Bound proteins were eluted by boiling in Laemmli buffer and analyzed by immunoblotting.

helices, four β sheets, and three loops (L1 to L3) in the order α1-β1-β2-L1-α2-L2-α3-β3-L3-β4 (51). As SFSV NSs (i) interferes with the promoter binding activity of IRF3 but (ii) does not interact with other IRF family members, one could speculate that it targets amino acid residues that are involved in DNA binding but that are not conserved within the IRF family. IRF3 residues L42, R78, and R86 are both nonconserved and involved in specific DNA promoter binding (51). However, R78 and R86 are also part of the bipartite IRF3 NLS. Since SFSV NSs does not interfere with the nuclear importation of IRF3, these residues are less likely to mediate the interaction with SFSV NSs. That leaves DNA binding residue L42 (situated in loop L1) as well as less-conserved strands β3 and β4 and loops L2 and L3 as the most probable candidate binding sites for SFSV NSs.

Among the other viral proteins known to target IRF3, only US1 (also ICP22) of herpes simplex virus 2 and NP1 of human bocavirus have been described to employ a similar mechanism (72, 73). Like SFSV, both these viruses target the IRF3 DBD and disrupt promoter binding, but whether this is restricted to IRF3 or also true for any other member of the IRF family was not addressed. Kaposi's sarcoma-associated herpesvirus proteins K-bZIP and LANA-1 also prevent the binding of activated IRF3 to its cognate promoter sites but do so by occupying the promoter sites themselves (74, 75), which we did not observe for SFSV NSs. In addition to these DNA viruses, bovine viral diarrhea virus interferes with promoter binding and then induces the degradation of nuclear IRF3 via its NPro protein (76, 77). A direct interaction between NPro and IRF3 could not be demonstrated, however. Hence, to our knowledge SFSV NSs seems to be the only virulence factor from an RNA virus which acts by directly masking the DBD of IRF3 to prevent promoter binding and IFN induction.

Given the remarkable diversity of the phleboviral NSs proteins with respect to sequences, subcellular localizations, and molecular mechanisms, it is tempting to speculate on a correlation between the specific anti-IFN strategy of a given NSs protein and the degree of virulence of the respective phlebovirus. The NSs of highly virulent RVFV uses multiple strategies, mostly based on proteasomal degradation, to globally and rapidly blunt host gene expression at the transcriptional and posttranscriptional levels (3, 32). The NSs of the highly virulent SFTSV abrogates IFN induction by sequestering several key signaling components, including RIG-I and TBK1, into cytoplasmic aggregates (40–43). The intermediately pathogenic TOSV acts by degrading RIG-I itself (39), but its NSs seems to be degraded along with its host target, cutting down its inhibitory efficiency (78). The NSs of the apathogenic Uukuniemi virus (UUKV), in contrast, does not significantly inhibit IFN induction (79, 80). How does the intermediately pathogenic SFSV fit into this picture? On the one hand, by masking the DBD to sterically hinder IRF3 from binding the IFN-β promoter, SFSV NSs blocks IRF3 independently of its conformation or activation state. On the other hand, however, this stoichiometric mechanism requires NSs to accumulate to levels that are sufficient for sequestering the cellular pool of IRF3, which, during the early phase of infection, outnumbers NSs. Moreover, SFSV NSs inhibition does not include IRF7, the master regulator of innate immunity (66). Thus, SFSV NSs fail to impair IFN induction in cells where upregulation of IRF7 took place before infection or in cells with physiologically high basic levels of IRF7, such as plasmacytoid dendritic cells (81). In other words, the stoichiometric and IRF3-specific nature of the anti-IFN induction strategy makes SFSV NSs a modulator rather than a full antagonist of IFN induction. This places SFSV between TOSV and UUKV with regard to both anti-IFN strategy (RIG-I degradation versus weak IFN antagonism) and virulence (fever and meningitis/encephalitis versus no disease).

Curiously, PTV-A does not seem to quite fit the picture; while its NSs protein seems to act as a global host transcription inhibitor, infection of humans has so far been associated only with febrile symptoms. In rodent models, such as mouse and hamster, however, PTV-A and chimeric RVFVs that express PTV-A NSs are also highly virulent (50, 82, 83), suggesting that PTV may be an outlier with respect to humans but not other mammals. Thus, the demonstration that the intermediately virulent SFSV specifically targets IRF3 in a highly specific and stoichiometric (i.e. nondestructive) manner supports our hypothesis that the molecular strategy employed by the NSs protein can correlate with the degree of virulence of the parental phlebovirus, although other factors, e.g., cell tropism, RNA polymerase activity, species-specific host protein interactions, and escape from adaptive immunity, are of course equally important.

MATERIALS AND METHODS

Cells, viruses, and plasmids. A549, BHK-21, HEK293, HEK293T, Vero B4, and Vero E6 cells were cultured in Dulbecco's minimal essential medium (DMEM) and CCM34 medium (DMEM with addition of 17.8 mg/liter L-alanine, 0.7 g/liter glycine, 75 mg/liter L-glutamic acid, 25 mg/liter L-proline, 0.1 mg/liter biotin, 25 mg/liter hypoxanthine, and 3.7 g/liter sodium bicarbonate) supplemented with 10% fetal calf serum (FCS), 2 mM glutamine, 100 U/ml penicillin, and 100 μg/ml streptomycin.

The Sabin strain of SFSV was obtained from the World Reference Center for Emerging Viruses and Arboviruses (WRCEVA) and propagated in Vero B4 cells. Attenuated RVFV strains MP12 and clone 13 were propagated in BHK-21 cells. Recombinant RVFV strains rZH548, rZH548ΔNSs, rZH548ΔNSs::NSsSFSV, and rZH548ΔNSs::NSsTOSV have been described previously (44, 84, 85). rZH548ΔNSs::NSsPTV-A, rZH548ΔNSs::PTV-B, and rZH548ΔNSs::NSsSFSV-CTAP were generated using a polymerase I (Pol I)/Pol II-based rescue system as described for the other recombinant RVFV strains (35, 53, 85). In brief, NSs coding sequences for PTV-A and PTV-B NSs (GenBank accession no. EF201835 and EF201834, respectively) were obtained by gene synthesis (Mr. Gene) and inserted into modified S-segment rescue plasmid pHH21_RVFV_vN_TCS. The reading frame of SFSV NSs was amplified from cDNA of infected cells and inserted into rescue plasmid pHH21_RVFV_vN_MCS_CTAP, which contains a C-terminal tag for tandem affinity purification (TAP). Primer sequences are available on request. The resulting plasmids were transfected together with L- and M-segment rescue plasmids pHH21_RVFV_vL and pHH21_RVFV_vM, respectively, as well as helper plasmids pl.18_RVFV_L and pl.18_RVFV_N into cocultures of HEK293T and BHK-21 cells. Recombinant RVFV strains were harvested 5 days after transfection, propagated in Vero E6 cells, and characterized by RT-PCR and sequencing of the N- and NSs-coding

regions. Titers of all virus strains were determined on Vero E6 cells via plaque assay. Both the cell lines and the virus stocks were routinely tested for mycoplasma contamination.

To generate constructs encoding 3×FLAG-tagged NSs of SFSV (GenBank accession no. EF201822.1), PTV-A, or PTV-B, the viral open reading frames were amplified from cDNA (SFSV) or synthesized DNA (PTV-A and PTV-B) and inserted into pl.18 by ligation-dependent cloning via the use of 5′ BamHI and 3′ XhoI restriction sites. Primer sequences are available on request. pl.18-NSsRVFV-3×FLAG and pl.18-3×FLAG-ΔMx were described before (35). Firefly luciferase reporter constructs p-125Luc, p-55C1BLuc, and p-55A2Luc (52) were kindly donated by Takashi Fujita, and pRL-SV40 was purchased from Promega. Expression plasmids for human TBK1 (86) and IRF3(5D) (55) were kindly provided by John Hiscott, for human MAVS by Shizuo Akira (87), and for full-length pEGFP-C1-IRF3 (88) and all other pEGFP-C1-IRFs by Luis Martinez-Sobrido and Adolfo Garcia-Sastre. pEGFP-C1 was from Clontech. pcDNA3.1(+)-eGFP-IRF7, pEGFP-C1-IRF3(1-190), pEGFP-C1-IRF3(190-427), pEGFP-C1-IRF3(385A/S386A), pEGFP-C1-IRF3(S385A/S386A-R211A/R213A), and pEGFP-C1-IRF3(S385A/S386A-R285A/H288A/H290A) were generated via gene synthesis and subcloning (BioCat and Eurofins Genomics).

siRNA-mediated knockdown and infection. Reverse transfection of A549 cells (1×10^5 per 24-well) with either control siRNA (1027280; Qiagen) or a pool of four custom-designed siRNA oligonucleotides targeting SFSV NSs (siNSs1 [5′-TTG GGT CTT AGT GAT GAG CAT-3′], siNSs2 [5′-AAG GGA TCA GCT AAT GTC TTA-3′], siNSs3 [5′-TAC AAT AAA TTT CAC ACT CAT-3′], and siNSs4 [5′-AAG GCT CTT AGC TGG CCA CTA-3′]; Qiagen) via the use of Lipofectamine RNAiMax (Life Technologies) was performed according to the manufacturer's recommendations. Cells were washed with sterile phosphate-buffered saline (PBS) at 24 h posttransfection and inoculated with virus diluted to a multiplicity of infection (MOI) of 1 in CCM34 supplemented with 2% FCS and antibiotics. After 1 h of incubation at 37°C, the inoculate was replaced by CCM34 supplemented with 10% FCS and antibiotics. For concomitant transfection of siRNA and plasmid DNA, Lipofectamine 2000 was used instead.

Reverse transcriptase PCR (RT-PCR). RNA was isolated using an RNeasy minikit (Qiagen) as recommended by the manufacturer. RNA from infected cells was subjected to DNase I digestion and cDNA synthesis using a PrimeScript RT reagent kit with genomic DNA (gDNA) Eraser (TaKaRa). Transcript levels of host genes were detected with SYBR Premix Ex *Taq* (Tli RNaseH Plus) (TaKaRa) and QuantiTect primers (human *IFNB*, QT00203763; *RRN18S*, QT00199367; Qiagen), whereas viral genomic segments were detected with Premix Ex *Taq* (Probe qPCR) (TaKaRa) and previously published primers and probes for the SFSV and RVFV S and L segments (for SFSV S, fwd, 5′-TGC ACT CAT CCA AGC TAT GTG-3′, rev, 5′-GAG GGC TAC AAA CAA GGG ATC-3′, probe, 6-carboxyfluorescein [FAM]-TCC CCC ATT CTC AGA ATG TAA GAC ATT AGC-black hole quencher 1 [BHQ-1] [89]; for SFSV L, fwd, 5′-TCT GAG AAC TGA GCT ACA AGT GTT TAT TA-3′, rev, 5′-TTC CCA TCT CTC TTC TGA AGA GTG-3′, probe, FAM-AGG TCA TAG ACA GTA TCA TGA GAA TTG CTA GGT G-BHQ-1 [4]; for RVFV S, fwd, 5′-TGC CAC GAG TYA GAG CCA-3′, rev, 5′-GTG GGT CCG AGA GTY TGC-3′, probe, FAM-TCC TTC TCC CAG TCA GCC CCA C-BHQ-1 [89]). Fold induction was calculated according to the threshold cycle ($\Delta\Delta C_T$) method using 18S rRNA as a housekeeping gene.

RNA from transfected cells was subjected to DNase I digestion (Fermentas), and NSs transcripts were amplified via OneStep RT-PCR (Qiagen) according to the manufacturer's instructions (for SFSV NSs, fwd, 5′-ATA TGG ATC CAT GAA CAG CCA GTA CAT GTT-3′, rev, 5′-GAC ACT CGA GTC AAA AGT CAG AGT CAG ACG-3′; for PTV-A NSs, fwd, 5′-GAG AGG ATC CAT GTC CAA CAT AAA CTA TTA TG-3′, rev, 5′-GAC ACT CGA GTT ATA TGT CTT GAT TTA GCA TTG-3′). Amplification products were run on 1.5% agarose gels and visualized with ethidium bromide.

Immunoblot analysis. Protein samples were run on 12% acrylamide gels and transferred to polyvinylidene fluoride (PVDF) membranes (Millipore) via semidry blotting. After blocking in Tris-buffered saline (TBS) with 5% bovine serum albumin (BSA) or milk powder, primary antibody staining was performed for 1 h at room temperature or overnight at 4°C. Membranes were washed in TBS–0.1% Tween 20, stained with secondary antibodies for 45 min, and washed again in TBS–0.1% Tween 20 and once in TBS. Finally, membranes were developed with a SuperSignal West Femto kit (Pierce) and bands visualized using a ChemiDoc imaging system (Bio-Rad).

Primary antibodies were as follows: RIG-I (ag-20b-0009; AdipoGen) (1:1,000), MAVS (ALX-210-929; Alexis) (1:1,000), TBK1 (IMG-139A; Imgenex) (1:1,000), PKR (610764; BD Transduction Laboratories) (1:1,000), IRF3 (sc-9082; Santa Cruz) (1:500), p62 (ab55199; Abcam) (1:2,000), GFP (3h9; Chromotek) (1:2,000), FLAG (F3165; Sigma) (1:2,000), p-IRF3 (catalog no. 4947; Cell Signaling) (1:1,000), tubulin (ab6046; Abcam) (1:2,500), SFSV N (mouse immune ascites fluid, provided by WRCEVA) (1:1,000), and RVFV N (rabbit hyperimmune serum, provided by Alenjandro Brun) (1:1,000). Secondary antibodies comprised anti-mouse (0031430 1892913; Thermo Fisher), anti-rabbit (0031460 1892914; Thermo Fisher), and anti-rat (712-036-150; Jackson Immuno Research) antibodies or were substituted by protein A horseradish peroxidase (HRP) conjugate (18-160; Millipore) (1:10,000).

Dual-luciferase assay. HEK293 cells seeded into 96-well plates (1.5×10^4 per well) were transfected the following day with firefly and *Renilla* luciferase reporter constructs (40 ng each), as well as expression constructs for MAVS (10 ng) and NSs proteins or the control protein ΔMx (0.1 ng, 1 ng, and 10 ng) via the use of TransIT-LT1 (Mirus Bio LLC). The total plasmid DNA amounts were adjusted to equal levels with empty vector pl.18. Cells were processed 24 h after transfection, and luciferase activities were measured with a dual-luciferase reporter assay system (Promega) according to the manufacturer's recommendations. Firefly luciferase activities were normalized to those of *Renilla* luciferase, and the stimulated control samples were set to 100% within each biological replicate. Means and standard deviations (SD) were calculated across the indicated number of biological replicate data sets.

Proteomics. As described previously (35, 53), approximately 2×10^8 HEK293T cells were infected with the recombinant RVFV strain expressing TAP-tagged SFSV NSs (rZH548ΔNSs::NSsSFSV-CTAP) at an

MOI of 5. The cells were washed with and scraped off in prechilled PBS at 16 h postinfection (hpi). The cell pellet was snap-frozen in liquid nitrogen, lysed in TAP buffer (50 mM Tris-HCl [pH 7.5], 100 mM NaCl, 0.2% NP-40, 5% glycerol) supplemented with protease and phosphatase inhibitors, snap-frozen again, and stored at −80°C until further processing. TAP purification was performed by sequential pulldowns using streptavidin agarose and HA-agarose beads. Bound protein complexes were eventually eluted in Laemmli buffer and subjected to one-dimensional SDS-PAGE prior to trypsin digestion and peptide analysis by liquid chromatography-tandem mass spectrometry (LC-MS/MS), which was described in detail elsewhere (53).

Coimmunoprecipitation. HEK293 cells (2.5×10^6 per 10-cm-diameter dish) were transfected with expression plasmids (4 μg each) via the calcium phosphate method. Cells were washed twice in PBS the following day and lysed in prechilled lysis buffer (50 mM Tris-HCl [pH 7.0], 150 mM NaCl, 1% IGEPAL-630) freshly supplemented with protease (Roche) (complete, EDTA-free) and phosphatase inhibitors (Phosphatase Inhibitor Cocktail set II; Calbiochem). Finally, cell debris was removed by centrifugation (10,000 × *g*, 10 min, 4°C), and the supernatants were used for further processing.

For immunoprecipitation via the use of GFP, supernatants were applied to prewashed wells of a GFP-multiTrap (Chromotek) and incubated at 4°C for 60 to 90 min under conditions of mild shaking. Wells were washed extensively with lysis buffer and bound proteins eluted for 20 min with preheated Laemmli buffer under conditions of strong agitation. For immunoprecipitation via the use of FLAG, magnetic beads (143-21D; Invitrogen) were covalently coupled with FLAG M2 antibody (F3165; Sigma) overnight and processed according to the manufacturer's recommendations. Lysates were then added to the coupled beads followed by incubation under conditions of rotation at 4°C for 4 h. After extensive washing, bound proteins were eluted by boiling in Laemmli buffer at 94°C for 5 min.

To map the binding region within IRF3, constructs comprising a T7 promoter, the open reading frames (ORF) of the respective truncated IRF3 mutants fused to eGFP, a stop codon, and a poly(A) stretch were assembled via PCR (primer sequences available on request) and purified via gel extraction (Omega Bio-tek) and DNA precipitation. The respective proteins were then produced by coupled *in vitro* transcription-translation using rabbit reticulocyte lysate (L4610; Promega) and added to lysate of HEK293 cells transiently expressing SFSV NSs. Immunoprecipitation via GFP was performed according to the aforementioned protocol.

IRF3 dimerization assay. A549 cells infected with SFSV were lysed as described above and then processed as described before (90). In brief, 10% native polyacrylamide gels were prerun at 25 mA for 30 min in native running buffer (25 mM Tris, 192 mM glycine, pH 8.3), with 1% deoxycholate added to the cathode buffer. Samples were supplemented with native loading buffer (250 mM Tris-HCl [pH 6.8], 50% glycerol, 1% deoxycholate, 0.5% bromophenol blue), run at 20 mA for the desired duration, and finally transferred to PVDF membranes via semidry blotting.

Immunofluorescence assay. A549 cells were seeded onto glass coverslips (1×10^5 per 24 wells) 1 day prior to infection at an MOI of 1. The cells were washed with PBS at 12 hpi and fixed overnight in PBS–4% paraformaldehyde (PFA) at 4°C. The coverslips were then washed with PBS, and the cells were permeabilized with PBS–0.1% Triton X-100, washed again, and blocked in PBS–1% FCS. Staining with primary antibodies diluted in blocking buffer (IRF3 FL-425, 1:200; SFSV, 1:2,500) was performed for 1 h in a humid chamber. Afterward, the coverslips were washed with PBS and incubated with secondary antibodies (Alexa Fluor 488 donkey anti-mouse [A21202] and Alexa Fluor 647 donkey anti-rabbit [A31573]; Thermo Fisher Scientific) (both 1:500) and 4′,6-diamidino-2-phenylindole (DAPI) (0.1 μg/ml) for 45 min in a humid chamber. Samples were washed again in PBS, rinsed in demineralized water, and mounted on microscopic slides using FluorSave reagent (Calbiochem). Confocal microscopy was performed using a Leica SP5 microscope and the accompanying software.

Promoter binding assay. Biotinylated DNA covering the IRF3-responsive positive regulatory domains within the human IFN-β promoter and the downstream sequence as a linker (GenBank accession no. EF064725.1) was ordered as complementary single DNA strands (sense, 5′-GAC ATA GGA AAA CTG AAA GGG AGA AGT GAA AGT GGG AAA TTC CTC TGA ATA GAG AGA GGA CCA TCT CAT ATA AAT AGG CCA TAC CCA TGG AGA AAG GAC ATT-biotin-3′; antisense, 5′-AAT GTC CTT TCT CCA TGG GTA TGG CCT ATT TAT ATG AGA TGG TCC TCT CTC TAT TCA GAG GAA TTT CCC ACT TTC ACT TCT CCC TTT CAG TTT TCC TAT GTC-3′) and subsequently annealed by initial denaturation at 95°C for 5 min, followed by slow cooling (1°C/min) to room temperature (91). The double-stranded biotinylated oligonucleotide (10 pmol per sample) was bound to streptavidin-coated magnetic beads (Dynabeads M-280 streptavidin; Invitrogen) (25 μl per sample) according to the manufacturer's instructions. HEK293 cells seeded into 6 wells (2.5×10^5 per well) were transfected with plasmids coding for eGFP-IRF3 or for eGFP (250 ng), MAVS (500 ng), 3×FLAG-tagged SFSV NSs, or ΔMx (25, 250, or 500 ng) and empty vector (to adjust plasmid amounts) via the use of TransIT-LT1 and lysed in the presence of protease and phosphatase inhibitors as described above. Lysates were then incubated with 250 pmol of the corresponding untagged IFN-β promoter oligonucleotide or 250 pmol of scrambled control oligonucleotide (sense, 5′-TTA CAG GAA AGA GGT ACC CAT ACC GGA TAA ATA TAC TCT ACC AGG AGA GAG ATA AGT CTC CTT AAA GGG TGA AAG TGA AGA GGG AAA GTC AAA AGG ATA CAG-3′; antisense, 5′-CTG TAT CCT TTT GAC TTT CCC TCT TCA CTT TCA CCC TTT AAG GAG ACT TAT CTC TCT CCT GGT AGA GTA TAT TTA TCC GGT ATG GGT ACC TCT TTC CTG TAA-3′) or were left untreated. After addition of oligonucleotide-coupled magnetic beads, samples were incubated under conditions of rotation for 90 min. The beads were washed four times in lysis buffer prior to elution of bound proteins in Laemmli buffer at 94°C for 5 min and analysis via SDS-PAGE and Western blotting.

ACKNOWLEDGMENTS

We are grateful to Besim Berisha for excellent technical assistance. We are indebted to Patricia Aguilar and Robert Tesh from the World Reference Center for Emerging Viruses and Arboviruses (WRCEVA) for providing the Sabin strain of SFSV along with mouse immune ascites fluid and to Alejandro Brun for providing anti-RVFV antiserum. Expression and luciferase reporter constructs were kind gifts from John Hiscott, Takashi Fujita, Luis Martinez-Sobrido, Adolfo Garcia-Sastre, and Shizuo Akira.

Work in our laboratories was supported by the Deutsche Forschungsgemeinschaft (grant SFB 1021 to F.W. and grants PI1084/2, PI1084/3, TRR179, and TRR237 to A.P.), by an ERC starting grant (ERC-StG iVIP no. 311339) to A.P., and by the Bundesministerium für Bildung und Forschung (Infect-ERA; grants "ESCential" and "ERASE" to F.W. and A.P., respectively).

REFERENCES

1. Elliott RM, Brennan B. 2014. Emerging phleboviruses. Curr Opin Virol 5:50–57. https://doi.org/10.1016/j.coviro.2014.01.011.
2. McMullan LK, Folk SM, Kelly AJ, MacNeil A, Goldsmith CS, Metcalfe MG, Batten BC, Albarino CG, Zaki SR, Rollin PE, Nicholson WL, Nichol ST. 2012. A New phlebovirus associated with severe febrile illness in Missouri. N Engl J Med 367:834–841. https://doi.org/10.1056/NEJMoa1203378.
3. Wuerth JD, Weber F. 2016. Phleboviruses and the type I interferon response. Viruses 8:174. https://doi.org/10.3390/v8060174.
4. Carhan A, Uyar Y, Ozkaya E, Ertek M, Dobler G, Dilcher M, Wang Y, Spiegel M, Hufert F, Weidmann M. 2010. Characterization of a sandfly fever Sicilian virus isolated during a sandfly fever epidemic in Turkey. J Clin Virol 48:264–269. https://doi.org/10.1016/j.jcv.2010.05.011.
5. Anagnostou V, Pardalos G, Athanasiou-Metaxa M, Papa A. 2011. Novel phlebovirus in febrile child, Greece. Emerg Infect Dis 17:940–941. https://doi.org/10.3201/eid1705.101958.
6. Charrel RN, Moureau G, Temmam S, Izri A, Marty P, Parola P, da Rosa AT, Tesh RB, de Lamballerie X. 2009. Massilia virus, a novel Phlebovirus (Bunyaviridae) isolated from sandflies in the Mediterranean. Vector Borne Zoonotic Dis 9:519–530. https://doi.org/10.1089/vbz.2008.0131.
7. Palacios G, da Rosa AT, Savji N, Sze W, Wick I, Guzman H, Hutchison S, Tesh R, Lipkin WI. 2011. Aguacate virus, a new antigenic complex of the genus Phlebovirus (family Bunyaviridae). J Gen Virol 92:1445–1453. https://doi.org/10.1099/vir.0.029389-0.
8. Alkan C, Vaziri VM, Ayhan N, Badakhshan M, Bichaud L, Rahbarian N, Javadian EA, Alten B, de Lamballerie X, Charrel RN. 2017. Isolation and sequencing of Dashli virus, a novel Sicilian-like virus in sandflies from Iran; genetic and phylogenetic evidence for the creation of one novel species within the Phlebovirus genus in the Bunyaviridae family. PLoS Negl Trop Dis 11:e0005978. https://doi.org/10.1371/journal.pntd.0005978.
9. Bartelloni PJ, Tesh RB. 1976. Clinical and serologic responses of volunteers infected with phlebotomus fever virus (Sicilian type). Am J Trop Med Hyg 25:456–462. https://doi.org/10.4269/ajtmh.1976.25.456.
10. Birt C. 1915. Phlebotomus or sandfly fever. Br Med J 2:168–169. https://doi.org/10.1136/bmj.2.2848.168.
11. Sabin AB. 1951. Experimental studies on Phlebotomus (pappataci, sandfly) fever during World War II. Arch Gesamte Virusforsch 4:367–410. https://doi.org/10.1007/BF01241161.
12. Alwassouf S, Christodoulou V, Bichaud L, Ntais P, Mazeris A, Antoniou M, Charrel RN. 2016. Seroprevalence of sandfly-borne phleboviruses belonging to three serocomplexes (sandfly fever Naples, sandfly fever Sicilian and Salehabad) in dogs from Greece and Cyprus using neutralization test. PLoS Negl Trop Dis 10:e0005063. https://doi.org/10.1371/journal.pntd.0005063.
13. Alwassouf S, Maia C, Ayhan N, Coimbra M, Cristovao JM, Richet H, Bichaud L, Campino L, Charrel RN. 2016. Neutralisation-based seroprevalence of Toscana virus and sandfly fever Sicilian virus in dogs and cats from Portugal. J Gen Virol 97:2816–2823. https://doi.org/10.1099/jgv.0.000592.
14. Ergunay K, Ayhan N, Charrel RN. 2017. Novel and emergent sandfly-borne phleboviruses in Asia Minor: a systematic review. Rev Med Virol 27:e1898. https://doi.org/10.1002/rmv.1898.
15. Gaĭdamovich SY, Khutoretskaya NV, Asyamov YV, Tsyupa VI, Mel'nikova EE. 1990. Sandfly fever in central Asia and Afghanistan. Arch Virol Suppl 1:287–293.
16. Goverdhan MK, Dhanda V, Modi GB, Bhatt PN, Bhagwat RB, Dandawate CN, Pavri KM. 1976. Isolation of phlebotomus (sandfly) fever virus from sandflies and humans during the same season in Aurangabad District, Maharashtra State, India. Indian J Med Res 64:57–63.
17. Sakhria S, Alwassouf S, Fares W, Bichaud L, Dachraoui K, Alkan C, Zoghlami Z, de Lamballerie X, Zhioua E, Charrel RN. 2014. Presence of sandfly-borne phleboviruses of two antigenic complexes (sandfly fever Naples virus and sandfly fever Sicilian virus) in two different biogeographical regions of Tunisia demonstrated by a microneutralisation-based seroprevalence study in dogs. Parasit Vectors 7:476. https://doi.org/10.1186/s13071-014-0476-8.
18. Woyessa AB, Omballa V, Wang D, Lambert A, Waiboci L, Ayele W, Ahmed A, Abera NA, Cao S, Ochieng M, Montgomery JM, Jima D, Fields B. 2014. An outbreak of acute febrile illness caused by sandfly fever Sicilian virus in the Afar region of Ethiopia, 2011. Am J Trop Med Hyg 91:1250–1253. https://doi.org/10.4269/ajtmh.14-0299.
19. Ayhan N, Sherifi K, Taraku A, Berxholi K, Charrel RN. 2017. High Rates of neutralizing antibodies to Toscana and sandfly fever Sicilian viruses in livestock, Kosovo. Emerg Infect Dis 23:989–992. https://doi.org/10.3201/eid2306.161929.
20. Eitrem R, Stylianou M, Niklasson B. 1991. High prevalence rates of antibody to three sandfly fever viruses (Sicilian, Naples, and Toscana) among Cypriots. Epidemiol Infect 107:685–691. https://doi.org/10.1017/S0950268800049384.
21. Eitrem R, Niklasson B, Weiland O. 1991. Sandfly fever among Swedish tourists. Scand J Infect Dis 23:451–457. https://doi.org/10.3109/00365549109075093.
22. Eitrem R, Vene S, Niklasson B. 1990. Incidence of sand fly fever among Swedish United Nations Soldiers on Cyprus during 1985. Am J Trop Med Hyg 43:207–211. https://doi.org/10.4269/ajtmh.1990.43.207.
23. Newman ENC, Johnstone P, Bridge H, Wright D, Jameson L, Bosworth A, Hatch R, Hayward-Karlsson J, Osborne J, Bailey MS, Green A, Ross D, Brooks T, Hewson R. 2014. Seroconversion for infectious pathogens among UK military personnel deployed to Afghanistan, 2008–2011. Emerg Infect Dis 20:2015–2022. https://doi.org/10.3201/eid2012.131830.
24. Sabin AB, Philip CB, Paul JR. 1944. Phlebotomus (Pappataci or sandfly) fever a disease of military importance summary of existing knowledge and preliminary report of original investigations. JAMA 125:603–606. https://doi.org/10.1001/jama.1944.02850270001001.
25. Ferron F, Weber F, de la Torre JC, Reguera J. 2017. Transcription and replication mechanisms of Bunyaviridae and Arenaviridae L proteins. Virus Res 234:118–134. https://doi.org/10.1016/j.virusres.2017.01.018.
26. Weber M, Gawanbacht A, Habjan M, Rang A, Borner C, Schmidt AM, Veitinger S, Jacob R, Devignot S, Kochs G, García-Sastre A, Weber F. 2013. Incoming RNA virus nucleocapsids containing a 5′-triphosphorylated genome activate RIG-I and antiviral signaling. Cell Host Microbe 13:336–346. https://doi.org/10.1016/j.chom.2013.01.012.
27. Yoneyama M, Onomoto K, Jogi M, Akaboshi T, Fujita T. 2015. Viral RNA detection by RIG-I-like receptors. Curr Opin Immunol 32:48–53. https://doi.org/10.1016/j.coi.2014.12.012.
28. Marsili G, Perrotti E, Remoli AL, Acchioni C, Sgarbanti M, Battistini A. 2016. IFN regulatory factors and antiviral innate immunity: how viruses

can get better. J Interferon Cytokine Res 36:414–432. https://doi.org/10.1089/jir.2016.0002.
29. Honda K, Takaoka A, Taniguchi T. 2006. Type I interferon gene induction by the interferon regulatory factor family of transcription factors. Immunity 25:349–360. https://doi.org/10.1016/j.immuni.2006.08.009.
30. Marie I, Durbin JE, Levy DE. 1998. Differential viral induction of distinct interferon-alpha genes by positive feedback through interferon regulatory factor-7. EMBO J 17:6660–6669. https://doi.org/10.1093/emboj/17.22.6660.
31. Sato M, Suemori H, Hata N, Asagiri M, Ogasawara K, Nakao K, Nakaya T, Katsuki M, Noguchi S, Tanaka N, Taniguchi T. 2000. Distinct and essential roles of transcription factors IRF-3 and IRF-7 in response to viruses for IFN-alpha/beta gene induction. Immunity 13:539–548. https://doi.org/10.1016/S1074-7613(00)00053-4.
32. Ly HJ, Ikegami T. 2016. Rift Valley fever virus NSs protein functions and the similarity to other bunyavirus NSs proteins. Virol J 13:118. https://doi.org/10.1186/s12985-016-0573-8.
33. Billecocq A, Spiegel M, Vialat P, Kohl A, Weber F, Bouloy M, Haller O. 2004. NSs protein of Rift Valley fever virus blocks interferon production by inhibiting host gene transcription. J Virol 78:9798–9806. https://doi.org/10.1128/JVI.78.18.9798-9806.2004.
34. Copeland AM, Van Deusen NM, Schmaljohn CS. 2015. Rift Valley fever virus NSS gene expression correlates with a defect in nuclear mRNA export. Virology 486:88–93. https://doi.org/10.1016/j.virol.2015.09.003.
35. Kainulainen M, Habjan M, Hubel P, Busch L, Lau S, Colinge J, Superti-Furga G, Pichlmair A, Weber F. 2014. Virulence factor NSs of Rift Valley fever virus recruits the F-box protein FBXO3 to degrade subunit p62 of general transcription factor TFIIH. J Virol 88:3464–3473. https://doi.org/10.1128/JVI.02914-13.
36. Kalveram B, Lihoradova O, Ikegami T. 2011. NSs protein of Rift Valley fever virus promotes posttranslational downregulation of the TFIIH subunit p62. J Virol 85:6234–6243. https://doi.org/10.1128/JVI.02255-10.
37. Le May N, Dubaele S, Proietti De Santis L, Billecocq A, Bouloy M, Egly JM. 2004. TFIIH transcription factor, a target for the Rift Valley hemorrhagic fever virus. Cell 116:541–550. https://doi.org/10.1016/S0092-8674(04)00132-1.
38. Le May N, Mansuroglu Z, Leger P, Josse T, Blot G, Billecocq A, Flick R, Jacob Y, Bonnefoy E, Bouloy M. 2008. A SAP30 complex inhibits IFN-beta expression in Rift valley fever virus infected cells. PloS Pathog 4:e13. https://doi.org/10.1371/journal.ppat.0040013.
39. Gori-Savellini G, Valentini M, Cusi MG. 2013. Toscana virus NSs protein inhibits the induction of type I interferon by interacting with RIG-I. J Virol 87:6660–6667. https://doi.org/10.1128/JVI.03129-12.
40. Chaudhary V, Zhang S, Yuen KS, Li C, Lui PY, Fung SY, Wang PH, Chan CP, Li DX, Kok KH, Liang MF, Jin DY. 2015. Suppression of type I and type III IFN signalling by NSs protein of severe fever with thrombocytopenia syndrome virus through inhibition of STAT1 phosphorylation and activation. J Gen Virol 96:3204–3211. https://doi.org/10.1099/jgv.0.000280.
41. Ning YJ, Wang M, Deng M, Shen S, Liu W, Cao WC, Deng F, Wang YY, Hu Z, Wang H. 2014. Viral suppression of innate immunity via spatial isolation of TBK1/IKKepsilon from mitochondrial antiviral platform. J Mol Cell Biol 6:324–337. https://doi.org/10.1093/jmcb/mju015.
42. Santiago FW, Covaleda LM, Sanchez-Aparicio MT, Silvas JA, Diaz-Vizarreta AC, Patel JR, Popov V, Yu X-J, García-Sastre A, Aguilar PV. 2014. Hijacking of RIG-I signaling proteins into virus-induced cytoplasmic structures correlates with the inhibition of type I interferon responses. J Virol 88:4572–4585. https://doi.org/10.1128/JVI.03021-13.
43. Wu XD, Qi X, Qu BQ, Zhang ZR, Liang MF, Li C, Cardona CJ, Li DX, Xing Z. 2014. Evasion of antiviral immunity through sequestering of TBK1/IKK epsilon/IRF3 into viral inclusion bodies. J Virol 88:3067–3076. https://doi.org/10.1128/JVI.03510-13.
44. Habjan M, Pichlmair A, Elliott RM, Overby AK, Glatter T, Gstaiger M, Superti-Furga G, Unger H, Weber F. 2009. NSs protein of Rift Valley fever virus induces the specific degradation of the double-stranded RNA-dependent protein kinase. J Virol 83:4365–4375. https://doi.org/10.1128/JVI.02148-08.
45. Lihoradova OA, Indran SV, Kalveram B, Lokugamage N, Head JA, Gong B, Tigabu B, Juelich TL, Freiberg AN, Ikegami T. 2013. Characterization of Rift Valley fever virus MP-12 strain encoding NSs of Punta Toro virus or sandfly fever Sicilian virus. PLoS Negl Trop Dis 7:e2181. https://doi.org/10.1371/journal.pntd.0002181.
46. Ikegami T, Narayanan K, Won S, Kamitani W, Peters CJ, Makino S. 2009. Rift Valley fever virus NSs protein promotes post-transcriptional downregulation of protein kinase PKR and inhibits eIF2alpha phosphorylation. PLoS Pathog 5:e1000287. https://doi.org/10.1371/journal.ppat.1000287.
47. Kainulainen M, Lau S, Samuel CE, Hornung V, Weber F. 2016. NSs virulence factor of Rift Valley fever virus engages the F-box proteins FBXW11 and beta-TRCP1 to degrade the antiviral protein kinase PKR. J Virol 90:6140–6147. https://doi.org/10.1128/JVI.00016-16.
48. Mudhasani R, Tran JP, Retterer C, Kota KP, Whitehouse CA, Bavari S. 2016. Protein kinase R degradation is essential for Rift Valley fever virus infection and is regulated by SKP1-CUL1-F-box (SCF)(FBXW11-NSs) E3 ligase. PloS Pathog 12:e1005437. https://doi.org/10.1371/journal.ppat.1005437.
49. Kalveram B, Ikegami T. 2013. Toscana virus NSs protein promotes degradation of double-stranded RNA-dependent protein kinase. J Virol 87:3710–3718. https://doi.org/10.1128/JVI.02506-12.
50. Perrone LA, Narayanan K, Worthy M, Peters CJ. 2007. The S segment of Punta Toro virus (Bunyaviridae, Phlebovirus) is a major determinant of lethality in the Syrian hamster and codes for a type I interferon antagonist. J Virol 81:884–892. https://doi.org/10.1128/JVI.01074-06.
51. Panne D, Maniatis T, Harrison SC. 2007. An atomic model of the interferon-beta enhanceosome. Cell 129:1111–1123. https://doi.org/10.1016/j.cell.2007.05.019.
52. Yoneyama M, Suhara W, Fukuhara Y, Fukuda M, Nishida E, Fujita T. 1998. Direct triggering of the type I interferon system by virus infection: activation of a transcription factor complex containing IRF-3 and CBP/p300. EMBO J 17:1087–1095. https://doi.org/10.1093/emboj/17.4.1087.
53. Pichlmair A, Kandasamy K, Alvisi G, Mulhern O, Sacco R, Habjan M, Binder M, Stefanovic A, Eberle CA, Goncalves A, Burckstummer T, Muller AC, Fauster A, Holze C, Lindsten K, Goodbourn S, Kochs G, Weber F, Bartenschlager R, Bowie AG, Bennett KL, Colinge J, Superti-Furga G. 2012. Viral immune modulators perturb the human molecular network by common and unique strategies. Nature 487:486–490. https://doi.org/10.1038/nature11289.
54. Lin R, Mamane Y, Hiscott J. 1999. Structural and functional analysis of interferon regulatory factor 3: localization of the transactivation and autoinhibitory domains. Mol Cell Biol 19:2465–2474. https://doi.org/10.1128/MCB.19.4.2465.
55. Lin RT, Heylbroeck C, Pitha PM, Hiscott J. 1998. Virus-dependent phosphorylation of the IRF-3 transcription factor regulates nuclear translocation, transactivation potential, and proteasome-mediated degradation. Mol Cell Biol 18:2986–2996. https://doi.org/10.1128/MCB.18.5.2986.
56. Wathelet MG, Lin CH, Parekh BS, Ronco LV, Howley PM, Maniatis T. 1998. Virus infection induces the assembly of coordinately activated transcription factors on the IFN-beta enhancer in vivo. Mol Cell 1:507–518. https://doi.org/10.1016/S1097-2765(00)80051-9.
57. Weaver BK, Kumar KP, Reich NC. 1998. Interferon regulatory factor 3 and CREB-binding protein/p300 are subunits of double-stranded RNA-activated transcription factor DRAF1. Mol Cell Biol 18:1359–1368. https://doi.org/10.1128/MCB.18.3.1359.
58. Takahasi K, Suzuki NN, Horiuchi M, Mori M, Suhara W, Okabe Y, Fukuhara Y, Terasawa H, Akira S, Fujita T, Inagaki F. 2003. X-ray crystal structure of IRF-3 and its functional implications. Nat Struct Biol 10:922–927. https://doi.org/10.1038/nsb1001.
59. Escalante CR, Nistal-Villán E, Shen L, García-Sastre A, Aggarwal AK. 2007. Structure of IRF-3 bound to the PRDIII-I regulatory element of the human interferon-beta enhancer. Mol Cell 26:703–716. https://doi.org/10.1016/j.molcel.2007.04.022.
60. Kumar KP, McBride KM, Weaver BK, Dingwall C, Reich NC. 2000. Regulated nuclear-cytoplasmic localization of interferon regulatory factor 3, a subunit of double-stranded RNA-activated factor 1. Mol Cell Biol 20:4159–4168. https://doi.org/10.1128/MCB.20.11.4159-4168.2000.
61. Zhu M, Fang T, Li S, Meng K, Guo D. 2015. Bipartite nuclear localization signal controls nuclear import and DNA-binding activity of IFN regulatory factor 3. J Immunol 195:289–297. https://doi.org/10.4049/jimmunol.1500232.
62. Taniguchi T, Ogasawara K, Takaoka A, Tanaka N. 2001. IRF family of transcription factors as regulators of host defense. Annu Rev Immunol 19:623–655. https://doi.org/10.1146/annurev.immunol.19.1.623.
63. Lohoff M, Mak TW. 2005. Roles of interferon-regulatory factors in T-helper-cell differentiation. Nat Rev Immunol 5:125–135. https://doi.org/10.1038/nri1552.
64. Qin BY, Liu C, Lam SS, Srinath H, Delston R, Correia JJ, Derynck R, Lin K. 2003. Crystal structure of IRF-3 reveals mechanism of autoinhibition and virus-induced phosphoactivation. Nat Struct Biol 10:913–921. https://doi.org/10.1038/nsb1002.

65. Qin BY, Liu C, Srinath H, Lam SS, Correia JJ, Derynck R, Lin K. 2005. Crystal structure of IRF-3 in complex with CBP. Structure 13:1269–1277. https://doi.org/10.1016/j.str.2005.06.011.
66. Honda K, Yanai H, Negishi H, Asagiri M, Sato M, Mizutani T, Shimada N, Ohba Y, Takaoka A, Yoshida N, Taniguchi T. 2005. IRF-7 is the master regulator of type-I interferon-dependent immune responses. Nature 434:772–777. https://doi.org/10.1038/nature03464.
67. Yanai H, Chiba S, Hangai S, Kometani K, Inoue A, Kimura Y, Abe T, Kiyonari H, Nishio J, Taguchi-Atarashi N, Mizushima Y, Negishi H, Grosschedl R, Taniguchi T. 2018. Revisiting the role of IRF3 in inflammation and immunity by conditional and specifically targeted gene ablation in mice. Proc Natl Acad Sci U S A 115:5253–5258. https://doi.org/10.1073/pnas.1803936115.
68. Ronco LV, Karpova AY, Vidal M, Howley PM. 1998. Human papillomavirus 16 E6 oncoprotein binds to interferon regulatory factor-3 and inhibits its transcriptional activity. Genes Dev 12:2061–2072. https://doi.org/10.1101/gad.12.13.2061.
69. Irie T, Kiyotani K, Igarashi T, Yoshida A, Sakaguchi T. 2012. Inhibition of interferon regulatory factor 3 activation by paramyxovirus V protein. J Virol 86:7136–7145. https://doi.org/10.1128/JVI.06705-11.
70. Xing JJ, Ni LW, Wang S, Wang KZ, Lin RT, Zheng CF. 2013. Herpes simplex virus 1-encoded tegument protein VP16 abrogates the production of beta interferon (IFN) by inhibiting NF-kappa B activation and blocking IFN regulatory factor 3 to recruit its coactivator CBP. J Virol 87:9788–9801. https://doi.org/10.1128/JVI.01440-13.
71. Barro M, Patton JT. 2005. Rotavirus nonstructural protein 1 subverts innate immune response by inducing degradation of IFN regulatory factor 3. Proc Natl Acad Sci U S A 102:4114–4119. https://doi.org/10.1073/pnas.0408376102.
72. Zhang M, Liu Y, Wang P, Guan X, He S, Luo S, Li C, Hu K, Jin W, Du T, Yan Y, Zhang Z, Zheng Z, Wang H, Hu Q. 2015. HSV-2 immediate-early protein US1 inhibits IFN-beta production by suppressing association of IRF-3 with IFN-beta promoter. J Immunol 194:3102–3115. https://doi.org/10.4049/jimmunol.1401538.
73. Zhang Z, Zheng Z, Luo H, Meng J, Li H, Li Q, Zhang X, Ke X, Bai B, Mao P, Hu Q, Wang H. 2012. Human bocavirus NP1 inhibits IFN-beta production by blocking association of IFN regulatory factor 3 with IFNB promoter. J Immunol 189:1144–1153. https://doi.org/10.4049/jimmunol.1200096.
74. Cloutier N, Flamand L. 2010. Kaposi sarcoma-associated herpesvirus latency-associated nuclear antigen inhibits interferon (IFN) beta expression by competing with IFN regulatory factor-3 for binding to IFNB promoter. J Biol Chem 285:7208–7221. https://doi.org/10.1074/jbc.M109.018838.
75. Lefort S, Soucy-Faulkner A, Grandvaux N, Flamand L. 2007. Binding of Kaposi's sarcoma-associated herpesvirus K-bZIP to interferon-responsive factor 3 elements modulates antiviral gene expression. J Virol 81:10950–10960. https://doi.org/10.1128/JVI.00183-07.
76. Baigent SJ, Zhang G, Fray MD, Flick-Smith H, Goodbourn S, McCauley JW. 2002. Inhibition of beta interferon transcription by noncytopathogenic bovine viral diarrhea virus is through an interferon regulatory factor 3-dependent mechanism. J Virol 76:8979–8988. https://doi.org/10.1128/JVI.76.18.8979-8988.2002.
77. Hilton L, Moganeradj K, Zhang G, Chen YH, Randall RE, McCauley JW, Goodbourn S. 2006. The NPro product of bovine viral diarrhea virus inhibits DNA binding by interferon regulatory factor 3 and targets it for proteasomal degradation. J Virol 80:11723–11732. https://doi.org/10.1128/JVI.01145-06.
78. Savellini GG, Gandolfo C, Cusi MG. 2015. Truncation of the C-terminal region of Toscana virus NSs protein is critical for interferon-beta antagonism and protein stability. Virology 486:255–262. https://doi.org/10.1016/j.virol.2015.09.021.
79. Rezelj VV, Li P, Chaudhary V, Elliott RM, Jin DY, Brennan B. 2017. Differential antagonism of human innate immune responses by tick-borne phlebovirus nonstructural proteins. mSphere 2:e00234-17. https://doi.org/10.1128/mSphere.00234-17.
80. Rezelj VV, Overby AK, Elliott RM. 2015. Generation of mutant Uukuniemi viruses lacking the nonstructural protein NSs by reverse genetics indicates that NSs is a weak interferon antagonist. J Virol 89:4849–4856. https://doi.org/10.1128/JVI.03511-14.
81. Reizis B, Bunin A, Ghosh HS, Lewis KL, Sisirak V. 2011. Plasmacytoid dendritic cells: recent progress and open questions. Annu Rev Immunol 29:163–183. https://doi.org/10.1146/annurev-immunol-031210-101345.
82. Anderson GW, Slayter MV, Hall W, Peters CJ. 1990. Pathogenesis of a phleboviral infection (Punta Toro virus) in Golden Syrian hamsters. Arch Virol 114:203–212. https://doi.org/10.1007/BF01310749.
83. Nishiyama S, Slack OAL, Lokugamage N, Hill TE, Juelich TL, Zhang LH, Smith JK, Perez D, Gong B, Freiberg AN, Ikegami T. 2016. Attenuation of pathogenic Rift Valley fever virus strain through the chimeric S-segment encoding sandfly fever phlebovirus NSs or a dominant-negative PKR. Virulence 7:871–881. https://doi.org/10.1080/21505594.2016.1195528.
84. Gori Savellini G, Weber F, Terrosi C, Habjan M, Martorelli B, Cusi MG. 2011. Toscana virus induces interferon although its NSs protein reveals antagonistic activity. J Gen Virol 92:71–79. https://doi.org/10.1099/vir.0.025999-0.
85. Habjan M, Penski N, Spiegel M, Weber F. 2008. T7 RNA polymerase-dependent and -independent systems for cDNA-based rescue of Rift Valley fever virus. J Gen Virol 89:2157–2166. https://doi.org/10.1099/vir.0.2008/002097-0.
86. Sharma S, tenOever BR, Grandvaux N, Zhou GP, Lin RT, Hiscott J. 2003. Triggering the interferon antiviral response through an IKK-related pathway. Science 300:1148–1151. https://doi.org/10.1126/science.1081315.
87. Kawai T, Takahashi K, Sato S, Coban C, Kumar H, Kato H, Ishii KJ, Takeuchi O, Akira S. 2005. IPS-1, an adaptor triggering RIG-I- and Mda5-mediated type I interferon induction. Nat Immunol 6:981–988. https://doi.org/10.1038/ni1243.
88. Basler CF, Mikulasova A, Martinez-Sobrido L, Paragas J, Mühlberger E, Bray M, Klenk H-D, Palese P, García-Sastre A. 2003. The Ebola virus VP35 protein inhibits activation of interferon regulatory factor 3. J Virol 77:7945–7956. https://doi.org/10.1128/JVI.77.14.7945-7956.2003.
89. Weidmann M, Sanchez-Seco MP, Sall AA, Ly PO, Thiongane Y, Lo MM, Schley H, Hufert FT. 2008. Rapid detection of important human pathogenic phleboviruses. J Clin Virol 41:138–142. https://doi.org/10.1016/j.jcv.2007.10.001.
90. Kuri T, Zhang X, Habjan M, Martinez-Sobrido L, Garcia-Sastre A, Yuan Z, Weber F. 2009. Interferon priming enables cells to partially overturn the SARS coronavirus-induced block in innate immune activation. J Gen Virol 90:2686–2694. https://doi.org/10.1099/vir.0.013599-0.
91. Hallikas O, Taipale J. 2006. High-throughput assay for determining specificity and affinity of protein-DNA binding interactions. Nat Protoc 1:215–222. https://doi.org/10.1038/nprot.2006.33.

4.3 Research article:

NSs of the mildly virulent sandfly fever Sicilian virus is unable to inhibit interferon signaling and upregulation of interferon-stimulated genes

Own contribution:

I designed and performed all experiments and contributed to writing the manuscript.

_____

Jennifer Würth

JOURNAL OF
GENERAL VIROLOGY

RESEARCH ARTICLE
Wuerth and Weber, *Journal of General Virology* 2021;102:001676
DOI 10.1099/jgv.0.001676

MICROBIOLOGY SOCIETY
OPEN ACCESS

NSs of the mildly virulent sandfly fever Sicilian virus is unable to inhibit interferon signaling and upregulation of interferon-stimulated genes

Jennifer Deborah Wuerth[1,2] and Friedemann Weber[1,*]

Abstract

Phleboviruses (order *Bunyavirales*, family *Phenuiviridae*) are globally emerging arboviruses with a wide spectrum of virulence. Sandfly fever Sicilian virus (SFSV) is one of the most ubiquitous members of the genus *Phlebovirus* and associated with a self-limited, incapacitating febrile disease in travellers and military troops. The phleboviral NSs protein is an established virulence factor, acting as antagonist of the antiviral interferon (IFN) system. Consistently, we previously reported that SFSV NSs targets the induction of IFN mRNA synthesis by specifically binding to the DNA-binding domain of the IFN transcription factor IRF3. Here, we further characterized the effect of SFSV and its NSs towards IFN induction, and evaluated its potential to affect the downstream IFN-stimulated signalling and the subsequent transactivation of antiviral interferon-stimulated genes (ISGs). We found that SFSV dampened, but did not entirely abolish type I and type III IFN induction. Furthermore, SFSV NSs did not affect IFN signalling, resulting in substantial ISG expression in infected cells. Hence, although SFSV targets IRF3 to reduce IFN induction, it is not capable of entirely disarming the IFN system in the presence of high basal IRF3 and/or IRF7 levels, and we speculate that this significantly contributes to its low level of virulence.

INTRODUCTION

Phleboviruses (order *Bunyavirales*, family *Phenuiviridae*, genus *Phlebovirus*) are gobally emerging arboviruses that cover a broad range of virulence [1–3]. The disease spectrum among well-known members ranges from seasonal, self-limited febrile disease (sandfly fever Sicilian virus (SFSV), Punta Toro virus (PTV)), via fever complicated by meningitis and encephalitis (Toscana virus, TOSV) to acute hepatitis, encephalitis, ocular complications, or haemorrhagic fever (Rift Valley fever virus, RVFV) [1–3]. While some novel virulent members were isolated from clinically apparent patients [4, 5], the majority of novel phleboviruses is curently identified by vector screening and subsequent sequence analysis, leaving their disease potential only partially explored or entirely elusive [6–10].

Historically, an outbreak of an incapacitating febrile disease accompanied by sudden onset generalized myalgia, headaches, malaise, ocular and gastrointestinal symptoms, termed *'sandfly fever'*, *'3 day fever'*, *'pappataci fever'*, or *'dog disease'* during the Sicilian invasion of World War II led to the first isolation of SFSV from infected soldiers [11, 12]. SFSV is also one of the most widespread phlebovirus, with its endemic area ranging from Portugal across the Mediterranean basin to as far east as Bangladesh, and south to Somalia, and seroprevalence levels reaching up to 50% in humans and around 80% in domestic animals [5, 13–17]. Consequently, SFSV continues to cause disease in immunologically naïve groups such as deployed military personnel and travellers [18–22]. Furthermore, several SFSV-like viruses were recently identified, such as sandfly fever Turkey, Dashli, Toros and Zerdali viruses [4, 23, 24].

Received 15 February 2021; Accepted 23 August 2021; Published 02 November 2021
Author affiliations: [1]Institute for Virology, FB10-Veterinary Medicine, Justus-Liebig University, Giessen, Germany; [2]Institute of Innate Immunity, University of Bonn, Bonn, Germany.
***Correspondence:** Friedemann Weber, friedemann.weber@vetmed.uni-giessen.de
Keywords: interferon antagonism; interferon-stimulated gene; interferon-regulatory factor; NSs protein; phlebovirus; sandfly fever Sicilian virus.
Abbreviations: DDX, DExD/H-box helicase; FF-Luc, firefly luciferase; IFN, interferon; IRF, interferon-regulatory factor; ISG, interferon-stimulated gene; JAK, Janus kinase; MAVS, mitochondrial antiviral signaling protein; Mx, myxovirus resistance; NSs, non-structural protein encoded on the S segment; PKR, protein kinase R; RIG-I, retinoic-acid inducible gene I; Rux, ruxolitinib; RVFV, Rift Valley fever virus; SFSV, sandfly fever Sicilian virus; SFTSV, severe fever with thrombocytopenia syndrome virus; STAT, signal transducer and activator of transcription; TOSV, Toscana virus; UUKV, Uukuniemi virus.
Four supplementary figures are available with the online version of this article.

Phleboviruses contain a tri-segmented, mainly negative-sense single-stranded RNA genome. While the large (L) and the medium (M) segment encode the viral RNA-dependent RNA polymerase and the glycoproteins, respectively, the small (S) segment codes for the nucleocapsid protein N that packages the genomic and antigenomic RNA into viral nucleoprotein complexes [2]. Additionally, the M segment encodes the non-structural protein NSm and the 78 kDa protein, whereas the S segment contains the gene for the NSs protein in an ambisense orientation. Phlebovirus replication takes place exclusively in the cytoplasm of the host cell, where the viral RNA is sensed by pattern-recognition receptor retinoic-acid inducible gene I (RIG-I) [25]. Upon activation, RIG-I engages the adapter, mitochondrial antiviral signalling protein (MAVS), providing a platform for the phosphorylation of interferon-regulatory factors IRF3 and IRF7 and culminating in the induction of type I and type III interferons (IFN-α/β and IFN-λ, respectively) [26, 27]. Secreted IFNs then stimulate their cognate receptors in a para- and autocrine manner, which in turn mediates the phosphorylation of the signal transducers and activators of transcription 1 (STAT1) and STAT2. A complex of STAT1, STAT2 and IRF9, so-called IFN-stimulated gene factor 3 (ISGF3), transactivates an assortment of interferon-stimulated genes (ISGs) to establish an antiviral state in the cell [28]. The dynamin-like GTPase MxA and ubiquitin-like protein ISG15 are examples of ISGs with anti-phleboviral activity [29–31] and the protective effect of the IFN response has been illustrated for several phleboviruses, including SFSV [29, 32–41]. With NSs, however, phleboviruses express an IFN antagonist that can display a multitude of strategies for curbing IFN induction [3, 42, 43]. Depending on the virus, IFN antagonisms range from a global, general block of host-gene expression to fine-adjusted targeting of specific host factors. Mechanistically, some NSs proteins are driving proteasomal degradation of target host factors, whereas others engage in their stoichiometric binding and sequestration [34, 44–48]. For SFSV NSs, we previously reported that it acts as suppressor of type IFN induction by obstructing the DNA-binding domain of the IFN transcription factor IRF3 [47]. Thus, SFSV employs a specific rather than a global or destructive strategy as used by other, more virulent phleboviruses. Here, given its stoichiometric and highly IRF3-specific mechanism of action, we evaluated the efficiency and breadth by which SFSV is counteracting the induction of different types of IFNs, and extended our analyses to downstream events like IFN signalling and ISG expression. Our results indicate that SFSV NSs is a modulator rather than a strong antagonist of IFN induction that is exclusively acting on IRF3, implying a possible correlation between the strength of a particular phleboviral NSs protein and the associated virulence.

METHODS

Cells, viruses, infection, and plasmids

A549, BHK-21, HEK293, HepG2, Vero B4 and Vero E6 cells were maintained in CCM34 medium (DMEM with addition of 17.8 mg l^{-1} L-alanine, 0.7 g l^{-1} glycine, 75 mg l^{-1} L-glutamic acid, 25 mg l^{-1} L-proline, 0.1 mg l^{-1} biotin, 25 mg l^{-1} hypoxanthine, and 3.7 g l^{-1} sodium bicarbonate) supplemented with 10% FCS, 2 mM glutamine, 100 U ml^{-1} penicillin, and 100 µg ml^{-1} streptomycin.

The Sabin strain of SFSV was propagated in Vero B4 cells, attenuated RVFV strains MP12 and clone 13 in BHK-21 cells. Virus titres were determined via plaque assay on Vero E6 cells with Avicel overlay and crystal violet staining. Cell lines and virus stocks were routinely tested for mycoplasma contamination, and virus stocks were tested for the presence of defective interfering particles. For infection, A549 cells (1×10^5 per 24-well) were washed with sterile PBS and inoculated with virus diluted to the respective multiplicity of infection (MOI) in serum-free medium for 1 h at 37 °C, after which the inoculate was replaced with fully supplemented medium. For super-stimulation or inhibition of IFN signalling, cells were treated with 100 U ml^{-1} of pan-species IFN-α (B/D) (PBL Assay Science) [49], IFN-β (Betaferon, Schering) or ruxolitinib (INCB018424, Selleckchem), respectively, from 1 h prior to infection until cell lysis.

Expression constructs encoding 3×FLAG-tagged NSs of SFSV (GenBank EF201822.1), pI.18-NSsRVFV-3×FLAG and pI.18–3×FLAG-ΔMx were described before [45, 47]. Expression constructs for the NSs proteins of TOSV prototype strain ISS.Phl.3 and SFTSV strain HB29 (GenBank X53794.1 and NC_018137.1, respectively) were synthesized (BioCat and Eurofins Genomics) and subcloned into pI.18. Luciferase reporter constructs p-125Luc [50] and pGL3-Mx1P-Luc [51] were kindly provided by Takashi Fujita and Georg Kochs, respectively. pRL-SV40 was purchased from Promega.

Immunoblot analysis

Samples were run on 12% acrylamide gels using the Tris-glycine buffer system and transferred to polyvinylidene fluoride (PVDF) membranes (Millipore) via semidry blotting. Membranes were blocked in TBS containing 5% BSA or milk powder, stained with primary antibody for 1 h at room temperature or overnight at 4 °C, washed in TBS/0.1% Tween-20, stained with secondary antibodies for 45 min, washed again in TBS/0.1% Tween-20 and once in TBS, and finally developed with SuperSignal West Femto kit (Pierce). Bands were detected using a ChemiDoc Imaging System (Bio-Rad) or a Sapphire Biomolecular Imager (Azure Biosystems).

Primary antibodies comprised: ISG15 (ab36765, Abcam, 1:500), MxA (Sigma, MABF938, 1:1000), RIG-I (ag-20b-0009, AdipoGen, 1:1000), RVFV N (rabbit hyperimmune serum, provided by Alenjandro Brun, 1:1000), SFSV N (mouse immune ascites fluid, provided by WRCEVA, 1:1000), p-STAT1(Y701) (7649, Cell Signalling, 1:1000), STAT1 (610186, BD Transduction Laboratories, 1:1000), p-STAT2(Y690) (88410, Cell Signalling, 1:1000), STAT2 (610188, BD Transduction Laboratories, 1:1000), tubulin (ab6046, Abcam, 1:2500). Secondary antibodies were

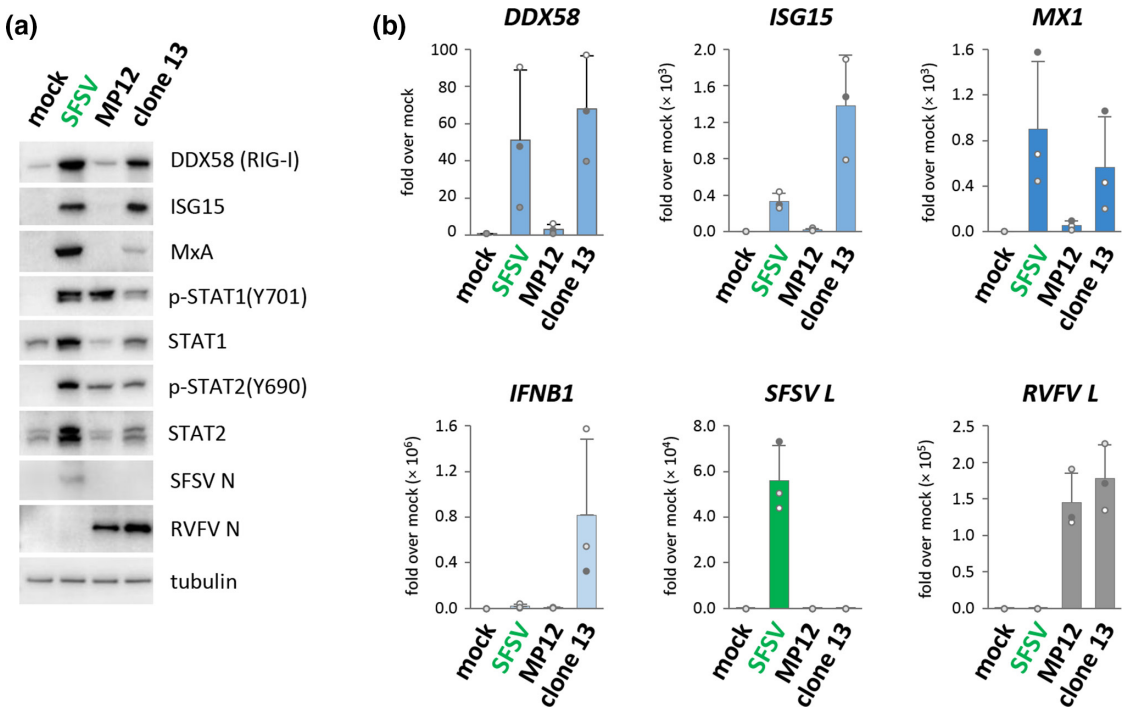

Fig. 1. ISG expression and IFN signalling under SFSV infection. (a) A549 cells were infected with SFSV, MP12 or clone 13 (MOI 1) and harvested 12 hpi. Lysates were analysed by immunoblot for ISG levels and phosphorylation of STAT1 and STAT2 (*n*=3). (b) Matching RNA samples were subjected to quantitative RT-PCR for *IFNB1*, ISGs *DDX58* (encoding RIG-I), *ISG15*, and *MX1*, as well as viral L segments (*n*=3, mean±SD). Please note that, for immunoblotting, antisera with very different signal-to-noise ratio were being used (mouse ascites fluid vs rabbit serum), not permitting any quantitative comparisons between the viral N signals.

anti-mouse (0031430 1892913) and anti-rabbit (0031460 1892914, both Thermo Fisher).

Human IFN-λ1/3 ELISA

Supernatants of infected A549 cells were diluted 1:5 in medium and subjected to human IFN-lambda 1/3 DuoSet ELISA (DY1598B, R and D Systems) according to the manufacturer's specifications.

Reverse transcriptase (RT)-PCR

RNA was isolated using the RNeasy Mini Kit (Qiagen) and then subjected to DNase I digest and cDNA synthesis using PrimeScript RT reagent Kit with gDNA Eraser (TaKaRa) as recommended by the manufacturers. Host transcripts were detected with SYBR Premix Ex Taq (Tli RNaseH Plus) (TaKaRa) and QuantiTect primers (*DDX58:* QT00040509; *IFNB1*: QT00203763; *IFNL1*: QT01033564; *IFNL2/3*: QT00222488; *IRF3:* QT00012866; *IRF5*: QT00210595, *IRF7*: QT00210595; *ISG15*: QT00072814; *MX1*: QT00090895; *RRN18S*: QT00199367, Qiagen). Premix Ex Taq (Probe qPCR) (TaKaRa) was used to detect viral RNA with previously published primers and probes for the SFSV and RVFV L segments (SFSV L: fwd 5′-TCT GAG AAC TGA GCT ACA AGT GTT TAT TA-3′, rev 5′-TTC CCA TCT CTC TTC TGA AGA GTG-3′, probe 6-FAM-AGG TCA TAG ACA GTA TCA TGA GAA TTG CTA GGT G-BHQ-1 [4]; SFSV S, fwd, 5′-TGC ACT CAT CCA AGC TAT GTG-3′, rev, 5′-GAG GGC TAC AAA CAA GGG ATC-3′, probe, FAM-TCC CCC ATT CTC AGA ATG TAA GAC ATT AGC-BHQ-1 [52]; RVFV L: fwd 5′-TGA AAA TTC CTG AGA CAC ATG G-3′, rev 5′-ACT TCC TTG CAT CAT CTG ATG-3′, probe 6-FAM-CAA TGT AAG GGG CCT GTG TGG ACT TGT G-BHQ-1 [53]). 18S rRNA was used as housekeeping gene to calculate fold induction according to the $\Delta\Delta C_T$ method.

Dual luciferase assay

HEK293 cells seeded into 96-well plates (1.5×10^4 per well) were transfected using TransIT-LT1 (Mirus Bio LLC). Transfection mixes included the indicated firefly and *Renilla* luciferase reporter constructs (40 ng each), as well as NSs proteins or the control protein ΔMx (0.1 ng, 1 ng and 10 ng), and were filled up to equal plasmid amounts with empty vector pI.18. For stimulation of IFN induction, an expression plasmid for MAVS was added to the transfection mix (50 ng). Gene expression was allowed for 24 h. Subsequently, cells were either harvested or stimulated with IFN-β or IFN-α B/D (100 U ml^{-1}) for 24 h. Cell lysis and determination of luciferase activities were performed using the Dual Luciferase Reporter Assay System (Promega) and a LB 942 TriStar² multimode reader (Berthold Technologies). Firefly luciferase activities were normalized to those

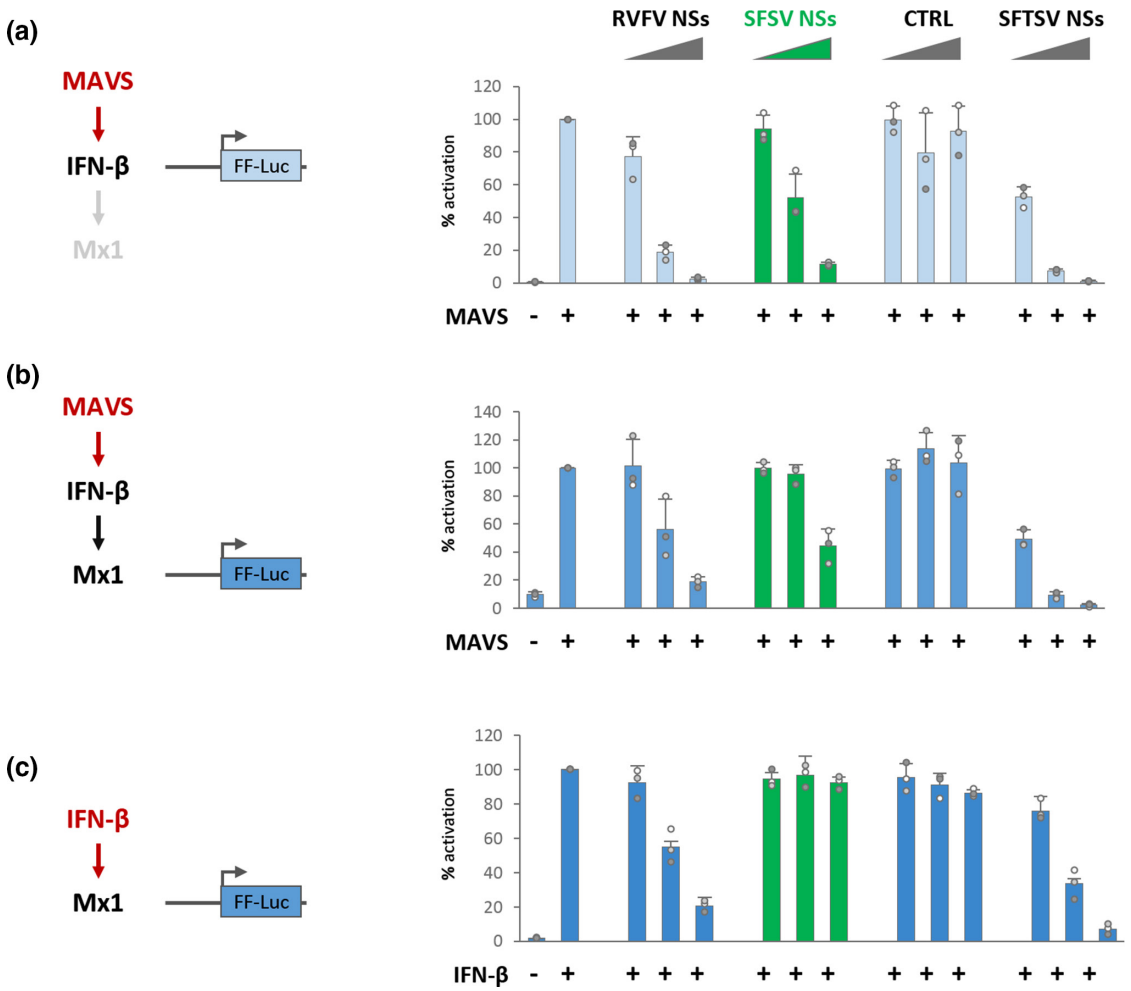

Fig. 2. IFN signalling and ISG induction under ectopic SFSV NSs expression. (a–c) HEK293 cells were co-transfected with indicated reporter constructs and increasing doses (0.1 ng, 1.0 ng, 10.0 ng) of expression plasmids for 3×FLAG-tagged NSs or negative control (CTRL). IFN induction or signalling was stimulated by concomitant overexpression of MAVS (a, b) or addition of 100 IU ml^{-1} IFN-β 12 h after transfection (c). Lysates were interrogated for IFN induction (*IFNB1* promoter, a) or IFN-dependent ISG induction (*Mx1* promoter, b, c) 24 h after stimulation (n=3, mean±SD). The respective stimulant is coloured in red.

of *Renilla* luciferase and the stimulated control samples set to 100% within each biological replicate. Finally, mean and SD values were calculated across the indicated number of biological replicate datasets.

siRNA-mediated knockdown and infection

A549 cells (1×10^5 per 24-well) were subjected to reverse transfection via Lipofectamine RNAiMax (Life Technologies) according to the manufacturer's recommendations. siRNA (all from Qiagen) comprised control siRNA (1027280), siIRF3 (1027416), siIRF5 (1027416), siIRF7 (1027416) or a pool of four custom-designed siRNA oligonucleotides targeting SFSV NSs (siNSs1 5′-TTG GGT CTT AGT GAT GAG CAT-3′, siNSs2 5′-AAG GGA TCA GCT AAT GTC TTA-3′, siNSs3 5′-TAC AAT AAA TTT CAC ACT CAT-3′, siNSs4 5'- AAG GCT CTT AGC TGG CCA CTA-3′) [47].

RESULTS

SFSV infection induces IFN signaling and ISG expression despite inhibition of type I IFN induction

SFSV NSs inhibits induction of the *IFNB1* promoter by masking the DNA-binding activity of IRF3 [47]. Nonetheless, the ISG RIG-I is upregulated under infection with parental SFSV or with a recombinant chimeric RVFV expressing SFSV NSs (rZH548ΔNSs::NSsSFSV) [47]. To test whether this was specific to RIG-I or whether ISGs are spared by NSs in general, we interrogated the protein and mRNA levels of two other ISGs, namely ISG15 and MxA [28]. As expected, both these ISGs were strongly upregulated by RVFV strain clone 13, which possesses a large deletion within the NSs gene and is thus a strong IFN and ISG inducer [32], whereas the RVFV strain MP12, harbouring a fully functional NSs, activated them

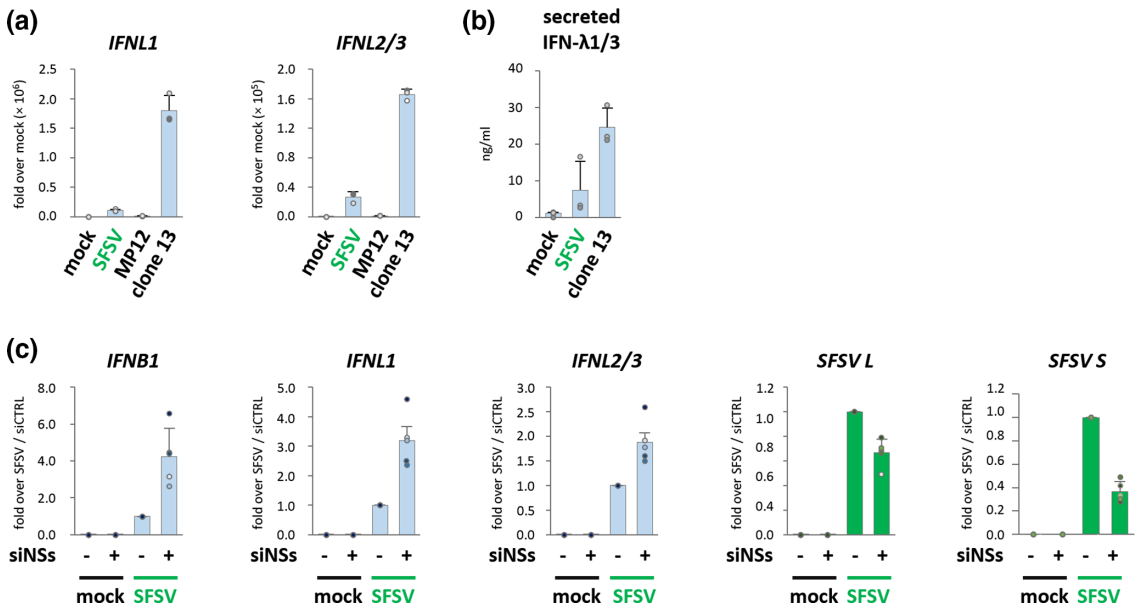

Fig. 3. Type III IFN expression under SFSV infection. Samples from Fig. 1b (MOI 1, 12 hpi) were interrogated for type III IFN expression by RT-qPCR (a) and supernatants for secreted type III IFNs by ELISA (b) (*n*=3, mean±SD). (c) A549 cells were subjected to reverse transfection with control siRNA or an siRNA pool targeting SFSV NSs. After 24 h, cells were infected with SFSV (MOI 1) for 12 h and subsequently analysed by RT-qPCR for type I and III IFN, as well as viral L segment and NSs-encoding viral S segment. Control siRNA-treated, SFSV-infected cells were set to 1 (*n*=5, mean±SD).

only marginally (Fig. 1a). Infection with SFSV, however, also resulted in elevated levels of RIG-I, MxA, and ISG15 proteins (Fig. 1a). With respect to mRNAs, SFSV infection caused intermediate activation of the *ISG15* gene and strong upregulation of *MX1* and *DDX58* (RIG-I), although only negligible levels of *IFNB1* mRNAs were induced (Fig. 1b). *MX1* is a conserved and strictly IFN-dependent ISG [54]. We therefore assessed the phosphorylation levels of transcription factors STAT1 and STAT2 as proxy for IFN signalling. Indeed, ISG induction under SFSV infection was accompanied by phosphorylation of both STAT1 and STAT2 (Fig. 1a). Additionally, STAT1 (and STAT2), which are also ISGs [28], were elevated on both transcript and protein levels under SFSV infection (Figs 1a and S1a, available in the online version of this article), consistent with their inducibility by IFNs. For STAT1 phosphorylation, we also performed a time course and show that it is detectable already at four hpi and steadily increases until 12 hpi (Fig. S1b).

Of note, pre-treatment with IFN-α prior to infection could not further enhance STAT phosphorylation or ISG expression (fold increase <2, Fig. S2 and data not shown), suggesting that SFSV infection alone already results in maximal ISG induction.

We wondered about the trigger of the IFN signalling and ISG upregulation that occur despite the inhibition of IFN induction by SFSV NSs. One possibility could be the contamination of virus stocks with high amounts of bioactive type III IFNs, as it had been reported previously for hantaviruses [55]. However, inactivation of viral stocks with β-propiolactone, which does not affect IFN bioactivity [56], abolished SFSV replication as expected, but also IFN and ISG induction (Fig. S3 and data not shown). Similarly, when we subjected viral stocks to ultrafiltration, the ISG-inducing activity was retained together with the viral particles by the filter membrane (data not shown). Thus, SFSV itself appears to stimulate the observed IFN signalling.

SFSV NSs does not affect IFN signaling or ISG induction

To dissect the impact of SFSV NSs on IFN induction vs. IFN signalling, we tested ectopically expressed SFSV NSs in luciferase reporter assays. Different promoters and inducers were combined in three experimental set-ups to distinguish the ability of SFSV NSs to block (i) *Ifnb1* promoter induction (Fig. 2a), (ii) indirect *Mx1* promoter stimulation by induced IFN (Fig. 2b), or (iii) direct *Mx1* promoter activation (Fig. 2c). For *Ifnb1* and indirect *Mx1* promoter stimulation, we concomitantly overexpressed the RIG-I adaptor MAVS, as described before [47], whereas direct ISG induction was stimulated by the addition of IFN-β to the medium. Along with SFSV NSs and RVFV NSs, we employed the NSs of the related severe fever with thrombocytopenia syndrome virus (SFTSV, recently reclassified as Dabie bandavirus [57]) as a well-established specific antagonist of both IFN induction and signalling [58–62]. As expected, ectopic SFSV NSs was able to efficiently inhibit *Ifnb1* promoter induction by MAVS (Fig. 2a).

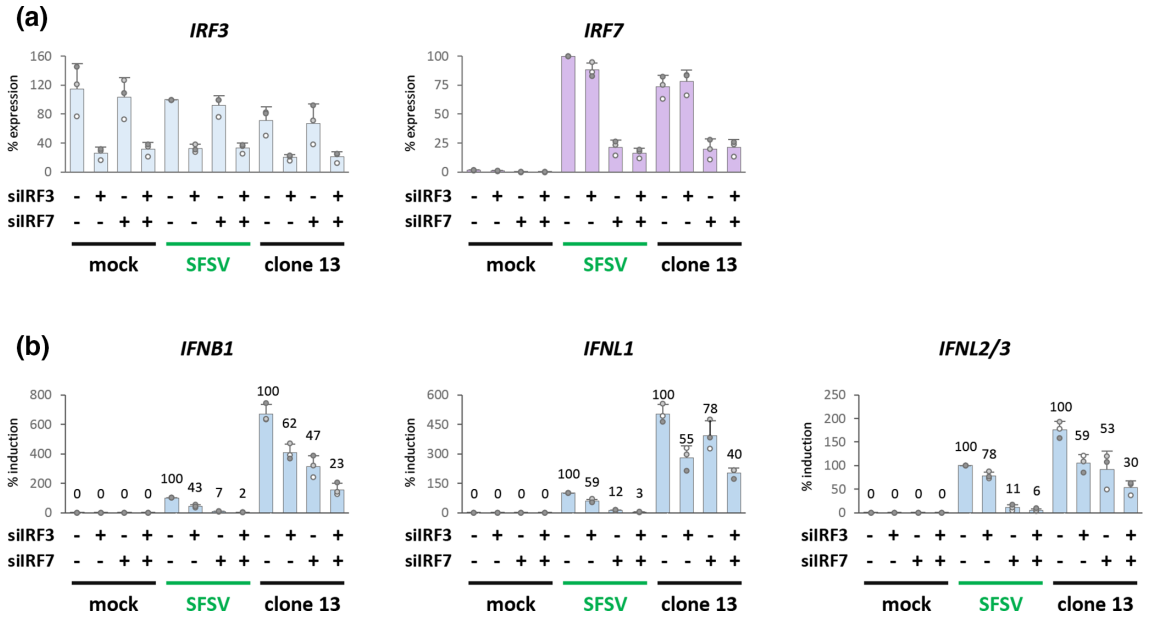

Fig. 4. IFN and ISG induction under IRF knockdown. A549 cells were subjected to reverse transfection with control siRNA or siRNA pools targeting IRF3 and IRF7 alone or in combination. After 24 h, cells were infected with SFSV (MOI 1) for 12 h and subsequently analysed for transcript levels of (a) IRF3 and IRF7 and (b) type I and III IFN (*n*=3, mean±SD). Expression and induction levels were normalized to cells treated with control siRNA and infected with SFSV, and the latter set to 100%. Data labels represent the percent of IFN induction normalized to the control siRNA condition of the respective virus group.

In contrast, when the reporter under control of the *Mx1* promoter was employed to measure ISG stimulation by MAVS (i.e. indirectly via secreted IFN), SFSV NSs was less efficient and only inhibitory when given at the highest dose (Fig. 2b). Finally, SFSV NSs completely failed to interfere when *Mx1* promoter activity was stimulated with ectopic IFN-β (Fig. 2c) or IFN-α (data not shown). Thus, SFSV NSs can affect IFN induction, but not IFN signalling.

SFSV NSs also modulates type III IFN induction

We found that also the type III IFNs *IFNL1* and *IFNL2/3* were moderately induced by SFSV in A549 cells on the transcriptional level, and low amounts of secreted IFN-λ1 and -λ3 could be detected in cell culture supernatants (Fig. 3a). Moreover, siRNA experiments revealed that the suppression of IFN induction was mediated by NSs (Fig. 3b). Thus, the ISG expression in response to SFSV is most likely due to active infection and reflects a failure of SFSV NSs to fully abrogate type I and III IFN production.

SFSV NSs fails to sufficiently control IRF-mediated IFN induction

SFSV NSs might be only a weak IFN induction antagonist due to incomplete sequestration of the cellular IRF3 pool, its inability to target IRF7 [47], or a combination thereof. To test these possibilities, we knocked down either IRF3, IRF7, or both with specific siRNA pools prior to SFSV and clone 13 infection (Fig. 4a). The knockdown of *IRF3* alone partially decreased *IFNB1*, *IFNL1*, and *IFNL2/3* mRNA levels in both clone 13- and SFSV-infected cells (Fig. 4b), suggesting that IRF3 participated in IFN induction in response to SFSV. The knockdown of *IRF7* alone resulted in an even stronger reduction of IFN transcripts in the case of SFSV, whereas for clone 13 the effect was comparable to the one of the *IRF3*-targeting siRNA. This implies that IFN induction under SFSV relied more on IRF7. Finally, the simultaneous knockdown of both IRFs had an additive effect for both viruses, but again for SFSV it led to a stronger reduction of IFN transcripts. Thus, both IRF3 and IRF7 appeared to be responsible for IFN type I and III induction during SFSV infection.

ISG expression in infected cells depends on IFN signaling

While IRF3 is constitutively expressed and not regulated by IFN, IRF7 is an ISG itself with only low basic levels in most cell types. Upon IFN signalling, IRF7 is rapidly upregulated on the transcriptional and translational levels, activated along with IRF3, and thereby amplifies IFN induction [28, 63–65] (Fig. 5a). To further differentiate between basally expressed and IFN-induced IRF7, we compared IRF, IFN, and ISG induction under treatment with the JAK1/2 inhibitor ruxolitinib that blocks signalling by IFNs and other cytokines [66]. As expected, ruxolitinib left *IRF3* levels unaffected but blocked the upregulation of *IRF7* (Fig. 5b) and *MX1* (Fig. 5c and data not shown). Similarly, ruxolitinib further decreased the already low inductions of *IFNB1*, *IFNL1*, and *IFNL2/3* in SFSV-infected cells, whereas it had no or only a partially reducing effect on the IFN transcripts in clone 13-infected cells. Finally, *ISG15* expression remained

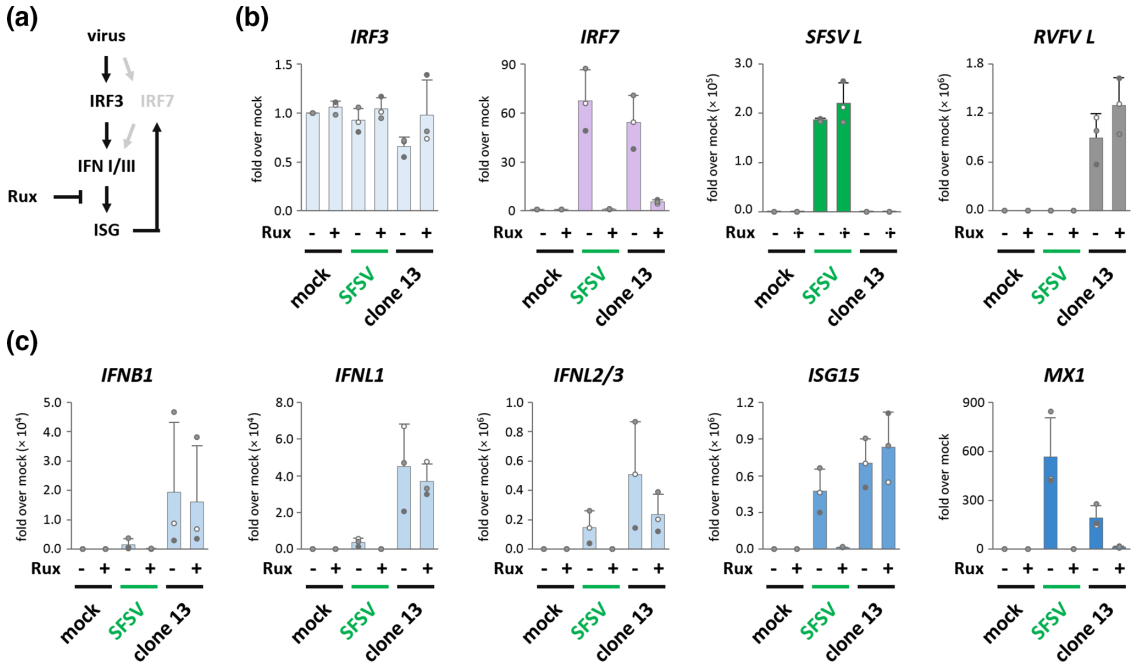

Fig. 5. IFN and ISG induction under ruxolitinib treatment. (a) In steady-state, type I and III IFN induction relies on IRF3 in most cell types. Upon IFN signalling, however, IRF7 transcription and translation are induced. IRF7 then is activated alongside IRF3 and participates in a positive feedback loop that results in the amplification and diversification of the IFN response. IFN signalling and ISG induction can be abrogated by JAK1/JAK2 inhibitor ruxolitinib (Rux). (b, c) A549 cells treated with ruxolitinib or vehicle control from 1 h prior and throughout the infection (MOI 1) until harvest 12 hpi. Cellular RNA was subsequently analysed for transcript levels of IRF3 and IRF7, viral gene segment L, type I and III IFN, as well as ISGs (n=3, mean±SD). All samples were normalized to vehicle-treated mock cells.

at baseline level under simultaneous ruxolitinib treatment and SFSV infection, whereas it was readily induced by clone 13 also when JAK-dependent signalling was inhibited. Hence, the IRF7-mediated positive feedback loop via secreted IFNs and perhaps other cytokines seems to be critical for the IFN and ISG inductions that are observed in SFSV-infected cells.

DISCUSSION

Phleboviruses cover a wide spectrum of virulence. As the majority of novel phleboviruses are currently identified by screening of putative arthropod vectors, their potential to cause disease in humans is mostly unknown.

The importance of the IFN system in the outcome of phlebovirus infection has been illustrated in animal models of infection by (a) the increased susceptibility of IFN-deficient mice, (b) the protective effect of prophylactic and early therapeutic application of type I IFNs, and (c) the association of an early type I IFN response with survival (see introduction). A major part of the antiviral activity is thereby mediated by ISGs acting on at multiple levels of the viral replication cycle [28]. To date, a systematic analysis of ISGs for anti-phleboviral activity is lacking. Nevertheless, a small set of ISGs has been shown to restrict the replication of RVFV [3, 43]. Similar to RVFV, SFSV is restricted by both overexpression of MxA and ectopic type I IFN if present during early stages of the viral replication cycle [30, 33]. Accordingly, phleboviruses have evolved a number of strategies to counteract IFN induction. Well established examples are the NSs proteins of virulent RVFV and TOSV that promote proteasomal degradation of host factors, either by recruiting the host ubiquitination machinery to target proteins or by NSs acting as ubiquitin ligase itself, respectively [45, 48]. In contrast, NSs of the only mildly virulent SFSV acts by stoichiometric interaction with IRF-3. In a similar manner, NSs of the related, highly virulent SFTSV bandavirus sequesters multiple factors of the IFN induction pathway into inclusion bodies, whereas NSs of the apathogenic Uukuniemi virus (UUKV) is a weak IFN antagonist [59–62, 67]. It has been discussed that the IFN-antagonistic activity of an NSs protein may correlate with the virulence of the respective phlebovirus [3, 43, 62], and that novel phleboviruses (or their NSs proteins) are more habitually tested for inhibition of IFN induction. Interestingly, NSs proteins of the virulent tick-borne bandaviruses also specifically target IFN signalling, whereas UUKV NSs does not [62]. This may suggest that, besides differences in breadth and speed of host factor inactivation, antagonism of both IFN induction and IFN signalling is required for high virulence. To our knowledge, such a comparative analysis has not been reported yet for phleboviruses - probably due to the fact that RVFV NSs blunts host gene expression and is therefore expected to abrogate IFN signalling and ISG induction. Here, we thus characterized the antagonistic capacity of mildly pathogenic SFSV towards IFN signalling and ISG induction in comparison with RVFV.

As reported previously for *IFNB1* [47], the induction of type III IFNs was dampened but not abrogated by SFSV NSs. IFN signalling was clearly activated in response to SFSV infection, and ISGs were induced on both the transcript and protein levels. IFN signalling upon addition of ectopic IFN did not increase ISG expression further and was inhibited neither by SFSV infection nor by NSs overexpression, in agreement with the observation that NSs did not interact with STAT1 or STAT2 (data not shown) and the absence of any IFN signalling factors from the NSs interactome [68, 69]. Interestingly, IFN and subsequent ISG induction were driven predominantly by IRF7, consistent with the failure of SFSV NSs to target IRF7 in our previous study [68]. In addition to IRF7, a role for IRF5 has been implied in IFN induction and a mouse model for Oropouche and LaCrosse orthobunyavirus infection [70]. Similar to IRF7, IRF5 is not targeted by SFSV NSs [47]. However, unlike what we observed for IRF7, knockdown of *IRF5* did not lead to any reduction in IFN or ISG levels in our experimental system (data not shown). In summary, the IFN-antagonistic activity of SFSV NSs is limited to and thereby relying entirely on its ability to modulate IRF3-driven *IFNB1* induction. Given that NSs needs to be produced freshly in infected cells and that already incoming viral genome segments can activate innate sensing [25], SFSV NSs appears to be a rather weak and inefficient IFN antagonist. All taken together, we propose the following model for SFSV infection: although type I and III IFN induction are down-modulated by NSs-mediated IRF3 sequestration, they cannot be sufficiently abrogated due to an (initial) excess of IRF3 over newly generated NSs. Secretion of small amounts of first-wave IFN-β and IFN-λ then triggers IFN signalling, unhindered by NSs, and the transcriptional and translational upregulation of IRF7. The latter, again unaffected by SFSV NSs, further amplifies the IFN and ISG response in the infected cells, resulting in substantial ISG induction. Of note, we recently found that SFSV NSs, in order to evade restriction by the powerful ISG product PKR, interacts with the translation initiation factor 2B (eIF2B), resulting in enhanced cap-dependent translation [69]. While ensuring the synthesis of viral proteins, this probably also augments the production of IFNs and ISGs within infected cells. Thereby, IFN from SFSV-infected cells can not only establish an antiviral state in bystander cells, but also in cells already infected.

Unfortunately, no small animal model is available to study SFSV infection [12]. However, early reports firmly established the self-limited nature of the febrile disease caused by SFSV in men [11, 12] and it is conceivable that, when spreading in a mammalian organism, the virus quickly encounters cells with high IRF levels. Accordingly, while targeting IRF3 might allow the virus a head start, considerable IFN induction through the IRF7-dependent positive feedback loop and possibly also by professional cell types with intrinsically high IRF7 levels can quickly limit viral spread. Hence, it is tempting to speculate that the failure of SFSV NSs to sufficiently blunt IFN induction and to affect IFN signalling significantly contributes to its limited virulence in mammalian hosts. While additional factors such as polymerase efficiency and receptor tropism, both of which remain unexplored in the case of SFSV, are contributing to virulence, studies using recombinant chimeric phleboviruses support a lead role of SFSV NSs in virulence: when replacing RVFV NSs with other NSs genes, the substitution with SFSV NSs conferred substantial attenuation in the mouse model and the chimeric virus has even been suggested as vaccine candidate for RVFV [46, 71].

Together with the mentioned studies using the phlebo-like bandaviruses in cells or chimeric phleboviruses in the mouse model, our data now provides further evidence that the ability of a particular NSs to interfere with both IFN induction and signalling are required for high virulence. Therefore, we propose that, rather than testing only for IFN induction, both IFN induction and signalling should be taken into considerationwhen rating the potential virulence of a novel phlebo- or bandavirus.

Funding information
Work in the authors' laboratory was supported by the Deutsche Forschungsgemeinschaft (DFG; German Research Foundation) (project number 197785619–SFB 1021), the Bundesministerium für Bildung und Forschung (Infect- ERA, grant 'ESCential'), and the Swedish Research Council (VR; no. 2018–05766).

Acknowledgements
We are grateful to Besim Berisha for excellent technical assistance and Andreas Schoen for helpful discussion. We are indebted to Patricia Aguilar and Robert Tesh from the World Reference Centre for Emerging Viruses and Arboviruses (WRCEVA) for kindly providing the Sabin strain of SFSV along with mouse immune ascites fluid. Luciferase reporter constructs and antibodies were kindly provided by Takashi Fujita and Georg Kochs.

Author contributions
J.D.W., performed the experiments, F.W., supervised the study. J.D.W. and F.W., wrote the manuscript.

Conflicts of interest
The authors declare that there are no conflicts of interest.

References
1. Alkan C, Bichaud L, de Lamballerie X, Alten B, Gould EA, *et al*. Sandfly-borne phleboviruses of Eurasia and Africa: epidemiology, genetic diversity, geographic range, control measures. *Antiviral Res* 2013;100:54–74.
2. Elliott RM, Brennan B. Emerging phleboviruses. *Curr Opin Virol* 2014;5:50–57.
3. Wuerth JD, Weber F. Phleboviruses and the type I interferon response. *Viruses* 2016;8.
4. Carhan A, Uyar Y, Ozkaya E, Ertek M, Dobler G, *et al*. Characterization of a sandfly fever Sicilian virus isolated during a sandfly fever epidemic in Turkey. *J Clin Virol* 2010;48:264–269.
5. Ergunay K, Ayhan N, Charrel RN. Novel and emergent sandfly-borne phleboviruses in Asia Minor: A systematic review. *Rev Med Virol* 2017;27.
6. Ayhan N, Velo E, de Lamballerie X, Kota M, Kadriaj P, *et al*. Detection of Leishmania infantum and a novel phlebovirus (balkan virus) from sand flies in Albania. *Vector Borne Zoonotic Dis* 2016;16:802–806.
7. Marklewitz M, Dutari LC, Paraskevopoulou S, Page RA, Loaiza JR, *et al*. Diverse novel phleboviruses in sandflies from the Panama Canal area, central Panama. *J Gen Virol* 2019;100:938–949.

8. Marklewitz M, Tchouassi DP, Hieke C, Heyde V, Torto B, *et al*. Insights into the evolutionary origin of Mediterranean sandfly fever viruses. *mSphere* 2020;5.
9. Ohlendorf V, Marklewitz M, Kopp A, Yordanov S, Drosten C, *et al*. Huge diversity of phleboviruses in ticks from Strandja Nature Park, Bulgaria. *Ticks Tick Borne Dis* 2019;10:697–703.
10. Papa A, Velo E, Bino S. A novel phlebovirus in *Albanian sandflies*. *Clin Microbiol Infect* 2011;17:585–587.
11. Bartelloni PJ, Tesh RB. Clinical and serologic responses of volunteers infected with phlebotomus fever virus (Sicilian type. *Am J Trop Med Hyg* 1976;25:456–462.
12. Sabin AB. Experimental studies on Phlebotomus (pappataci, sandfly) fever during World War II. *Arch Gesamte Virusforsch* 1951;4:367–410.
13. Alwassouf S, Christodoulou V, Bichaud L, Ntais P, Mazeris A, *et al*. Seroprevalence of sandfly-borne phleboviruses belonging to three serocomplexes (Sandfly fever Naples, Sandfly fever Sicilian and Salehabad) in dogs from Greece and cyprus using neutralization test. *PLoS Negl Trop Dis* 2016;10:e0005063.
14. Ayhan N, Sherifi K, Taraku A, Berxholi K, Charrel RN. High rates of neutralizing antibodies to toscana and sandfly fever sicilian viruses in Livestock, Kosovo. *Emerg Infect Dis* 2017;23:989–992.
15. Eitrem R, Stylianou M, Niklasson B. High prevalence rates of antibody to three sandfly fever viruses (Sicilian, Naples, and Toscana) among Cypriots. *Epidemiol Infect* 1991;107:685–691.
16. Sakhria S, Alwassouf S, Fares W, Bichaud L, Dachraoui K, *et al*. Presence of sandfly-borne phleboviruses of two antigenic complexes (Sandfly fever Naples virus and Sandfly fever Sicilian virus) in two different bio-geographical regions of Tunisia demonstrated by a microneutralisation-based seroprevalence study in dogs. *Parasit Vectors* 2014;7:476.
17. Tesh RB, Saidi S, Gajdamovic SJ, Rodhain F, Vesenjak-Hirjan J. Serological studies on the epidemiology of sandfly fever in the Old World. *Bull World Health Organ* 1976;54:663–674.
18. Eitrem R, Vene S, Niklasson B. Incidence of sand fly fever among Swedish United Nations soldiers on Cyprus during 1985. *Am J Trop Med Hyg* 1990;43:207–211.
19. Eitrem R, Niklasson B, Weiland O. Sandfly fever among Swedish tourists. *Scand J Infect Dis* 1991;23:451–457.
20. Kniha E, Obwaller AG, Dobler G, Poeppl W, Mooseder G, *et al*. Phlebovirus seroprevalence in Austrian Army personnel returning from missions abroad. *Parasit Vectors* 2019;12:416.
21. Papa A, Konstantinou G, Pavlidou V, Antoniadis A. Sandfly fever virus outbreak in Cyprus. *Clin Microbiol Infect* 2006;12:192–194.
22. Shiraly R, Khosravi A, Farahangiz S. Seroprevalence of sandfly fever virus infection in military personnel on the western border of Iran. *J Infect Public Health* 2017;10:59–63.
23. Alkan C, Erisoz Kasap O, Alten B, Lamballerie de, Charrel RN. Sandfly-Borne Phlebovirus Isolations from Turkey: New Insight into the Sandfly fever Sicilian and Sandfly fever Naples Species. *PLoS Negl Trop Dis* 2016;10:e0004519.
24. Alkan C, Moin Vaziri V, Ayhan N, Badakhshan M, Bichaud L, *et al*. Isolation and sequencing of Dashli virus, a novel sicilian-like virus in sandflies from Iran; Genetic and phylogenetic evidence for the creation of one novel species within the phlebovirus genus in the Phenuiviridae family. *PLoS Negl Trop Dis* 2017;11:e0005978.
25. Weber M, Gawanbacht A, Habjan M, Rang A, Borner C, *et al*. Incoming RNA virus nucleocapsids containing a 5'-triphosphorylated genome activate RIG-I and antiviral signaling. *Cell Host Microbe* 2013;13:336–346.
26. Liu G, Gack MU. Distinct and orchestrated functions of RNA sensors in innate immunity. *Immunity* 2020;53:26–42.
27. Yoneyama M, Onomoto K, Jogi M, Akaboshi T, Fujita T. Viral RNA detection by RIG-I-like receptors. *Curr Opin Immunol* 2015;32:48–53.
28. Schoggins JW. Interferon-stimulated genes: what do they all do? *Annu Rev Virol* 2019;6:567–584.
29. do Valle TZ, Billecocq A, Guillemot L, Alberts R, Gommet C, *et al*. A new mouse model reveals a critical role for host innate immunity in resistance to Rift Valley fever. *J Immunol* 2010;185:6146–6156.
30. Frese M, Kochs G, Feldmann H, Hertkorn C, Haller O. Inhibition of bunyaviruses, phleboviruses, and hantaviruses by human MxA protein. *J Virol* 1996;70:915–923.
31. Sandrock M, Frese M, Haller O, Kochs G. Interferon-induced rat Mx proteins confer resistance to Rift Valley fever virus and other arthropod-borne viruses. *J Interferon Cytokine Res* 2001;21:663–668.
32. Bouloy M, Janzen C, Vialat P, Khun H, Pavlovic J, *et al*. Genetic evidence for an interferon-antagonistic function of Rift Valley fever virus nonstructural protein NSs. *J Virol* 2001;75:1371–1377.
33. Crance JM, Gratier D, Guimet J, Jouan A. Inhibition of sandfly fever Sicilian virus (Phlebovirus) replication in vitro by antiviral compounds. *Res Virol* 1997;148:353–365.
34. Habjan M, Pichlmair A, Elliott RM, Overby AK, Glatter T, *et al*. NSs protein of Rift Valley fever virus induces the specific degradation of the double-stranded RNA-dependent protein kinase. *J Virol* 2009;83:4365–4375.
35. Kende M. Prophylactic and therapeutic efficacy of poly(I,C)-LC against Rift Valley fever virus infection in mice. *J Biol Response Mod* 1985;4:503–511.
36. Liu Y, Wu B, Paessler S, Walker DH, Tesh RB, *et al*. The pathogenesis of severe fever with thrombocytopenia syndrome virus infection in alpha/beta interferon knockout mice: insights into the pathologic mechanisms of a new viral hemorrhagic fever. *J Virol* 2014;88:1781–1786.
37. Mendenhall M, Wong MH, Skirpstunas R, Morrey JD, Gowen BB. Punta Toro virus (Bunyaviridae, Phlebovirus) infection in mice: strain differences in pathogenesis and host interferon response. *Virology* 2009;395:143–151.
38. Morrill JC, Jennings GB, Cosgriff TM, Gibbs PH, Peters CJ. Prevention of Rift Valley fever in rhesus monkeys with interferon-alpha. *Rev Infect Dis* 1989;11:S815–S825.
39. Morrill JC, Jennings GB, Johnson AJ, Cosgriff TM, Gibbs PH, *et al*. Pathogenesis of Rift Valley fever in rhesus monkeys: role of interferon response. *Arch Virol* 1990;110:195–212.
40. Peters CJ, Reynolds JA, Slone TW, Jones DE, Stephen EL. Prophylaxis of Rift Valley fever with antiviral drugs, immune serum, an interferon inducer, and a macrophage activator. *Antiviral Res* 1986;6:285–297.
41. Sidwell RW, Huffman JH, Smee DF, Gilbert J, Gessaman A, *et al*. Potential role of immunomodulators for treatment of phlebovirus infections of animals. *Ann N Y Acad Sci* 1992;653:344–355.
42. Eifan S, Schnettler E, Dietrich I, Kohl A, Blomstrom AL. Non-structural proteins of arthropod-borne bunyaviruses: roles and functions. *Viruses* 2013;5:2447–2468.
43. Ly HJ, Ikegami T. Rift Valley fever virus NSs protein functions and the similarity to other bunyavirus NSs proteins. *Virol J* 2016;13:118.
44. Ikegami T, Narayanan K, Won S, Kamitani W, Peters CJ, *et al*. Rift Valley fever virus NSs protein promotes post-transcriptional downregulation of protein kinase PKR and inhibits eIF2alpha phosphorylation. *PLoS Pathog* 2009;5:e1000287.
45. Kainulainen M, Habjan M, Hubel P, Busch L, Lau S, *et al*. Virulence factor NSs of rift valley fever virus recruits the F-box protein FBXO3 to degrade subunit p62 of general transcription factor TFIIH. *J Virol* 2014;88:3464–3473.
46. Lihoradova OA, Indran SV, Kalveram B, Lokugamage N, Head JA, *et al*. Characterization of Rift Valley fever virus MP-12 strain encoding NSs of Punta Toro virus or sandfly fever Sicilian virus. *PLoS Negl Trop Dis* 2013;7:e2181.
47. Wuerth JD, Habjan M, Wulle J, Superti-Furga G, Pichlmair A, *et al*. NSs Protein of Sandfly Fever Sicilian Phlebovirus Counteracts Interferon (IFN) Induction by Masking the DNA-Binding Domain of IFN Regulatory Factor 3. *J Virol* 2018;92:23.

48. Gori Savellini G, Anichini G, Gandolfo C, Prathyumnan S, Cusi MG. Toscana virus non-structural protein NSS acts as E3 ubiquitin ligase promoting rig-i degradation. *PLoS Pathog* 2019;15:e1008186.
49. Horisberger MA, de Staritzky K. A recombinant human interferon-alpha B/D hybrid with a broad host-range. *J Gen Virol* 1987;68:945–948.
50. Yoneyama M, Suhara W, Fukuhara Y, Fukuda M, Nishida E, *et al*. Direct triggering of the type I interferon system by virus infection: activation of a transcription factor complex containing IRF-3 and CBP/p300. *EMBO J* 1998;17:1087–1095.
51. Kochs G, Garcia-Sastre A, Martinez-Sobrido L. Multiple anti-interferon actions of the influenza A virus NS1 protein. *J Virol* 2007;81:7011–7021.
52. Weidmann M, Sanchez-Seco MP, Sall AA, Ly PO, Thiongane Y, *et al*. Rapid detection of important human pathogenic Phleboviruses. *J Clin Virol* 2008;41:138–142.
53. Bird BH, Bawiec DA, Ksiazek TG, Shoemaker TR, Nichol ST. Highly sensitive and broadly reactive quantitative reverse transcription-PCR assay for high-throughput detection of Rift Valley fever virus. *J Clin Microbiol* 2007;45:3506–3513.
54. Holzer M, Schoen A, Wulle J, Muller MA, Drosten C, *et al*. Virus- and interferon alpha-induced transcriptomes of cells from the microbat *Myotis daubentonii*. *iScience* 2019;19:647–661.
55. Prescott J, Hall P, Acuna-Retamar M, Ye C, Wathelet MG, *et al*. New World hantaviruses activate IFNlambda production in type I IFN-deficient vero E6 cells. *PLoS One* 2010;5:e11159.
56. Kuri T, Habjan M, Penski N, Weber F. Species-independent bioassay for sensitive quantification of antiviral type I interferons. *Virol J* 2010;7:50.
57. International Committee on Taxonomy of Viruses. Virus Taxonomy: 2019 Release; 2019. https://talk.ictvonline.org/taxonomy/
58. Chaudhary V, Zhang S, Yuen KS, Li C, Lui PY, *et al*. Suppression of type I and type III IFN signalling by NSs protein of severe fever with thrombocytopenia syndrome virus through inhibition of STAT1 phosphorylation and activation. *J Gen Virol* 2015;96:3204–3211.
59. Ning YJ, Wang M, Deng M, Shen S, Liu W, *et al*. Viral suppression of innate immunity via spatial isolation of TBK1/IKKepsilon from mitochondrial antiviral platform. *J Mol Cell Biol* 2014;6:324–337.
60. Qu B, Qi X, Wu X, Liang M, Li C, *et al*. Suppression of the interferon and NF-kappaB responses by severe fever with thrombocytopenia syndrome virus. *J Virol* 2012;86:8388–8401.
61. Santiago FW, Covaleda LM, Sanchez-Aparicio MT, Silvas JA, Diaz-Vizarreta AC, *et al*. Hijacking of RIG-I signaling proteins into virus-induced cytoplasmic structures correlates with the inhibition of type I interferon responses. *J Virol* 2014;88:4572–4585.
62. Rezelj VV, Li P, Chaudhary V, Elliott RM, Jin DY, *et al*. Differential antagonism of human innate immune responses by tick-borne phlebovirus nonstructural proteins. *mSphere* 2017;2.
63. Ning S, Pagano JS, Barber GN. IRF7: activation, regulation, modification and function. *Genes Immun* 2011;12:399–414.
64. Marie I, Durbin JE, Levy DE. Differential viral induction of distinct interferon-alpha genes by positive feedback through interferon regulatory factor-7. *EMBO J* 1998;17:6660–6669.
65. Sato M, Hata N, Asagiri M, Nakaya T, Taniguchi T, *et al*. Positive feedback regulation of type I IFN genes by the IFN-inducible transcription factor IRF-7. *FEBS Lett* 1998;441:106–110.
66. Stewart CE, Randall RE, Adamson CS. Inhibitors of the interferon response enhance virus replication in vitro. *PLOS ONE* 2014;9:e112014.
67. Wu X, Qi X, Qu B, Zhang Z, Liang M, *et al*. Evasion of antiviral immunity through sequestering of TBK1/IKKepsilon/IRF3 into viral inclusion bodies. *J Virol* 2014;88:3067–3076.
68. Pichlmair A, Kandasamy K, Alvisi G, Mulhern O, Sacco R, *et al*. Viral immune modulators perturb the human molecular network by common and unique strategies. *Nature* 2012;487:486–490.
69. Wuerth JD, Habjan M, Kainulainen M, Berisha B, Bertheloot D, *et al*. eIF2B as a target for viral evasion of PKR-Mediated Translation Inhibition. *mBio* 2020;11.
70. Proenca-Modena JL, Hyde JL, Sesti-Costa R, Lucas T, Pinto AK, *et al*. Interferon-Regulatory Factor 5-dependent signaling restricts orthobunyavirus dissemination to the central nervous System. *J Virol* 2016;90:189–205.
71. Nishiyama S, Slack OA, Lokugamage N, Hill TE, Juelich TL, *et al*. Attenuation of pathogenic Rift Valley fever virus strain through the chimeric S-segment encoding sandfly fever phlebovirus NSs or a dominant-negative PKR. *Virulence* 2016;7:871–881.

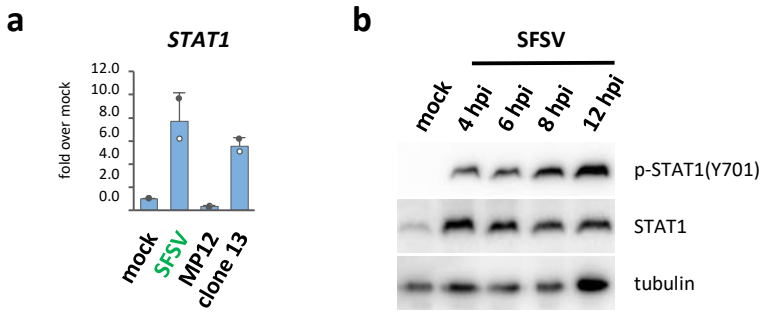

Supporting Fig. 1: STAT1 expression and phosphorylation under infection

a Samples of Fig. 1b were analysed via RT-qPCR with primers for *STAT1* (n = 2, mean ± SD). **b** A549 cells were infected with SFSV (MOI 1), harvested at the indicated time points, and analysed by immunoblotting for STAT1 phosphorylation and total STAT1 levels as described for Fig. 1a.

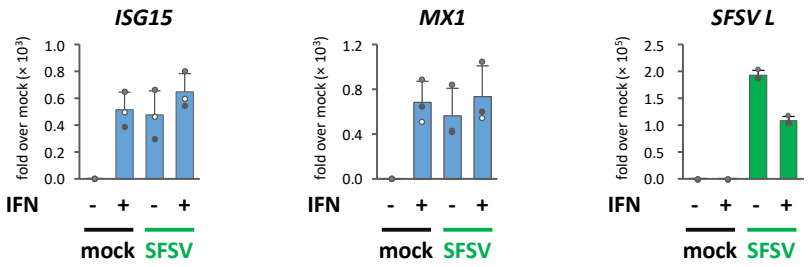

Supporting Fig. 2: ISG induction under IFN pre-treatment
A549 cells were pre-treated with 100 IU/ml pan-species IFN-α (B/D) for 1 h, subsequently infected with SFSV (MOI 1) or mock-treated, and IFN or mock treatment was continued until harvesting for RT-qPCR analysis 12 hpi (n = 3, mean ± SD).

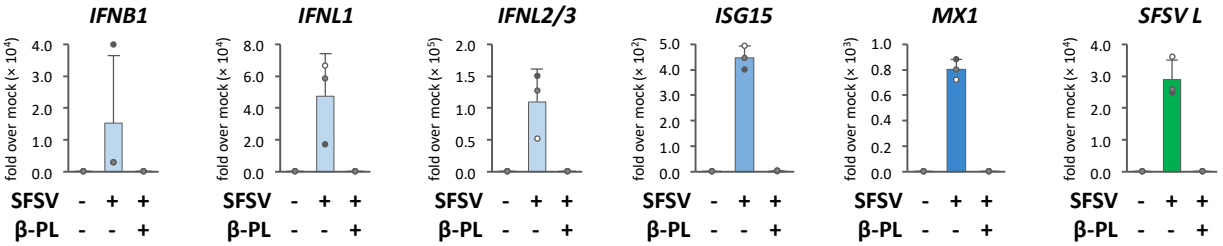

Supporting Fig. 3: Interferon and ISG induction after virus inactivation

A549 cells were infected with β-propiolactone-inactivated or matching mock-treated SFSV (MOI 1), and harvested 12 hpi for RT-qPCR analysis (n = 3, mean ± SD).

4.4 Research article:
eIF2B as Target for Viral Evasion of PKR-Mediated Translation Inhibition

Own contribution:
I performed all experiments shown in the main figures with exceptions of fig. 1 and 6c. I further contributed to the design of the study, as well as writing and illustrating the manuscript.

Generation of recombinant viruses and the infection experiment displayed in fig. 1 were performed by Matthias Habjan. Infection and Western Blot analysis in suppl. fig. 2 were performed by Markus Kainulainen. Bacterial expression and purification of eIF2B subunits and SFSV NSs (data not shown), as well as part of the molecular cloning, and the experiment shown in fig. 6c were performed by Besim Berisha.

_____

Jennifer Würth

AMERICAN SOCIETY FOR MICROBIOLOGY | mBio®

RESEARCH ARTICLE
Host-Microbe Biology

eIF2B as a Target for Viral Evasion of PKR-Mediated Translation Inhibition

Jennifer Deborah Wuerth,[a,b,c] Matthias Habjan,[d] Markus Kainulainen,[b] Besim Berisha,[a] Damien Bertheloot,[c] Giulio Superti-Furga,[e,f] Andreas Pichlmair,[d,g,h] Friedemann Weber[a,b,h]

[a]Institute for Virology, FB10-Veterinary Medicine, Justus-Liebig University, Giessen, Germany
[b]Institute for Virology, Philipps-University Marburg, Marburg, Germany
[c]Institute of Innate Immunity, University of Bonn, Bonn, Germany
[d]Innate Immunity Laboratory, Max-Planck Institute of Biochemistry, Munich, Germany
[e]CeMM Research Center for Molecular Medicine of the Austrian Academy of Sciences, Vienna, Austria
[f]Center for Physiology and Pharmacology, Medical University of Vienna, Vienna, Austria
[g]Institute of Virology, Technical University of Munich, School of Medicine, Munich, Germany
[h]German Center for Infection Research (DZIF), partner sites Giessen and Munich, Germany

ABSTRACT RNA-activated protein kinase (PKR) is a major innate immune factor that senses viral double-stranded RNA (dsRNA) and phosphorylates eukaryotic initiation factor (eIF) 2α. Phosphorylation of the α subunit converts the eIF2$\alpha\beta\gamma$ complex into a stoichiometric inhibitor of eukaryotic initiation factor eIF2B, thus halting mRNA translation. To escape this protein synthesis shutoff, viruses have evolved countermechanisms such as dsRNA sequestration, eIF-independent translation by an internal ribosome binding site, degradation of PKR, or dephosphorylation of PKR or of phospho-eIF2α. Here, we report that sandfly fever Sicilian phlebovirus (SFSV) confers such a resistance without interfering with PKR activation or eIF2α phosphorylation. Rather, SFSV expresses a nonstructural protein termed NSs that strongly binds to eIF2B. Although NSs still allows phospho-eIF2α binding to eIF2B, protein synthesis and virus replication are unhindered. Hence, SFSV encodes a unique PKR antagonist that acts by rendering eIF2B resistant to the inhibitory action of bound phospho-eIF2α.

IMPORTANCE RNA-activated protein kinase (PKR) is one of the most powerful antiviral defense factors of the mammalian host. PKR acts by phosphorylating mRNA translation initiation factor eIF2α, thereby converting it from a cofactor to an inhibitor of mRNA translation that strongly binds to initiation factor eIF2B. To sustain synthesis of their proteins, viruses are known to counteract this on the level of PKR or eIF2α or by circumventing initiation factor-dependent translation altogether. Here, we report a different PKR escape strategy executed by sandfly fever Sicilian virus (SFSV), a member of the increasingly important group of phleboviruses. We found that the nonstructural protein NSs of SFSV binds to eIF2B and protects it from inactivation by PKR-generated phospho-eIF2α. Protein synthesis is hence maintained and the virus can replicate despite ongoing full-fledged PKR signaling in the infected cells. Thus, SFSV has evolved a unique strategy to escape the powerful antiviral PKR.

KEYWORDS PKR, phospho-eIF2α, translation inhibition, integrated stress response, viral PKR antagonist, eIF2B, sandfly fever Sicilian phlebovirus, NSs protein

Protein kinase R (PKR) is a major host defense factor against viruses that acts by inhibiting mRNA translation (1). PKR senses viral double-stranded RNA (dsRNA) and phosphorylates Ser51 of the α subunit of eukaryotic initiation factor (eIF) 2. The heterotrimeric eIF2$\alpha\beta\gamma$ complex is a GTPase pivotal for initiation of mRNA translation.

Citation Wuerth JD, Habjan M, Kainulainen M, Berisha B, Bertheloot D, Superti-Furga G, Pichlmair A, Weber F. 2020. eIF2B as a target for viral evasion of PKR-mediated translation inhibition. mBio 11:e00976-20. https://doi.org/10.1128/mBio.00976-20.

Invited Editor Tetsuro Ikegami, The University of Texas Medical Branch at Galveston

Editor Thomas E. Morrison, University of Colorado School of Medicine

Address correspondence to Friedemann Weber, friedemann.weber@vetmed.uni-giessen.de.

Received 21 April 2020
Accepted 11 June 2020
Published 14 July 2020

In its GTP-bound form, the eIF2$\alpha\beta\gamma$ complex loads initiator tRNAi-Met onto 40S ribosome subunits. AUG recognition on the mRNA then stimulates GTP hydrolysis, followed by eIF2·GDP release and 60S subunit joining. eIF2·GTP is then recycled by the guanine nucleotide exchange factor eIF2B. Phosphorylation by PKR, however, converts eIF2α from a substrate to a competitive inhibitor of eIF2B, forcing eIF2B into a so-called nonproductive state that halts the translation of mRNAs. To sustain synthesis of their proteins, viruses have therefore evolved escape mechanisms for the PKR-eIF2α signaling cascade, the so-called PKR antagonists. The strategies known so far involve sequestration of dsRNA, circumventing eIFs by means of a special internal ribosome entry site (IRES), PKR sequestration, inhibition of PKR phosphorylation, degradation of PKR, or dephosphorylation of eIF2α (2, 3).

Members of the arthropod-transmitted genus *Phlebovirus* (order *Bunyavirales*, family *Phenuiviridae*) are globally emerging pathogens with significant public health and economic impacts (4). The long-known Rift Valley fever virus (RVFV) can cause encephalitis or hemorrhagic fever in humans and abortion storms and high death rates in ruminants (5). Human infection with the recently emerged severe fever with thrombocytopenia syndrome virus in Asia or the related Heartland virus in North America lead to multiorgan dysfunction with a high case fatality rate (6). Moreover, intermediately virulent phleboviruses such as sandfly fever Sicilian virus (SFSV), Punta Toro virus (PTV), or Toscana virus (TOSV) can cause an incapacitating febrile disease with sudden onset, myalgia, headache, malaise, leukocytopenia, and ocular or gastrointestinal symptoms that may (in the case of TOSV) develop into severe encephalitis (7). SFSV in particular, originally isolated by Albert Sabin after an outbreak of so-called sandfly fever (or "dog disease") among Allied forces during the invasion of Sicily in 1943 (8), turned out to be one the most widespread and prevalent phleboviruses. SFSV is found in a geographic area from Portugal to India in Eurasia and to Somalia in Africa, with seroprevalences up to 50% in humans and nearly 80% in domestic animals (9–12). While SFSV continues to cause disease in immunologically naive soldiers deployed to areas of endemicity, it becomes increasingly relevant also in travel medicine (9, 12–15). Despite their wide geographical spread, the high risk for exposure, continuing case reports, and their emerging nature, only little is known about SFSV and SFSV-like viruses at the molecular level.

Phleboviruses possess a single-stranded trisegmented RNA genome. The large (L) and medium (M) segments carry the genes for the viral polymerase L or multiple nonstructural proteins and the glycoproteins Gn and Gc, respectively, in negative-sense orientation. In contrast, the small (S) segment uses an antisense configuration to carry the gene for the nonstructural protein NSs in addition to the one for the nucleocapsid protein N.

Replication and transcription of the phlebovirus genome take place in the cytoplasm and can activate PKR (16, 17). For two phleboviruses, RVFV and TOSV, it was previously shown that they express a nonstructural protein (NSs) that triggers proteasomal degradation of PKR (16, 17). However, for the related human pathogen SFSV, although it also encodes an NSs, there is no such PKR degradation, and it remained unclear whether it can escape PKR at all (17, 18). Of note, the NSs proteins of different phleboviruses show only little sequence conservation, which is reflected by the differences in their subcellular localization, host interactomes, and the molecular mechanisms employed to perturb host cell responses (4). Here, we investigated whether and how SFSV, one of the most widespread and prevalent phleboviruses, may be coping with the PKR system. We show that its NSs confers PKR resistance by a unique strategy that targets the downstream factor eIF2B rather than PKR or phospho-eIF2α.

RESULTS

PKR escape activity is a trait of several phleboviral NSs proteins. In a first set of experiments addressing potential effects of SFSV NSs on PKR, we employed a recombinant RVFV (rRVFVΔNSs::SFSV NSs), in which the RVFV NSs gene was replaced by the NSs of SFSV (19), along with recombinant wild-type (wt) RVFV and RVFV NSs deletion

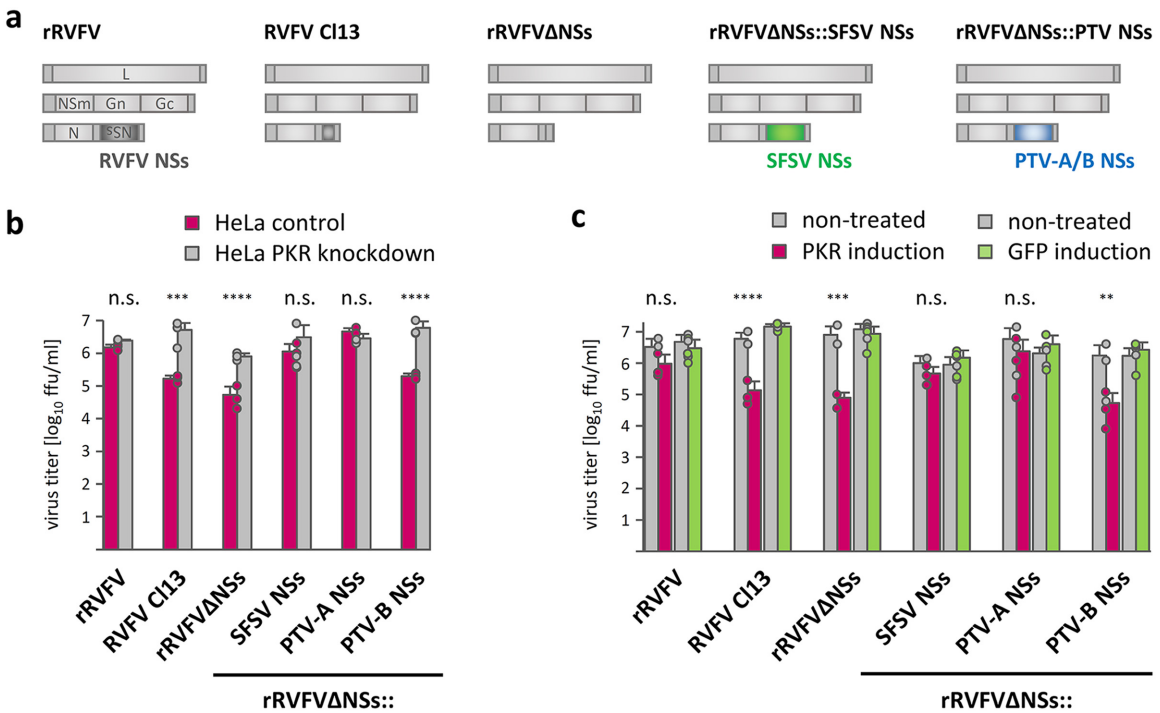

FIG 1 SFSV NSs rescues PKR-sensitive virus replication. (a) Tripartite single-stranded RNA genomes of the virus panel used: wt rRVFV (strain ZH548), natural NSs-deleted RVFV strain clone 13 (Cl13), and recombinant RVFVs expressing no NSs (rRVFVΔNSs) or the NSs genes of SFSV, PTV-A, or PTV-B. (b and c) Replication of the viruses in the absence or presence of PKR. HeLa cells with a stable PKR knockdown and PKR-expressing control cells (b) or doxycycline-induced HEK293 FLP-IN PKR or GFP cells (c) were infected at an MOI of 0.01, and viral titers were determined 24 h later ($n = 3$, mean ± SD). ****, $P \leq 0.0001$; ***, $P < 0.001$; **, $P < 0.01$; n.s., not significant, $P > 0.05$ (two-way analysis of variance [ANOVA]).

mutants as controls (Fig. 1a). Here, we also included rRVFV expressing NSs of the PTV phlebovirus strains Adames (PTV-A; virulent) or Balliet (PTV-B; avirulent), but these could not be followed up later due their transcription shutoff activity (see below). The replicative capacity of the various RVFV recombinants was first compared in PKR knockdown versus PKR-expressing control cell lines. As expected from the PKR-destroying activity of RVFV NSs (17, 20), recombinant wild-type RVFV (rRVFV) grew to similar titers in both cell lines, whereas recombinant (rRVFVΔNSs) or natural (RVFV clone 13) NSs deletion mutants exhibited reduced replication in control cells but reached levels comparable to those of rRVFV in PKR knockdown cells (Fig. 1b). The NSs proteins of SFSV as well as of PTV-A also enabled similar growth efficiencies in both cell lines, whereas PTV-B NSs had no such activity. Of note, clone 13 and PTV-B are natural isolates from febrile humans (21, 22), and the NSs protein of PTV-B (but not clone 13) retains type-I interferon (IFN) antagonist function in murine cells (23). We also infected HEK293 FLP-IN cells in which the expression of PKR (or green fluorescent protein [GFP] as control) was induced by doxycycline treatment. Also, both NSs-deficient control viruses as well as the PTV-B NSs recombinant were highly and specifically sensitive to PKR, whereas recombinants containing the NSs genes of SFSV or PTV-A showed only a minor reduction in titers under conditions of PKR induction, similarly to recombinant wild-type RVFV (Fig. 1c). Thus, PKR depletion and overexpression experiments suggest that the NSs proteins of SFSV (and PTV-A) confer PKR resistance.

PKR escape activity that does not affect PKR signaling. We then investigated the influence of the phleboviral NSs proteins on the PKR signaling pathway. Infection with the recombinant viruses (Fig. 2a) confirmed that the NSs of RVFV, but not of SFSV or PTV, reduces PKR levels (17, 18, 20). Consequently, autophosphorylated PKR, an indicator of PKR activity, was undetectable in the presence of RVFV NSs. Curiously, however, when cells were infected with viruses expressing SFSV or PTV NSs, phosphorylation of

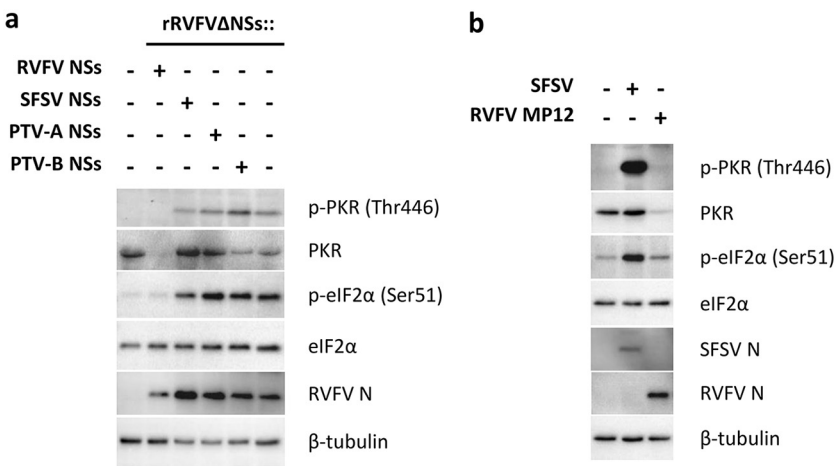

FIG 2 SFSV NSs affects neither PKR activation nor eIF2α phosphorylation. (a) A549 cells were infected with the recombinant RVFVs expressing the various NSs genes presented in Fig. 1 at an MOI of 1 and harvested 8 hpi for immunoblot analysis (representative of 2 experiments). Staining of RVFV N served as marker for viral infection common to all recombinant viruses. (b) A549 cells infected with SFSV or RVFV strain MP12 (MOI 1) and harvested 12 hpi were analyzed by immunoblotting (representative of 5 experiments).

both PKR and its substrate eIF2α was upregulated similar to that in the NSs deletion virus rRVFVΔNSs (Fig. 2a). Time course analyses showed that PKR and eIF2α phosphorylation persisted despite the presence of SFSV or PTV NSs (see Fig. S1 in the supplemental material). In line with this, parental SFSV also triggered PKR and eIF2α phosphorylation, unlike the PKR-destroying RVFV (Fig. 2b). Thus, on one hand, the NSs proteins of SFSV and PTV are required to counter the antiviral activity of PKR (Fig. 1), indicating a PKR escape phenotype. On the other hand, however, these NSs proteins seem to act in a manner that is different from that of prototypical PKR antagonists, as they do not interfere with the PKR-eIF2α phosphorylation axis.

SFSV NSs enhances eIF2-dependent translation. Transfection of DNA plasmids is known to activate PKR (24). Hence, we aimed to assess the impact of SFSV NSs on cellular mRNA translation by using a transiently transfected luciferase reporter system. PTV NSs could not be included in these and further experiments as it impairs general host transcription (18) (data not shown). The luciferase reporter system encodes a bicistronic mRNA in which translation of the upstream firefly luciferase open reading frame (ORF) is canonically initiated from the 5′ cap (and hence requires eIF2), whereas translation of the downstream *Renilla* luciferase ORF is initiated from the cricket paralysis virus IRES ($IRES_{CrPV}$) that does not require any eIFs (25). Cotransfection of SFSV NSs with the bicistronic reporter construct amplified firefly luciferase activity, i.e., eIF-dependent gene expression, in a dose-dependent manner (Fig. 3a), whereas it had no detectable effect on eIF-independent *Renilla* luciferase activity (Fig. 3b). Of note, the boost of firefly luciferase activity was observable only for C-terminally epitope-tagged NSs (SFSV NSs-3×FLAG), but not for the N-terminally tagged variant (3×FLAG-SFSV NSs) or the inert negative control (3×FLAG-ΔMx) (Fig. 3a). Both the C-terminally and the N-terminally tagged NSs proteins were, however, expressed at comparable levels (Fig. 3c) and exhibited the previously reported (19) inhibitory activity toward transcriptional induction of type I interferon (see Fig. S2a and c). Consistent with the results from the bicistronic luciferase assay, C-terminally tagged SFSV NSs also boosted an eIF-dependent SV40 luciferase reporter (Fig. S2b). Furthermore, puromycin labeling of *de novo* synthesized proteins showed that mRNA translation was comparable to that in noninfected cells during wt SFSV infection, whereas infection with the PKR-activating NSs mutant clone 13 (Fig. S1) led to a shutdown of protein synthesis (Fig. 3d). Thus, unlike other previously characterized viral PKR antagonists, SFSV NSs enables both viral replication and canonical eIF-dependent mRNA translation without blocking PKR activation or affecting the phosphorylation state of eIF2α.

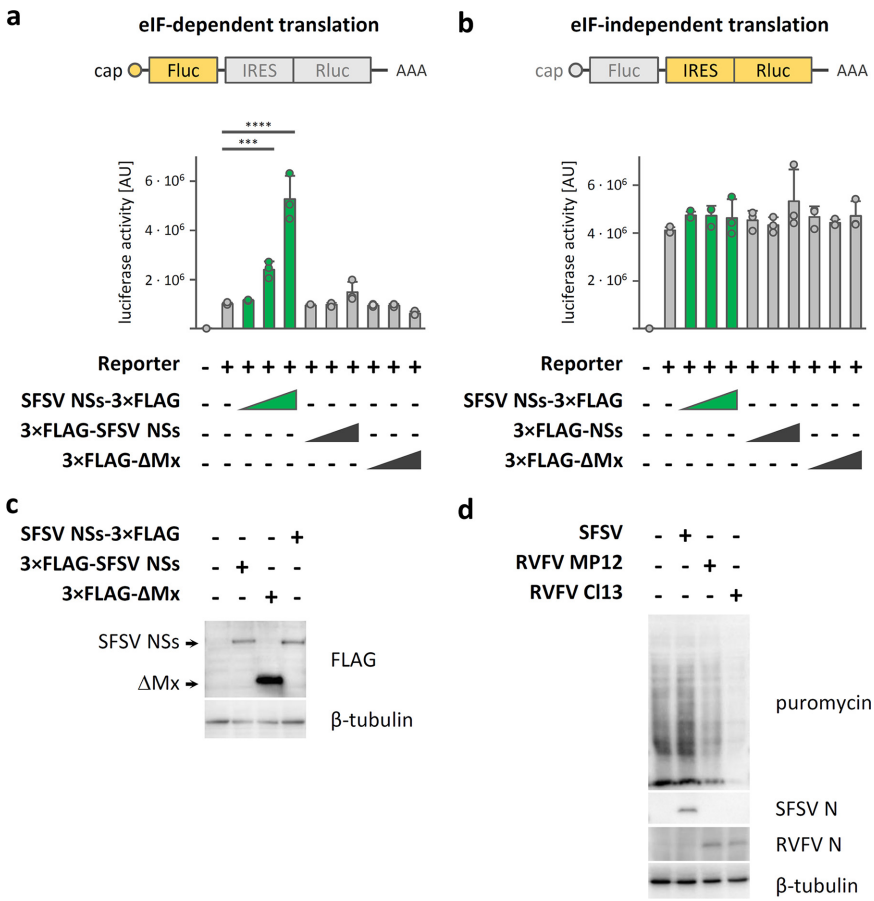

FIG 3 Effect of SFSV NSs on mRNA translation. (a and b) Influence of SFSV NSs on a bicistronic reporter system with an upstream canonical (i.e., eIF-dependent) firefly luciferase ORF and a downstream *Renilla* luciferase ORF initiated from the eIF-independent $IRES_{CrPV}$. HEK293 cells were transfected with the bicistronic reporter plasmid and expression plasmids for SFSV NSs containing either a C- or N-terminal 3×FLAG tag (SFSV NSs-3×FLAG and 3×FLAG-NSs SFSV, respectively) or for an irrelevant negative control (3×FLAG-ΔMx). Lysates were assayed for eIF2-dependent firefly (Fluc) (a) and IRES-dependent *Renilla* luciferase (Rluc) (b) activities (arbitrary units [AU]). Shown are data from 1 of 3 independent experiments. Each of these was conducted with three technical (i.e., parallel) replicates. Bars show means ± SDs. ****, $P \leq 0.0001$; ***, $P < 0.001$ (one-way ANOVA, corrected for multiple comparisons using Dunnett test). For the Rluc data, none of the tests reached the significance level. (c) C- and N-terminally tagged SFSV NSs (SFSV NSs-3×FLAG and 3×FLAG-NSs SFSV, respectively) were transiently expressed in HEK293 cells, and expression levels were analyzed by immunoblotting (representative of 3 experiments). (d) A549 cells were infected with SFSV, MP12, or clone 13 (MOI, 1), and currently translated proteins were labeled by the addition of puromycin 12 h postinfection, followed by subsequent immunoblot analysis (representative of 4 experiments). Staining of viral N proteins served as marker for infection. Data are representative and from 1 of 3 independent experiments each with 3 technical replicates (a and b), from 1 of 3 independent experiments (c), or from 1 of 4 independent experiments (d).

SFSV NSs interacts with the eIF2B complex. SFSV NSs seems to protect protein synthesis by neutralizing antiviral PKR action downstream of eIF2α. Ser51 phosphorylation of eIF2α is known to convert the eIF2αβγ complex from a substrate into an inhibitor of its guanine nucleotide exchange factor eIF2B (26). Strikingly, our previous mass spectrometry-based approach to map the host interactome of SFSV NSs returned all five subunits of the eIF2B complex as the highest scoring candidate interactors (see Fig. S3) (27). To verify the interaction, we overexpressed the eIF2B subunits from cDNA plasmids together with C-terminally 3×FLAG-tagged SFSV NSs and performed immunoprecipitations for NSs or eIF2B with antibodies to epitope tags. Immunoprecipitation of FLAG-tagged NSs, but not the FLAG-tagged control protein (ΔMx), coprecipitated all five eIF2B subunits in a highly reproducible manner (Fig. 4a). Vice versa, when using an expression construct for epitope-tagged eIF2Bε-mCitrine-hemagglutinin (HA), we were

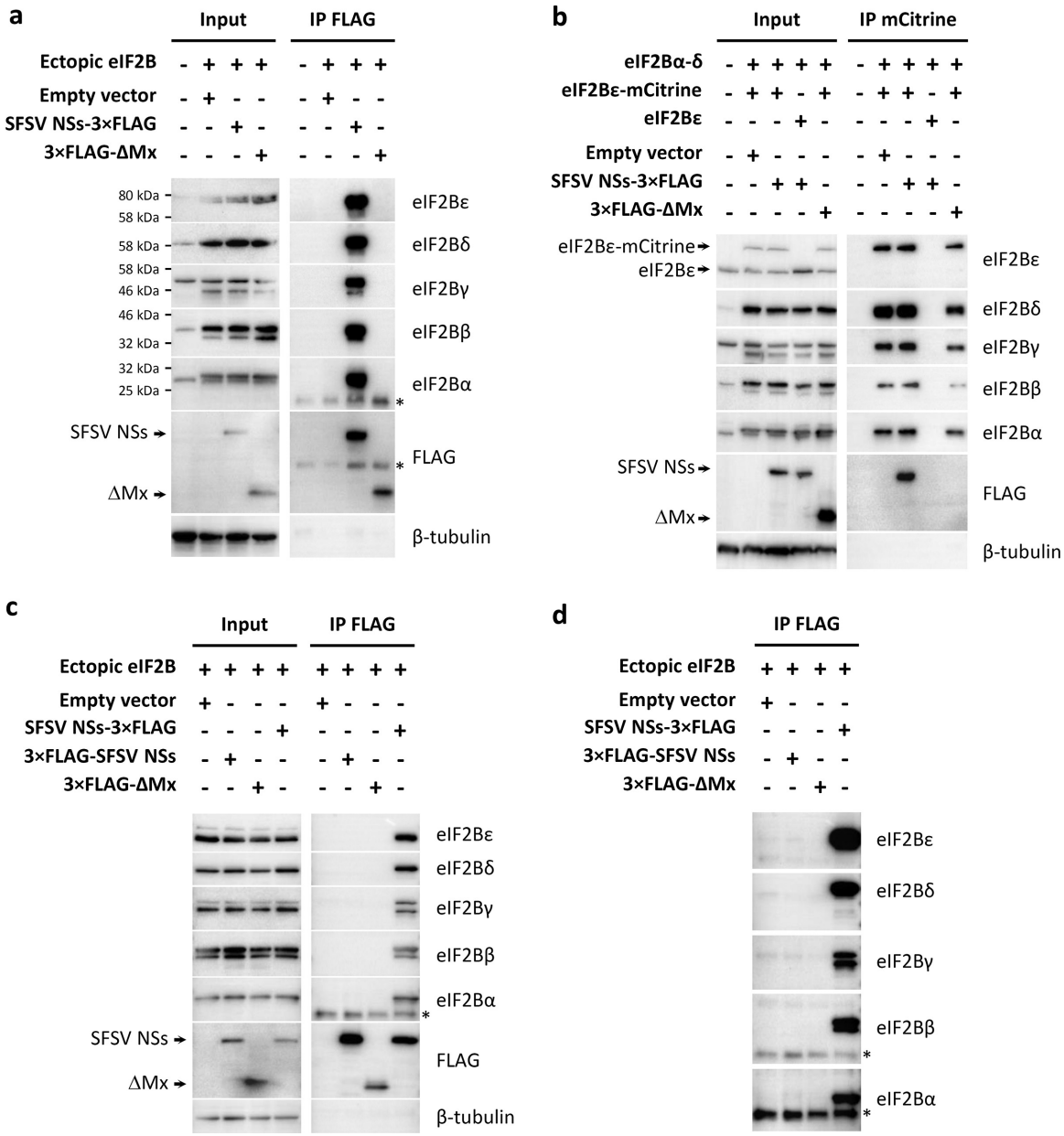

FIG 4 Interaction of SFSV NSs with the eIF2B complex. Coimmunoprecipitation experiments. HEK293 cells were transiently transfected with expression plasmids for all eIF2B subunits as well as 3×FLAG-tagged SFSV NSs variants or the unrelated control 3×FLAG-ΔMx. Proteins in the cell lysates were precipitated via specific tags and analyzed by immunoblotting with the indicated antibodies. (a) Overexpression of eIF2B subunits along with C-terminally 3×FLAG-tagged NSs (SFSV NSs-3×FLAG). Immunoprecipitation was performed with anti-FLAG antibody. (b) mCitrine-HA-tagged eIF2Bε (eIF2Bε-mCitrine-HA) was expressed along with eIF2B subunits α, β, γ, and δ as well as SFSV NSs-3×FLAG. Untagged eIF2Bε served as control for unspecific binding. The eIF2B complex was precipitated using an mCitrine-binding matrix. (c) Overexpression of untagged eIF2B subunits along with C- or N-terminally 3×FLAG-tagged NSs (SFSV NSs-3×FLAG and 3×FLAG-NSs SFSV, respectively). Immunoprecipitation was performed with anti-FLAG antibody. (d) Immunoprecipitated proteins from the experiment shown in panel c after prolonged exposure. Shown data are representatives of 3 (a, c, and d) or 5 (b) experiments. *, light chain of the IP antibody.

able to pull down the entire eIF2B complex via the mCitrine tag and also SFSV NSs (Fig. 4b). As a specificity control, we expressed untagged eIF2Bε instead of eIF2Bε-mCitrine-HA and observed no such precipitations, as expected. Furthermore, SFSV NSs also enabled specific coprecipitation of endogenous eIF2B from both A549 and HEK293 cells (Fig. S4a and data not shown), and superinfection with a PKR-activating NSs-deficient RVFV did not affect its interaction with eIF2B (Fig. S4b). Finally, only the translation-rescuing SFSV NSs with the C-terminal FLAG tag (SFSV NSs-3×FLAG) but not

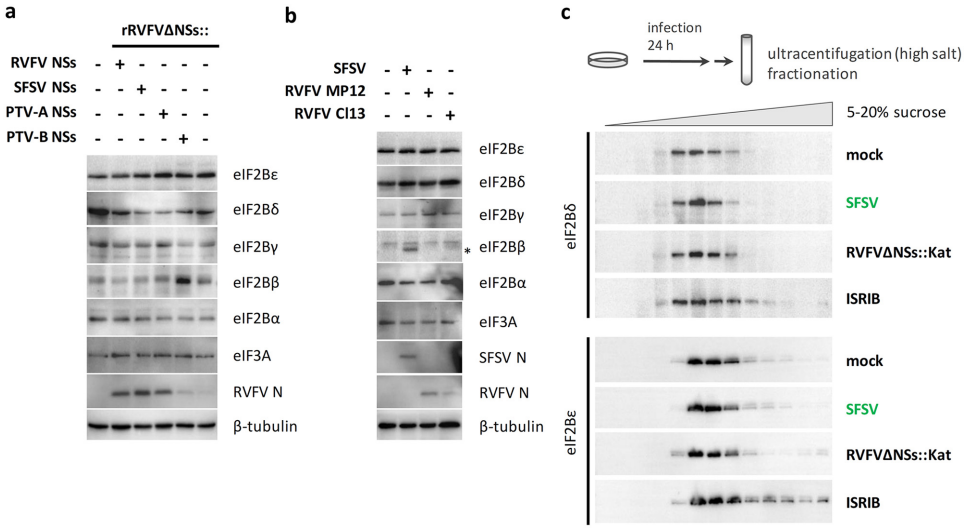

FIG 5 SFSV NSs and established mechanisms of eIF2B regulation. (a and b) Monitoring expression levels of eIF2B subunits in the presence of NSs. A549 cells were either infected with the indicated recombinant viruses (MOI, 1) and lysed 16 hpi (a) or infected with parental viruses SFSV, RVFV MP12, and Cl13 (MOI, 1) and lysed 12 hpi (b) and analyzed by immunoblotting. Staining of viral N proteins served as marker for infection. *, leftover SFSV N signal, for which the blot was probed before detecting eIF2B beta. (c) Monitoring eIF2B decamer formation. HEK293 cells were infected with SFSV or NSs-deficient RVFV strain rRVFVΔNSs::Katushka (rRVFVΔNSs::Kat) or treated with ISRIB. rRVFVΔNSs::Kat served as negative control for infection-induced but NSs-independent effects on eIF2B stoichiometry, whereas ISRIB was included as positive control for eIF2B decamerization. Cell lysates were fractionated via 5% to 20% sucrose gradients, and fractions were analyzed for a shift of eIF2B subunits toward fractions of higher density by immunoblotting. Shown data are representatives of 2 (a) or 3 (b and c) experiments.

the inactive N-terminally tagged version (3×FLAG-SFSV NSs) interacted with eIF2B (Fig. 4c and d). This result correlates with the functional data from the bicistronic reporter system (Fig. 3), suggesting that SFSV NSs boosts eIF-dependent translation and enables PKR-sensitive virus replication by acting directly on eIF2B.

Further attempts at identifying the eIF2B subunit(s) targeted by SFSV NSs using Far-Western blotting (employing cells that transiently expressed NSs-3×FLAG as bait and individual, bacterially expressed nondenatured eIF2B subunits as prey) did not reveal any interaction (data not shown). Moreover, bacterially produced SFSV NSs lost its ability to interact with cellular eIF2B in coimmunoprecipitation experiments, precluding binding studies with NSs produced in an eIF2B-free background (data not shown).

Established mechanisms of cellular eIF2B modulation are not applicable to SFSV NSs. Phosphorylation of eIF2α is not only mediated by PKR but also by other kinases of the so-called integrated stress response (ISR) (28). Besides virus infection, the ISR can also be activated by compounds such as arsenite. Due to its low cellular levels and tight regulation, eIF2B is considered the central hub of translation regulation by the ISR (26). Cancer cells, for example, elevate eIF2B expression to satisfy their demand for increased protein synthesis (29). Moreover, the stabilization of the decameric form of eIF2B (consisting of two copies of each of the five subunits), a process facilitated by the small molecule ISRIB (integrated stress response inhibitor), enables translation despite the presence of phospho-eIF2α (30–32). However, when testing for these mechanisms, we did not find SFSV NSs to elevate eIF2B levels under ectopic expression or infection (Fig. 5a and b and data not shown). Moreover, after sucrose gradient ultracentrifugation of cell lysates, a shift of eIF2Bδ and eIF2Bε toward high-density fractions that is indicative of decamer formation was only detected for the ISRIB control and not for NSs-expressing SFSV or the ISR-activating rRVFVΔNSs::Kat virus (Fig. 5c and data not shown). Thus, despite strongly binding to eIF2B, SFSV NSs seems not to act by any of the established phospho-eIF2α bypass mechanisms.

SFSV NSs does not interfere with binding of phospho-eIF2α to eIF2B. Comparative cryo-electron microscopy (cryo-EM) analyses have recently elucidated that non-

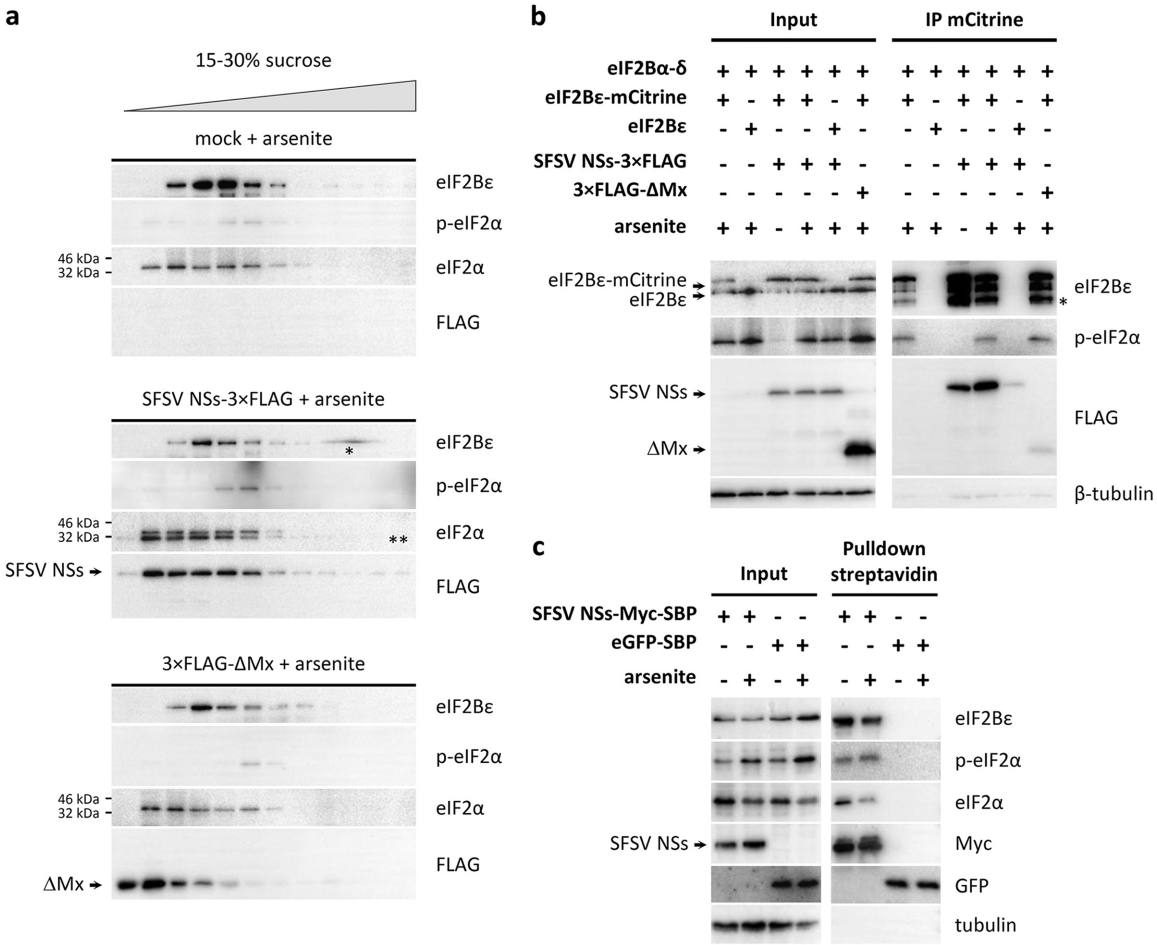

FIG 6 SFSV NSs allows binding of phospho-eIF2α to eIF2B. (a) Cofractionation experiments. HEK293 cells were transfected with expression plasmids for SFSV NSs-3×FLAG or 3×FLAG-ΔMx (negative control) or left untransfected. Half of the cells was stimulated with arsenite to induce eIF2α phosphorylation prior to lysis (see Fig. S5 in the supplemental material for results with the unstimulated cells). Sucrose gradient ultracentrifugation was performed, and fractions were analyzed by immunoblotting for phospho-eIF2α with eIF2B. *, gel artifact; **, remaining signal for SFSV NSs-3×FLAG (lower band) from previous FLAG antibody staining due to incomplete stripping of the anti-FLAG antibody. (b and c) Coprecipitation experiments. HEK293 cells were transfected with expression plasmids, treated with arsenite to induce eIF2α phosphorylation, and lysed, and protein complexes were precipitated via specific tags and analyzed by immunoblotting. (b) eIF2B pulldown. eIF2Bε-mCitrine, SFSV NSs, and ΔMx were expressed, and eIF2B was precipitated via the mCitrine tag. *, cleavage or partial degradation product of eIF2Bε. (c) NSs pulldown. SFSV NSs-Myc-SBP and eGFP-SBP were expressed, and NSs was precipitated via the SBP tag. Shown data are representatives of 2 (a), 5 (b), or 3 (c) experiments.

phosphorylated and phosphorylated eIF2 bind to distinct sites on eIF2B (33–36). Binding of nonphosphorylated eIF2α triggers the so-called productive mode of eIF2B in which eIF2·GTP is recycled and translation of mRNAs enabled. In contrast, phospho-eIF2α is structurally rearranged and consequently excluded from the productive binding site of eIF2B. Instead, it associates with eIF2B in a nonproductive binding mode, through which access of nonphosphorylated eIF2 to eIF2B is blocked and hence eIF2B activity abrogated, halting translation. To test the influence of SFSV NSs on the binding of phospho-eIF2α to eIF2B, we performed cofractionation as well as coimmunoprecipitation experiments. In the cofractionation experiments, lysates from cells that were treated with the ISR activator arsenite were separated by sucrose gradient ultracentrifugation, and the fractions were analyzed by immunoblotting. In lysates from control cells, the phospho-eIF2α peak was found to overlap that for fractions containing eIF2Bε, suggesting complex formation (Fig. 6a and Fig. S5). However, expression of SFSV NSs did not shift the phospho-eIF2α peak toward lower-density fractions, as would have been expected if it interfered with the binding of phospho-eIF2α to eIF2B. Rather, phospho-eIF2α was exclusively recovered in the fractions containing eIF2Bε, similar to the situation in untransfected or control (ΔMx) transfected cells (Fig. 6a).

For the coimmunoprecipitations, two different approaches were chosen. First, we coexpressed the eIF2Bε-mCitrine-HA-containing eIF2B complex with SFSV NSs, stimulated eIF2α phosphorylation with arsenite, and subsequently immunoprecipitated eIF2B via the mCitrine moiety. Phospho-eIF2α specifically and reproducibly coprecipitated with eIF2B as expected (Fig. 6b). eIF2α phosphorylation had no effect on the amount of SFSV NSs binding to eIF2B. Vice versa, the presence of SFSV NSs also did not reduce the signal of coprecipitated phospho-eIF2α. To further support these findings, we directly investigated whether phospho-eIF2α is attached to NSs-precipitated eIF2B. To this aim, we constructed an expression plasmid for NSs (NSs-Myc-streptavidin-binding peptide [SBP]) that was C-terminally tagged with Myc (for immunoblot detection) and streptavidin-binding peptide (for precipitation with streptavidin-coated beads). eGFP-SBP served as negative control. Cells were transfected with these cDNA constructs, the ISR was stimulated with arsenite, and the lysates were subjected to streptavidin-mediated precipitation. As observed previously with the NSs-3×FLAG construct, NSs-Myc-SBP coprecipitated the endogenous eIF2B (represented by the eIF2Bε subunit), whereas eGFP-SBP did not (Fig. 6c). Importantly, endogenous phospho-eIF2α also specifically coprecipitated along with the NSs-eIF2B complex, demonstrating that NSs does not impede the binding of phospho-eIF2α to eIF2B. Thus, the results from the fractionation and coprecipitation experiments argue for a model in which SFSV NSs is binding to the eIF2B-phospho-eIF2 complex. Because, on the other hand, SFSV NSs enables virus replication despite the presence of phospho-PKR and phospho-eIF2α, our data suggest that it renders eIF2B resistant to inhibition by bound phospho-eIF2.

DISCUSSION

Phleboviruses are gaining increased attention as agents of emerging zoonoses (4, 7, 37). As RNA viruses infecting vertebrates, they have to cope with the broadly antiviral PKR system, and the virulent phleboviruses RVFV and TOSV rapidly destroy PKR itself as a countermeasure (17). SFSV, one of the most widespread phleboviruses, is a more moderate pathogen and, as we show here, inhibits the PKR-mediated translation block by targeting eIF2B. All phleboviruses investigated so far also inhibit induction of the antiviral interferons (IFN-α/β) (7, 38, 39). Interestingly, virulent RVFV and TOSV do this by NSs-mediated destruction of key host factors, whereas SFSV NSs obstructs the DNA-binding domain of transcription factor IRF3, blocking its access to the IFN promoter (19). Thus, there seems to be a correlation between the mode of NSs action against host defenses (rapid and enzymatic versus slowly building up and stoichiometric) and the respective virulence level of the particular phlebovirus, observed not only in humans but also in an outbred mouse model (23).

Viruses have evolved a plethora of measures to avoid translation inhibition by the antiviral PKR system (Fig. 7a and b). The destruction of PKR by RVFV and TOSV NSs proteins was mentioned above. At the upper end of the signaling chain, PKR-triggering dsRNA is sequestered by the influenza A NS1 protein and the vaccinia virus E3L, among others (40). dsRNA-induced PKR autophosphorylation is inhibited by the Kaposi's sarcoma herpesvirus vIRF2 (41), vaccinia virus K3L acts as a PKR pseudosubstrate (42), and herpes simplex virus ICP34.5 recruits a protein phosphatase to revert eIF2α phosphorylation (43). Besides these examples, all viral strategies reported so far act on the level of PKR, affect phosphorylation of its substrate eIF2α (2, 3), or circumvent eIF-dependent translation with a special IRES that directly binds to the 40S ribosome (25). Although, mechanistically, viruses may not necessarily target PKR itself, they nonetheless neutralize its negative effect on viral replication by a variety of other means, i.e., biologically, they encode a PKR escape activity. As shown by our knockdown and overexpression experiments, the NSs of SFSV only offers a growth advantage when PKR is present, i.e., phenotypically, it is a PKR antagonist. By targeting eIF2B, however, it employs a distinct and apparently novel PKR escape mechanism (Fig. 7c). There are several modes of cellular eIF2B regulation that can relieve the negative influence of phosphorylated eIF2α, most prominently, upregulation of eIF2B subunits and eIF2B

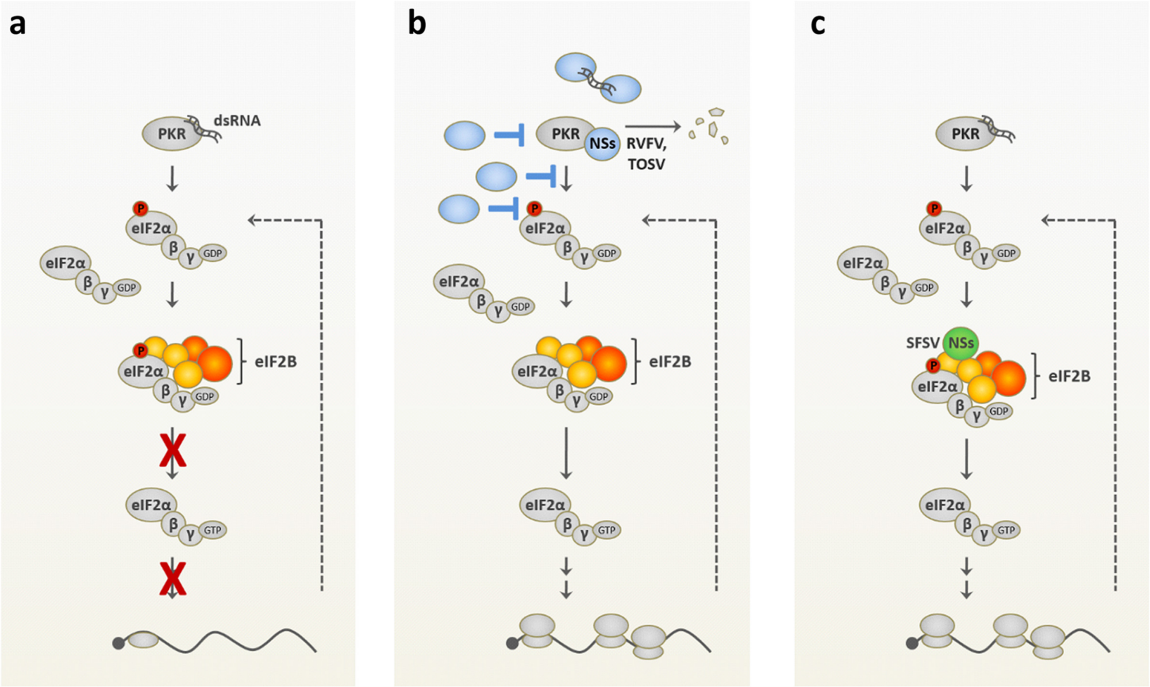

FIG 7 PKR-mediated shutdown of translation and antagonistic strategies employed by viral proteins. (a) Shutdown of translation initiation mediated by PKR: in response to recognition of double-stranded RNA (dsRNA), PKR phosphorylates eIF2αSer51, resulting in nonproductive binding of the latter to eIF2B and, consequently, global inhibition of translation. Due to limiting concentrations of eIF2B compared to that of eIF2, partial eIF2α phosphorylation is sufficient to shutdown protein synthesis. (b) Previously reported viral strategies for PKR antagonism: viral proteins (blue) sequester viral RNA or affect PKR levels (such as NSs proteins of phleboviruses RVFV and TOSV), PKR activation, or the phosphorylation state of eIF2α. (c) Mechanism used by SFSV NSs: while PKR activation, PKR phosphorylation, and eIF2α phosphorylation occur in response to the virus infection and even the binding of p-eIF2α to eIF2B occurs, SFSV NSs enables cap-dependent translation by targeting eIF2B in a way that somehow neutralizes the nonproductive mode of eIF2B imposed by p-eIF2α binding.

decamerization, but none of these apply to SFSV NSs and NSs did not displace phospho-eIF2α from eIF2B. Thus, NSs can enable eIF2-dependent protein synthesis in the presence of activated PKR by a novel mechanism that protects eIF2B from the nonproductive mode that is normally imposed by phospho-eIF2α.

It remains to be shown where on the eIF2B complex NSs is binding and how NSs manages to force phospho-eIF2-bound eIF2B into the productive mode. One possibility would be that SFSV NSs enables binding of phospho-eIF2 to the productive site that is normally occupied by nonphosphorylated eIF2. However, since phospho-eIF2 is excluded from the productive binding site due to electrostatic repulsion by the eIF2Bβ subunit (35), this possibility appears unlikely. Alternatively, due to its complex architecture, eIF2B offers potential for manifold posttranslational modifications. For instance, Ser539 of the catalytic eIF2Bε subunit is a regulatory site for enzymatic eIF2B activity (44). Although we did not observe differential eIF2Bε Ser539 phosphorylation in the presence of SFSV NSs when using commercial antibodies (data not shown), other posttranslational modifications cannot be ruled out. Moreover, in addition to its known binding sites for phosphorylated and nonphosphorylated eIF2, GDP, and GTP, eIF2B possesses a significant amount of further surface area without an assigned physiological function. It could thus be envisioned that NSs acts as mimic of an as-yet-unidentified host protein with eIF2B regulatory activity. Further elucidation of the supercomplex of eIF2B, phosphorylated eIF2α, and SFSV NSs might aid the ongoing efforts to understand the intricate regulation of eIF2B.

MATERIALS AND METHODS

Cell culture. A549, BHK-21, HEK293, HEK293T, Vero B4, and Vero E6 cells were cultured in Dulbecco's minimal essential medium (DMEM) and CCM34 medium (DMEM with addition of 17.8 mg/liter L-alanine, 0.7 g/liter glycine, 75 mg/liter L-glutamic acid, 25 mg/liter L-proline, 0.1 mg/liter biotin, 25 mg/liter hypoxanthine, and 3.7 g/liter sodium bicarbonate) supplemented with 10% fetal calf serum (FCS), 100 U/ml penicillin, and 100 μg/ml streptomycin. HeLa PKR knockdown and control cells, generated by stable

transfection with the pSUPER vector encoding a short hairpin RNA against the PKR gene or with the empty pSUPER, respectively (kindly obtained from Charles Samuel, UC Santa Barbara) (45), were maintained in full DMEM or CCM34 additionally supplemented with 2 μg/ml puromycin. HEK293 FLP-IN T Rex cells with inducible expression of PKR or GFP were as described previously (17) or obtained from Ju-Tao Guo (Baruch S. Blumberg Institute) (46) and maintained in full DMEM or CCM34 medium additionally supplemented with 50 μg/ml hygromycin and 5 μg/ml blasticidin, respectively. All cell lines were routinely tested for mycoplasma contamination.

Viruses. Previously described recombinant RVFV strains rZH548, rZH548ΔNSs, rZH548ΔNSs::NSsSFSV, rZH548ΔNSs::NSsPTV-A, rZH548ΔNSs::PTV-B, and rZH548ΔNSs::NSsSFSV-CTAP (17, 19, 47) were propagated in Vero E6 cells under biosafely level 3 (BSL3) conditions. The prototype Sabin strain of SFSV was obtained from the World Reference Center for Emerging Viruses and Arboviruses (WRCEVA) and propagated in Vero B4 cells. rZH548ΔNSs::Katushka (48) was also propagated in Vero E6 cells, whereas rZH548ΔNSs::Ren (49) as well as attenuated RVFV strains MP12 and clone 13 were propagated in BHK-21 cells. All viruses were titrated on Vero E6 cells under an overlay of 0.6% Avicel (FMC BioPolymer) (50), and plaques were visualized via crystal violet staining. Virus stocks were routinely tested for mycoplasma contamination.

For infection, viruses were diluted to the desired multiplicity of infection (MOI) in serum-free medium and incubated with the cells for 1 h at 37°C, after which, the inoculate was replaced by full cell culture medium.

Plasmids. Expression constructs for 3×FLAG-tagged NSs of RVFV and SFSV (GenBank EF201822.1) as well as 3×FLAG-ΔMx were described previously (19, 51). C-terminally tagged SFSV NSs was generated by amplification of the ORF with specific primers, of which, the reverse primer contained the 3×FLAG or Myc-SBP tag sequence, restriction with BamHI and XhoI, and subsequent ligation-dependent cloning into pI.18 (kindly provided by Jim Robertson, National Institute for Biological Standards and Control, Hertfordshire, UK) and pcDNA3.1 (Invitrogen). Coding sequences for eIF2B subunits *eIF2B1* (NG_015862.1), *eIF2B2-B10* (NG_013333.1), *eIF2B3* (NG_015864.1), and *eIF2B4* (NG_009305.1) were amplified from pDONR223 constructs (kindly provided by BIOSS Centre for Biological Signaling Studies, University of Freiburg, Germany), inserted into pcDNA3.1/V5-His-TOPO via TA cloning, and finally subcloned into pcDNA3 via the HindIII and NotI restriction sites. The *eIF2B5* ORF (NM_003907.2) was amplified and subcloned from pRevTRE2-hIF2Bε-GFP (52) (kind gift of Dirk Görlich, Max Planck Institute for Biophysical Chemistry, Germany) and additionally supplemented with an mCitrine-HA cassette using the NotI and ApaI sites. Primer and insert sequences are available upon request. All expression constructs were confirmed by Sanger sequencing with primers covering the respective inserts and multiple-cloning sites.

Translation reporter pFR_CrPV_xb, constructed by Philipp Sharp (53), was obtained from Addgene (plasmid 11509). Subsequently, the HSV-TK promoter was replaced with an SV40 promoter by directional cloning using the BglII and HindIII restriction sites. Firefly reporter construct p-125Luc was kindly donated by Takashi Fujita (54); pGL3-Control and pRL-SV40 were purchased from Promega.

Replication assays. HeLa cells were seeded into 6-well plates and infected with recombinant viruses (MOI, 0.01). HEK293 FLP-IN T Rex cells were seeded into 6-well plates, induced with 2 μg/ml doxycycline (Sigma) for 24 h, and infected with recombinant viruses (MOI 0.01) under continuing induction. Culture supernatants were harvested 24 h postinfection (hpi), and virus titers were determined by immunoplaque assay as follows: BHK-21 cells were infected with serial dilutions of cell culture supernatant and incubated under an overlay of 0.6% Avicel (FMC BioPolymer) (50) for 24 h prior to fixation and permeabilization. After staining with polyclonal mouse ascites fluid raised against recombinant RVFV N (kindly provided by Michèle Bouloy, Institut Pasteur Paris, France) (55) and horseradish peroxidase (HRP)-coupled secondary antibody, plaques were visualized using TrueBlue peroxidase substrate (KPL) and titers were calculated.

Immunoblot analysis. Protein samples were run on 12% or 15% acrylamide gels and transferred to polyvinylidene fluoride (PVDF) membranes (Millipore) via semidry blotting. After blocking in Tris-buffered saline (TBS) with 5% bovine serum albumin (BSA) or milk powder, primary antibody staining was performed for 1 h at room temperature or overnight at 4°C. Membranes were washed in TBS-0.1% Tween 20, stained with secondary antibodies for 45 min, and washed again in TBS-0.1% Tween 20 and once in TBS. Finally, membranes were developed with a SuperSignal West Femto kit (Pierce), and bands were visualized using a ChemiDoc imaging system and Image Lab software (Bio-Rad). For kinetic analysis after infection with the recombinant virus panel, proteins were blotted onto nitrocellulose membranes (Whatman Protran) and stained as described above, and bands were detected using an Odyssey imaging system (LI-COR).

Primary antibodies were used as follows: β-actin (1:1,000, number [no.] 3700; Cell Signaling); eIF2α (1:1,000, no. 2103; Cell Signaling); phospho (p)-eIF2α (1:500, no. 3597 [Cell Signaling] and 1:1,000, no. 44728G [Invitrogen]); eIF2Bα (sc-98323 [Santa Cruz Biotechnology] and 18010-1-AP [Proteintech], both 1:1,000); eIF2Bβ (1:1,000, sc-100729; Santa Cruz Biotechnology); eIF2Bγ (1:1,000, sc-137248; Santa Cruz Biotechnology); eIF2Bδ (1:500, sc-271795; Santa Cruz Biotechnology); eIF2Bε (1:1,000, sc-55558; Santa Cruz Biotechnology); eIF3A (1:1,000, no. 3411; Cell Signaling); FLAG M2 (1:2,000, F3165; Sigma); GFP (1:1,000, 3h9; Chromotek); HA (1:1,000, no. 901515; BioLegend); Myc (1:1,000, M4439; Sigma); PKR (1:1,000, no. 610764; BD Transduction Laboratories); p-PKR (1:1,000, ab32036; Abcam); puromycin (1:1,000, EQ0001; Kerafast); tubulin (1:2,500, ab6046; Abcam); SFSV N (mouse immune ascites fluid, provided by WRCEVA, 1:1,000); RVFV N (rabbit hyperimmune serum, kindly provided by Alenjandro Brun, 1:1,000). Secondary antibodies comprised anti-mouse (0031430 and 1892913), anti-rabbit (0031460 and 1892914; both Thermo Fisher), and anti-rat (712-036-150; Jackson ImmunoResearch) (all 1:20,000) antibodies, anti-mouse and anti-rabbit conjugated IRDyes

(1:5,000, 610-130-121, 610-132-121, and 611-132-122; Rockland), or were replaced by TrueBlot (1:1,000, 18-8816-33 or 18–8817-33; Biomol).

Bicistronic translation and interferon reporter assay. HEK293 cells seeded into 96-well plates were transfected the following day with a bicistronic firefly and *Renilla* luciferase reporter construct (40 ng) as well as expression constructs for NSs proteins or the control protein ΔMx (0.1 ng, 1 ng, and 10 ng) via TransIT-LT1. Total transfected DNA was adjusted to equal amounts with the empty vector pI.18. Cells were processed 48 h after transfection, and luciferase activities were determined using the Dual Luciferase Reporter Assay system (Promega) according to the manufacturer's instructions and a LB 942 TriStar^2 multimode reader (Berthold Technologies). Means and standard deviations (SDs) were calculated from three technical replicates within each biological replicate.

For interferon reporter assays, cells were seeded and transfected as described above, using p125Luc and pRL-SV40 as reporter plasmids (40 ng each). Luciferase activities were determined 24 h after transfection, and means and SDs were calculated as described above.

Puromycin labeling. To monitor ongoing translation, medium was supplemented with 10 ng/ml puromycin and incubated for a further 10 to 30 min at 37°C prior to harvesting (56). Incorporation of puromycin was visualized via immunoblotting as described above.

Proteomics. As described previously (19, 27, 51), approximately 2×10^8 HEK293T cells were infected with the recombinant RVFV strain expressing C-terminally TAP-tagged SFSV NSs (rZH548ΔNSs::NSsSFSV-CTAP) at an MOI of 5. The cells were washed with and scraped off in prechilled phosphate-buffered saline (PBS) 16 h postinfection (hpi). The cell pellet was snap-frozen in liquid nitrogen, lysed in TAP buffer (50 mM Tris-HCl [pH 7.5], 100 mM NaCl, 0.2% NP-40, 5% glycerol) supplemented with protease and phosphatase inhibitors, snap-frozen again, and stored at −80°C until further processing. TAP purification was performed by sequential pulldowns using streptavidin-agarose and HA-agarose beads. Bound protein complexes were eventually eluted in Laemmli buffer and subjected to one-dimensional SDS-PAGE prior to trypsin digestion and peptide analysis by liquid chromatography-tandem mass spectrometry (LC-MS/MS), which was described in detail elsewhere (27). Network visualization of high-confidence interactors was generated using STRING database (57).

Coimmunoprecipitation. HEK293 cells seeded into 10-cm dishes were transfected with expression plasmids (2 μg each per eIF2B subunit and NSs or control constructs) via the calcium phosphate method (58) and lysed 16 to 24 h after transfection or after additional infection with rZH548ΔNSs::Ren (MOI of 5, 5 hpi). A549 cells were transfected with 4 μg expression plasmids for SFSV NSs or ΔMx using Lipofectamine 2000 (Thermo Fisher). Cells were scraped into PBS and lysed in prechilled lysis buffer (50 mM Tris-HCl [pH 7.0], 150 mM NaCl, 1% IGEPAL-630, 1× protease inhibitor cocktail, 1× phosphatase inhibitor cocktail). Cell debris was removed (10,000 × *g*, 10 min, 4°C), and supernatants were used for further processing. For immunoprecipitation via FLAG or HA, FLAG M2 or HA antibodies were coupled to magnetic beads (143-21D or 10004D; Invitrogen) overnight; for immunoprecipitation of SBP-tagged proteins, streptavidin-coated beads (11205; Invitrogen) were used. Coated beads were then processed according to the manufacturer's recommendations, equilibrated to lysis buffer, and incubated with cell lysate under rotation at 4°C for 4 h or overnight. After extensive washing, bound proteins were eluted by heating in Laemmli gel sample buffer at 94°C for 5 min. For immunoprecipitation via mCitrine, supernatants were applied to prewashed wells of a GFP-multiTrap (Chromotek) and incubated at 4°C for 60 to 90 min. Wells were then washed extensively with lysis buffer, and bound proteins were finally eluted with preheated Laemmli buffer (60°C) under strong agitation for 15 to 20 min.

Sucrose gradients. HEK293 cells seeded into 145-mm dishes were either transfected with SFSV NSs or ΔMx expression plasmids (10 μg) or infected the following day with SFSV or rRVFVΔNSs::Katushka (MOI 0.1) or left untreated and harvested 24 h later. Control cells were treated with 1 μM ISRIB (Cay16258-5; Cayman) 1 h prior to harvest. Cells were scraped into PBS and lysed, debris was pelleted (20,000 × *g*, 10 min, 4°C), and 450 μl of the supernatant was loaded onto the gradients. To monitor eIF2B decamerization, 5% to 20% sucrose gradients were poured manually by layering five steps of high-salt lysis buffer [50 mM Tris-HCl (pH 7.4), 400 mM KCl, 4 mM magnesium acetate, 0.5% Triton X-100, 1 mM Tris(2-carboxyethyl)phosphine hydrochloride [TCEP]) supplemented with decreasing sucrose concentrations (5% to 20% sucrose gradient for eIF2B decamerization: 20%, 16.25%, 12.5%, 8.75%, and 5%; 15% to 30% sucrose gradient for eIF2B-phospho-eIF2α association: 15%, 18.75%, 22.5%, 26.25%, and 30%). The gradients were stored at −80°C until usage and allowed to linearize at 4°C overnight prior to loading and ultracentrifugation (SW55, 40,000 rpm, 14 h, 4°C, Beckmann Optima XPN-80). To examine phospho-eIF2$\alpha\beta\gamma$ binding to eIF2B, 15% to 30% sucrose gradients were poured in low-salt lysis buffer (50 mM Tris-HCl [pH 7.4], 100 mM KCl, 0.5% Triton X-100, 1 mM TCEP) and subjected to ultracentrifugation (SW55, 45,000 rpm, 6 h 20 min, 4°C). Afterwards, gradients were fractionated manually into 13 or 12 fractions, and aliquots of the crude fractions were finally analyzed by immunoblotting.

Data availability. The data sets generated during the present study are available from the corresponding author on reasonable request.

SUPPLEMENTAL MATERIAL

Supplemental material is available online only.

FIG S1, TIF file, 1.8 MB.

FIG S2, TIF file, 0.6 MB.

FIG S3, TIF file, 1.7 MB.

FIG S4, TIF file, 1.4 MB.

FIG S5, TIF file, 1.2 MB.

ACKNOWLEDGMENTS

We thank Charles Samuel, Ju-Tao Guo, and David Ron for providing cell lines. We also thank Patricia Aguilar and Robert Tesh from the World Reference Center for Emerging Viruses and Arboviruses (WRCEVA) for providing the Sabin strain of SFSV along with mouse immune ascites fluid and Michèle Bouloy and Alejandro Brun for providing anti-RVFV sera. Expression and luciferase reporter constructs were kindly obtained from BIOSS Centre for Biological Signaling Studies, Jim Robertson, Dirk Görlich, Phil Sharp via Addgene, and Takashi Fujita.

Work in the authors' laboratories was supported by the Deutsche Forschungsgemeinschaft (DFG; German Research Foundation) (project number 197785619–SFB 1021 to F.W. and PI1084/2, PI1084/3, TRR179, and TRR237 to A.P.), an ERC starting grant (ERC-StG iVIP, 311339 to A.P.), the Bundesministerium für Bildung und Forschung (Infect-ERA, grants ESCential and ERASE to F.W. and A.P., respectively), and the Swedish Research Council (VR; no. 2018-05766 to F.W.).

J.D.W., G.S.-F., A.P., and F.W. designed the research. J.D.W., M.H., M.K., B.B., D.B., and A.P. acquired the data. J.D.W., M.H., M.K., B.B., G.S.-F., A.P., and F.W. analyzed and interpreted the data. J.D.W. and F.W. wrote the paper.

We declare no competing interests.

REFERENCES

1. Pindel A, Sadler A. 2011. The role of protein kinase R in the interferon response. J Interferon Cytokine Res 31:59–70. https://doi.org/10.1089/jir.2010.0099.
2. Dauber B, Wolff T. 2009. Activation of the antiviral kinase PKR and viral countermeasures. Viruses 1:523–544. https://doi.org/10.3390/v1030523.
3. Walsh D, Mohr I. 2011. Viral subversion of the host protein synthesis machinery. Nat Rev Microbiol 9:860–875. https://doi.org/10.1038/nrmicro2655.
4. Elliott RM, Brennan B. 2014. Emerging phleboviruses. Curr Opin Virol 5:50–57. https://doi.org/10.1016/j.coviro.2014.01.011.
5. McMillen CM, Hartman AL. 2018. Rift Valley fever in animals and humans: current perspectives. Antiviral Res 156:29–37. https://doi.org/10.1016/j.antiviral.2018.05.009.
6. Li P, Tong ZD, Li KF, Tang A, Dai YX, Yan JB. 2017. Seroprevalence of severe fever with thrombocytopenia syndrome virus in China: a systematic review and meta-analysis. PLoS One 12:e0175592. https://doi.org/10.1371/journal.pone.0175592.
7. Wuerth JD, Weber F. 2016. Phleboviruses and the type I interferon response. Viruses 8:174. https://doi.org/10.3390/v8060174.
8. Sabin AB. 1951. Experimental studies on *Phlebotomus* (pappataci, sandfly) fever during World War II. Arch Gesamte Virusforsch 4:367–410. https://doi.org/10.1007/BF01241161.
9. Atkinson B, Hewson R. 2018. Emerging arboviruses of clinical importance in Central Asia. J Gen Virol 99:1172–1184. https://doi.org/10.1099/jgv.0.001125.
10. Alwassouf S, Christodoulou V, Bichaud L, Ntais P, Mazeris A, Antoniou M, Charrel RN. 2016. Seroprevalence of sandfly-borne phleboviruses belonging to three serocomplexes (sandfly fever Naples, sandfly fever Sicilian and Salehabad) in dogs from Greece and Cyprus using neutralization test. PLoS Negl Trop Dis 10:e0005063. https://doi.org/10.1371/journal.pntd.0005063.
11. Alwassouf S, Maia C, Ayhan N, Coimbra M, Cristovao JM, Richet H, Bichaud L, Campino L, Charrel RN. 2016. Neutralisation-based seroprevalence of Toscana virus and Sandfly fever Sicilian virus in dogs and cats from Portugal. J Gen Virol 97:2816–2823. https://doi.org/10.1099/jgv.0.000592.
12. Ergunay K, Ayhan N, Charrel RN. 2017. Novel and emergent sandfly-borne phleboviruses in Asia Minor: a systematic review. Rev Med Virol 27:e1898. https://doi.org/10.1002/rmv.1898.
13. Eitrem R, Stylianou M, Niklasson B. 1991. High prevalence rates of antibody to three sandfly fever viruses (Sicilian, Naples, and Toscana) among Cypriots. Epidemiol Infect 107:685–691. https://doi.org/10.1017/s0950268800049384.
14. Kniha E, Obwaller AG, Dobler G, Poeppl W, Mooseder G, Walochnik J. 2019. Phlebovirus seroprevalence in Austrian Army personnel returning from missions abroad. Parasit Vectors 12:416. https://doi.org/10.1186/s13071-019-3674-6.
15. Shiraly R, Khosravi A, Farahangiz S. 2017. Seroprevalence of sandfly fever virus infection in military personnel on the western border of Iran. J Infect Public Health 10:59–63. https://doi.org/10.1016/j.jiph.2016.02.014.
16. Kalveram B, Ikegami T. 2013. Toscana virus NSs protein promotes degradation of double-stranded RNA-dependent protein kinase. J Virol 87:3710–3718. https://doi.org/10.1128/JVI.02506-12.
17. Habjan M, Pichlmair A, Elliott RM, Overby AK, Glatter T, Gstaiger M, Superti-Furga G, Unger H, Weber F. 2009. NSs protein of Rift Valley fever virus induces the specific degradation of the double-stranded RNA-dependent protein kinase. J Virol 83:4365–4375. https://doi.org/10.1128/JVI.02148-08.
18. Lihoradova OA, Indran SV, Kalveram B, Lokugamage N, Head JA, Gong B, Tigabu B, Juelich TL, Freiberg AN, Ikegami T. 2013. Characterization of Rift Valley fever virus MP-12 strain encoding NSs of Punta Toro virus or sandfly fever Sicilian virus. PLoS Negl Trop Dis 7:e2181. https://doi.org/10.1371/journal.pntd.0002181.
19. Wuerth JD, Habjan M, Wulle J, Superti-Furga G, Pichlmair A, Weber F. 2018. NSs protein of sandfly fever sicilian phlebovirus counteracts interferon (IFN) induction by masking the DNA-binding domain of IFN regulatory factor 3. J Virol 92:e01202-18. https://doi.org/10.1128/JVI.01202-18.
20. Ikegami T, Narayanan K, Won SY, Kamitani W, Peters CJ, Makino S. 2009. Rift Valley fever virus NSs protein promotes post-transcriptional downregulation of protein kinase PKR and inhibits eIF2 alpha phosphorylation. PLoS Pathog 5:e1000287. https://doi.org/10.1371/journal.ppat.1000287.
21. Muller R, Saluzzo JF, Lopez N, Dreier T, Turell M, Smith J, Bouloy M. 1995. Characterization of clone-13, a naturally attenuated avirulent isolate of Rift-Valley fever virus, which is altered in the small segment. Am J Trop Med Hyg 53:405–411. https://doi.org/10.4269/ajtmh.1995.53.405.
22. Perrone LA, Narayanan K, Worthy M, Peters CJ. 2007. The S segment of Punta Toro virus (*Bunyaviridae*, *Phlebovirus*) is a major determinant of lethality in the Syrian hamster and codes for a type I interferon antagonist. J Virol 81:884–892. https://doi.org/10.1128/JVI.01074-06.
23. Nishiyama S, Slack OAL, Lokugamage N, Hill TE, Juelich TL, Zhang LH, Smith JK, Perez D, Gong B, Freiberg AN, Ikegami T. 2016. Attenuation of pathogenic Rift Valley fever virus strain through the chimeric S-segment encoding sandfly fever phlebovirus NSs or a dominant-negative PKR. Virulence 7:871–881. https://doi.org/10.1080/21505594.2016.1195528.
24. Terenzi F, deVeer MJ, Ying H, Restifo NP, Williams BR, Silverman RH. 1999.

The antiviral enzymes PKR and RNase L suppress gene expression from viral and non-viral based vectors. Nucleic Acids Res 27:4369–4375. https://doi.org/10.1093/nar/27.22.4369.

25. Wilson JE, Pestova TV, Hellen CUT, Sarnow P. 2000. Initiation of protein synthesis from the A site of the ribosome. Cell 102:511–520. https://doi.org/10.1016/S0092-8674(00)00055-6.
26. Pavitt GD. 2018. Regulation of translation initiation factor eIF2B at the hub of the integrated stress response. Wiley Interdiscip Rev RNA 9:e1491. https://doi.org/10.1002/wrna.1491.
27. Pichlmair A, Kandasamy K, Alvisi G, Mulhern O, Sacco R, Habjan M, Binder M, Stefanovic A, Eberle CA, Goncalves A, Burckstummer T, Muller AC, Fauster A, Holze C, Lindsten K, Goodbourn S, Kochs G, Weber F, Bartenschlager R, Bowie AG, Bennett KL, Colinge J, Superti-Furga G. 2012. Viral immune modulators perturb the human molecular network by common and unique strategies. Nature 487:486–490. https://doi.org/10.1038/nature11289.
28. Pakos-Zebrucka K, Koryga I, Mnich K, Ljujic M, Samali A, Gorman AM. 2016. The integrated stress response. EMBO Rep 17:1374–1395. https://doi.org/10.15252/embr.201642195.
29. Balachandran S, Barber GN. 2004. Defective translational control facilitates vesicular stomatitis virus oncolysis. Cancer Cell 5:51–65. https://doi.org/10.1016/s1535-6108(03)00330-1.
30. Tsai JC, Miller-Vedam LE, Anand AA, Jaishankar P, Nguyen HC, Renslo AR, Frost A, Walter P. 2018. Structure of the nucleotide exchange factor eIF2B reveals mechanism of memory-enhancing molecule. Science 359:eaaq0939. https://doi.org/10.1126/science.aaq0939.
31. Sidrauski C, Tsai JC, Kampmann M, Hearn BR, Vedantham P, Jaishankar P, Sokabe M, Mendez AS, Newton BW, Tang EL, Verschueren E, Johnson JR, Krogan NJ, Fraser CS, Weissman JS, Renslo AR, Walter P. 2015. Pharmacological dimerization and activation of the exchange factor eIF2B antagonizes the integrated stress response. Elife 4:e07314. https://doi.org/10.7554/eLife.07314.
32. Zyryanova AF, Weis F, Faille A, Alard AA, Crespillo-Casado A, Sekine Y, Harding HP, Allen F, Parts L, Fromont C, Fischer PM, Warren AJ, Ron D. 2018. Binding of ISRIB reveals a regulatory site in the nucleotide exchange factor eIF2B. Science 359:1533–1536. https://doi.org/10.1126/science.aar5129.
33. Adomavicius T, Guaita M, Zhou Y, Jennings MD, Latif Z, Roseman AM, Pavitt GD. 2019. The structural basis of translational control by eIF2 phosphorylation. Nat Commun 10:2136. https://doi.org/10.1038/s41467-019-10167-3.
34. Gordiyenko Y, Llacer JL, Ramakrishnan V. 2019. Structural basis for the inhibition of translation through eIF2 alpha phosphorylation. Nat Commun 10:2640. https://doi.org/10.1038/s41467-019-10606-1.
35. Kashiwagi K, Yokoyama T, Nishimoto M, Takahashi M, Sakamoto A, Yonemochi M, Shirouzu M, Ito T. 2019. Structural basis for eIF2B inhibition in integrated stress response. Science 364:495–499. https://doi.org/10.1126/science.aaw4104.
36. Kenner LR, Anand AA, Nguyen HC, Myasnikov AG, Klose CJ, McGeever LA, Tsai JC, Miller-Vedam LE, Walter P, Frost A. 2019. eIF2B-catalyzed nucleotide exchange and phosphoregulation by the integrated stress response. Science 364:491–495. https://doi.org/10.1126/science.aaw2922.
37. Silvas JA, Aguilar PV. 2017. The emergence of severe fever with thrombocytopenia syndrome virus. Am J Trop Med Hyg 97:992–996. https://doi.org/10.4269/ajtmh.16-0967.
38. Ly HJ, Ikegami T. 2016. Rift Valley fever virus NSs protein functions and the similarity to other bunyavirus NSs proteins. Virol J 13:118. https://doi.org/10.1186/s12985-016-0573-8.
39. Rezelj VV, Li P, Chaudhary V, Elliott RM, Jin DY, Brennan B. 2017. Differential antagonism of human innate immune responses by tick-borne phlebovirus nonstructural proteins. mSphere 2:e00234-17. https://doi.org/10.1128/mSphere.00234-17.
40. Chang HW, Watson JC, Jacobs BL. 1992. The E3L gene of vaccinia virus encodes an inhibitor of the interferon-induced, double-stranded RNA-dependent protein kinase. Proc Natl Acad Sci U S A 89:4825–4829. https://doi.org/10.1073/pnas.89.11.4825.
41. Burysek L, Pitha PM. 2001. Latently expressed human herpesvirus 8-encoded interferon regulatory factor 2 inhibits double-stranded RNA-activated protein kinase. J Virol 75:2345–2352. https://doi.org/10.1128/JVI.75.5.2345-2352.2001.
42. Davies MV, Elroy-Stein O, Jagus R, Moss B, Kaufman RJ. 1992. The vaccinia virus K3L gene product potentiates translation by inhibiting double-stranded-RNA-activated protein kinase and phosphorylation of the alpha subunit of eukaryotic initiation factor 2. J Virol 66:1943–1950. https://doi.org/10.1128/JVI.66.4.1943-1950.1992.
43. He B, Gross M, Roizman B. 1997. The gamma(1)34.5 protein of herpes simplex virus 1 complexes with protein phosphatase 1alpha to dephosphorylate the alpha subunit of the eukaryotic translation initiation factor 2 and preclude the shutoff of protein synthesis by double-stranded RNA-activated protein kinase. Proc Natl Acad Sci U S A 94:843–848. https://doi.org/10.1073/pnas.94.3.843.
44. Woo CW, Kutzler L, Kimball SR, Tabas I. 2012. Toll-like receptor activation suppresses ER stress factor CHOP and translation inhibition through activation of eIF2B. Nat Cell Biol 14:192–200. https://doi.org/10.1038/ncb2408.
45. Zhang P, Samuel CE. 2007. Protein kinase PKR plays a stimulus- and virus-dependent role in apoptotic death and virus multiplication in human cells. J Virol 81:8192–8200. https://doi.org/10.1128/JVI.00426-07.
46. Jiang D, Guo HT, Xu CX, Chang JH, Gu BH, Wang LJ, Block TM, Guo JT. 2008. Identification of three interferon-inducible cellular enzymes that inhibit the replication of hepatitis C virus. J Virol 82:1665–1678. https://doi.org/10.1128/JVI.02113-07.
47. Habjan M, Penski N, Spiegel M, Weber F. 2008. T7 RNA polymerase-dependent and -independent systems for cDNA-based rescue of Rift Valley fever virus. J Gen Virol 89:2157–2166. https://doi.org/10.1099/vir.0.2008/002097-0.
48. Islam MK, Baudin M, Eriksson J, Oberg C, Habjan M, Weber F, Overby AK, Ahlm C, Evander M. 2016. High-throughput screening using a whole-cell virus replication reporter gene assay to identify inhibitory compounds against Rift Valley fever virus infection. J Biomol Screen 21:354–362. https://doi.org/10.1177/1087057115625184.
49. Kuri T, Habjan M, Penski N, Weber F. 2010. Species-independent bioassay for sensitive quantification of antiviral type I interferons. Virol J 7:50. https://doi.org/10.1186/1743-422X-7-50.
50. Matrosovich M, Matrosovich T, Garten W, Klenk HD. 2006. New low-viscosity overlay medium for viral plaque assays. Virol J 3:63. https://doi.org/10.1186/1743-422X-3-63.
51. Kainulainen M, Habjan M, Hubel P, Busch L, Lau S, Colinge J, Superti-Furga G, Pichlmair A, Weber F. 2014. Virulence factor NSs of Rift Valley fever virus recruits the F-box protein FBXO3 to degrade subunit p62 of general transcription factor TFIIH. J Virol 88:3464–3473. https://doi.org/10.1128/JVI.02914-13.
52. Bohnsack MT, Regener K, Schwappach B, Saffrich R, Paraskeva E, Hartmann E, Gorlich D. 2002. Exp5 exports eEF1A via tRNA from nuclei and synergizes with other transport pathways to confine translation to the cytoplasm. EMBO J 21:6205–6215. https://doi.org/10.1093/emboj/cdf613.
53. Petersen CP, Bordeleau ME, Pelletier J, Sharp PA. 2006. Short RNAs repress translation after initiation in mammalian cells. Mol Cell 21:533–542. https://doi.org/10.1016/j.molcel.2006.01.031.
54. Yoneyama M, Suhara W, Fukuhara Y, Fukuda M, Nishida E, Fujita T. 1998. Direct triggering of the type I interferon system by virus infection: activation of a transcription factor complex containing IRF-3 and CBP/p300. EMBO J 17:1087–1095. https://doi.org/10.1093/emboj/17.4.1087.
55. Bouloy M, Janzen C, Vialat P, Khun H, Pavlovic J, Huerre M, Haller O. 2001. Genetic evidence for an interferon-antagonistic function of Rift Valley fever virus nonstructural protein NSs. J Virol 75:1371–1377. https://doi.org/10.1128/JVI.75.3.1371-1377.2001.
56. Schmidt EK, Clavarino G, Ceppi M, Pierre P. 2009. SUnSET, a nonradioactive method to monitor protein synthesis. Nat Methods 6:275–277. https://doi.org/10.1038/nmeth.1314.
57. Szklarczyk D, Gable AL, Lyon D, Junge A, Wyder S, Huerta-Cepas J, Simonovic M, Doncheva NT, Morris JH, Bork P, Jensen LJ, Mering CV. 2019. STRING v11: protein-protein association networks with increased coverage, supporting functional discovery in genome-wide experimental datasets. Nucleic Acids Res 47:D607–D613. https://doi.org/10.1093/nar/gky1131.
58. Sambrook J, Russell DW. 2006. Calcium-phosphate-mediated transfection of eukaryotic cells with plasmid DNAs. CSH Protoc 2006:pdb.prot3871. https://doi.org/10.1101/pdb.prot3871.
59. Hovanessian AG, Galabru J, Meurs E, Buffet-Janvresse C, Svab J, Robert N. 1987. Rapid decrease in the levels of the double-stranded RNA-dependent protein kinase during virus infections. Virology 159:126–136. https://doi.org/10.1016/0042-6822(87)90355-2.

Suppl. Fig. 1

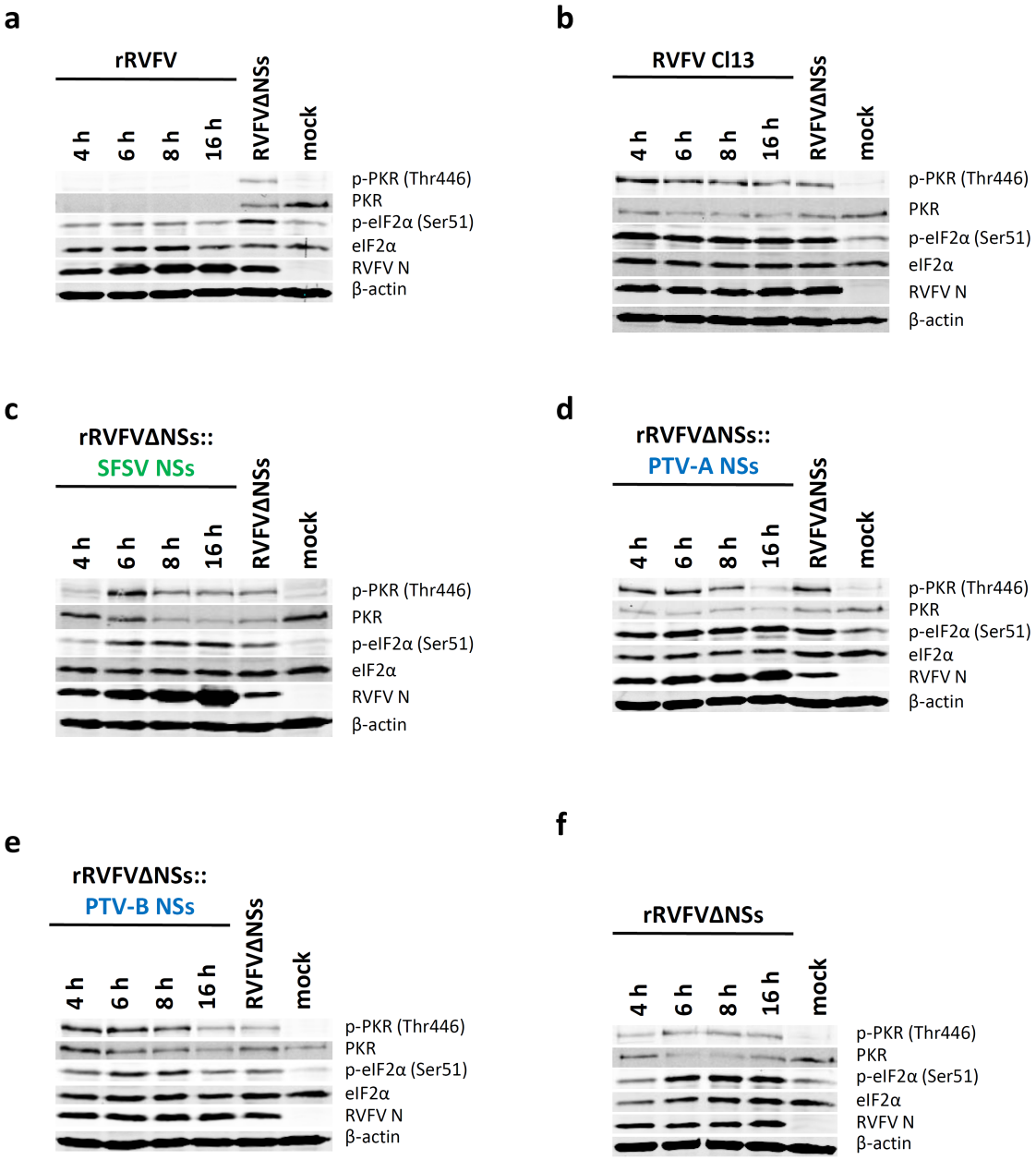
a
rRVFV
4 h
6 h
8 h
16 h
RVFVΔNSs
mock
p-PKR (Thr446)
PKR
p-eIF2α (Ser51)
eIF2α
RVFV N
β-actin
b
RVFV Cl13
4 h
6 h
8 h
16 h
RVFVΔNSs
mock
p-PKR (Thr446)
PKR
p-eIF2α (Ser51)
eIF2α
RVFV N
β-actin
c
rRVFVΔNSs::
SFSV NSs
4 h
6 h
8 h
16 h
RVFVΔNSs
mock
p-PKR (Thr446)
PKR
p-eIF2α (Ser51)
eIF2α
RVFV N
β-actin
d
rRVFVΔNSs::
PTV-A NSs
4 h
6 h
8 h
16 h
RVFVΔNSs
mock
p-PKR (Thr446)
PKR
p-eIF2α (Ser51)
eIF2α
RVFV N
β-actin
e
rRVFVΔNSs::
PTV-B NSs
4 h
6 h
8 h
16 h
RVFVΔNSs
mock
p-PKR (Thr446)
PKR
p-eIF2α (Ser51)
eIF2α
RVFV N
β-actin
f
rRVFVΔNSs
4 h
6 h
8 h
16 h
mock
p-PKR (Thr446)
PKR
p-eIF2α (Ser51)
eIF2α
RVFV N
β-actin

Suppl. Fig. 2

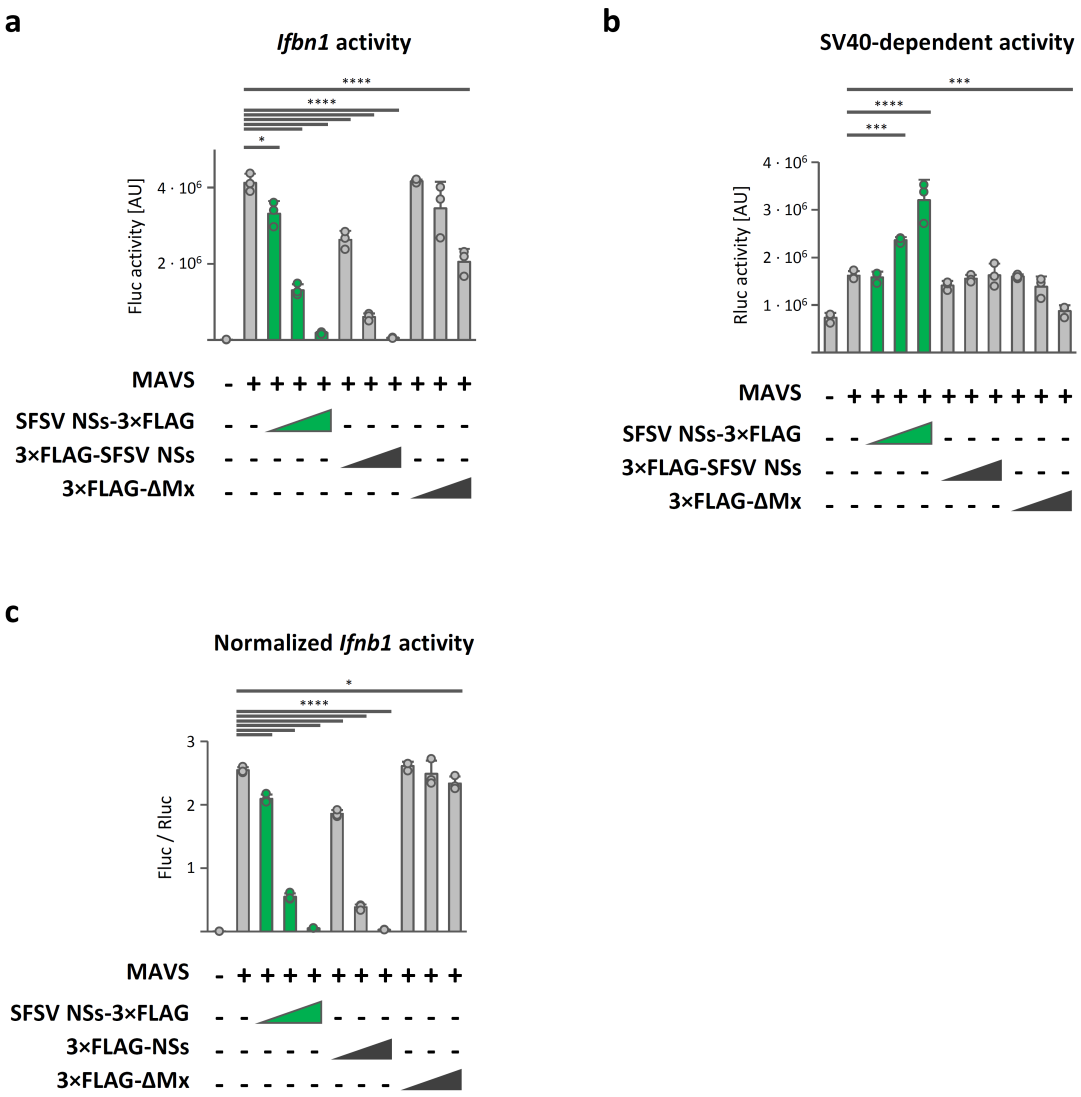
a
Ifbn1 activity
Fluc activity [AU]
4 · 10^6
2 · 10^6
MAVS
SFSV NSs-3×FLAG
3×FLAG-SFSV NSs
3×FLAG-ΔMx
b
SV40-dependent activity
Rluc activity [AU]
4 · 10^6
3 · 10^6
2 · 10^6
1 · 10^6
MAVS
SFSV NSs-3×FLAG
3×FLAG-SFSV NSs
3×FLAG-ΔMx
c
Normalized Ifnb1 activity
Fluc / Rluc
3
2
1
MAVS
SFSV NSs-3×FLAG
3×FLAG-NSs
3×FLAG-ΔMx

Suppl. Fig. 3

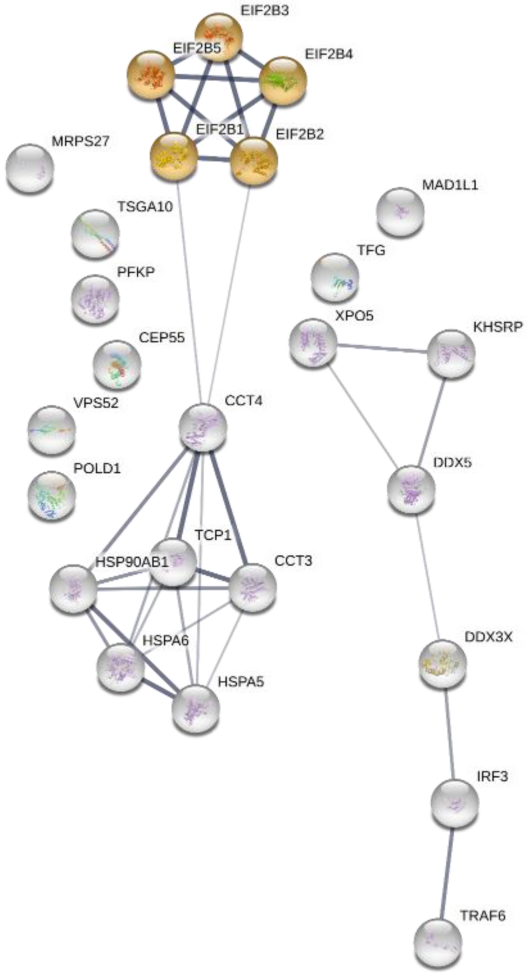
EIF2B3
EIF2B5
EIF2B4
EIF2B1
EIF2B2
MRPS27
TSGA10
PFKP
CEP55
VPS52
POLD1
CCT4
TCP1
HSP90AB1
CCT3
HSPA6
HSPA5
MAD1L1
TFG
XPO5
KHSRP
DDX5
DDX3X
IRF3
TRAF6

Suppl. Fig. 4

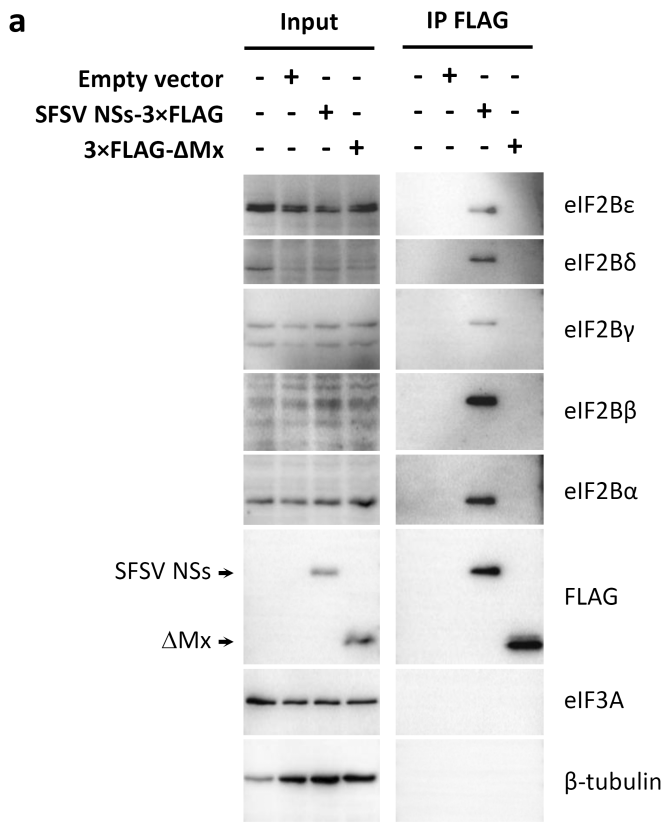
a
Input
IP FLAG
Empty vector - + - - - + - -
SFSV NSs-3×FLAG - - + - - - + -
3×FLAG-ΔMx - - - + - - - +
eIF2Bε
eIF2Bδ
eIF2Bγ
eIF2Bβ
eIF2Bα
SFSV NSs
ΔMx
FLAG
eIF3A
β-tubulin

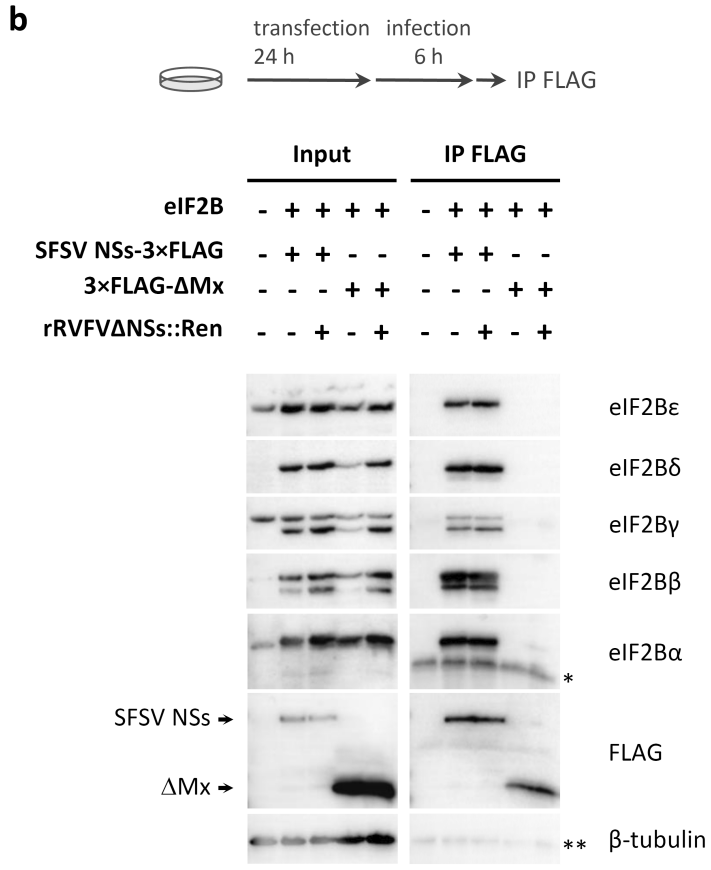
b
transfection
24 h
infection
6 h
IP FLAG
Input
IP FLAG
eIF2B - + + + + - + + + +
SFSV NSs-3×FLAG - + + - - - + + - -
3×FLAG-ΔMx - - - + + - - - + +
rRVFVΔNSs::Ren - - + - + - - + - +
eIF2Bε
eIF2Bδ
eIF2Bγ
eIF2Bβ
eIF2Bα
*
SFSV NSs
ΔMx
FLAG
**
β-tubulin

Suppl. Fig. 5

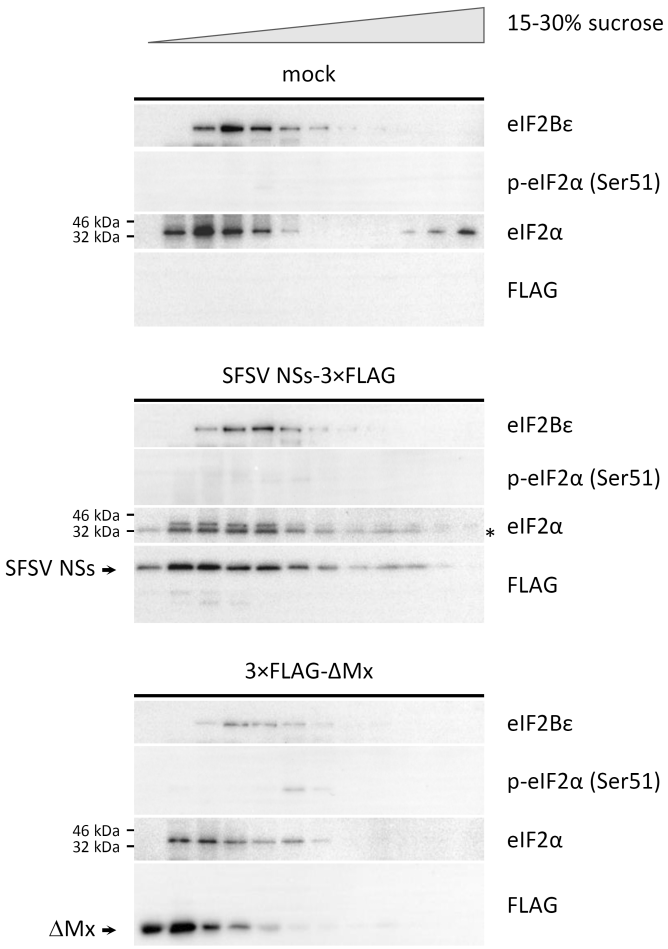
15-30% sucrose
mock
eIF2Bε
p-eIF2α (Ser51)
46 kDa
32 kDa
eIF2α
FLAG
SFSV NSs-3×FLAG
eIF2Bε
p-eIF2α (Ser51)
46 kDa
32 kDa
eIF2α
*
SFSV NSs
FLAG
3×FLAG-ΔMx
eIF2Bε
p-eIF2α (Ser51)
46 kDa
32 kDa
eIF2α
FLAG
ΔMx

4.5 Reasearch article:

Viral Evasion of the Integrated Stress Response Through Antagonism of eIF2-P Binding to eIF2B

Own contribution:

I contributed to the design of NSs constructs and NSs purification strategy, and provided input to writing the manuscript.

_____

Jennifer Würth

Viral Evasion of the Integrated Stress Response Through Antagonism of eIF2-P Binding to eIF2B

Michael Schoof[1,2,#], Lan Wang[1,2,#], J Zachery Cogan[1,2], Rosalie E Lawrence[1,2], Morgane Boone[1,2], Jennifer Deborah Wuerth[3], Adam Frost[2,4], Peter Walter[1,2,*]

Affiliations

[1]Howard Hughes Medical Institute, University of California at San Francisco, San Francisco, CA, USA.

[2]Department of Biochemistry and Biophysics, University of California at San Francisco, San Francisco, CA, USA.

[3]Institute of Innate Immunity, Medical Faculty, University of Bonn, Bonn, Germany

[4]Chan Zuckerberg Biohub, San Francisco, CA, USA.

[#] These authors contributed equally

* To whom correspondence should be addressed; Email: Peter@walterlab.ucsf.edu

Abstract

Viral infection triggers activation of the integrated stress response (ISR). In response to viral double-stranded RNA (dsRNA), RNA-activated protein kinase (PKR) phosphorylates the translation initiation factor eIF2, converting it from a translation initiator into a potent translation inhibitor and this restricts the synthesis of viral proteins. Phosphorylated eIF2 (eIF2-P) inhibits translation by binding to eIF2's dedicated, heterodecameric nucleotide exchange factor eIF2B and conformationally inactivating it. We show that the NSs protein of Sandfly Fever Sicilian virus (SFSV) allows the virus to evade the ISR. Mechanistically, NSs tightly binds to eIF2B (K_D = 30 nM), blocks eIF2-P binding, and rescues eIF2B GEF activity. Cryo-EM structures demonstrate that SFSV NSs and eIF2-P directly compete, with the primary NSs contacts to eIF2Bα mediated by five 'aromatic fingers'. NSs binding preserves eIF2B activity by maintaining eIF2B's conformation in its active A-State.

Introduction

The Integrated Stress Response (ISR) is a conserved eukaryotic stress response network that, upon activation by a diverse set of stressors, profoundly reprograms translation. It is coordinated by at least four stress-responsive kinases: PERK (responsive to protein misfolding in the endoplasmic reticulum), PKR (responsive to viral infection), HRI (responsive to heme deficiency and oxidative and mitochondrial stresses), and GCN2 (responsive to nutrient deprivation) [1-4]. All four known ISR kinases converge on the phosphorylation of a single serine (S51) of the α subunit of the general translation initiation factor eIF2. Under non-stress conditions, eIF2 forms a ternary complex (TC) with methionyl initiator tRNA (Met-tRNA^{i}) and GTP. This complex performs the critical task of delivering the first amino acid to ribosomes at AUG initiation codons. Upon S51 phosphorylation, eIF2 is converted from a substrate to an inhibitor of its dedicated nucleotide exchange factor (GEF) eIF2B. GEF inhibition results from binding of eIF2-P in a new, inhibitory binding orientation on eIF2B, where it elicits allosteric changes to antagonize eIF2 binding and additionally compromise eIF2B's intrinsic enzymatic activity [5, 6].

eIF2B is a two-fold symmetric heterodecamer composed of 2 copies each of α, β, δ, γ, and ε subunits [7-10]. eIF2B can exist in a range of stable subcomplexes (eIF2Bβδγε tetramers and eIF2Bα_2 dimers) if the concentrations of its constituent subunits are altered [5, 8, 9, 11]. While earlier models suggested eIF2B assembly to be rate-limiting and a potential regulatory step, recent work by us and others show that eIF2B in cells primarily exists in its fully assembled decameric, enzymatically active state [5, 6]. Cryo-EM studies of various eIF2B complexes elucidated the mechanisms of nucleotide exchange and ISR inhibition through eIF2-P binding [5, 6, 12-15]. Under non-stress conditions, eIF2 engages eIF2B through multiple interfaces along a path spanning the heterodecamer. In this arrangement, eIF2α binding to eIF2B critically positions the GTPase domain in eIF2's γ subunit, allowing for efficient catalysis of nucleotide exchange [12, 14]. eIF2B's catalytically active conformation ('A-State') becomes switched to an inactive conformation upon eIF2-P binding (Inhibited or 'I-State'), which displays altered substrate-binding interfaces [5, 6]. I-State eIF2B$(\alpha\beta\delta\gamma\varepsilon)_2$ exhibits enzymatic activity and substrate engagement akin to the tetrameric eIF2Bβδγε subcomplex, hence eIF2-P inhibition of eIF2B converts the decamer into conjoined

67 tetramers, which reduces its GEF activity, lowers the cell's TC concentration, and results
68 in ISR-dependent translational reprogramming [5, 6].
69
70 Viruses hijack the host cell's protein synthesis machinery to produce viral proteins and
71 package new viral particles. Numerous host countermeasures have evolved. In the
72 context of the ISR, double-stranded RNA (dsRNA), a by-product of viral replication,
73 triggers dimerization and autophosphorylation of PKR [3, 16]. In this activated state PKR
74 phosphorylates eIF2, which then binds to and inhibits eIF2B. As such, cells
75 downregulate mRNA translation as a strategy to slow the production of virions. Viruses,
76 in turn, enact strategies of evasion. Indeed, viral evasion strategies acting at each step
77 of ISR activation have been observed. Influenza virus, for example, masks its dsRNA
78 [17, 18]. Rift Valley Fever virus (RVFV) encodes an effector protein that degrades PKR
79 [19]. Hepatitis C virus blocks PKR dimerization [20]. Vaccinia virus encodes a
80 pseudosubstrate as a PKR decoy [21]. Herpes simplex virus can dephosphorylate eIF2-
81 P [22]. And some coronavirus and picornavirus proteins appear to block the eIF2B-eIF2-
82 P interaction [23]. This evolutionary arms race between host and pathogen can provide
83 invaluable tools and insights into the critical mechanisms of the ISR, as well as other
84 cellular stress responses.
85
86 Here, we investigated the previously unknown mechanism by which Sandfly Fever
87 Sicilian virus (SFSV) evades the ISR. SFSV and RVFV are both members of the genus
88 *Phlebovirus* (order *Bunyavirales*) which encode an evolutionarily related non-structural
89 protein (NSs) [24-26]. Across the phleboviruses, NSs serves to counteract the antiviral
90 interferon response, but NSs proteins perform other functions as well [27, 28]. Unlike the
91 RVFV NSs which degrades PKR, SFSV NSs does not impact the levels or
92 phosphorylation status of PKR or eIF2 [19, 29]. Instead, it binds to eIF2B, inhibiting the
93 ISR. The mechanistic basis of this inhibition was previously unclear. We here provide
94 cellular, biochemical, and structural insight into this question, showing that the SFSV
95 NSs evades all branches of the ISR by binding to eIF2B and selectively blocking eIF2-P
96 binding, thereby maintaining eIF2B in its active A-State.

Results

The SFSV NSs is a pan ISR inhibitor

To dissect the role of the SFSV NSs (henceforth referred to as NSs) in ISR modulation, we engineered cells stably expressing either an empty vector, a functional NSs (NSs::FLAG), or a non-functional NSs (FLAG::NSs) (Supplementary Fig. 1). As previously reported, the NSs with a C-terminal FLAG tag (NSs::FLAG) should retain its PKR-evading properties while tagging at the N-terminus (FLAG::NSs) blocks this functionality [29]. These constructs were genomically integrated into our previously generated ISR reporter system, in which both changes in ATF4 translation and general translation can be monitored [5]. Both NSs::FLAG and FLAG::NSs were stably expressed in these cells without impacting the levels of key ISR components (eIF2B, eIF2, PKR, PERK) (Fig. 1a). The apparent differences in band intensity between NSs::FLAG and FLAG::NSs may reflect differences in protein stability or, perhaps more likely, differences in antibody affinity for the FLAG epitope at the respective C- and N-terminal tagging locations.

To ask whether NSs is a pan-ISR inhibitor capable of dampening ISR activation irrespective of any particular ISR activating kinase, we chemically activated PERK, HRI, and GCN2 with thapsigargin, oligomycin, and glutamine deprivation / synthetase inhibition through L-methionine sulfoximine, respectively. NSs::FLAG expression dampened the increases in ATF4 translation brought about by activation of any of the kinases (Fig. 1b-d). NSs::FLAG also maintained general translation levels in the thapsigargin and oligomycin treated cells (Fig. 1b,c). Notably, in the context of GCN2 activation, general translation comparably decreased at the highest levels of stress regardless of NSs status (Fig. 1d). This observation likely reflects the additional stress responses that react to reduced amino acid levels, as well as the fact that while the ISR controls translation initiation, ribosome-engaged mRNAs still need sufficient levels of amino acids to be successfully translated. On the whole, these data therefore show that the NSs is a pan-ISR inhibitor akin to the small molecule ISRIB, which binds to eIF2B and counteracts the ISR by allosterically blocking eIF2-P binding and promoting eIF2B complex assembly when eIF2B's decameric state is compromised [5, 6, 30].

NSs binds decameric eIF2B exclusively

131 To explain the mechanism by which NSs inhibits the ISR, we purified NSs expressed in
132 mammalian cells (Fig. 2a,b). We next validated that NSs binds to eIF2B *in vitro* by
133 immobilizing distinct eIF2B complexes on agarose beads and incubating them with an
134 excess of NSs (Fig. 2c). As expected, NSs binds to the fully assembled eIF2B$(\alpha\beta\delta\gamma\varepsilon)_2$
135 decamers (Lane 4). Notably, it did not bind to eIF2Bβδγε tetramers (Lane 5) or to
136 eIF2Bα_2 dimers (Lane 6). The NSs interaction with eIF2B thus either spans multiple
137 interfaces that are only completed in the fully assembled complex or interacts with a
138 region of eIF2B that undergoes a conformational change when in the fully assembled
139 state.
140
141 To quantitatively assess NSs binding to eIF2B, we employed surface plasmon
142 resonance (SPR) experiments to determine the affinity of NSs for the various eIF2B
143 complexes (Fig. 2d-f). The NSs interaction with decameric eIF2B could be modeled
144 using one-phase association and dissociation kinetics. NSs binds to decameric eIF2B
145 with a K_D of 30 nM (k_a = 3.0 x 10^5 $M^{-1}s^{-1}$, k_d = 8.9 x 10^{-3} s^{-1}) (Fig. 2d). This affinity is
146 comparable to the low nanomolar affinity of ISRIB for decameric eIF2B (Supplementary
147 Fig. 3) [10]. In this orthogonal approach, we again observed no detectable binding of
148 NSs to eIF2Bβδγε tetramers or eIF2Bα_2 dimers (Fig. 2e,f).
149
150 **NSs rescues eIF2B activity by blocking eIF2-P binding**
151 We next sought to explain the mechanism of NSs inhibition of the ISR using our
152 established *in vitro* systems for studying eIF2B. As is the case with the small molecule
153 ISRIB, NSs did not impact the intrinsic nucleotide exchange activity of eIF2B as
154 monitored by a fluorescent BODIPY-FL-GDP loading assay (Supplementary Fig. 2). To
155 mimic the conditions during ISR activation, we repeated our nucleotide exchange assay
156 in the presence of the inhibitory eIF2α-P (Fig. 3a). As expected, eIF2α-P inhibited eIF2B
157 GEF activity ($t_{1/2}$ = 13.4 min, s.e.m. = 1.5 min), but increasing concentrations of NSs (25
158 nM: $t_{1/2}$ = 9.2 min, s.e.m. = 1.2 min; 100 nM: $t_{1/2}$ = 6.2 min, s.e.m. = 0.5 min) overcame
159 the inhibitory effects of eIF2α-P and fully rescued eIF2B GEF activity (uninhibited $t_{1/2}$ =
160 6.3 min, s.e.m. = 0.6 min).
161
162 As NSs' ability to affect eIF2B activity markedly manifests in the presence of eIF2α-P,
163 we wondered whether NSs blocks eIF2α-P binding to eIF2B. To test this notion, we
164 utilized a fluorescent ISRIB analog (FAM-ISRIB) that emits light with a higher degree of

165 polarization when bound to eIF2B, compared to being free in solution (Fig. 3b, black and
166 red dots on the Y axis, respectively). It has been previously shown that eIF2α-P binding
167 to eIF2B antagonizes FAM-ISRIB binding by shifting eIF2B into a conformation
168 incapable of binding ISRIB or its analogs (Fig. 3b, blue dot on the Y axis) [5, 6]. A
169 titration of NSs into this reaction recovered FAM-ISRIB polarization (EC_{50} = 72 nM,
170 s.e.m. = 9 nM), indicating that NSs engages eIF2B and disrupts eIF2α-P's inhibitory
171 binding. To directly show this antagonism, we immobilized eIF2B decamers on agarose
172 beads and incubated with combinations of NSs and eIF2α-P (Fig. 3c). While individually,
173 both eIF2α-P and NSs bound to eIF2B (Fig. 3c, lanes 4 and 5, respectively), in the
174 presence of saturating NSs, eIF2α-P no longer bound eIF2B (Fig. 3c, lane 6). We next
175 sought to analyze the impact of NSs binding on full-length substrate (eIF2) and inhibitor
176 (eIF2-P) binding through SPR experiments. In this assay we first flowed one analyte
177 over immobilized eIF2B (to saturate the binding site) immediately followed by a mixture
178 of both analytes (to assess whether the second analyte could co-bind elsewhere).
179 Consistent with the nucleotide exchange assay in Fig. 3a, eIF2 and NSs co-bound eIF2B
180 (Fig. 3d,f, increases in RU at 60 s). However, as with the phosphorylated eIF2α subunit
181 alone, the full phosphorylated heterotrimer (eIF2-P) and NSs did not co-bind (Fig. 3e,g,
182 no increases in RU at 60 s). Together, these results demonstrate that the NSs is a
183 potent inhibitor of eIF2-P binding while preserving eIF2 binding.
184
185 **NSs binds to eIF2B at the eIF2α-P binding site and keeps eIF2B in the active A-**
186 **State**
187 Having established that the NSs blocks eIF2-P binding to eIF2B, we next assessed
188 whether NSs is an allosteric regulator of eIF2-P binding (as is the case with ISRIB) or,
189 alternatively, whether it directly competes with eIF2-P binding. To answer this question
190 and to rigorously determine NSs' interactions with eIF2B, we turned to cryoEM. To
191 obtain a homogeneous sample suitable for structural studies, we mixed full-length NSs
192 with decameric eIF2B at a 3:1 molar ratio. We then prepared the sample for cryo-EM
193 imaging and determined the structure of the eIF2B-NSs complex.
194
195 3D classification with no symmetry assumptions yielded a distinct class of 137,093
196 particles. Refinement of this class resulted in a map with an average resolution of 2.6 Å
197 (Supplementary Fig. 4). After docking the individual eIF2B subunits into the recorded
198 density, we observed significant extra density next to both eIF2Bα subunits, indicating

199 that two copies of NSs are bound to each eIF2B decamer (Fig. 4a, Supplementary Fig.
200 4). The local resolution of the NSs ranges from 2.5 Å (regions close to eIF2B) to >4.0 Å
201 (periphery), with most of the side chain densities clearly visible (Supplementary Fig. 4.
202 To build the molecular model for NSs, we split the protein into two domains. The C-
203 terminal domain was built using the crystal structure of the C-terminal domain of the
204 RVFV NSs (PDB ID: 5OOO) as a homology model (43.8% sequence similarity with the
205 C-terminal domain of the SFSV NSs (residues 85-261)) (Supplementary Fig. 5) [31]. The
206 N-terminal domain of the NSs (residues 1-84) was built *de novo* (Supplementary Table
207 1). The high resolution map allowed us to build a model for the majority of NSs. The map
208 quality of both NSs molecules are comparable, and their molecular models are nearly
209 identical (root mean square deviation (RMSD) ≈ 0.2 Å). We henceforth focus our
210 analysis on one of them (chain K).
211
212 Two copies of NSs bind to one decameric eIF2B in a symmetric manner (Fig. 4a). An
213 overlay of the NSs-bound eIF2B and the eIF2α-P-bound eIF2B structures (PDB ID:
214 6O9Z) shows a significant clash between the NSs and eIF2-αP, indicating that, unlike
215 the allosteric regulator ISRIB, NSs binds in direct competition with eIF2α-P (Fig. 4d-f).
216 Interestingly, whereas eIF2α-P forms extensive interactions with both the α and the δ
217 subunits of eIF2B, the NSs mainly interacts with the eIF2Bα subunit. The expansive
218 interactions between eIF2α-P and both eIF2Bα and eIF2Bδ mediate a shift in eIF2B's
219 conformation from eIF2B's enzymatically active A-state to its inhibited I-state [5, 6].
220 Thus, despite binding to a region known to influence eIF2B's conformation, an overlay of
221 the NSs-bound eIF2B and apo-eIF2B shows that the overall conformation of eIF2B in
222 the two structures are virtually identical (Fig. 4b). By contrast, the eIF2B-NSs and eIF2B-
223 eIF2α-P overlay shows major conformational differences (Fig. 4c). Together, these
224 structural data, paired with our *in vitro* assays, show that the NSs grants SFSV evasion
225 of the ISR by directly competing off eIF2-P and restoring eIF2B to its enzymatically
226 active A-State.
227
228 **NSs uses a novel protein fold containing aromatic fingers to bind eIF2B**
229 Next, we sought to interrogate the molecular details of the NSs-eIF2B interaction. As
230 mentioned above, NSs consists of two domains. Its N-terminal domain (amino acids 1-
231 84) consists of six β strands and interacts directly with eIF2B. A search in the DALI
232 protein structure comparison server did not reveal any hits, suggesting a novel protein

233 fold. β strands 1 and 2 and β strands 3 and 4 form two antiparallel β sheets and fold on
234 top of the C-terminal domain (Supplementary Fig. 6b). The C-terminal domain (amino
235 acids 85-261) is largely α-helical and presumably supports the folding of the N-terminal
236 domain, as truncating the C-terminal domain results in the complete loss of NSs activity
237 in terms of ISR evasion (Supplementary Fig. 7). Also, despite the moderate sequence
238 conservation of the C-terminal domain of the SFSV NSs and the RVFV NSs, their
239 structures overlay extensively (RMSD ≈ 0.2 Å, Supplementary Fig. 6).
240
241 The surface of the N-terminal domain forms a hand shape that grips the alpha helices of
242 eIF2Bα, akin to a koala grabbing a eucalyptus branch (Fig. 5a, Supplementary Fig. 10).
243 In this arrangement, the N-terminal domain extends three loops that contact eIF2Bα. The
244 first two loops sit in a groove between helices α3 and α4 and the third loop just below
245 helix α3, effectively sandwiching helix α3 (Fig. 5b). Together, the three loops extend five
246 aromatic amino acids to contact eIF2Bα. We refer to these aromatic amino acids as
247 "aromatic fingers". On the top side of helix α3, the side chain of NSs Y5 forms a cation-π
248 interaction with eIF2Bα R74 and its backbone carbonyl forms a hydrogen bond with
249 eIF2Bα R46 (Fig. 5d). NSs F7 forms a cation-π interaction with eIF2Bα R46, and
250 hydrophobic stacking with eIF2Bα I42. NSs F33 stacks against the backbone of eIF2Bα
251 Y304 and L305, as well as the aliphatic region of eIF2Bα R74. On the bottom side of
252 helix α3, NSs F80 stacks against a hydrophobic groove formed by eIF2Bα I7, F33 and
253 A52 (Fig. 5e). NSs Y79 forms a polar interaction with eIF2Bα D37, completing the
254 extensive interaction network of the NSs' aromatic fingers with the α helices in eIF2Bα.
255 In addition, the side chain of NSs H36 and the backbone carbonyl of NSs T35 both
256 contact eIF2Bδ R321. The side chain of NSs D37 also forms an ionic interaction with
257 eIF2Bδ R321, although the distance is close to 4.0 Å, suggesting a weak interaction.
258 These three amino acids account for the only interactions with eIF2Bδ (Fig. 5c).
259
260 To validate the functional importance of the eIF2Bα-facing aromatic fingers, we mutated
261 them in pairs or singly to alanines (Y5A/F7A, Y79A/F80A, and F33A) and stably
262 expressed these NSs variants in the dual ISR reporter cells. The point mutations did not
263 compromise NSs stability and, as with WT NSs, did not affect eIF2 or eIF2B subunit
264 levels (Fig. 6a). Upon stress, eIF2α became phosphorylated in all cell lines, but only in
265 cells expressing WT NSs::FLAG was ATF4 translation blunted (Fig. 6a). A similar picture
266 emerged from analysis of the fluorescent ISR reporter signals. Whereas WT NSs

267 inhibited the translation of ATF4 and maintained general translation at roughly normal
268 levels, all the point mutants tested broke the NSs' function as an ISR evader (Fig. 6b).
269 All 5 eIF2Bα-facing aromatic fingers thus appear critical for NSs modulation of the ISR,
270 likely through reducing the binding affinity of NSs for eIF2B. Indeed, alanine substitutions
271 of the aromatic fingers was independently shown to reduce NSs binding affinity to eIF2B
272 [32].
273
274 We additionally assessed the importance of the eIF2Bδ-facing residues – generating
275 stable lines with alanine mutations (H36A and D37A). As we saw with mutation of the
276 aromatic fingers, neither H36A nor D37A impaired NSs translation or impacted eIF2 or
277 eIF2B subunit levels, but ISR evasion as monitored by ATF4 translation became
278 compromised (Fig. 6c). Notably, NSs::FLAG (H36A) displayed an intermediate
279 phenotype in the ATF4 and general translation reporter assays, suggesting that while
280 this mutation compromises NSs binding it does not appear to entirely break the
281 interaction (Fig. 6d). In contrast, NSs::FLAG (D37A) expressing cells appear unable to
282 resist ISR activation. Although the structure suggests only a mild ionic interaction
283 between NSs D37 and eIF2Bδ R321, we reason the D37A mutation might not only break
284 the ionic interaction, but also potentially alter the conformation of the loop. As a result,
285 V38 would move, disrupting its stacking with M6, an amino acid next to two aromatic
286 fingers (Y5 and F7) (Supplementary Fig. 8). Thus, changes to D37 and H36 could result
287 in the repositioning of the eIF2Bα-facing aromatic fingers, leading to a complete loss of
288 NSs interaction with eIF2B. Together, these data provide a rationale for NSs' potent and
289 selective binding to only fully assembled eIF2B$(\alpha\beta\delta\gamma\varepsilon)_2$ decamers.

290 **Discussion**

291

292 As one of the strategies in the evolutionary arms race between viruses and the host cells
293 they infect, mammalian cells activate the ISR to temporarily shut down translation, thus
294 preventing the synthesis of viral proteins. Viruses, in turn, have evolved ways to evade
295 the ISR, typically by disarming the PKR branch through countermeasures that lead to
296 decreased levels of eIF2-P, thus allowing translation to continue. In this study, we show
297 that SFSV expresses a protein (NSs) that allows it to evade not just PKR-mediated ISR
298 activation, but all four branches of the ISR, through a mechanism that exploits the
299 conformational flexibility of eIF2B. NSs is an antagonist of eIF2B's inhibitor eIF2-P,
300 deploying an overlapping binding site. Whereas eIF2-P shifts eIF2B to its inactive I-State
301 conformation by closing the angle between the eIF2Bα and eIF2Bδ subunits, NSs
302 engages the enzyme to opposite effect, binding to an overlapping site with eIF2-P but
303 preserving the angle between eIF2Bα and eIF2Bδ and locking it into its active A-State
304 conformation (Figure 7).

305

306 Previously, we and others showed that the GEF activity of eIF2B is modulated
307 conformationally: eIF2B's substrate (eIF2) binding stabilizes it in the A-State, whereas its
308 inhibitor (eIF2-P) binding induces a hinge motion between the two tetrameric halves,
309 resulting in a conformation that cannot engage the substrate optimally (I-state) [5, 6].
310 Our structure shows that NSs antagonizes the endogenous inhibitor (eIF2-P) by directly
311 competing it off and stabilizing eIF2B in the active conformation. Owing to the reported
312 single digit nM affinity of eIF2-P for eIF2B, this likely entails a cellular excess of NSs
313 relative to eIF2-P (which should be expected given the high levels at which viral proteins
314 are typically expressed) [33-35]. While NSs binds to the inhibitor-binding site, it does not
315 induce the conformational change that the inhibitor binding induces. This mechanism is
316 reminiscent of the antagonistic inhibition of GPCRs, such as the β adrenergic receptors,
317 where binding of an agonist ligand shifts the receptor to its active conformation, whereas
318 binding of an antagonist ligand occupies an overlapping but not identical binding site that
319 lacks contacts required to induce the activating conformational change [36-39]. NSs,
320 however, is an antagonist of an inhibitor (eIF2-P). Thus, by inhibiting an inhibition, it
321 actually works as an eIF2B activator under conditions where eIF2-P is present and the
322 ISR is induced.

323

324 In its ability to modulate eIF2B, NSs is not unique among viral proteins. The beluga
325 whale coronavirus (Bw-CoV) protein AcP10 likewise allows evasion of the host cell ISR
326 by interacting with eIF2B, as does the picornavirus AiVL protein [23]. It was suggested
327 that AcP10 makes contacts with eIF2Bα and eIF2Bδ, akin to NSs, and hence may act
328 through a similar mechanism by antagonizing eIF2-P, although no structural information
329 is yet available. By primary sequence comparison, AcP10, AiVL, and NSs show no
330 recognizable homology with one another, indicating that viruses have evolved at least
331 three – and likely more – different ways to exploit the eIF2α-P binding site on eIF2B to
332 shut off the ISR. Therefore, inhibiting the eIF2B-eIF2-P interaction through the
333 antagonism of eIF2-P binding could also be a general strategy used by many viruses.
334
335 Our structure and mutational analysis suggest that the binding of different parts of NSs
336 to eIF2B occurs in a highly synergistic manner. While the amino acids facing eIF2Bδ do
337 not seem to make sufficiently intimate contacts to provide a significant contribution to the
338 enthalpic binding energy, changing them disrupts binding. It is plausible that the contacts
339 of NSs with eIF2Bδ allow the optimal positioning of the aromatic fingers through
340 allosteric communications between the loops and thus license NSs for tight binding.
341
342 The structure of the eIF2B-NSs complex reveals a previously unknown site on eIF2B
343 that is potentially druggable. Unlike ISRIB, which stabilizes eIF2B's A-State through
344 binding to a narrow pocket at the center of eIF2B and stapling the two tetrameric halves
345 together at a precise distance and angle, NSs binds to a different interface on the
346 opposite side of the protein. With ISRIB-derivatives showing extreme promise to
347 alleviate cognitive dysfunction in animal studies of various neurological disorders and
348 recently progressing into the clinic for Phase I human trials, developing therapeutics that
349 modulate the ISR has never been more relevant [40].
350
351 Across phleboviruses, all characterized members of the family of related NSs proteins
352 also counteract the host's interferon response [25, 26]. For RVFV, this functionality is
353 contained within the structurally conserved C-terminal domain, which nonetheless varies
354 quite heavily in sequence space [27, 28, 41, 42]. A strict functional conservation does
355 not appear to be the case for the N-terminal domain. Although this domain serves to
356 evade PKR in some phleboviruses such as RVFV and SFSV, it accomplishes it through
357 entirely different means: degradation of PKR in RVFV and antagonism of eIF2-P binding

358 to eIF2B in SFSV [19, 29]. The NSs is thus a bispecific molecule – a multitool of sorts.
359 The C-terminal domain may serve as a scaffold containing a core functionality upon
360 which the N-terminal domain may be free to evolve, exploring diverse functionalities and
361 mechanisms. It is exciting to speculate whether anti-PKR properties of the N-terminal
362 domain, as we identified for SFSV NSs, are commonly found across phleboviruses and
363 whether still other PKR evasion strategies can be found.
364
365 Aberrant ISR activation underlies many neurological disorders (Traumatic Brain Injury,
366 Down's Syndrome, Alzheimer's Disease, Amyotrophic Lateral Sclerosis), as well as
367 certain cancers (metastatic prostate cancer) [40, 43-47]. Virotherapy, where viruses are
368 used as a therapeutic agent for particular diseases, has seen the most success in the
369 realm of cancer treatment where the infection either directly attacks cancer cells
370 (oncolytic virotherapy) or serves to activate host defenses which target virus and cancer
371 alike [48, 49]. Indeed, decades of evidence have shown that cancer patients that
372 experience an unrelated viral infection can show signs of improvement, paving the way
373 for the generation of genetically engineered oncolytic viruses that have only just received
374 FDA approval in the last decade [50, 51]. With our ever-growing understanding of
375 diverse host-virus interactions, a whole host of new virotherapies are imaginable that
376 can exploit the evolved functionalities of viral proteins such as the NSs.

377 **Figures**

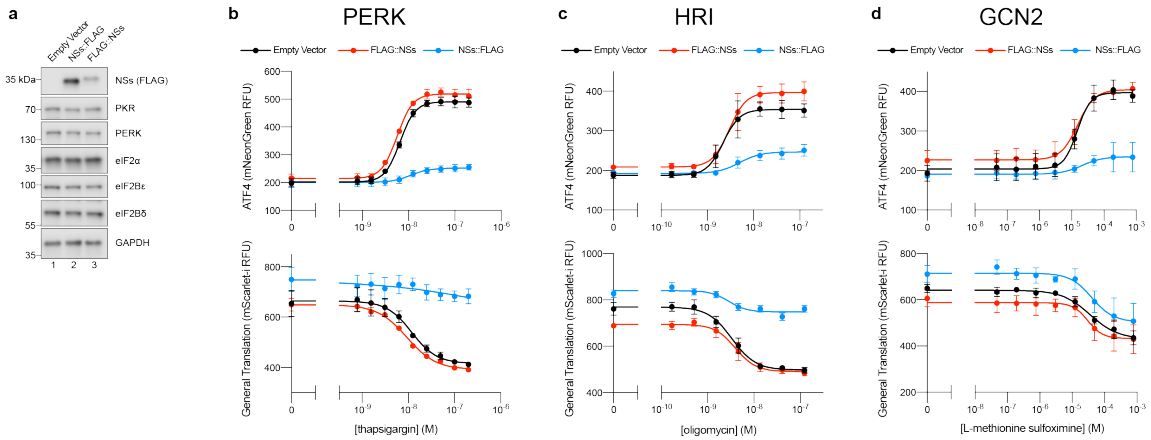

378

379 **Fig. 1: The SFSV NSs is a pan-ISR inhibitor**

380 **(a)** Western blot of K562 cell extracts. Loading of all lanes was normalized to total
381 protein. **(b-d)** ATF4 and General Translation reporter levels as monitored by flow
382 cytometry. Trimethoprim, which is necessary to stabilize the ecDHFR::mScarlet-i and
383 ecDHFR::mNeonGreen translation reporters, was at 20 μM for all conditions. (b)
384 Samples after 3 h of thapsigargin and trimethoprim treatment. (c) Samples after 3 h of
385 oligomycin and trimethoprim treatment. (d) Samples after 4 h of glutamine deprivation, L-
386 methionine sulfoximine, and trimethoprim treatment.
387 For (a), PERK and GAPDH, PKR and eIF2α, and eIF2Bε and NSs (FLAG) are from the
388 same gels, respectively. eIF2Bδ is from its own gel. For (b-d), biological replicates: n = 3.
389 All error bars represent s.e.m. Source data are provided as a Source Data file.

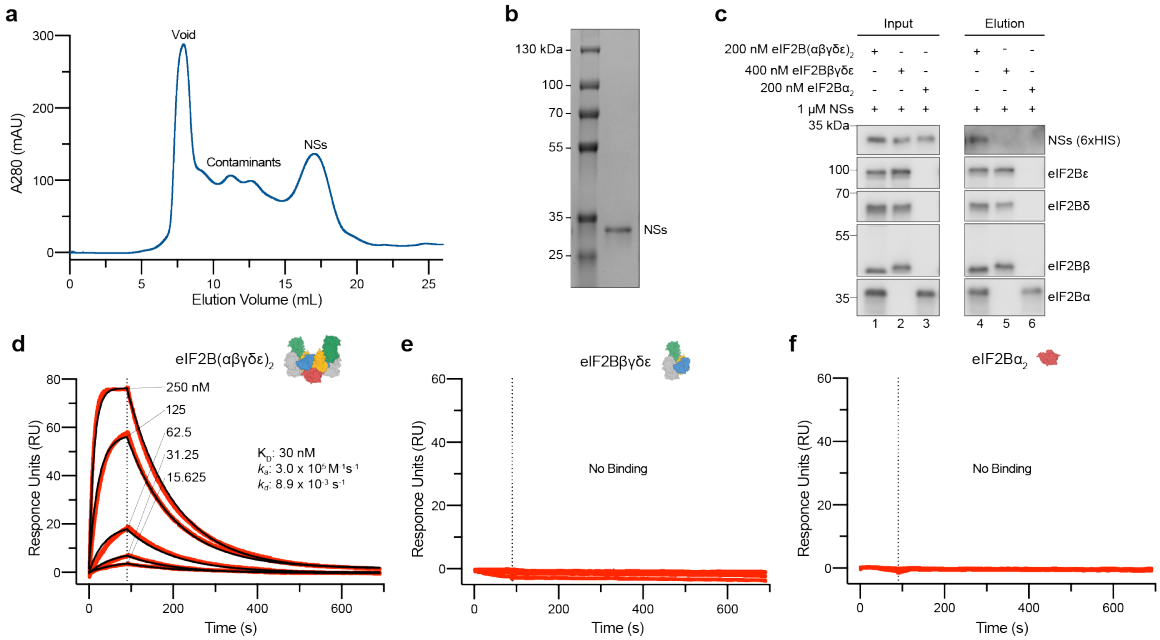

Fig. 2: NSs specifically binds to eIF2B(αβδγε)$_2$ decamers

(a) Size exclusion chromatogram (Superdex 200 Increase 10/300 GL) during NSs purification from Expi293 cells. **(b)** Coomassie Blue staining of purified NSs. **(c)** Western blot of purified protein recovered after incubation with eIF2B(αβδγε)$_2$, eIF2Bβδγε, or eIF2Bα$_2$ immobilized on Anti-protein C antibody conjugated resin. For eIF2B(αβδγε)$_2$ and eIF2Bα$_2$, eIF2Bα was protein C tagged. eIF2Bβ was protein C tagged for eIF2Bβδγε. **(d-f)** SPR of immobilized (d) eIF2B(αβδγε)$_2$, (e) eIF2Bβδγε, and (f) eIF2Bα$_2$ binding to NSs. For eIF2B(αβδγε)$_2$ and eIF2Bβδγε, eIF2Bβ was Avi-tagged and biotinylated. For eIF2Bα$_2$, eIF2Bα was Avi-tagged and biotinylated. For (d), concentration series: (250 nM - 15.625 nM) For (e-f), concentration series: (125 nM – 15.625 nM). For (c), eIF2Bβ and eIF2Bα, and eIF2Bδ and NSs (6xHIS) are from the same gels, respectively. eIF2Bε is from its own gel. For (b-f), a single biological replicate. Source data are provided as a Source Data file.

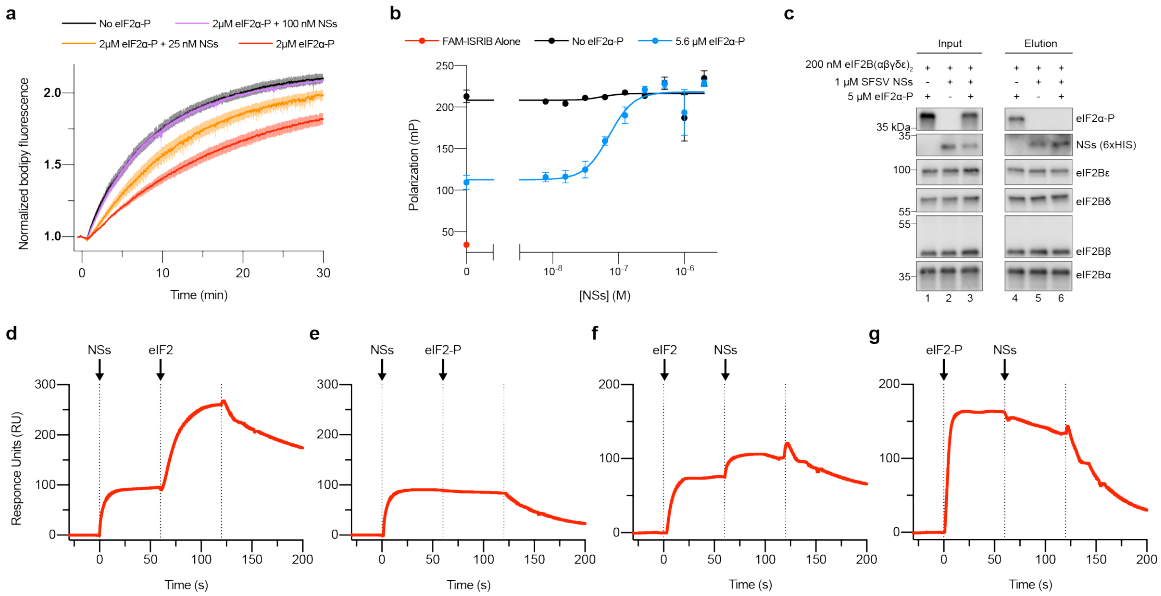

Fig. 3: NSs grants ISR evasion by antagonizing eIF2α-P binding to eIF2B

(a) GEF activity of eIF2B as assessed by BODIPY-FL-GDP exchange. eIF2B(αβδγε)$_2$ at 10 nM throughout. $t_{1/2}$ = 6.3 min (No eIF2α-P), 6.2 min (2 μM eIF2α-P + 100 nM NSs), 9.2 min (2 μM eIF2α-P + 25 nM NSs), and 13.4 min (2 μM eIF2α-P). **(b)** Plot of fluorescence polarization signal before (*red*) and after incubation of FAM-ISRIB (2.5 nM) with 100 nM eIF2B(αβδγε)$_2$ (*black*) or 100 nM eIF2B(αβδγε)$_2$ + 5.6 μM eIF2α-P (*blue*) and varying concentrations of NSs. **(c)** Western blot of purified protein recovered after incubation with eIF2B(αβδγε)$_2$ immobilized on Anti-protein C antibody conjugated resin. eIF2Bα was protein C tagged. **(d-g)** SPR of immobilized eIF2B(αβδγε)$_2$ binding to saturating (d-e) 500 nM NSs, (f) 125 nM eIF2, or (g) 125 nM eIF2-P followed by (d) 125 nM eIF2, (e) 125 nM eIF2-P, or (f-g) 500 nM NSs. eIF2Bα was Avi-tagged and biotinylated.

For (c), eIF2Bε and eIF2α-P, eIF2Bβ and eIF2Bα, and eIF2Bδ and NSs (6xHIS) are from the same gels, respectively. For (a-b), biological replicates: n = 3. For (c-g), a single biological replicate. All error bars represent s.e.m. Source data are provided as a Source Data file.

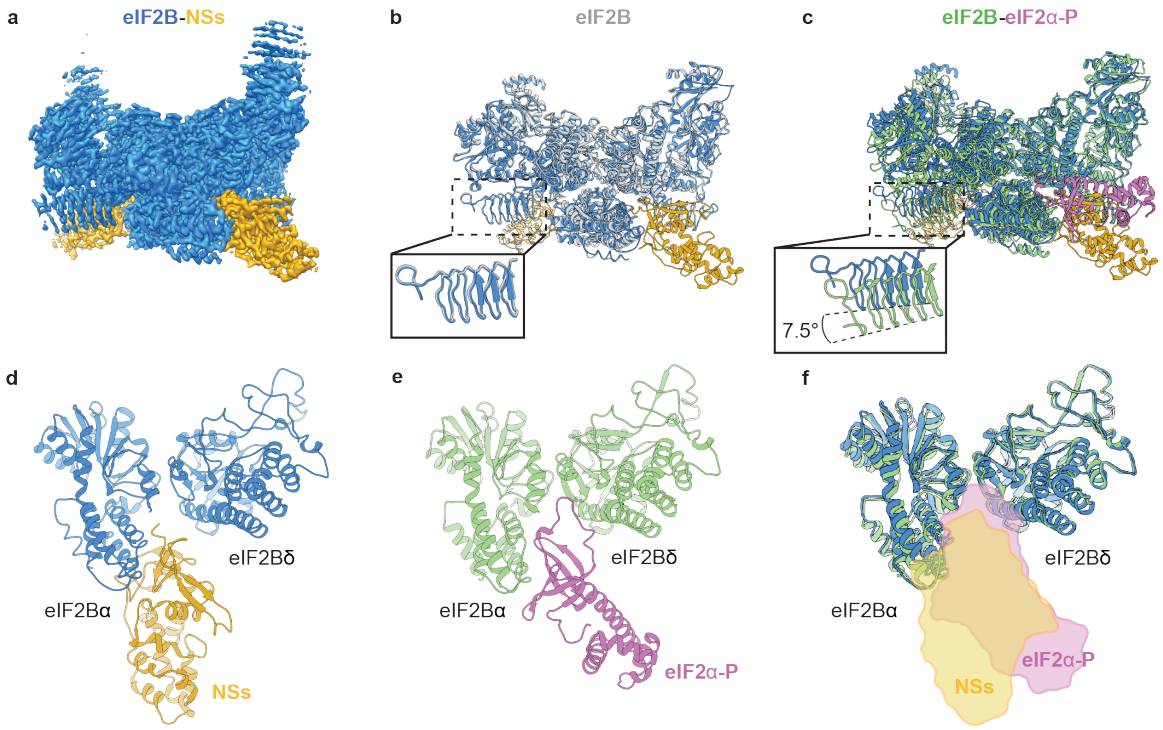

Fig. 4: Overall architecture of the eIF2B-NSs complex

(a) Cryo-EM map of the eIF2B-NSs complex. **(b)** Overlay of the apo eIF2B structure (PDB ID: 7L70) and the eIF2B-NSs structure shows that the overall conformation of eIF2B is nearly identical between the NSs-bound state and the apo state. **(c)** Overlay of the eIF2B-eIF2α-P complex structure (PDB ID: 6O9Z) and the eIF2B-NSs structure shows a 7.5° hinge movement between the two eIF2B halves. **(d)** and **(e)** Both NSs and eIF2α-P bind to eIF2B at the cleft between eIF2Bα and eIF2Bδ. **(d)** NSs mainly contacts eIF2Bα, whereas **(e)** eIF2α-P makes extensive contacts to both eIF2Bα and eIF2Bδ. **(f)** Comparison between the surfaces of NSs and eIF2α-P showing a significant overlay between the two. eIF2B in the eIF2B-NSs complex is colored in blue and NSs in gold. eIF2B in its apo form is colored white. eIF2B in the eIF2α-P-bound complex is colored in green, and eIF2α-P in pink.

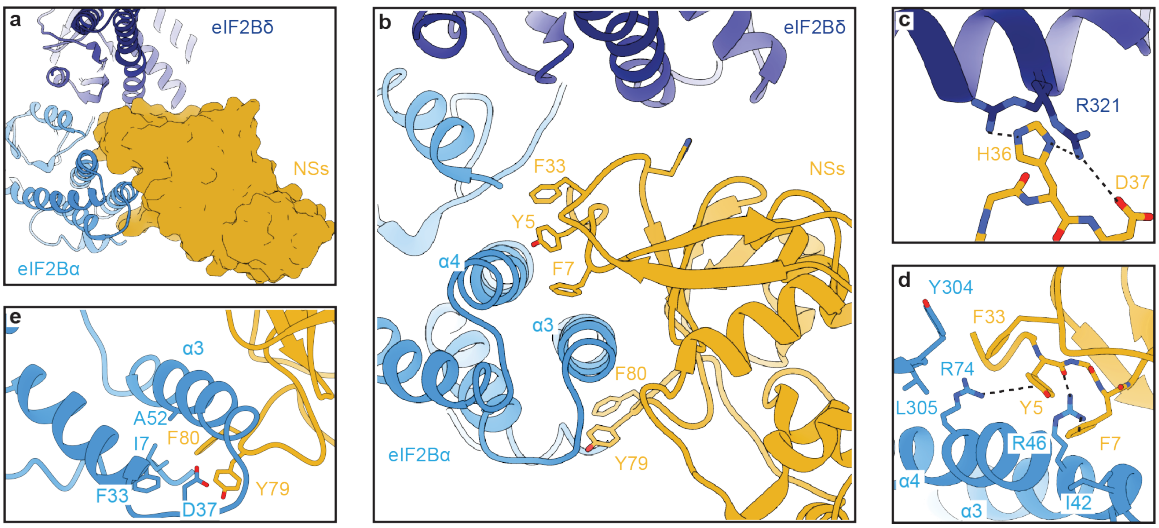

Fig. 5: NSs latches on to eIF2B with its aromatic fingers

(a) Surface representation of NSs showing that it grips the alpha helices of eIF2Bα. **(b)** NSs extends five aromatic amino acids in three short loops to contact eIF2Bα. They contact helices α3 and α4 of eIF2Bα. The backbone of T35 and the side chains of H36 and D37 of NSs make contact with eIF2Bδ **(c)** Zoomed in view of panel b showing the interaction between H36 and D37 with eIF2Bδ. **(d)** and **(e)** Zoomed-in view of panel b showing the detailed interactions between the five main aromatic amino acids and eIF2Bα. Each polar-polar or cation-π interaction is denoted by a dashed line. NSs is colored in gold, eIF2Bα in blue, and eIF2Bδ in purple.

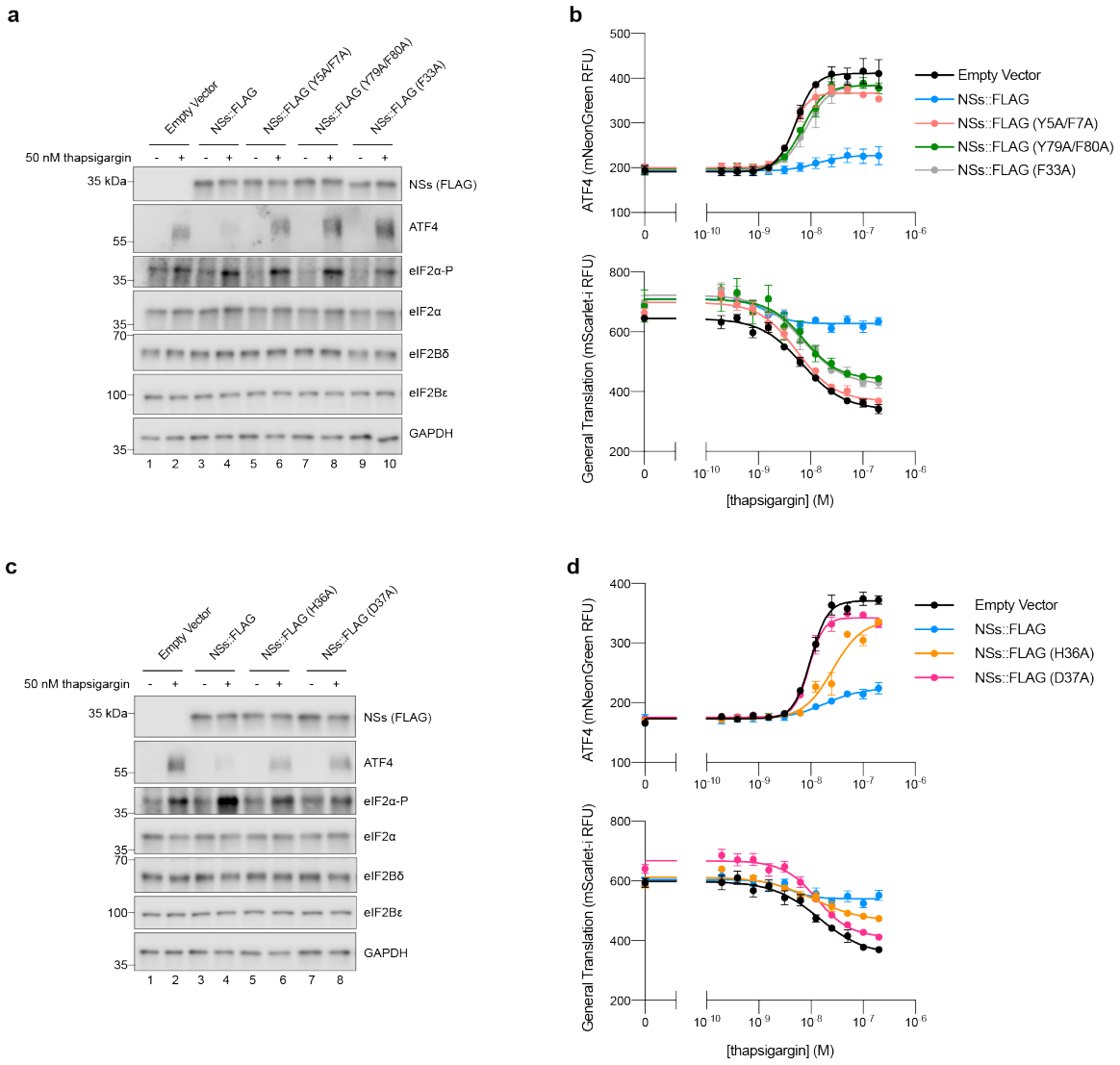

Fig. 6: All 5 aromatic fingers are required for NSs evasion of the ISR

(a and c) Western blot of K562 cell extracts 3 h after treatment with 50 nM thapsigargin. Loading of all lanes was normalized to total protein. **(b and d)** ATF4 and General Translation reporter levels as monitored by flow cytometry after 3 h of thapsigargin and trimethoprim (20 μM) treatment.

For (a), ATF4 and eIF2α, eIF2Bε and NSs (FLAG), and eIF2Bδ and eIF2α-P are from the same gels, respectively. GAPDH is from its own gel. For (c), ATF4 and GAPDH, eIF2Bε and NSs (FLAG), and eIF2Bδ and eIF2α-P are from the same gels, respectively. eIF2α is from its own gel. For (b), biological replicates: n = 3. For (d), biological replicates: n = 4. All error bars represent s.e.m. Source data are provided as a Source Data file.

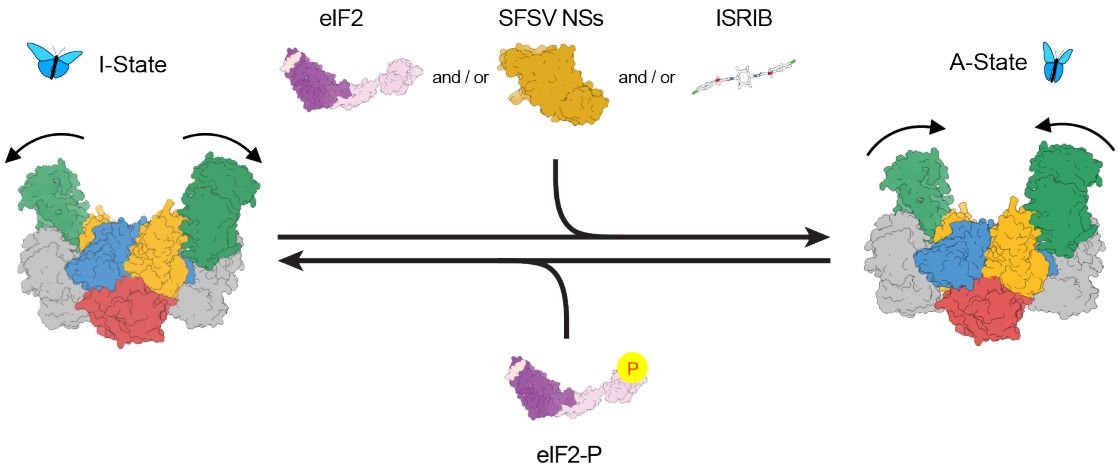

Fig. 7: Model for regulation of eIF2B activity.

Like the small molecule ISRIB and the substrate eIF2, NSs binds to and stabilizes the active, “wings up” conformation of eIF2B (A-State). eIF2-P induces the inhibited “wings down” conformation of eIF2B (I-State).

462 **Methods**

463 **Cloning of NSs expression plasmids**

464 The NSs::6xHIS Expi293 expression plasmid for transient transfection was generated
465 using In-Fusion HD cloning. The SFSV NSs sequence [29] was inserted into the pXSN
466 vector backbone and a 6xHIS tag was added at the C-terminus. The various NSs
467 overexpression plasmids for stable lentiviral integration were generated using In-Fusion
468 HD cloning. The SFSV NSs sequence was inserted into the pDBR vector backbone and
469 a FLAG tag was added at the C-terminus (pMS110, pMS127, pMS128, pMS129,
470 pMS130, pMS131, pMS132, pMS133) or N-terminus (pMS111). The various NSs
471 truncations did not have a FLAG tag (pMS119, pMS120, pMS121, pMS122, pMS123).
472 An empty vector control plasmid with no NSs insertion was also generated (pMS085).
473 An IRES followed by the puromycin resistance gene, a T2A self-cleaving peptide, and
474 the BFP sequence allows for selection based on antibiotic resistance or BFP signal
475 (what was used in this study) (Supplementary Fig. 1). Full plasmid details are shown in
476 Supplementary Table 2.

477

478 **Cloning of tagged human eIF2B expression plasmids**

479 *eIF2B2* (encoding eIF2Bβ) and *eIF2B4* (encoding eIF2Bδ) had previously been inserted
480 into sites 1 and 2 of pACYCDuet-1, respectively (pJT073) [8]. In-Fusion HD cloning
481 (Takarabio) was used to edit this plasmid further and insert an Avi tag
482 (GLNDIFEAQKIEWHE) or a Protein C tag (EDQVDPRLIDGK) at the N-terminus of
483 *eIF2B2,* immediately following the pre-existing 6xHIS tag (pMS001 and pMS003).
484 *eIF2B1* (encoding eIF2Bα) had previously been inserted into site 1 of pETDuet-1
485 (pJT075) [8]. In-Fusion HD cloning was used to edit this plasmid further and insert an Avi
486 tag at the N-terminus of *eIF2B1*, immediately following the pre-existing 6xHIS tag
487 (pMS026). The Avi tag allows selective, single, and complete biotinylation of the tagged
488 protein.

489

490 **Generation of stable NSs-expressing cells in an ISR reporter cell line**

491 Our previously generated dual ISR reporter K562 cells expressing a stably integrated
492 ATF4 reporter (pMS086), general translation reporter (pMS078), and dCas9-KRAB was
493 used as the parental line [5]. The various NSs overexpression constructs
494 (Supplementary Table 2) were integrated using a lentiviral vector. Vesicular stomatitis
495 virus (VSV)-G pseudotyped lentivirus was prepared using standard protocols and

496 293METR packaging cells. Viral supernatants were filtered (0.45 µm low protein binding
497 filter unit (EMD Millipore)) and concentrated 10-20-fold (Amicon Ultra-15 concentrator
498 with a 100,000-dalton molecular mass cutoff). Concentrated supernatant was then used
499 the same day or frozen for future use. For spinfection, approximately 1,000,000 K562
500 cells were mixed with concentrated lentivirus and fresh media (RPMI containing 4.5 g/l
501 glucose and 25 mM HEPES supplemented with 10% FBS, 2 mM L-alanyl-L-glutamine
502 (Gibco GlutaMAX), and penicillin/streptomycin), supplemented with polybrene to 8 µg/ml,
503 brought to 1.5 mL in a 6-well plate, and centrifuged for 1.5 h at 1000 g. Cells were then
504 allowed to recover and expand for ~1 week before sorting on a Sony SH800 cytometer
505 to isolate cells that had integrated the reporter. Roughly 100,000 BFP positive cells
506 (targeting the highest 1-3% of expressers) were then sorted into a final pooled
507 population and allowed to recover and expand. Cells expressing NSs truncations
508 (pMS119-pMS123) were not sorted and instead analyzed as a polyclonal population,
509 gating for BFP positive cells during data analysis.
510
511 **Western Blotting**
512 Western blotting was performed as previously described [5]. In brief, approximately
513 1,000,000 cells of the appropriate cell type were drugged as described in individual
514 assays and then pelleted, washed, pelleted again, and resuspended in lysis buffer. Cells
515 were then rotated for 30 min at 4 °C and then spun at 12,000 g for 20 min to pellet cell
516 debris. Protein concentration was measured using a bicinchoninic acid assay (BCA
517 assay) and within an experiment, total protein concentration was normalized to the least
518 concentrated sample. Equal protein content for each condition (targeting 10 µg) was run
519 on 10% Mini-PROTEAN TGX precast protein gels (Biorad). After electrophoresis,
520 samples were transferred onto a nitrocellulose membrane. Primary antibody / blocking
521 conditions for each protein of interest are outlined in Supplementary Table 3.
522 Membranes were developed with SuperSignal West Dura (Thermo Fisher Scientific).
523 Developed membranes were imaged on a LI-COR Odyssey gel imager for 0.5-10 min
524 depending on band intensity.
525
526 **ATF4 / general translation reporter assays**
527 ISR reporter cells (at ~500,000 / ml) were co-treated with varying combinations of drugs
528 (20 µM trimethoprim plus one of the following: thapsigargin, oligomycin, or glutamine
529 deprivation (and no FBS) + L-methionine sulfoximine) and incubated at 37 °C until the

530 appropriate timepoint had been reached. At this time, the plate was removed from the
531 incubator and samples were incubated on ice for 10 min. Then ATF4 (mNeonGreen) and
532 General Translation (mScarlet-i) reporter levels were monitored using a high throughput
533 sampler (HTS) attached to a BD FACSCelesta cytometer running BD FACSDiva v9.0.
534 Data was analyzed in FlowJo version 10.6.1, and median fluorescence values for both
535 reporters were exported and plotted in GraphPad Prism 8 (Supplementary Fig. 9). No
536 BFP positive sorting was performed on the lines expressing NSs truncations. For
537 analysis of these samples, BFP positive cells were gated in FlowJo and analysis
538 performed on this population. Where appropriate, curves were fit to log[inhibitor] versus
539 response function with variable slope.
540
541 **Purification of human eIF2B subcomplexes**
542 Human eIFBα$_2$ (pJT075), Avi-tagged eIFBα$_2$ (pMS026), protein C-tagged eIFBα$_2$
543 (pMS027), eIF2Bβγδε (pJT073 and pJT074 co-expression), Avi-tagged eIF2Bβγδε
544 (pMS001 and pJT074 co-expression), and ProteinC-tagged eIF2Bβγδε (pMS003 and
545 pJT074 co-expression) were purified as previously described with a minor modification
546 for purification of the Avi-tagged species [8]. One Shot BL21 Star (DE3) chemically
547 competent *E. coli* cells (Invitrogen) were transformed with the requisite expression
548 plasmids and grown in LB with kanamycin and chloramphenicol (eIF2B tetramer preps)
549 or ampicillin (eIF2Bα$_2$ preps). At an OD_{600} of ~0.8 1 mM IPTG (Gold Biotechnology) was
550 added and the culture was grown overnight at 16 °C. Using the EmulsiFlex-C3 (Avestin),
551 Cells were harvested and lysed through 3 cycles of high-pressure homogenization in
552 lysis buffer (20 mM HEPES-KOH, pH 7.5, 250 mM KCl, 1 mM dithiothreitol (DTT), 5 mM
553 $MgCl_2$, 15 mM imidazole, and cOmplete EDTA-free protease inhibitor cocktail (Roche)).
554 For eIF2Bα$_2$ preps 20 mM imidazole was used.The lysate was clarified at 30,000 g for
555 30 min at 4 °C. Lysate was then clarified at 30,000 g for 60 min at 4 °C.
556
557 All following purification steps were conducted on the ÄKTA Pure (GE Healthcare)
558 system at 4 °C. Clarified lysate was loaded onto a 5 ml HisTrap HP column (GE
559 Healthcare). For eIF2B tetramer preps the column was then washed in a buffer
560 containing 20 mM HEPES-KOH, pH 7.5, 200 mM KCl, 1 mM DTT, 5 mM $MgCl_2$, and 15
561 mM imidazole. For eIF2Bα$_2$ preps 30 mM KCl and 20 mM imidazole were used. The
562 sample was then eluted with a linear gradient up to 300 mM imidazole. eIF2B containing
563 fractions were collected and applied to a MonoQ HR 10/100 GL column (GE Healthcare)

564 equilibrated in 20 mM HEPES-KOH pH 7.5, 200 mM KCl, 1 mM DTT, and 5 mM $MgCl_2$.
565 For eIF2Bα_2 preps 30 mM KCl was used. The column was washed in the same buffer,
566 and the protein was eluted with a linear gradient up to 500 mM KCl. eIF2B containing
567 fractions were collected and concentrated with an Amicon Ultra-15 concentrator (EMD
568 Millipore) with a 30 kDa (tetramer preps) or 10 kDa (eIF2Bα_2 preps) molecular mass
569 cutoff and spun down for 10 min at 10,000 g to remove aggregates. The supernatant
570 was then injected onto a Superdex 200 10/300 GL (GE Healthcare) column equilibrated
571 in a buffer containing 20 mM HEPES-KOH pH 7.5, 200 mM KCl, 1 mM DTT, 5 mM
572 $MgCl_2$, and 5% glycerol, and concentrated using the appropriate Amicon Ultra-15
573 concentrators (EMD Millipore).
574
575 For Avi-tagged species, after running samples over a MonoQ HR 10/10 column the
576 eluted fractions were combined and concentrated to a target concentration of 40 μM.
577 The sample was then incubated at 4 °C overnight according to manufacturer's
578 instructions with 2.5 μg BirA for every 10 nmol substrate, 10mM ATP, 50 μM d-biotin,
579 and 100mM $Mg(OAc)^2$ in a 50 mM bicine buffer, pH 8.3 (Avidity BirA biotin-protein ligase
580 standard reaction kit). Incubation with BirA yields selective and efficient biotinylation of
581 Avi-tagged species. After the biotinylation reaction, purification of biotinylated species
582 proceeded as described above.
583
584 All eIF2B$(\alpha\beta\gamma\delta\varepsilon)_2$ used throughout was assembled by mixing purified eIF2B$\beta\gamma\delta\varepsilon$ and
585 eIF2Bα_2 (either tagged or untagged versions as needed) at the appropriate molar ratios.
586
587 **Purification of human eIF2αβγ heterotrimer and eIF2α-P**
588 Human eIF2 was purified as previously described [52]. This material was a generous gift
589 of Calico Life Sciences LLC. eIF2-P was prepared by mixing eIF2 in 50-fold excess with
590 PERK kinase and 1 mM ATP. The mixture was incubated at room temperature for 60
591 min before incubation on ice until use. The purification of human eIF2α-P was performed
592 as previously described [5]. One Shot BL21 Star (DE3) chemically competent *E. coli*
593 cells (Invitrogen) were transformed with the expression plasmid for N-terminally 6x-His-
594 tagged human eIF2α, (pAA007) along with a tetracycline-inducible, chloramphenicol-
595 resistant plasmid (pG-Tf2) containing the chaperones groES, groEL, and Tig (Takara
596 Bio). Transformed cells were grown in LB with kanamycin and chloramphenicol for
597 selection. Chaperone expression was induced at an OD600 of ~0.2, by addition of

598 tetracycline (1 ng/ml). At an OD_{600} of ~0.8 the culture was cooled to room temperature
599 and eIF2α expression was induced with 1 mM IPTG (Gold Biotechnology) and the
600 culture was grown for at least 16 h more at 16 °C. Using the EmulsiFlex-C3 (Avestin),
601 Cells were harvested and lysed through 3 cycles of high-pressure homogenization in
602 lysis buffer (100 mM HEPES-KOH, pH 7.5, 300 mM KCl, 2 mM dithiothreitol (DTT), 5
603 mM $MgCl_2$, 5 mM imidazole, 10% glycerol, 0.1% IGEPAL CA-630, and cOmplete EDTA-
604 free protease inhibitor cocktail (Roche)). The lysate was clarified at 30,000 g for 30 min
605 at 4 °C.
606 Subsequent purification steps were conducted on the ÄKTA Pure (GE Healthcare)
607 system at 4 °C. Clarified lysate was loaded onto a 5 ml HisTrap FF Crude column (GE
608 Healthcare), washed in a buffer containing 20 mM HEPES-KOH, pH 7.5, 100 mM KCl,
609 5% glycerol, 1 mM DTT, 5 mM $MgCl_2$, 0.1% IGEPAL CA-630, and 20 mM imidazole, and
610 eluted with 75 ml linear gradient of 20 to 500 mM imidazole. The eIF2α-containing
611 fractions were collected and applied to a MonoQ HR 10/100 GL column (GE Healthcare)
612 equilibrated in anion exchange buffer (20 mM HEPES-KOH pH 7.5, 100 mM KCl, 1 mM
613 DTT, 5% glycerol, and 5 mM $MgCl_2$). The column was washed in the same buffer, and
614 the protein was eluted with a linear gradient of 100 mM to 1 M KCl. eIF2α containing
615 fractions were collected and concentrated with an Amicon Ultra-15 concentrator (EMD
616 Millipore) with a 30 kDa molecular mass cutoff and spun down for 10 min at 10,000 g to
617 remove aggregates. Before size exclusion, the pooled anion exchange fractions were
618 phosphorylated *in vitro* overnight at 4 °C with 1 mM ATP and 1 µg of $PKR_{(252-551)}$-GST
619 enzyme (Thermo Scientific) per mg of eIF2α. The supernatant was then injected onto a
620 Superdex 75 10/300 GL (GE Healthcare) column equilibrated in a buffer containing 20
621 mM HEPES-KOH pH 7.5, 100 mM KCl, 1 mM DTT, 5 mM $MgCl_2$, and 5% glycerol, and
622 concentrated using Amicon Ultra-15 concentrators (EMD Millipore) with a 10 kDa
623 molecular mass cutoff. Complete phosphorylation was confirmed by running the samples
624 on a 12.5% Super-Sep PhosTag gel (Wako Chemicals).
625
626 **Purification of NSs::6xHIS**
627 We used the pMS113 construct to express and purify NSs::6xHIS. Expi293T cells
628 (ThermoFisher) were transfected with the NSs construct per the manufacturer's
629 instructions for the MaxTiter protocol and harvested 5 days after transfection. Cells were
630 pelleted (1000 g, 4 min) and resuspended in Lysis Buffer (130 mM KCl, 2.5 mM $MgCl_2$,
631 25 mM HEPES-KOH pH 7.4, 2 mM EGTA ,1% triton, 1mM TCEP, 1x cOmplete protease

632 inhibitor cocktail (Roche)). Cells were then incubated for 30 min at 4 °C and then spun at
633 30,000 g for 1 h to pellet cell debris. Lysate was applied to a 5 ml HisTrap HP column
634 (GE Healthcare) equilibrated in Buffer A (20 mM HEPES-KOH, pH 7.5, 200 mM KCl, 5
635 mM $MgCl_2$, 15mM imidazole) and then eluted using a gradient of Buffer B (20 mM
636 HEPES-KOH, pH 7.5, 200 mM KCl, 5 mM $MgCl_2$, 300mM imidazole). NSs::6xHIS was
637 concentrated using a 10 kDa MWCO spin concentrator (Amicon) and further purified by
638 size exclusion chromatography over a Superdex 200 Increase 10/300 GL column (GE
639 Healthcare) in Elution Buffer (20 mM HEPES, pH 7.5, 200 mM KCl, 5mM $MgCl_2$, 1mM
640 TCEP, and 5% Glycerol). The resulting fractions were pooled and flash frozen in liquid
641 nitrogen.
642
643 ***In vitro* NSs/eIF2α-P immunoprecipitation**
644 Varying combinations of purified eIF2α-P, NSs::6xHIS, eIF2B$(\alpha\beta\delta\gamma\varepsilon)_2$, eIF2Bβδγε, and
645 eIF2Bα_2 were incubated (with gentle rocking) with Anti-protein C antibody conjugated
646 resin (generous gift from Aashish Manglik) in Assay Buffer (20 mM HEPES-KOH, pH
647 7.5, 150 mM KCl, 5 mM $MgCl_2$, 1mM TCEP, 1 mg/ml bovine serum albumin (BSA), 5mM
648 $CaCl_2$). After 1.5 h the resin was pelleted by benchtop centrifugation and the supernatant
649 was removed. Resin was washed 3x with 1 mL of ice cold Assay Buffer before resin was
650 resuspended in Elution Buffer (Assay Buffer with 5 mM EDTA and 0.5 mg/mL protein C
651 peptide added) and incubated with gentle rocking for 1 h. The resin was then pelleted
652 and the supernatant was removed. Samples were analyzed by Western Blotting as
653 described above.
654
655 **GDP exchange assay**
656 *in vitro* detection of BODIPY-FL-GDP binding to eIF2 was performed as previously
657 described [5, 8]. The only modification was addition of NSs in certain conditions as
658 indicated. In brief, purified eIF2 (100 nM) was incubated with 100 nM BODIPY-FL-GDP
659 (Thermo Fisher Scientific) in assay buffer (20 mM HEPES-KOH, pH 7.5, 100 mM KCl, 5
660 mM $MgCl_2$, 1 mM TCEP, and 1 mg / ml BSA) to a volume of 18 µl in 384 square-well
661 black-walled, clear-bottom polystyrene assay plates (Corning). The GEF mix was
662 prepared by incubating a 10x solution of eIF2B$(\alpha\beta\gamma\delta\varepsilon)_2$ with or without 10x solutions of
663 eIF2α-P and / or NSs. To compare nucleotide exchange rates, the 10x GEF mixes were
664 spiked into the 384-well plate wells with a multi-channel pipette, such that the resulting
665 final concentration of eIF2B$(\alpha\beta\gamma\delta\varepsilon)_2$ was 10 nM and the final concentration of other

666 proteins and drugs are as indicated in the figures. Fluorescence intensity was recorded
667 every 10 s for 30-60 min using a Clariostar PLUS (BMG LabTech) plate reader
668 (excitation wavelength: 497 nm, bandwidth 14 nm, emission wavelength: 525 nm,
669 bandwidth: 30 nm). Data were fit to a first-order exponential and plotted in GraphPad
670 Prism 8.
671
672 **FAM-ISRIB binding assay**
673 All fluorescence polarization measurements were performed as previously described [5].
674 In brief, 20 µl reactions were set up with 100 nM eIF2B$(\alpha\beta\gamma\delta\varepsilon)_2$ + 2.5 nM FAM-ISRIB
675 (Praxis Bioresearch) in FP buffer (20 mM HEPES-KOH pH 7.5, 100 mM KCl, 5 mM
676 $MgCl_2$, 1 mM TCEP) and measured in 384-well non-stick black plates (Corning 3820)
677 using the ClarioStar PLUS (BMG LabTech) at room temperature. Prior to reaction setup,
678 eIF2B$(\alpha\beta\gamma\delta\varepsilon)_2$ was assembled in FP buffer using eIF2B$\beta\gamma\delta\varepsilon$ and eIF2Bα_2 in 2:1 molar
679 ratio for 1 h at room temperature. FAM-ISRIB was first diluted to 2.5 µM in 100% NMP
680 prior to dilution to 50 nM in 2% NMP and then added to the reaction. For titrations with
681 NSs, dilutions were again made in FP buffer, and the reactions with eIF2B, FAM-ISRIB,
682 and these dilutions +/- eIF2α-P were incubated at 22 °C for 30 min prior to measurement
683 of parallel and perpendicular intensities (excitation: 482 nm, emission: 530 nm). Data
684 were plotted in GraphPad Prism 8, and where appropriate, curves were fit to
685 log[inhibitor] vs response function with variable slope.
686
687 **Affinity determination and competition analysis by surface plasmon resonance**
688 NSs affinity determination experiments were performed on a Biacore T200 instrument
689 (Cytiva Life Sciences) by capturing the biotinylated eIF2B$(\alpha\beta\gamma\delta\varepsilon)_2$, eIF2B$\beta\gamma\delta\varepsilon$, and
690 eIF2Bα_2 at ~100nM on a Biotin CAPture Series S sensor chip (Cytiva Life Sciences) to
691 achieve maximum response (Rmax) of <100 response units (RUs) upon NSs binding. A
692 molar equivalent of each eIF2B species was immobilized. 2-fold serial dilutions of
693 purified NSs were flowed over the captured eIF2B complexes at 30 µL / min for 90
694 seconds followed by 600 seconds of dissociation flow. Following each cycle, the chip
695 surface was regenerated with 3 M guanidine hydrochloride. A running buffer of 20 mM
696 HEPES-KOH, pH 7.5, 100 mM KCl, 5 mM $MgCl_2$, and 1 mM TCEP was used throughout.
697 The resulting sensorgrams were fit to a 1:1 Langmuir binding model using the
698 association then dissociation model in GraphPad Prism 8.0.

699 For NSs and eIF2/eIF2-P competition experiments, eIF2B(αβγδε)$_2$ was immobilized as
700 described above. A solution containing 500 nM NSs, 125 nM eIF2, or 125 nM eIF2-P
701 was flowed over the captured eIF2B for 60 s at 30 µL / min to achieve saturation.
702 Following this binding reaction, a second injection of 500 nM NSs and either 125 nM
703 eIF2 or 125 nM eIF2-P was performed.
704
705 **Sample preparation for cryo-electron microscopy**
706 Decameric eIF2B(αβγδε)$_2$ was prepared by incubating 20 µM eIF2Bβγδε with 11 µM
707 eIF2Bα$_2$ in a final solution containing 20 mM HEPES-KOH, pH 7.5, 200 mM KCl, 5 mM
708 $MgCl_2$, and 1 mM TCEP. This 10 µM eIF2B(αβγδε)$_2$ sample was further diluted to 750
709 nM and incubated with 2.25 µM NSs::6xHIS on ice for 1 h before plunge freezing. A 3 µl
710 aliquot of the sample was applied onto the Quantifoil R 1.2/1/3 400 mesh Gold grid and
711 we waited for 30 s. A 0.5 µl aliquot of 0.1-0.2% Nonidet P-40 substitute was added
712 immediately before blotting. The entire blotting procedure was performed using Vitrobot
713 (FEI) at 10 ºC and 100% humidity.
714
715 **Electron microscopy data collection**
716 Cryo-EM data for the eIF2B-NSs complex was collected on a Titan Krios transmission
717 electron microscope operating at 300 keV, and micrographs were acquired using a
718 Gatan K3 direct electron detector. Serial EM was used to collect the EM data [53]. The
719 total dose was 67 e^-/ Å^2, and 117 frames were recorded during a 5.9 s exposure. Data
720 was collected at 105,000 x nominal magnification (0.835 Å/pixel at the specimen level),
721 and nominal defocus range of -0.6 to -2.0 µm.
722
723 **Image processing**
724 The micrograph frames were aligned using MotionCorr2 [54]. The contrast transfer
725 function (CTF) parameters were estimated with GCTF [55]. Particles were picked in
726 Cryosparc v2.15 using the apo eIF2B (EMDB: 23209) as a template. Particles were
727 extracted using a 80-pixel box size [56], and classified in 2D [57]. Classes that showed
728 clear protein features were selected and extracted for ab initio reconstruction followed by
729 homogenous and heterogeneous refinement. Particles belonging to the best class were
730 then re-extracted with a pixel size of 2.09 Å, and then subjected to nonuniform
731 refinement, yielding a reconstruction of 4.25 Å. These particles were subjected to
732 another round of heterogeneous refinement followed by nonuniform refinement to

generate a consensus reconstruction consisting of the best particles. These particles were re-extracted at a pixel size of 0.835 Å. Then, CTF refinement was performed to correct for the per-particle CTF as well as beam tilt. A final round of 2D classification followed by nonuniform refinement was performed to yield the final structure of 2.6 Å.

Atomic model building, refinement, and visualization

To build models for the eIF2B-NSs complex, the previously determined structures of the human eIF2B in its apo form (PDB ID: 7L70) was used as the starting model for the eIF2B part [5]. To build the NSs model, we first ran the structure prediction program RaptorX using the full-length NSs sequence [58]. The predicted structure is divided into two parts: the C-terminal domain predicted based on the structure of the RVFV NSs (PDB ID: 5OOO), and the N-terminal domain is predicted without a known PDB structure as a template [31]. The predicted full-length structure was docked into the EM density corresponding to the NSs in UCSF Chimera [59], and then subjected to rigid body refinement in Phenix [60]. The models were then manually adjusted in Coot [61] and then refined in phenix.real_space_refine [60] using global minimization, secondary structure restraints, Ramachandran restraints, and local grid search. Then iterative cycles of manual rebuilding in Coot and phenix.real_space_refine were performed. The final model statistics were tabulated using Molprobity [62]. Distances were calculated from the atomic models using UCSF Chimera. Molecular graphics and analyses were performed with the UCSF Chimera package [59]. UCSF Chimera is developed by the Resource for Biocomputing, Visualization, and Informatics and supported by NIGMS P41-GM103311. The atomic model is deposited in the PDB under accession code 7RLO. The EM map is deposited into EMDB under accession code EMD-24535.

759 **Acknowledgments**
760 We thank the Walter lab for helpful discussions throughout the course of this project;
761 Cobar Wollemi for inspiring Supplementary Fig. 10; Calico Life Sciences LLC for a
762 generous gift of purified eIF2 heterotrimer; Z Yu and D Bulkley of the UCSF Center for
763 Advanced Cryo-EM facility, which is supported by NIH grants S10OD021741 and
764 S10OD020054; and the Howard Hughes Medical Institute (HHMI). We also thank the
765 QB3 shared cluster for computational support.
766
767 **Funding**
768 This work was supported by generous support from Calico Life Sciences LLC (to PW); a
769 generous gift from The George and Judy Marcus Family Foundation (To PW); the
770 Belgian-American Educational Foundation (BAEF) Postdoctoral Fellowship (to MB), the
771 Damon Runyon Cancer Research Foundation Postdoctoral fellowship (to LW); and the
772 Jane Coffin Child Foundation Postdoctoral Fellowship (to RL). AF is a HHMI faculty
773 scholar and a Chan Zuckerberg Biohub investigator. PW is an Investigator of the
774 Howard Hughes Medical Institute.
775
776 **Author Contributions**
777 P.W. supervised the research. M.S., L.W., J.Z.C., and R.L. designed the experiments.
778 M.S. performed all cloning. M.S., J.Z.C., R.L., and M.B. expressed and purified proteins.
779 M.S. and J.Z.C. generated the cell lines. M.S. and J.Z.C. performed the flow cytometry
780 experiments. M.S. performed the binding assays (SPR and bead immobilization). M.S.,
781 J.Z.C., and R.L. performed the nucleotide exchange assays. M.S., J.Z.C., and M.B.
782 performed the FAM-ISRIB binding assays. M.S. performed all western blotting. L.W.
783 performed cryo-EM sample preparation, data collection, processing, and model building
784 with A.F. providing additional model building input. M.S., L.W., and P.W., prepared the
785 rough manuscript draft, with finalizing input from all authors including J.Z.C., R.L., M.B.,
786 J.D.W., and A.F.
787
788 **Competing Interests**
789 PW is an inventor on U.S. Patent 9708247 held by the Regents of the University of
790 California that describes ISRIB and its analogs. Rights to the invention have been
791 licensed by UCSF to Calico. The remaining authors declare no competing interests.
792

793 **Data Availability**

794 The cryo-EM structure generated in this study has been deposited in the protein data
795 bank under the accsssion code 7RLO (https://www.rcsb.org/structure/7RLO). The
796 corresponding EM map has been deposited in the EM database under the accession
797 code EMD-24535 (https://www.ebi.ac.uk/emdb/entry/24535). The structure of the RVFV
798 NSs used for model building is available in the protein data bank under the accession
799 code 5OOO (https://www.rcsb.org/structure/5OOO).

800 **References**

801 1. Hinnebusch, A.G., *Translational regulation of GCN4 and the general amino acid*
802 *control of yeast.* Annu Rev Microbiol, 2005. **59**: p. 407-50.
803 2. Guo, X., et al., *Mitochondrial stress is relayed to the cytosol by an OMA1-DELE1-*
804 *HRI pathway.* Nature, 2020. **579**(7799): p. 427-432.
805 3. Dey, M., et al., *Mechanistic link between PKR dimerization,*
806 *autophosphorylation, and eIF2alpha substrate recognition.* Cell, 2005. **122**(6):
807 p. 901-13.
808 4. Shi, Y., et al., *Identification and characterization of pancreatic eukaryotic*
809 *initiation factor 2 alpha-subunit kinase, PEK, involved in translational control.*
810 Mol Cell Biol, 1998. **18**(12): p. 7499-509.
811 5. Schoof, M., et al., *eIF2B conformation and assembly state regulate the*
812 *integrated stress response.* Elife, 2021. **10**.
813 6. Zyryanova, A.F., et al., *ISRIB Blunts the Integrated Stress Response by*
814 *Allosterically Antagonising the Inhibitory Effect of Phosphorylated eIF2 on*
815 *eIF2B.* Mol Cell, 2021. **81**(1): p. 88-103.e6.
816 7. Kashiwagi, K., et al., *Crystal structure of eukaryotic translation initiation factor*
817 *2B.* Nature, 2016. **531**(7592): p. 122-5.
818 8. Tsai, J.C., et al., *Structure of the nucleotide exchange factor eIF2B reveals*
819 *mechanism of memory-enhancing molecule.* Science, 2018. **359**(6383).
820 9. Wortham, N.C., et al., *Analysis of the subunit organization of the eIF2B complex*
821 *reveals new insights into its structure and regulation.* Faseb j, 2014. **28**(5): p.
822 2225-37.
823 10. Zyryanova, A.F., et al., *Binding of ISRIB reveals a regulatory site in the*
824 *nucleotide exchange factor eIF2B.* Science, 2018. **359**(6383): p. 1533-1536.
825 11. Craddock, B.L. and C.G. Proud, *The alpha-subunit of the mammalian guanine*
826 *nucleotide-exchange factor eIF-2B is essential for catalytic activity in vitro.*
827 Biochem Biophys Res Commun, 1996. **220**(3): p. 843-7.
828 12. Kenner, L.R., et al., *eIF2B-catalyzed nucleotide exchange and*
829 *phosphoregulation by the integrated stress response.* Science, 2019.
830 **364**(6439): p. 491-495.
831 13. Gordiyenko, Y., J.L. Llácer, and V. Ramakrishnan, *Structural basis for the*
832 *inhibition of translation through eIF2α phosphorylation.* Nat Commun, 2019.
833 **10**(1): p. 2640.
834 14. Kashiwagi, K., et al., *Structural basis for eIF2B inhibition in integrated stress*
835 *response.* Science, 2019. **364**(6439): p. 495-499.
836 15. Adomavicius, T., et al., *The structural basis of translational control by eIF2*
837 *phosphorylation.* Nat Commun, 2019. **10**(1): p. 2136.
838 16. Galabru, J. and A. Hovanessian, *Autophosphorylation of the protein kinase*
839 *dependent on double-stranded RNA.* J Biol Chem, 1987. **262**(32): p. 15538-44.
840 17. Rosário-Ferreira, N., et al., *The Central Role of Non-Structural Protein 1 (NS1)*
841 *in Influenza Biology and Infection.* Int J Mol Sci, 2020. **21**(4).
842 18. Stasakova, J., et al., *Influenza A mutant viruses with altered NS1 protein*
843 *function provoke caspase-1 activation in primary human macrophages,*

844 *resulting in fast apoptosis and release of high levels of interleukins 1beta and*
845 *18.* J Gen Virol, 2005. **86**(Pt 1): p. 185-195.
846 19. Habjan, M., et al., *NSs protein of rift valley fever virus induces the specific*
847 *degradation of the double-stranded RNA-dependent protein kinase.* J Virol,
848 2009. **83**(9): p. 4365-75.
849 20. Gale, M.J., Jr., M.J. Korth, and M.G. Katze, *Repression of the PKR protein kinase*
850 *by the hepatitis C virus NS5A protein: a potential mechanism of interferon*
851 *resistance.* Clin Diagn Virol, 1998. **10**(2-3): p. 157-62.
852 21. Kawagishi-Kobayashi, M., et al., *Regulation of the protein kinase PKR by the*
853 *vaccinia virus pseudosubstrate inhibitor K3L is dependent on residues*
854 *conserved between the K3L protein and the PKR substrate eIF2alpha.* Mol Cell
855 Biol, 1997. **17**(7): p. 4146-58.
856 22. Li, Y., et al., *ICP34.5 protein of herpes simplex virus facilitates the initiation of*
857 *protein translation by bridging eukaryotic initiation factor 2alpha (eIF2alpha)*
858 *and protein phosphatase 1.* J Biol Chem, 2011. **286**(28): p. 24785-92.
859 23. Rabouw, H.H., et al., *Inhibition of the integrated stress response by viral*
860 *proteins that block p-eIF2-eIF2B association.* Nat Microbiol, 2020. **5**(11): p.
861 1361-1373.
862 24. Hedil, M. and R. Kormelink, *Viral RNA Silencing Suppression: The Enigma of*
863 *Bunyavirus NSs Proteins.* Viruses, 2016. **8**(7).
864 25. Ly, H.J. and T. Ikegami, *Rift Valley fever virus NSs protein functions and the*
865 *similarity to other bunyavirus NSs proteins.* Virol J, 2016. **13**: p. 118.
866 26. Wuerth, J.D. and F. Weber, *Phleboviruses and the Type I Interferon Response.*
867 Viruses, 2016. **8**(6).
868 27. Wuerth, J.D., et al., *NSs Protein of Sandfly Fever Sicilian Phlebovirus*
869 *Counteracts Interferon (IFN) Induction by Masking the DNA-Binding Domain of*
870 *IFN Regulatory Factor 3.* J Virol, 2018. **92**(23).
871 28. Billecocq, A., et al., *NSs protein of Rift Valley fever virus blocks interferon*
872 *production by inhibiting host gene transcription.* J Virol, 2004. **78**(18): p.
873 9798-806.
874 29. Wuerth, J.D., et al., *eIF2B as a Target for Viral Evasion of PKR-Mediated*
875 *Translation Inhibition.* mBio, 2020. **11**(4).
876 30. Sidrauski, C., et al., *Pharmacological brake-release of mRNA translation*
877 *enhances cognitive memory.* Elife, 2013. **2**: p. e00498.
878 31. Barski, M., et al., *Rift Valley fever phlebovirus NSs protein core domain*
879 *structure suggests molecular basis for nuclear filaments.* Elife, 2017. **6**.
880 32. Kashiwagi, K., et al., *eIF2B-capturing viral protein NSs suppresses the*
881 *integrated stress response.* bioRxiv, 2021: p. 2021.06.07.447466.
882 33. Bogorad, A.M., K.Y. Lin, and A. Marintchev, *eIF2B Mechanisms of Action and*
883 *Regulation: A Thermodynamic View.* Biochemistry, 2018. **57**(9): p. 1426-
884 1435.
885 34. Soday, L., et al., *Quantitative Temporal Proteomic Analysis of Vaccinia Virus*
886 *Infection Reveals Regulation of Histone Deacetylases by an Interferon*
887 *Antagonist.* Cell Reports, 2019. **27**(6): p. 1920-1933.e7.
888 35. Weekes, Michael P., et al., *Quantitative Temporal Viromics: An Approach to*
889 *Investigate Host-Pathogen Interaction.* Cell, 2014. **157**(6): p. 1460-1472.

890 36. Kobilka, B.K., *Structural insights into adrenergic receptor function and*
891 *pharmacology.* Trends Pharmacol Sci, 2011. **32**(4): p. 213-8.
892 37. Rasmussen, S.G., et al., *Structure of a nanobody-stabilized active state of the*
893 *β(2) adrenoceptor.* Nature, 2011. **469**(7329): p. 175-80.
894 38. Rasmussen, S.G., et al., *Crystal structure of the β2 adrenergic receptor-Gs*
895 *protein complex.* Nature, 2011. **477**(7366): p. 549-55.
896 39. Staus, D.P., et al., *Allosteric nanobodies reveal the dynamic range and diverse*
897 *mechanisms of G-protein-coupled receptor activation.* Nature, 2016.
898 **535**(7612): p. 448-52.
899 40. Chou, A., et al., *Inhibition of the integrated stress response reverses cognitive*
900 *deficits after traumatic brain injury.* Proc Natl Acad Sci U S A, 2017. **114**(31):
901 p. E6420-e6426.
902 41. Cyr, N., et al., *A ΩXaV motif in the Rift Valley fever virus NSs protein is essential*
903 *for degrading p62, forming nuclear filaments and virulence.* Proc Natl Acad Sci
904 U S A, 2015. **112**(19): p. 6021-6.
905 42. Sall, A.A., et al., *Variability of the NS(S) protein among Rift Valley fever virus*
906 *isolates.* J Gen Virol, 1997. **78 (Pt 11)**: p. 2853-8.
907 43. Zhu, P.J., et al., *Activation of the ISR mediates the behavioral and*
908 *neurophysiological abnormalities in Down syndrome.* Science, 2019.
909 **366**(6467): p. 843-849.
910 44. Ma, T., et al., *Suppression of eIF2α kinases alleviates Alzheimer's disease-*
911 *related plasticity and memory deficits.* Nat Neurosci, 2013. **16**(9): p. 1299-
912 305.
913 45. Atkin, J.D., et al., *Endoplasmic reticulum stress and induction of the unfolded*
914 *protein response in human sporadic amyotrophic lateral sclerosis.* Neurobiol
915 Dis, 2008. **30**(3): p. 400-7.
916 46. Nguyen, H.G., et al., *Development of a stress response therapy targeting*
917 *aggressive prostate cancer.* Sci Transl Med, 2018. **10**(439).
918 47. Costa-Mattioli, M. and P. Walter, *The integrated stress response: From*
919 *mechanism to disease.* Science, 2020. **368**(6489).
920 48. Harrington, K., et al., *Optimizing oncolytic virotherapy in cancer treatment.* Nat
921 Rev Drug Discov, 2019. **18**(9): p. 689-706.
922 49. Russell, S.J., *RNA viruses as virotherapy agents.* Cancer Gene Ther, 2002.
923 **9**(12): p. 961-6.
924 50. Pelner, L., G.A. Fowler, and H.C. Nauts, *EFFECT OF CONCURRENT INFECTIONS*
925 *AND THEIR TOXINS ON THE COURSE OF LEUKEMIA.* Acta Medica
926 Scandinavica, 1958. **162**(S338): p. 5-24.
927 51. Kelly, E. and S.J. Russell, *History of oncolytic viruses: genesis to genetic*
928 *engineering.* Mol Ther, 2007. **15**(4): p. 651-9.
929 52. Wong, Y.L., et al., *The small molecule ISRIB rescues the stability and activity of*
930 *Vanishing White Matter Disease eIF2B mutant complexes.* Elife, 2018. **7**.
931 53. Mastronarde, D.N., *SerialEM: A Program for Automated Tilt Series Acquisition*
932 *on Tecnai Microscopes Using Prediction of Specimen Position.* Microscopy and
933 Microanalysis, 2003. **9**(S02): p. 1182-1183.
934 54. Zheng, S.Q., et al., *MotionCor2: anisotropic correction of beam-induced motion*
935 *for improved cryo-electron microscopy.* Nat Methods, 2017. **14**(4): p. 331-332.

936 55. Zhang, K., *Gctf: Real-time CTF determination and correction.* J Struct Biol,
937 2016. **193**(1): p. 1-12.
938 56. Scheres, S.H., *RELION: implementation of a Bayesian approach to cryo-EM*
939 *structure determination.* J Struct Biol, 2012. **180**(3): p. 519-30.
940 57. Punjani, A., et al., *cryoSPARC: algorithms for rapid unsupervised cryo-EM*
941 *structure determination.* Nat Methods, 2017. **14**(3): p. 290-296.
942 58. Xu, J., M. McPartlon, and J. Li, *Improved protein structure prediction by deep*
943 *learning irrespective of co-evolution information.* Nature Machine Intelligence,
944 2021.
945 59. Pettersen, E.F., et al., *UCSF Chimera--a visualization system for exploratory*
946 *research and analysis.* J Comput Chem, 2004. **25**(13): p. 1605-12.
947 60. Adams, P.D., et al., *PHENIX: a comprehensive Python-based system for*
948 *macromolecular structure solution.* Acta Crystallogr D Biol Crystallogr, 2010.
949 **66**(Pt 2): p. 213-21.
950 61. Emsley, P. and K. Cowtan, *Coot: model-building tools for molecular graphics.*
951 Acta Crystallogr D Biol Crystallogr, 2004. **60**(Pt 12 Pt 1): p. 2126-32.
952 62. Chen, V.B., et al., *MolProbity: all-atom structure validation for macromolecular*
953 *crystallography.* Acta Crystallogr D Biol Crystallogr, 2010. **66**(Pt 1): p. 12-21.
954

Supplementary Information

Viral Evasion of the Integrated Stress Response Through Antagonism of eIF2-P binding to eIF2B

Michael Schoof[1,2,#], Lan Wang[1,2,#], J Zachery Cogan[1,2], Rosalie Lawrence[1,2], Morgane Boone[1,2], Jennifer Deborah Wuerth[3], Adam Frost[2,4], Peter Walter[1,2,*]

Affiliations

[1]Howard Hughes Medical Institute, University of California at San Francisco, San Francisco, CA, USA.

[2]Department of Biochemistry and Biophysics, University of California at San Francisco, San Francisco, CA, USA.

[3]Institute of Innate Immunity, Medical Faculty, University of Bonn, Bonn, Germany

[4]Chan Zuckerberg Biohub, San Francisco, CA, USA.

[#] These authors contributed equally

* To whom correspondence should be addressed; Email: Peter@walterlab.ucsf.edu

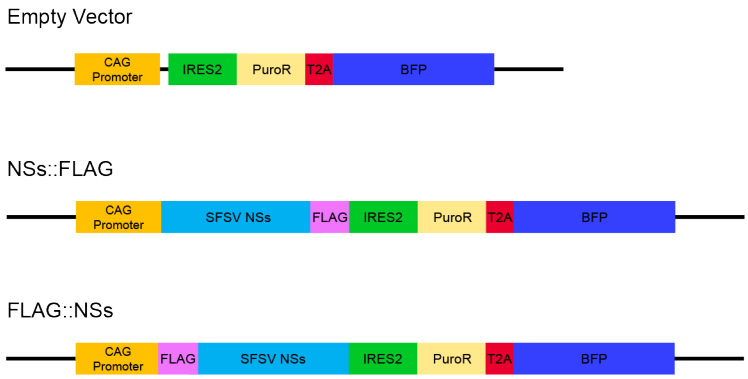

Supplementary Fig. 1: Design of NSs expression constructs

A schematic of the NSs expression constructs stably integrated (lentivirus) into the genome.

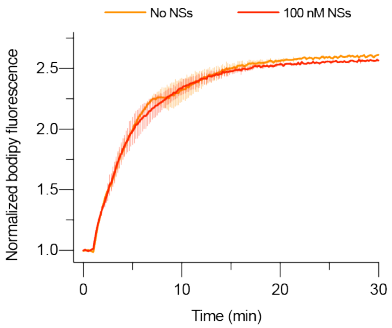

Supplementary Fig. 2: Effect of NSs alone on eIF2B nucleotide exchange

GEF activity of eIF2B as assessed by BODIPY-FL-GDP exchange. BODIPY-FL-GDP fluorescence increases when bound to protein. $t_{1/2}$ = 3.6 min, s.e.m. = 0.5 min (No NSs) and 3.4 min, s.e.m. = 0.5 min (100 nM NSs). eIF2B$(\alpha\beta\delta\gamma\varepsilon)_2$ at 10 nM throughout. Biological replicates: n = 2. Source data are provided as a Source Data file.

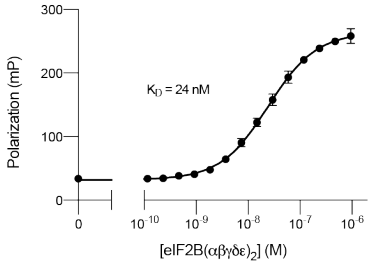

Supplementary Fig. 3: Binding affinity of ISRIB for decameric eIF2B

Plot of fluorescence polarization signal after incubation of FAM-ISRIB (2.5 nM) with a titration of eIF2B(αβδγε)$_2$. Biological replicates: n = 3. All error bars represent s.e.m. Source data are provided as a Source Data file.

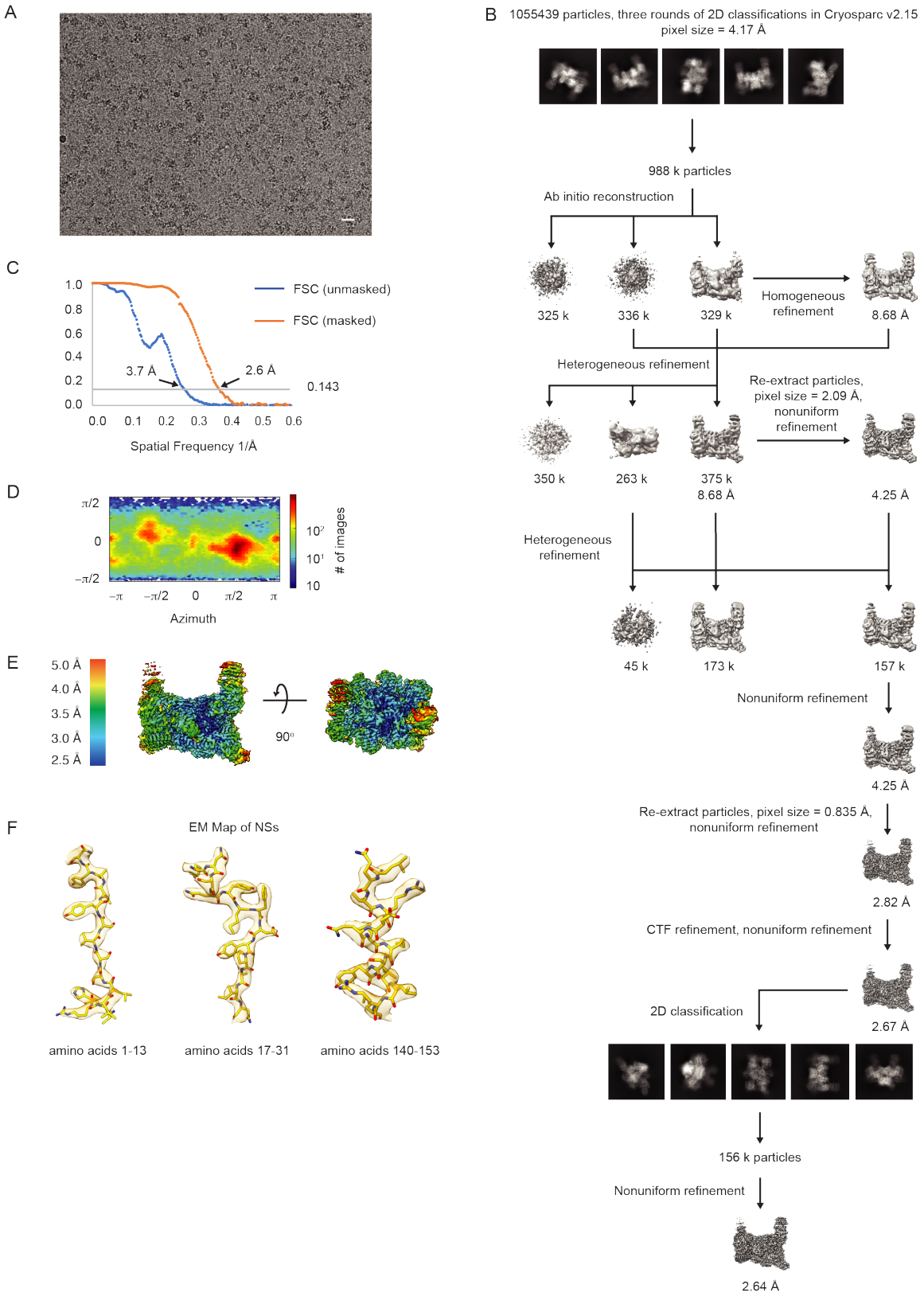

Supplementary Fig. 4: Cryo-EM data analysis flow

(**a**) Representative micrograph of a total of 2143 micrographs collected for the eIF2B-NSs sample. The scale bar shown in white at the bottom-right is 200 Å. (**b**) Data processing scheme for reconstruction of eIF2B-NSs assembly. (**c**) Fourier shell correlation (FSC) plots of the 3D reconstructions of the eIF2B-NSs complex masked (orange), unmasked (blue) (**d**) Orientation angle distribution of the eIF2B-NSs complex reconstruction. (**e**) Local resolution map of the eIF2B-NSs complex showing that the N-terminal region of NSs that contacts eIF2B is well-resolved, and the C-terminal region of NSs that faces the solution is more dynamic. (**f**) Electron microscopy maps of different regions of the NSs structure in the eIF2B-NSs complex showing the quality of the data and the fit of the model.

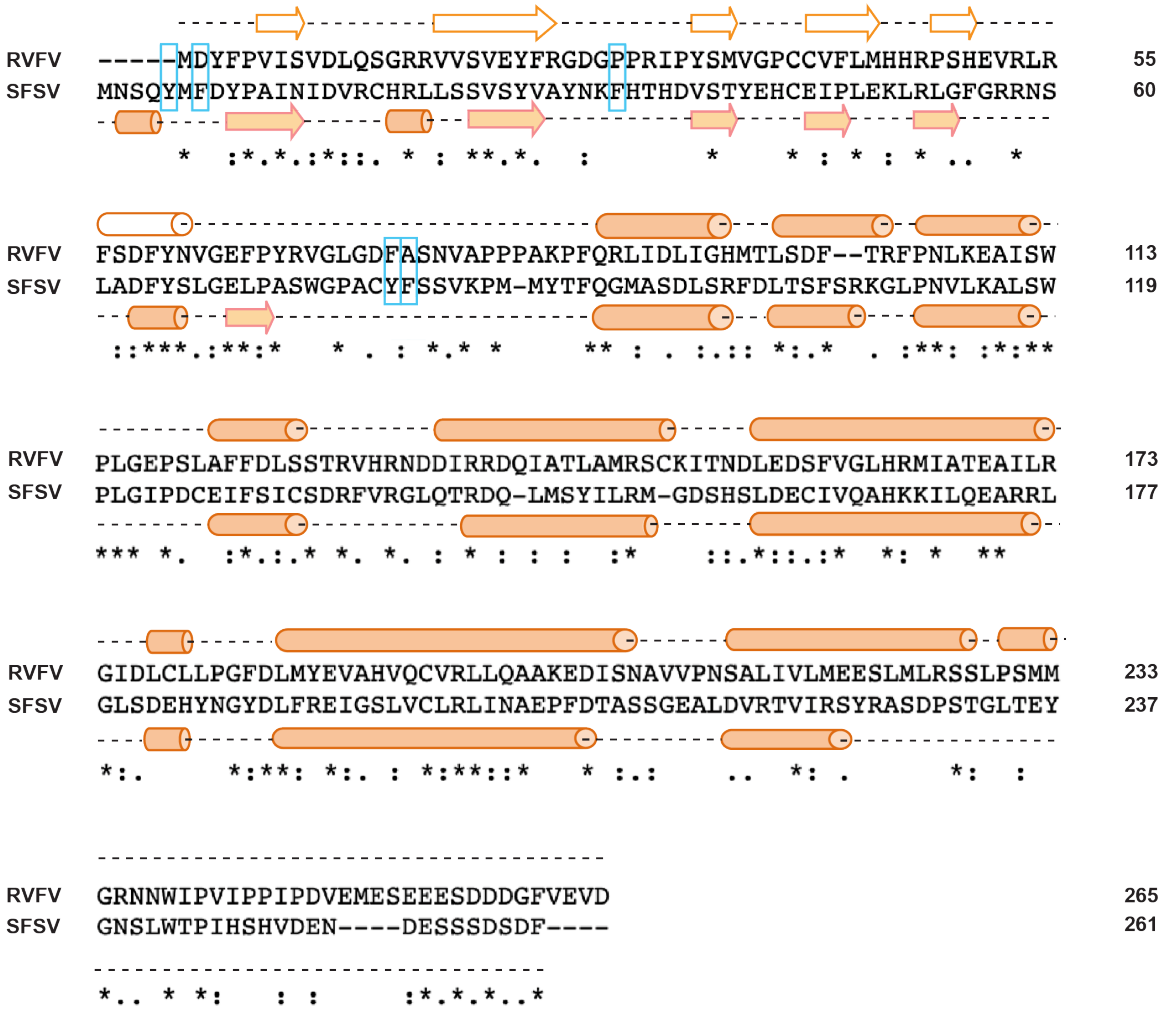

Supplementary Fig. 5: Primary sequence alignment of the SFSV NSs and the RVFV NSs

Alignment shows that the primary sequence between the two NSs shares 43.2% similarity and most of the aromatic finger amino acids (in cyan boxes) in the SFSV NSs are not conserved in the RVFV NSs. Secondary structures are shown in arrows (beta strands) and cylinders (helices). The secondary structure of the SFSV NSs is assigned based on the experimental structure. The secondary structure of the C-terminal domain of the RVFV NSs is assigned based on PDB ID: 5OOO, and the N-terminal domain based on predictions (shown as hollow arrows or cylinders [1].

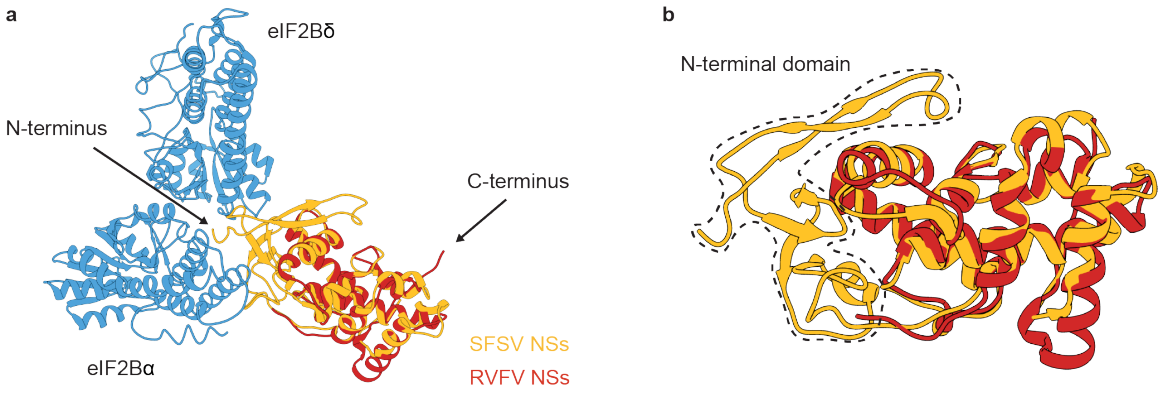

Supplementary Fig. 6: Structural comparision between the SFSV NSs and the RVFV NSs

(a) Overlay of the RVFV NSs C-terminal domain structure (PDB ID: 5OOO, chain A) to the SFSV NSs showing that the C-terminal domain of the two NSs share similar overal structures. However, it is the N-terminal domain that forms direct contact with eIF2B. **(b)** Zoomed in view of panel a showing the structural similarity between the C-terminal domains fo the two NSs. eIF2B is colored blue, the SFSV NSs in gold and the RVFV NSs in red.

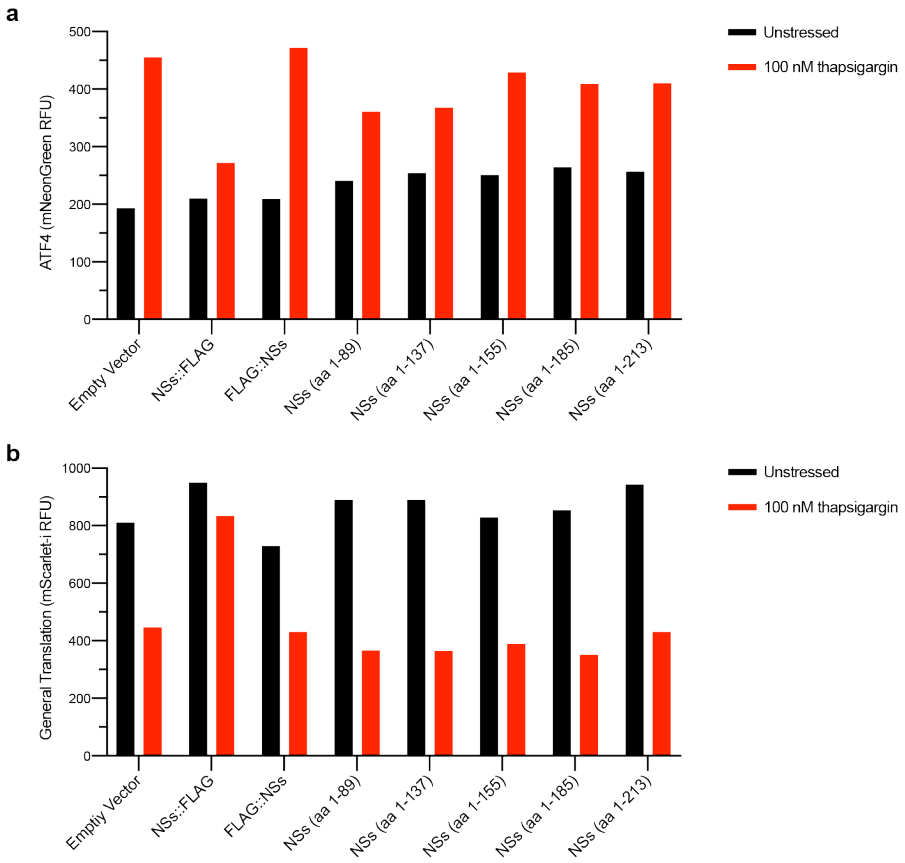

Supplementary Fig. 7: Effect of NSs truncations on protein function

(a) ATF4 and **(b)** General Translation reporter levels as monitored by flow cytometry after 3 h of thapsigargin (100 nM) and trimethoprim (20 μM) treatment. ATF4 and General Translation reporter levels are show for the population of BFP+ cells (that is, cells that have stably integrated the NSs expression constructs). NSs truncation abolishes its ISR evasion functionality, either by destabilizing protein synthesis or, more specifically, the interaction with eIF2B. Source data are provided as a Source Data file.

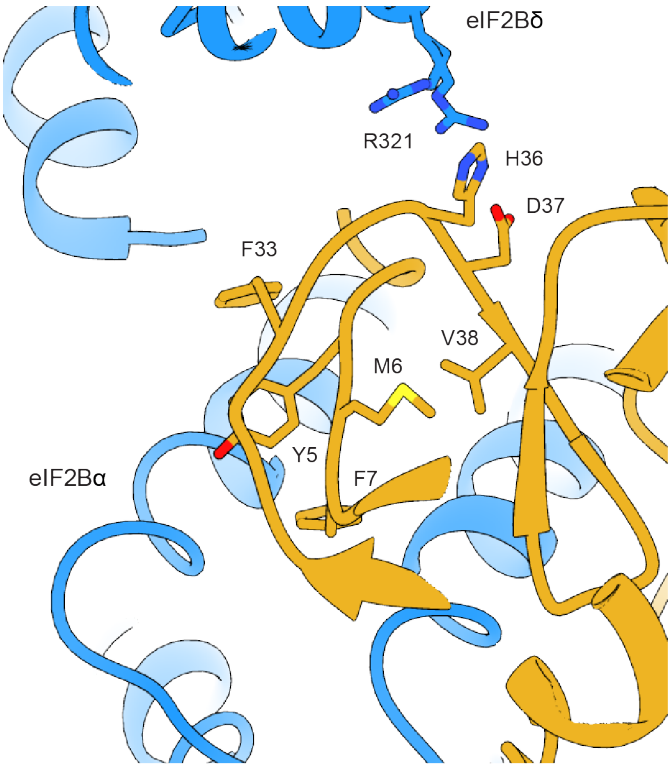

Supplementary Fig. 8: Synergistic binding of NSs loops

Zoomed in view of the NSs loops interaction with eIF2B. The conformation of the eIF2Bδ-facing amino acids (H36 and D37) could affect the positioning of V38, which forms hydrophobic stacking with M6. This stacking interaction may be important for the optimal positioning of Y5 and F7, the two main aromatic fingers facing eIF2Bα, thus contributing to NSs-eIF2B binding. eIF2B is colored in blue and NSs in gold.

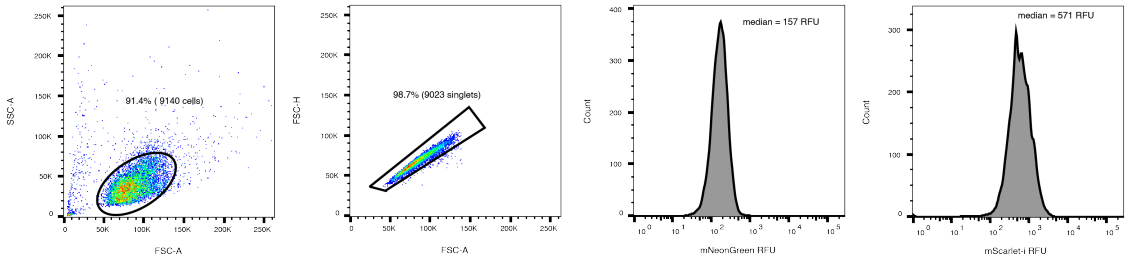

Supplementary Fig. 9: Representative gating strategy for flow cytometry experiments

An example of how flow cytometry data is analyzed. From 10,000 events collected the vast majority pass filtering and are included in median reporter signal calculations.

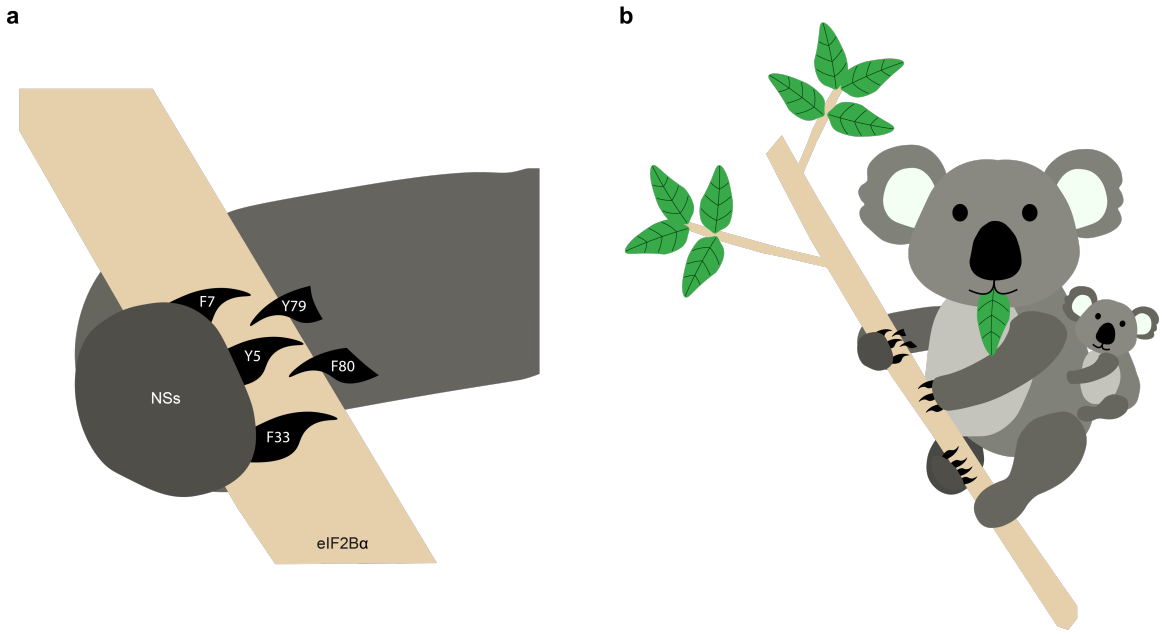

Supplementary Fig. 10: Schematic overview of the aromatic fingers

(a) Cartoon representation of the NSs aromatic fingers interacting with eIF2Bα. A koala was chosen to illustrate this interaction as their hands have three fingers and two opposable thumbs that grab onto branches from opposite sides in a geometry similar to how NSs grabs onto eIF2Bα **(b)** Zoomed out view of panel a.

Supplementary Table 1

Structure	eIF2B-NSs complex (PDB ID: 7RLO)
Data collection	
Microscope	Titan Krios
Voltage (keV)	300
Nominal magnification	105000x
Exposure navigation	Image shift
Electron dose ($e^{-}Å^{-2}$)	67
Dose rate (e^{-}/pixel/sec)	8
Detector	K3 summit
Pixel size (Å)	0.835
Defocus range (μm)	0.6-2.0
Micrographs	2143
Reconstruction	
Total extracted particles (no.)	1055439
Final particles (no.)	137093
Symmetry imposed	C1
FSC average resolution, masked (Å)	2.6
FSC average resolution, unmasked (Å)	3.7
Applied B-factor (Å)	76.2
Reconstruction package	Cryosparc 2.15
Refinement	
Protein residues	3670
Ligands	0
RMSD Bond lengths (Å)	0.002
RMSD Bond angles (°)	0.530
Ramachandran outliers (%)	0.08
Ramachandran allowed (%)	4.55
Ramachandran favored (%)	95.37
Poor rotamers (%)	3.20
CaBLAM outliers (%)	2.57
Molprobity score	2.08 (96th percentile)
Clash score (all atoms)	6.8 (99th percentile)
B-factors (protein)	102.73
B-factors (ligands)	N/A
EMRinger Score	2.77
Refinement package	Phenix 1.17.1-3660-000

Supplementary Table 2

Plasmid	Description	Antibiotic
pMS113	NSs::6xHIS for Expi293 expression / purification	Ampicillin
pMS085	Empty Vector for lentiviral integration	Ampicillin
pMS110	NSs::FLAG for lentiviral integration	Ampicillin
pMS111	FLAG::NSs for lentiviral integration	Ampicillin
pMS119	Truncated NSs (aa 1-89) for lentiviral integration	Ampicillin
pMS120	Truncated NSs (aa 1-137) for lentiviral integration	Ampicillin
pMS121	Truncated NSs (aa 1-155) for lentiviral integration	Ampicillin
pMS122	Truncated NSs (aa 1-185) for lentiviral integration	Ampicillin
pMS123	Truncated NSs (aa 1-213) for lentiviral integration	Ampicillin
pMS127	NSs::FLAG (Y5A/F7A) for lentiviral integration	Ampicillin
pMS128	NSs::FLAG (Y79A/F80A) for lentiviral integration	Ampicillin
pMS129	NSs::FLAG (F33A) for lentiviral integration	Ampicillin
pMS132	NSs::FLAG (H36A) for lentiviral integration	Ampicillin
pMS134	NSs::FLAG (D37A) for lentiviral integration	Ampicillin
pMS001	*E. coli* expression plasmid for eIF2Bδ and Avi-tagged eIF2Bβ	Chloramphenicol
pMS003	*E. coli* expression plasmid for eIF2Bδ and Protein C-tagged eIF2Bβ	Chloramphenicol
pMS026	*E. coli* expression plasmid for Avi-tagged eIF2Bα	Ampicillin

Supplementary Table 3

Antibody Target	Host	Dilution	Manufacturer / Catalog #	Blocking Conditions
GAPDH	Rabbit	1/2000	Abcam / ab9485	TBS-T + 3% BSA
eIF2Bα	Rabbit	1/1000	ProteinTech / 18010-1-AP	TBS-T + 3% milk
eIF2Bβ	Rabbit	1/1000	ProteinTech / 11034-1-AP	TBS-T + 3% milk
eIF2Bδ	Rabbit	1/1000	ProteinTech / 11332-1-AP	TBS-T + 3% milk
eIF2Bε	Mouse	1/1000	Santa Cruz Biotechnology / sc-55558	PBS-T + 3% milk
ATF4	Rabbit	1/1000	Cell Signaling / 11815S	PBS-T + 3% milk
eIF2α-P	Rabbit	1/1000	Cell Signaling / 9721S	PBS-T + 1% BSA
eIF2α	Rabbit	1/1000	Cell Signaling / 5324S	PBS-T + 3% milk
6xHIS	Goat (directly conjugated to HRP)	1/1000	Abcam / ab1269	TBS-T + 5% milk
FLAG	Mouse	1/1000	Sigma / F1804-1MG	PBS-T + 3% milk
PKR	Mouse	1/1000	BD Transduction Laboratories / 610764	TBS-T + 3% milk
PERK	Rabbit	1/1000	Cell Signaling / 3192S	TBS-T + 3% milk

4.6 News and Views: Ferreting out viral pathogenesis

Own contribution:

I contributed to writing and illustrating the manuscript.

_____

Jennifer Würth

VIRAL PATHOGENESIS

Ferreting out viral pathogenesis

Severe fever with thrombocytopenia virus is an emerging, highly lethal tick-borne pathogen with growing impact. In this issue of *Nature Microbiology*, two papers make major progress towards a better understanding of its so far incompletely understood mechanisms of virulence.

Jennifer Deborah Wuerth and Friedemann Weber

Severe fever with thrombocytopenia virus (SFTSV) is an RNA virus of the order Bunyavirales, genus *Phlebovirus*. It was first recognized in 2009 in China, but soon turned out to be present all over East Asia, with seroprevalence rates that can exceed 9%[1]. To date, there are more than 7,000 reported cases of the acute, high-fever illness with thrombocytopenia, leukocytopenia and multi-organ failure. The case fatality rate increases with age and can reach up to 30%[2].

Known virulence mechanisms of SFTSV centre on the non-structural protein NSs and its inhibitory interaction with the antiviral interferon (IFN)-α/β system[3]. IFNs are cytokines produced by virus-infected cells. Secreted IFNs bind to their cognate receptor and stimulate hundreds of genes with antiviral activity. SFTSV NSs, however, blocks both the induction of IFN and the subsequent IFN-triggered signalling (Fig. 1a), thus impeding antiviral gene expression. The role of NSs in IFN antagonism is well-investigated in cell culture, but not in vivo. The main reason, curiously, is that IFN-deficient mice are required to obtain SFTSV pathogenesis. In a recently published paper in *Nature Microbiology*, Park et al. overcame this drawback by establishing an infection model with immunocompetent ferrets[4]. Interestingly, these animals exhibited the same age dependency for clinical manifestations of SFTS as humans do. Moreover, gene expression profiles showed an IFN response that was early, strong and transient in the surviving young animals, whereas in the aged animals, it came later but persisted until they succumbed to the virus. Thus, in vivo, SFTSV NSs is able to dampen the IFN response, but cannot entirely shut it off. IFN signatures are a marker for ongoing viral replication, and the delay of their onset is paramount for productive infection. Inflammation on the other hand is a marker of severe viral disease[5] — exactly what was observed in the SFTSV ferret model. Only the aged animals had upregulated pathways of, for example, interleukin (IL)-6 signalling, macrophage recruitment and leukocyte extravasation, simultaneously with the late IFN response. This indicates an excessive immune activation that eventually leads to tissue damage and immune exhaustion.

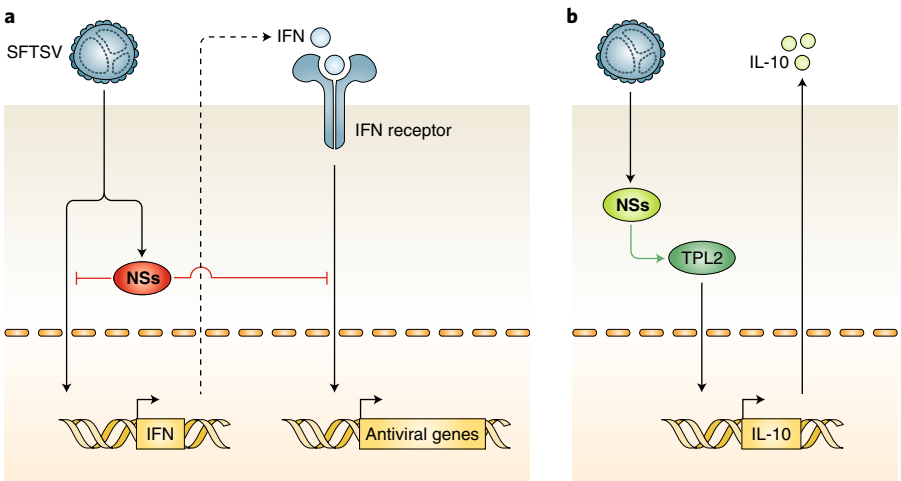

Fig. 1 | Suppressive and activating effects of SFTSV NSs on host signalling pathways. a, Following sensing of SFTSV infection, mammalian cells trigger the induction of IFN. The NSs protein of SFTSV, however, acts as an antagonist to both IFN induction and IFN signalling to evade the expression of antiviral genes. **b**, Now, SFTSV NSs has been discovered to additionally activate the cellular kinase TPL2, thereby driving the induction and secretion of the immunosuppressive cytokine IL-10.

Suppression of the IFN system is a basic pathogenicity mechanism of viruses, but a second recently published paper in *Nature Microbiology*[6] shows that other strategies play a significant role as well. Choi et al. discovered that SFTSV forces immune cells to produce the immunosuppressive cytokine IL-10 (ref. [6]). Again, the key player is the NSs protein, but here it stabilizes and activates the so-called tumour progression locus 2 (TPL2) kinase complex to trigger a signalling chain leading to IL-10 expression (Fig. 1b). Strikingly, in the IFN-deficient mouse model, both TPL2 and IL-10 were essential for SFTSV virulence. Thus, Choi et al. have identified a novel, activating mechanism of virulence mediated by the IFN-suppressive NSs.

Both papers[4,6] represent major steps towards a better understanding of SFTSV pathogenesis, but several points remain unsolved. First, unlike patients and IFN-deficient mice, the aged ferrets did not exhibit an IL-10 signature[4]. As ferrets do encode IL-10 (ref. [7]), there might be limitations of this animal model. Moreover, the observation that a SFTSV mouse model has to be IFN-deficient, whereas ferrets need just be old, may indicate that SFTSV NSs is not compatible with the murine IFN system. Finally, and more generally, it seems that in severe infections, the late-onset IFNs and inflammatory cytokines are sending orders to the immune system that are quite contrary to the ones sent by the anti-inflammatory cytokine IL-10 induced at the same time. Now that it is clear that the virus itself is upregulating IL-10, it is tempting to speculate that these conflicting immune signals are part of the reason why some viral infections can run out of control and exhaust the host response.

Pathogens are under strong selection pressure for maximal spread, and host damage is often an inevitable consequence[8]. Arthropod-borne viruses, like SFTSV,

in particular require a systemically and heavily infected host to guarantee the transit into the next vector organism, which could bite anywhere on the skin. Thus, viraemia is critical for transmission, and the novel mechanism of IL-10 induction is a substantial contributor. Furthermore, the findings suggest a general principle that may reach well beyond the phlebovirus SFTSV. IL-10 production has so far only been reported for DNA viruses like herpes or pox, which encode their own version[9]. For many other viral diseases, like Ebola, Rift Valley fever, Crimean-Congo haemorrhagic fever and SFTSV (ref. [6]), high production of IL-10 has been shown to be associated with poor outcomes, but the source of the cytokine has remained elusive. It seems to be time to pay more attention to this and to investigate whether these aggressive RNA viruses may actively induce IL-10, like SFTSV does through its NSs protein.

SFTSV is shortlisted by WHO as a major public health risk, with no approved therapy or prophylaxis available. The novel animal model and insights into the virulence mechanism reported by Park et al.[4] and Choi et al.[6] can now be exploited for developing and testing candidate antivirals and vaccines. ❐

Jennifer Deborah Wuerth and Friedemann Weber*

Institute for Virology, FB10-Veterinary Medicine, Justus-Liebig University, Giessen, Germany.
**e-mail: friedemann.weber@vetmed.uni-giessen.de*

Published online: 20 February 2019
https://doi.org/10.1038/s41564-019-0390-0

References

1. Li, P. et al. *PLoS ONE* **12**, e0175592 (2017).
2. Robles, N. J. C., Han, H. J., Park, S. J. & Choi, Y. K. *Clin. Exp. Vaccine Res.* **7**, 43–50 (2018).
3. Silvas, J. A. & Aguilar, P. V. *Am. J. Trop. Med. Hyg.* **97**, 992–996 (2017).
4. Park, S.-J. et al. *Nat. Microbiol.* https://doi.org/10.1038/s41564-018-0317-1 (2018).
5. Yamada, S. et al. *J. Virol.* **92**, e02246–17 (2018).
6. Choi, Y. et al. *Nat. Microbiol.* https://doi.org/10.1038/s41564-018-0329-x (2018).
7. Svitek, N. & von Messling, V. *Virology* **362**, 404–410 (2007).
8. Hedrick, S. M. *Trends Immunol.* **38**, 888–903 (2017).
9. Ouyang, P. et al. *J. Gen. Virol.* **95**, 245–262 (2014).

Competing interests

The authors declare no competing interests.

5 References

[1] Abudurexiti A et al. Taxonomy of the order Bunyavirales: update 2019. *Arch Virol* **164**; 1949-1965 (2019)

[2] Adams MJ et al. Changes to taxonomy and the International Code of Virus Classification and Nomenclature ratified by the International Committee on Taxonomy of Viruses (2017). *Arch Virol* **162**; 2505–2538 (2017)

[3] Adomavicius T et al. The structural basis of translational control by eIF2 phosphorylation. *Nat Commun* **10**; 2136 (2019)

[4] Albariño CG, Bird BH, Nichol ST. A shared transcription termination signal on negative and ambisense RNA genome segments of Rift Valley fever, sandfly fever Sicilian, and Toscana viruses. *J Virol* **81**; 5246-5256 (2007)

[5] Alexopoulou L et al. Recognition of double-stranded RNA and activation of NF-kappaB by Toll-like receptor 3. *Nature* **413**; 732-738 (2001)

[6] Al Hazmi M et al. Epidemic Rift Valley fever in Saudi Arabia: a clinical study of severe illness in humans. *Clin Infect Dis* **36**; 245-252 (2003)

[7] Alkan C et al. Sandfly-borne phleboviruses of Eurasia and Africa: epidemiology, genetic diversity, geographic range, control measures. *Antiviral Res* **100**; 54-74 (2013)

[8] Alkan C et al. Sandfly-Borne Phlebovirus Isolations from Turkey: New Insight into the Sandfly fever Sicilian and Sandfly fever Naples Species. *PLoS Negl Trop Dis* **10**; e0004519 (2016)

[9] Alkan C et al. Isolation and sequencing of Dashli virus, a novel Sicilian-like virus in sandflies from Iran; genetic and phylogenetic evidence for the creation of one novel species within the Phlebovirus genus in the Phenuiviridae family. *PLoS Negl Trop Dis* **11**; e0005978 (2017)

[10] Alwassouf S et al. Seroprevalence of Sandfly-Borne Phleboviruses Belonging to Three Serocomplexes (Sandfly fever Naples, Sandfly fever Sicilian and Salehabad) in Dogs from Greece and Cyprus Using Neutralization Test. *PLoS Negl Trop Dis* **10**; e0005063 (2016)

[11] Alwassouf S et al. Neutralization-based seroprevalence of Toscana virus and sandfly fever Sicilian virus in dogs and cats from Portugal. *J Gen Virol* **97**; 2816-2823 (2016)

[12] Anderson Jr GW et al. Pathogenesis of a phleboviral infection (Punta Toro virus) in golden Syrian hamsters. *Arch Virol* **114**; 203-212 (1990)

[13] Atasheva S et al. New PARP gene with an anti-alphavirus function. *J Virol* **86**; 8147-8160 (2012)

[14] Ayhan N et al. High Rates of Neutralizing Antibodies to Toscana and Sandfly Fever Sicilian Viruses in Livestock, Kosovo. *Emerg Infect Dis* **23**; 989-992 (2017)

[15] Baigent SJ et al. Inhibition of beta interferon transcription by noncytopathogenic bovine viral diarrhea virus is through an interferon regulatory factor 3-dependent mechanism. *J Virol* **76**; 8979-8988 (2002)

[16] Balachandran S and Barber GN. Defective translational control facilitates vesicular stomatitis virus oncolysis. *Cancer Cell* **5**; 51-65 (2004)

[17] Barr JN, Weber F, Schmaljohn CS. In: Howley PM, Knipe DM, and Whelan S (eds.): Fields Virology, 7th Edition, Volume 1: Emerging Viruses. Lipincott Williams & Wilkins, Philadelphia, USA (2020)

[18] Barro M and Patton JT. Rotavirus nonstructural protein 1 subverts innate immune response by inducing degradation of IFN regulatory factor 3. *Proc Natl Acad Sci USA* **102**; 4114-4119 (2005)

[19] Bartelloni PJ and Tesh RB. Clinical and serologic responses of volunteers infected with phlebotomus fever virus (Sicilian type). *Am J Trop Med Hyg* **25**; 456-462 (1976)

[20] Batieha A et al. Seroprevalence of West Nile, Rift Valley, and sandfly arboviruses in Hashimiah, Jordan. *Emerg Infect Dis* **6**; 358-362 (2000)

[21] Billecocq A et al. NSs Protein of Rift Valley Fever Virus Blocks Interferon Production by Inhibiting Host Gene Transcription. *J Virol* **78**; 9798-9806 (2004)

[22] Bino S et al. Detection of a Novel Phlebovirus (Drin Virus) from Sand Flies in Albania. *Viruses* **11**; 469 (2019)

[23] Bird BH. Rift Valley fever virus. *J Am Vet Med Assoc* **234**; 883-893 (2009)

[24] Blitvich BJ et al. Bunyavirus Taxonomy: Limitations and Misconceptions Associated with the Current ICTV Criteria Used for Species Demarcation. *Am J Trop Med Hyg* **99**; 11-16 (2018)

[25] Bouloy M et al. Genetic evidence for an interferon-antagonistic function of rift valley fever virus nonstructural protein NSs. *J Virol* **75**; 1371-1377 (2001)
[26] Brault AC et al. Heartland Virus Epidemiology, Vector Association, and Disease Potential. *Viruses* **10**; 498 (2018)
[27] Brennan B, Rezelj VV, Elliott RM. Mapping of Transcription Termination within the S Segment of SFTS Phlebovirus Facilitated Generation of NSs Deletant Viruses. *J Virol* **91**; e00743-17 (2017)
[28] Burýsek L and Pitha PM. Latently expressed human herpesvirus 8-encoded interferon regulatory factor 2 inhibits double-stranded RNA-activated protein kinase. *J Virol* **75**; 2345-2352 (2001)
[29] Caplen H, Peters CJ, Bishop DH. Mutagen-directed attenuation of Rift Valley fever virus as a method for vaccine development. *J Gen Virol* **66**; 2271-2277 (1985)
[30] Çarhan A et al. Characterization of a sandfly fever Sicilian virus isolated during a sandfly fever epidemic in Turkey. *J Clin Virol* **48**; 264-269 (2010)
[31] Chang HW, Watson JC, Jacobs BL. The E3L gene of vaccinia virus encodes an inhibitor of the interferon-induced, double-stranded RNA-dependent protein kinase. *Proc Natl Acad Sci USA* **89**; 4825-4829 (1992)
[32] Charrel RN, Bichaud L, de Lamballerie X. Emergence of Toscana virus in the mediterranean area. *World J Virol* **1**; 135-141 (2012)
[33] Chaudhary V et al. Suppression of type I and type III IFN signalling by NSs protein of severe fever with thrombocytopenia syndrome virus through inhibition of STAT1 phosphorylation and activation. *J Gen Virol* **96**; 3204-3211 (2015)
[34] Chevalier V. Relevance of Rift Valley fever to public health in the European Union. *Clin Microbiol Infect* **19**; 705-708 (2013)
[35] Choi Y et al. Severe fever with thrombocytopenia syndrome phlebovirus non-structural protein activates TPL2 signalling pathway for viral immunopathogenesis. *Nat Microbiol* **4**; 429-437 (2019)
[36] Choi Y et al. Severe Fever with Thrombocytopenia Syndrome Virus NSs Interacts with TRIM21 To Activate the p62-Keap1-Nrf2 Pathway. *J Virol* **94**; e01684-19 (2020)
[37] Chou A et al. Inhibition of the integrated stress response reverses cognitive deficits after traumatic brain injury. *Proc Natl Acad Sci USA* **114**; E6420-E6426 (2017)
[38] Cloutier N and Flamand L. Kaposi sarcoma-associated herpesvirus latency-associated nuclear antigen inhibits interferon (IFN) beta expression by competing with IFN regulatory factor-3 for binding to IFNB promoter. *J Biol Chem* **285**; 7208-7221 (2010)
[39] Colonna M, Trinchieri G, Liu YJ. Plasmacytoid dendritic cells in immunity. *Nat Immunol* **5**; 1219-1226 (2004)
[40] Copeland AM et al. Rift Valley fever virus NSs gene expression correlates with a defect in nuclear mRNA export. *Virology* **486**; 88-93 (2015)
[41] Costa-Mattioli M and Walter P. The integrated stress response: From mechanism to disease. *Science* **368**; eaat5314 (2020)
[42] Crabtree MB et al. Infection and transmission of Rift Valley fever viruses lacking the NSs and/or NSm genes in mosquitoes: potential role for NSm in mosquito infection. *PLoS Negl Trop Dis* **6**; e1639 (2012)
[43] Crance JM et al. Inhibition of sandfly fever Sicilian virus (Phlebovirus) replication in vitro by antiviral compounds. *Res Virol* **148**; 353-365 (1997)
[44] Dar O, Hogarth S, McIntyre S. Tempering the risk: Rift Valley fever and bioterrorism. *Trop Med Int Health* **18**; 1036-1041 (2013)
[45] Dauber B and Wolff T. Activation of the Antiviral Kinase PKR and Viral Countermeasures. *Viruses* **1**; 523-544 (2009)
[46] Daubney R, Hudson JR, Garnham PC. Enzootic Hepatitis or Rift Valley Fever. An Undescribed Virus Disease of Sheep Cattle and Man from East Africa. *J Pathol Bacteriol* **34**; 545-579 (1931)
[47] Davies MV et al. The vaccinia virus K3L gene product potentiates translation by inhibiting double-stranded-RNA-activated protein kinase and phosphorylation of the alpha subunit of eukaryotic initiation factor 2. *J Virol* **66**; 1943-1950 (1992)
[48] Dey R et al. Gut Microbes Egested during Bites of Infected Sand Flies Augment Severity of Leishmaniasis via Inflammasome-Derived IL-1β. *Cell Host Microbe* **23**; 134-143 (2018)

[49] Diebold SS et al. Innate antiviral responses by means of TLR7-mediated recognition of single-stranded RNA. *Science* **303**; 1529-1531 (2004)
[50] Dilcher M et al. Genetic characterization of Bhanja virus and Palma virus, two tick-borne phleboviruses. *Virus Genes* **45**; 311-315 (2012)
[51] do Valle TZ et al. A new mouse model reveals a critical role for host innate immunity in resistance to Rift Valley fever. *J Immunol* **185**; 6146-6156 (2010)
[52] Eitrem R, Niklasson B, Wieland O. Sandfly fever among Swedish tourists. *Scand J Infect Dis* **23**; 451-457 (1991)
[53] Eitrem R, Stylianou M, Niklasson B. High prevalence rates of antibody to three sandfly fever viruses (Sicilian, Naples, and Toscana) among Cypriots. *Epidemiol Infect* **107**; 685-691 (1991)
[54] Eitrem R, Vene S, Niklasson B. Incidence of sand fly fever among Swedish United Nations soldiers on Cyprus during 1985. *Am J Trop Med Hyg* **43**; 207-211 (1990)
[55] Elliott RM and Brennan B. Emerging phleboviruses. *Curr Opin Virol* **5**; 50-57 (2014)
[56] Ellis SB et al. Outbreak of sandfly fever in central Iraq, September 2007. *Mil Med* **173**; 949-953 (2008)
[57] Ergunay K et al. A case of central nervous system infection due to a novel Sandfly Fever Virus (SFV) variant: Sandfly Fever Turkey Virus (SFTV). *J Clin Virol* **54**; 79-82 (2012)
[58] Ergunay K, Ayhan N, Charrel RN. Novel and emergent sandfly-borne phleboviruses in Asia Minor: a systematic review. *Rev Med Virol* **27**; e1898 (2017)
[59] Ermler ME et al. RNA helicase signaling is critical for type I interferon production and protection against Rift Valley fever virus during mucosal challenge. *J Virol* **87**; 4846-4860 (2013)
[60] Escalante CR et al. Structure of IRF-3 bound to the PRDIII-I regulatory element of the human interferon-beta enhancer. *Mol Cell* **26**; 703-716 (2007)
[61] Ferron F et al. Transcription and replication mechanisms of Bunyaviridae and Arenaviridae L proteins. *Virus Res* **234**; 118-134 (2017)
[62] Fitzgerald KA et al. IKKepsilon and TBK1 are essential components of the IRF3 signaling pathway. *Nat Immunol* **4**; 491-496 (2003)
[63] Frese M et al. Inhibition of bunyaviruses, phleboviruses, and hantaviruses by human MxA protein. *J Virol* **70**; 915-923 (1996)
[64] Gaidamovich SY et al. Sandfly fever in central Asia and Afghanistan. In: Calisher CH (ed.) Hemorrhagic fever with renal syndrome, tick and mosquito-borne viruses. Springer, Vienna, Austria (1991)
[65] Gerrard SR and Nichol ST. Synthesis, proteolytic processing and complex formation of N-terminally nested precursor proteins of the Rift Valley fever virus glycoproteins. *Virology* **357**; 124-133 (2007)
[66] García MA et al. Impact of protein kinase PKR in cell biology: from antiviral to antiproliferative action. *Microbiol Mol Biol Rev* **70**; 1032-1060 (2006)
[67] Geiss GK et al. Cellular transcriptional profiling in influenza A virus-infected lung epithelial cells: the role of the nonstructural NS1 protein in the evasion of the host innate defense and its potential contribution to pandemic influenza. *PNAS* **99**; 10736-10741 (2002)
[68] Giorgi C et al. Sequences and coding strategies of the S RNAs of Toscana and Rift Valley fever viruses compared to those of Punta Toro, Sicilian Sandfly fever, and Uukuniemi viruses. *Virology* **180**; 738-753 (1991)
[69] Gordiyenko Y, Llacer JL, Ramakrishnan V. Structural basis for the inhibition of translation through eIF2α phosphorylation. *Nat Commun* **10**; 2640 (2019)
[70] Gori Savellini G et al. Toscana virus induces interferon although its NSs protein reveals antagonistic activity. *J Gen Virol* **92**; 71-79 (2011)
[71] Gori-Savellini G, Valentini M, Cusi MG. Toscana Virus NSs Protein Inhibits the Induction of Type I Interferon by Interacting with RIG-I. *J Virol* **87**; 6660-6667 (2013)
[72] Gori Savellini G, Gandolfo C, Cusi MG. Truncation of the C-terminal region of Toscana Virus NSs protein is critical for interferon-β antagonism and protein stability. *Virology* **486**; 255-262 (2015)
[73] Gori Savellini G et al. Toscana virus non-structural protein NSs acts as E3 ubiquitin ligase promoting RIG-I degradation. *PLoS Pathog* **15**; e1008186 (2019)

[74] Goverdhan MK et al. Isolation of phlebotomus (sandfly) fever virus from sandflies and humans during the same season in Aurangabad District, Maharashtra State, India. *Indian J Med Res* **64**; 57-63 (1976)
[75] Grandvaux N et al. Transcriptional profiling of interferon regulatory factor 3 target genes: direct involvement in the regulation of interferon-stimulated genes. *J Virol* **76**; 5532-5539 (2002)
[76] Gundacker ND et al. Clinical Manifestations of Punta Toro Virus Species Complex Infections, Panama, 2009. *Emerg Infect Dis* **23**; 872-874 (2017)
[77] Habjan M et al. Processing of genome 5' termini as a strategy of negative-strand RNA viruses to avoid RIG-I-dependent interferon induction. *PLoS One* **3**; e2032 (2008)
[78] Habjan M et al. T7 RNA polymerase-dependent and -independent systems for cDNA-based rescue of Rift Valley fever virus. *J Gen Virol* **89**; 2157-2166 (2008)
[79] Habjan M et al. NSs protein of rift valley fever virus induces the specific degradation of the double-stranded RNA-dependent protein kinase. *J Virol* **83**; 4365-4375 (2009)
[80] Habjan M et al. Efficient production of Rift Valley fever virus-like particles: The antiviral protein MxA can inhibit primary transcription of bunyaviruses. *Virology* **385**; 400-408 (2009)
[81] Haller O, Kochs G, Weber F. The interferon response circuit: induction and suppression by pathogenic viruses. *Virology* **344**; 119-130 (2006)
[82] Hao W, Wang L, Li S. Roles of the Non-Structural Proteins of Influenza A Virus. *Pathogens* **9**; 812 (2020)
[83] Harmon B et al. Rift Valley fever virus strain MP-12 enters mammalian host cells via caveola-mediated endocytosis. *J Virol* **86**; 12954-12970 (2012)
[84] Hassan A et al. Epidemiological Investigation of a Rift Valley Fever Outbreak in Humans and Livestock in Kenya, 2018. *Am J Trop Med Hyg* **103**; 1649-1655 (2020)
[85] Hassan OA et al. The 2007 Rift Valley fever outbreak in Sudan. *PLoS Negl Trop Dis* **5**; e1229 (2011)
[86] He B, Gross M, Roizman B. The gamma(1)34.5 protein of herpes simplex virus 1 complexes with protein phosphatase 1alpha to dephosphorylate the alpha subunit of the eukaryotic translation initiation factor 2 and preclude the shutoff of protein synthesis by double-stranded RNA-activated protein kinase. *Proc Natl Acad Sci USA* **94**; 843-848 (1997)
[87] Head JA, Kalveram B, Ikegami T. Functional analysis of Rift Valley fever virus NSs encoding a partial truncation. *PLoS One* **7**; e45730 (2012)
[88] Heil F et al. Species-specific recognition of single-stranded RNA via toll-like receptor 7 and 8. *Science* **303**; 1526-1529 (2004)
[89] Heirwegh E et al. Sandfly Fever Sicilian Virus-Leishmania major co-infection modulates innate inflammatory response favoring myeloid cell infections and skin hyperinflammation. *PLoS Negl Trop Dis* **15**; e0009638 (2021)
[90] Hilton L et al. The NPro product of bovine viral diarrhea virus inhibits DNA binding by interferon regulatory factor 3 and targets it for proteasomal degradation. *J Virol* **80**; 11723-11732 (2006)
[91] Holzinger D et al. Induction of MxA gene expression by influenza A virus requires type I or type III interferon signaling. *J Virol* **81**; 7776-7785 (2007)
[92] Honda K et al. IRF-7 is the master regulator of type-I interferon-dependent immune responses. *Nature* **434**; 772-777 (2005)
[93] Honda K and Taniguchi T. IRFs: master regulators of signalling by Toll-like receptors and cytosolic pattern-recognition receptors. *Nat Rev Immunol* **6**; 644-658 (2006)
[94] Honda K, Takaoka A, Taniguchi T. Type I interferon gene induction by the interferon regulatory factor family of transcription factors. *Immunity* **25**; 349-360 (2006)
[95] Ikegami T et al. Rescue of infectious rift valley fever virus entirely from cDNA, analysis of virus lacking the NSs gene, and expression of a foreign gene. *J Virol* **80**; 2933-2940 (2006)
[96] Ikegami T et al. Characterization of Rift Valley Fever Virus Transcriptional Terminations. *J Virol* **81**; 8421-8438 (2007)
[97] Ikegami T et al. Rift Valley fever virus NSs protein promotes post-transcriptional downregulation of protein kinase PKR and inhibits eIF2alpha phosphorylation. *PLoS Pathog* **5**; 41000287 (2009)
[98] Ikegami T et al. Rift Valley Fever Virus MP-12 Vaccine Is Fully Attenuated by a Combination of Partial Attenuations in the S, M, and L Segments. *J Virol* **89**; 7262-7276 (2015)

[99] Jackson RJ, Hellen CUT, Pestova TV. The mechanism of eukaryotic translation initiation and principles of its regulation. *Nat Rev Mol Cell Biol* **11**; 113-127 (2010)
[100] Jan E, Mohr I, Walsh D. A Cap-to-Tail Guide to mRNA Translation Strategies in Virus-Infected Cells. *Annu Rev Virol* **3**; 283-307 (2016)
[101] Jantsch M and Marcus GH. Alois PICK, the discoverer of pappataci fever. *Wien Med Wschr* **111**; 801-803 (1961)
[102] Jiao P et al. A single-amino-acid substitution in the NS1 protein changes the pathogenicity of H5N1 avian influenza viruses in mice. *J Virol* **82**; 1146-1154 (2008)
[103] Kainulainen M et al. Virulence Factor NSs of Rift Valley Fever Virus Recruits the F-Box Protein FBXO3 To Degrade Subunit p62 of General Transcription Factor TFIIH. *J Virol* **88**; 3464-3473 (2014)
[104] Kainulainen M et al. NSs Virulence Factor of Rift Valley Fever Virus Engages the F-Box Proteins FBXW11 and β-TRCP1 To Degrade the Antiviral Protein Kinase PKR. *J Virol* **90**; 6140-6147 (2016)
[105] Kalveram B, Lihoradova O, Ikegami T. NSs Protein of Rift Valley Fever Virus Promotes Posttranslational Downregulation of the TFIIH Subunit p62. *J Virol* **85**; 6234-6243 (2011)
[106] Kalveram B et al. Rift Valley fever virus NSs inhibits host transcription independently of the degradation of dsRNA-dependent protein kinase PKR. *Virology* **435**; 415-424 (2013)
[107] Kalveram B and Ikegami T. Toscana virus NSs protein promotes degradation of double-stranded RNA-dependent protein kinase. *J Virol* **87**; 3710-3718 (2013)
[108] Kashiwagi K et al. Structural basis for eIF2B inhibition in integrated stress response. *Science* **364**; 495-499 (2019)
[109] Kashiwagi K et al. eIF2B-capturing viral protein NSs suppresses the integrated stress response. *BioRxiv* 2021.06.07.447466 (2021)
[110] Kato H et al. Differential roles of MDA5 and RIG-I helicases in the recognition of RNA viruses. *Nature* **441**; 101-105 (2006)
[111] Kawai T et al. IPS-1, an adaptor triggering RIG-I- and Mda5-mediated type I interferon induction. *Nat Immunol* **6**; 981-988 (2005)
[112] Kende M. Prophylactic and therapeutic efficacy of poly(I,C)-LC against Rift Valley fever virus infection in mice. *J Biol Response Mod* **4**; 503-511 (1985)
[113] Kenner LR et al. eIF2B-catalyzed nucleotide exchange and phosphoregulation by the integrated stress response. *Science* **364**; 491-495 (2019)
[114] Khalil J, Kato H, Fujita T. The Role of Non-Structural Protein NSs in the Pathogenesis of Severe Fever with Thrombocytopenia Syndrome. *Viruses* **13**; 876 (2021)
[115] Kniha E et al. Phlebovirus seroprevalence in Austrian Army personnel returning from missions abroad. *Parasit Vectors* **12**; 416 (2019)
[116] Kobasa D et al. Aberrant innate immune response in lethal infection of macaques with the 1918 influenza virus. *Nature* **445**; 319-323 (2007)
[117] Koch J et al. Entry of Phenuiviruses into Mammalian Host Cells. *Viruses* **13**; 299 (2021)
[118] Kochs G, Garcia-Sastre A, Martinez-Sobrido L. Multiple anti-interferon actions of the influenza A virus NS1 protein. *J Virol* **81**; 7011-7021 (2007)
[119] Krammer F et al. Influenza. *Nat Rev Dis Primers* **4**; 3 (2018)
[120] Krishnamoorthy T et al. Tight binding of the phosphorylated alpha subunit of initiation factor 2 (eIF2alpha) to the regulatory subunits of guanine nucleotide exchange factor eIF2B is required for inhibition of translation initiation. *Mol Cell Biol* **21**; 5018-5030 (2001)
[121] Krug RM. Functions of the influenza A virus NS1 protein in antiviral defense. *Curr Opin Virol* **12**; 1-6 (2015)
[122] Kumar KP et al. Regulated nuclear-cytoplasmic localization of interferon regulatory factor 3, a subunit of double-stranded RNA-activated factor 1. *Mol Cell Biol* **20**; 4159-4168 (2000)
[123] Lara E et al. Characterization of wild-type and alternate transcription termination signals in the Rift Valley fever virus genome. *J Virol* **85**; 12134-12145 (2011)
[124] Lefort S et al. Binding of Kaposi's sarcoma-associated herpesvirus K-bZIP to interferon-responsive factor 3 elements modulates antiviral gene expression. *J Virol* **81**; 10950-10960 (2007)

[125] Le May N et al. TFIIH transcription factor, a target for the Rift Valley hemorrhagic fever virus. *Cell* **116**; 541-550 (2004)
[126] Le May N et al. A SAP30 complex inhibits IFN-beta expression in Rift Valley fever virus infected cells. *PLoS Pathog* **4**; e13 (2008)
[127] Lihoradova OA et al. Characterization of Rift Valley fever virus MP-12 strain encoding NSs of Punta Toro virus or sandfly fever Sicilian virus. *PLoS Negl Trop Dis* **7**; e2181 (2013)
[128] Lihoradova OA and Ikegami T. Countermeasure development for Rift Valley fever: deletion, modification or targeting of major virulence factor NSs. *Future Virol* **9**; 27-39 (2014)
[129] Lin R et al. Virus-dependent phosphorylation of the IRF-3 transcription factor regulates nuclear translocation, transactivation potential, and proteasome-mediated degradation. *Mol Cell Biol* **18**; 2986-2996 (1998)
[130] Lin R, Mamane Y, Hiscott J. Structural and functional analysis of interferon regulatory factor 3: localization of the transactivation and autoinhibitory domains. *Mol Cell Biol* **19**; 2465-2474 (1999)
[131] Liu S et al. MAVS recruits multiple ubiquitin E3 ligases to activate antiviral signaling cascades. *eLife* **2**; e00785 (2013)
[132] Liu S et al. Phosphorylation of innate immune adaptor proteins MAVS, STING, and TRIF induces IRF3 activation. *Science* **347**; aaa2630 (2015)
[133] Liu Y et al. The pathogenesis of severe fever with thrombocytopenia syndrome virus infection in alpha/beta interferon knockout mice: insights into the pathologic mechanisms of a new viral hemorrhagic fever. *J Virol* **88**; 1781-1786 (2014)
[134] Lozach PY et al. Entry of bunyaviruses into mammalian cells. *Cell Host Microbe* **7**; 488-499 (2010)
[135] Ly HJ and Ikegami T. Rift Valley fever virus NSs protein functions and the similarity to other bunyavirus NSs proteins. *Virol J* **13**; 118 (2016)
[136] Madani TA et al. Rift Valley fever epidemic in Saudi Arabia: epidemiological, clinical, and laboratory characteristics. *Clin Infect Dis* **37**; 1084-1092 (2003)
[137] Marie I, Durbin JE, Levy DE. Differential viral induction of distinct interferon-alpha genes by positive feedback through interferon regulatory factor-7. *EMBO J* **17**; 6660-6669 (1998)
[138] Matsuno K et al. Characterization of the Bhanja serogroup viruses (Bunyaviridae): a novel species of the genus Phlebovirus and its relationship with other emerging tick-borne phleboviruses. *J Virol* **87**; 3719-3728 (2013)
[139] Matsuoka Y, Chen SY, Compans RW. Bunyavirus protein transport and assembly. *Curr Top Microbiol Immunol* **169**; 161-179 (1991)
[140] McCormick C and Khaperskyy DA. Translation inhibition and stress granules in the antiviral immune response. *Nat Rev Immunol* **17**; 647-660 (2017)
[141] McMullan LK et al. A new phlebovirus associated with severe febrile illness in Missouri. *N Engl J Med* **367**; 834-841 (2012)
[142] McNab F et al. Type I interferons in infectious disease. *Nat Rev Immunol* **15**; 87-103 (2015)
[143] Medlock JM et al. A summary of the evidence for the change in European distribution of phlebotomine sand flies (Diptera: Psychodidae) of public health importance. *J Vector Ecol* **39**; 72-77 (2014)
[144] Mendenhall M et al. Punta Toro virus (Bunyaviridae, Phlebovirus) infection in mice: strain differences in pathogenesis and host interferon response. *Virology* **395**; 143-151 (2009)
[145] Mesev EV, LeDesma RA, Ploss A. Decoding type I and III interferon signalling during viral infection. *Nat Microbiol* **4**; 914-924 (2019)
[146] Meylan E et al. Cardif is an adaptor protein in the RIG-I antiviral pathway and is targeted by hepatitis C virus. *Nature* **437**; 1167-1172 (2005)
[147] Min YQ et al. The Nonstructural Protein of Guertu Virus Disrupts Host Defenses by Blocking Antiviral Interferon Induction and Action. *ACS Infect Dis* **6**; 857-870 (2020)
[148] Moriconi M et al. Phlebotomine sand fly-borne pathogens in the Mediterranean Basin: Human leishmaniasis and phlebovirus infections. *PLoS Negl Trop Dis* **11**; e0005660 (2017)
[149] Morill JC et al. Prevention of Rift Valley fever in rhesus monkeys with interferon-alpha. *Rev Infect Dis* **11 (Suppl 4)**; S815-S825 (1989)

[150] Morill JC et al. Pathogenesis of Rift Valley fever in rhesus monkeys: role of interferon response. *Arch Virol* **110**; 195-212 (1990)
[151] Mudhasani R et al. IFITM-2 and IFITM-3 but not IFITM-1 restrict Rift Valley fever virus. *J Virol* **87**; 8451-8464 (2013)
[152] Mudhasani R et al. Protein Kinase R Degradation Is Essential for Rift Valley Fever Virus Infection and Is Regulated by SKP1-CUL1-F-box (SCF)FBXW11-NSs E3 Ligase. *PLoS Pathog* **12**; e1005437 (2016)
[153] Muller R et al. Characterization of clone 13, a naturally attenuated avirulent isolate of Rift Valley fever virus, which is altered in the small segment. *Am J Trop Med Hyg* **53**; 405-411 (1995)
[154] Newman ENC et al. Seroconversion for infectious pathogens among UK military personnel deployed to Afghanistan, 2008-2011. *Emerg Infect Dis* **20**; 2015-2022 (2014)
[155] Niklasson B and Eitrem R. Sandfly fever among Swedish UN troops in Cyprus. *Lancet* **1**; 1212 (1985)
[156] Ning S, Pagano JS, Barber GN. IRF7: activation, regulation, modification and function. *Genes Immun* **12**; 399-414 (2011)
[157] Ning YJ et al. Viral suppression of innate immunity via spatial isolation of TBK1/IKKε from mitochondrial antiviral platform. *J Mol Cell Biol* **6**; 324-337 (2014)
[158] Ning YJ et al. Disruption of type I interferon signaling by the nonstructural protein of severe fever with thrombocytopenia syndrome virus via the hijacking of STAT2 and STAT1 into inclusion bodies. *J Virol* **89**; 4227-4236 (2015)
[159] Nishiyama S et al. Attenuation of pathogenic Rift Valley fever virus strain through the chimeric S-segment encoding sandfly fever phlebovirus NSs or a dominant-negative PKR. *Virulence* **7**; 871-881 (2016)
[160] Nogales A et al. Modulation of Innate Immune Responses by the Influenza A NS1 and PA-X Proteins. *Viruses* **10**; 708 (2018)
[161] Onoguchi K et al. Viral infections activate types I and III interferon genes through a common mechanism. *J Biol Chem* **282**; 7576-7581 (2007)
[162] Osterlund PI et al. IFN regulatory factor family members differentially regulate the expression of type III IFN (IFN-lambda) genes. *J Immunol* **179**; 3434-3442 (2007)
[163] Palacios G et al. Characterization of the Uukuniemi virus group (Phlebovirus: Bunyaviridae): evidence for seven distinct species. *J Virol* **87**; 3187-3195 (2013)
[164] Palacios G et al. Characterization of the Punta Toro species complex (genus Phlebovirus, family Bunyaviridae). *J Gen Virol* **96**; 2079-2085 (2015)
[165] Pakos-Zebrucka K. The integrated stress response. *EMBO Rep* **17**; 1374-1395 (2016)
[166] Panne D, Maniatis T, Harrison SC. Crystal structure of ATF-2/c-Jun and IRF-3 bound to the interferon-beta enhancer. *EMBO J* **23**; 4384-4393 (2004)
[167] Panne D, Maniatis T, Harrison SC. An atomic model of the interferon-beta enhanceosome. *Cell* **129**; 1111-1123 (2007)
[168] Pavitt GD. Regulation of translation initiation factor eIF2B at the hub of the integrated stress response. *Wiley Interdiscip Rev RNA* **9**; e1491 (2018)
[169] Peters CJ et al. Prophylaxis of Rift Valley fever with antiviral drugs, immune serum, an interferon inducer, and a macrophage activator. *Antiviral Res* **6**; 285-297 (1986)
[170] Peters NC et al. In vivo imaging reveals an essential role for neutrophils in leishmaniasis transmitted by sand flies. *Science* **321**; 970-974 (2008)
[171] Perrone LA et al. The S segment of Punta Toro virus (Bunyaviridae, Phlebovirus) is a major determinant of lethality in the Syrian hamster and codes for a type I interferon antagonist. *J Virol* **81**; 884-892 (2007)
[172] Pichlmair A et al. IFIT1 is an antiviral protein that recognizes 5'-triphosphate RNA. *Nat Immunol* **12**; 624-630 (2011)
[173] Pichlmair A et al. Viral immune modulators perturb the human molecular network by common and unique strategies. *Nature* **487**; 486-490 (2012)
[174] Pingen M et al. Host Inflammatory Response to Mosquito Bites Enhances the Severity of Arbovirus Infection. *Immunity* **44**; 1455-1469 (2016)

[175] Prescott J et al. New World hantaviruses activate IFNlambda production in type I IFN-deficient vero E6 cells. *PLoS One* **5**; e11159 (2010)
[176] Qu B et al. Suppression of the interferon and NF-κB responses by severe fever with thrombocytopenia syndrome virus. *J Virol* **86**; 8388-8401 (2012)
[177] Rabouw HH et al. Inhibition of the integrated stress response by viral proteins that block p-eIF2-eIF2B association. *Nat Microbiol* **5**; 1361-1373 (2020)
[178] Rath CT et al. Amazonian Phlebovirus (Bunyaviridae) potentiates the infection of Leishmania (Leishmania) amazonensis: Role of the PKR/IFN1/IL-10 axis. *PLoS Negl Trop Dis* **13**; e0007500 (2019)
[179] Rezelj VV, Överby AK, Elliott RM. Generation of mutant Uukuniemi viruses lacking the nonstructural protein NSs by reverse genetics indicates that NSs is a weak interferon antagonist. *J Virol* **89**; 4849-4856 (2015)
[180] Rezelj VV et al. Differential Antagonism of Human Innate Immune Responses by Tick-Borne *Phlebovirus* Nonstructural Proteins. *mSphere* **2**; e00234-17 (2017)
[181] Robles NJC et al. Epidemiology of severe fever and thrombocytopenia syndrome virus infection and the need for therapeutics for the prevention. *Clin Exp Vaccine Res* **7**; 43-50 (2018)
[182] Rolin AI, Berrang-Ford L, Kulkarni MA. The risk of Rift Valley fever virus introduction and establishment in the United States and European Union. *Emerg Microbes Infect* **2**; e81 (2013)
[183] Rossi M and Fasel N. The criminal association of Leishmania parasites and viruses. *Curr Opin Microbiol* **46**; 65-72 (2018)
[184] Sabin AB, Philip CB, Paul JR. Phlebotomus (pappataci or sandfly) fever: a disease of military importance - summary of existing knowledge and preliminary report of original investigations. *JAMA* **125**; 603-606 (1944)
[185] Sabin AB. Experimental studies on Phlebotomus (pappataci, sandfly) fever during World War II. *Arch Gesamte Virusforsch* **4**; 367-410 (1951)
[186] Saidi S et al. Studies on the epidemiology of sandfly fever in Iran. II. The prevalence of human and animal infection with five phlebotomus fever virus serotypes in Isfahan province. *Am J Trop Med Hyg* **26**; 288-293 (1977)
[187] Sakhria S et al. Presence of sandfly-borne phleboviruses of two antigenic complexes (Sandfly fever Naples virus and Sandfly fever Sicilian virus) in two different bio-geographical regions of Tunisia demonstrated by a microneutralisation-based seroprevalence study in dogs. *Parasit Vectors* **7**; 476 (2014)
[188] Salman M. Is the United States really at risk for introduction of Rift Valley fever virus? *J Am Vet Med Assoc* **242**; 606-608 (2013)
[189] Sandrock M et al. Interferon-induced rat Mx proteins confer resistance to Rift Valley fever virus and other arthropod-borne viruses. *J Interferon Cytokine Res* **21**; 663-668 (2001)
[190] Santiago FW et al. Hijacking of RIG-I signaling proteins into virus-induced cytoplasmic structures correlates with the inhibition of type I interferon responses. *J Virol* **88**; 4572-4585 (2014)
[191] Sato M et al. Positive feedback regulation of type I IFN genes by the IFN-inducible transcription factor IRF-7. *FEBS Lett* **441**; 106-110 (1998)
[192] Sato M et al. Distinct and essential roles of transcription factors IRF-3 and IRF-7 in response to viruses for IFN-alpha/beta gene induction. *Immunity* **13**; 539-548 (2000)
[193] Savage HM et al. First detection of heartland virus (Bunyaviridae: Phlebovirus) from field collected arthropods. *Am J Trop Med Hyg* **89**; 445-452 (2013)
[194] Schlee M. Master sensors of pathogenic RNA - RIG-I like receptors. *Immunobiology* **218**; 1322-1335 (2013)
[195] Schoggins JW. Interferon-Stimulated Genes: What Do They All Do? *Annu Rev Virol* **6**; 567-584 (2019)
[196] Schoof M et al. eIF2B conformation and assembly state regulate the integrated stress response. *eLife* **10**; e65703 (2021)
[197] Schümann M, Gantke T, Muehlberger E. Ebola virus VP35 antagonizes PKR activity through its C-terminal interferon inhibitory domain. *J Virol* **83**; 8993-8997 (2009)
[198] Schwanke H, Stempel M, Brinkmann MM. Of Keeping and Tipping the Balance: Host Regulation and Viral Modulation of IRF3-Dependent *IFNB1*Expression. *Viruses* **12**; 733 (2020)

[199] Sekine Y et al. Stress responses. Mutations in a translation initiation factor identify the target of a memory-enhancing compound. *Science* **348**; 1027-1030 (2015)
[200] Seth RB et al. Identification and characterization of MAVS, a mitochondrial antiviral signaling protein that activates NF-kappaB and IRF3. *Cell* **122**; 669-682 (2005)
[201] Sharma S et al. Triggering the interferon antiviral response through an IKK-related pathway. *Science* **300**; 1148-1151 (2003)
[202] Shaw ML et al. Nuclear localization of the Nipah virus W protein allows for inhibition of both virus- and toll-like receptor 3-triggered signaling pathways. *J Virol* **79**; 6078-6088 (2005)
[203] Shen S et al. A novel tick-borne phlebovirus, closely related to severe fever with thrombocytopenia syndrome virus and Heartland virus, is a potential pathogen. *Emerg Microbes Infect* **7**; 95 (2018)
[204] Sidrauski C et al. Pharmacological dimerization and activation of the exchange factor eIF2B antagonizes the integrated stress response. *eLife* **4**; e07314 (2015)
[205] Sidwell RW et al. Potential role of immunomodulators for treatment of phlebovirus infections of animals. *Ann N Y Acad Sci* **653**; 344-355 (1992)
[206] Siegal FP et al. The nature of the principal type 1 interferon-producing cells in human blood. *Science* **284**; 1835-1837 (1999)
[207] Sonenberg N and Hinnebusch AG. Regulation of translation initiation in eukaryotes: mechanisms and biological targets. *Cell* **136**; 731-745 (2009)
[208] Srihongse S and Johnson CM. Human infections with Chagres virus in Panama. *Am J Trop Med Hyg* **23**; 690-693 (1974)
[209] Stern-Ginossar N et al. Translational Control in Virus-Infected Cells. *Cold Spring Harb Perspect Biol* **11**; a033001 (2019)
[210] Tchouassi DP et al. Sand Fly-Associated Phlebovirus with Evidence of Neutralizing Antibodies in Humans, Kenya. *Emerg Infect Dis* **25**; 681-690 (2019)
[211] Tesh RB et al. Serological studies on the epidemiology of sandfly fever in the Old World. *Bull World Health Organ* **54**; 663-674 (1976)
[212] Tesh RB. The genus Phlebovirus and its vectors. *Ann Rev Entomol* **33**; 169-181 (1988)
[213] Travassos da Rosa AP et al. Characterization of eight new phlebotomus fever serogroup arboviruses (Bunyaviridae: Phlebovirus) from the Amazon region of Brazil. *Am J Trop Med Hyg* **32**; 1164-1171 (1983)
[214] Tsai JC et al. Structure of the nucleotide exchange factor eIF2B reveals mechanism of memory-enhancing molecule. *Science* **359**; eaaq0939 (2018)
[215] Vialat P et al. The S segment of rift valley fever phlebovirus (Bunyaviridae) carries determinants for attenuation and virulence in mice. *J Virol* **74**; 1538-1543 (2000)
[216] Wack A, Terczyńska-Dyla E, Hartmann R. Guarding the frontiers: the biology of type III interferons. *Nat Immunol* **16**; 802-809 (2015)
[217] Walsh MC, Lee JE, Choi Y. Tumor necrosis factor receptor- associated factor 6 (TRAF6) regulation of development, function, and homeostasis of the immune system. *Immunol Rev* **266**; 72-92 (2015)
[218] Wang J et al. Emerging Sand Fly-Borne Phlebovirus in China. *Emerg Infect Dis* **26**; 2435-2438 (2020)
[219] Wathelet MG et al. Virus infection induces the assembly of coordinately activated transcription factors on the IFN-beta enhancer in vivo. *Mol Cell* **1**; 507-518 (1998)
[220] Weber F et al. Double-stranded RNA is produced by positive-strand RNA viruses and DNA viruses but not in detectable amounts by negative-strand RNA viruses. *J Virol* **80**; 5059-5064 (2006)
[221] Weber M et al. Incoming RNA virus nucleocapsids containing a 5'-triphosphorylated genome activate RIG-I and antiviral signaling. *Cell Host Microbe* **13**; 336-346 (2013)
[222] Weber M and Weber F. Segmented negative-strand RNA viruses and RIG-I: divide (your genome) and rule. *Curr Opin Microbiol* **20**; 96-102 (2014)
[223] Weber-Gerlach M and Weber F. To Conquer the Host, Influenza Virus Is Packing It In: Interferon-Antagonistic Strategies beyond NS1. *J Virol* **90**; 8389-8394 (2016)
[224] Wilson JE et al. Initiation of protein synthesis from the A site of the ribosome. *Cell* **102**; 511-520 (2000)

[225] Won S et al. NSm and 78-kilodalton proteins of Rift Valley fever virus are nonessential for viral replication in cell culture. *J Virol* **80**; 8274-8278 (2006)
[226] Woo CW et al. Toll-like receptor activation suppresses ER stress factor CHOP and translation inhibition through activation of eIF2B. *Nat Cell Biol* **14**; 192-200 (2012)
[227] Woyessa AB et al. An outbreak of acute febrile illness caused by Sandfly Fever Sicilian Virus in the Afar region of Ethiopia, 2011. *Am J Trop Med Hyg* **91**; 1250-1253 (2014)
[228] Wu X et al. Evasion of antiviral immunity through sequestering of TBK1/IKKε/IRF3 into viral inclusion bodies. *J Virol* **88**; 3067-3076 (2014)
[229] Wu Y et al. Detecting protein-protein interactions by Far western blotting. *Nat Protoc* **2**; 3278-3284 (2007)
[230] Xu B et al. Metagenomic analysis of fever, thrombocytopenia and leukopenia syndrome (FTLS) in Henan Province, China: discovery of a new bunyavirus. *PLoS Pathog* **7**; e1002369 (2011)
[231] Xu F et al. Phylogenetic relationships among sandfly fever group viruses (Phlebovirus: Bunyaviridae) based on the small genome segment. *J Gen Virol* **88**; 2312-2319 (2007)
[232] Xu LG et al. VISA is an adapter protein required for virus-triggered IFN-beta signaling. *Mol Cell* **19**; 727-740 (2005)
[233] Xu Z et al. Isolation and Identification of a Novel Phlebovirus, Hedi Virus, from Sandflies Collected in China. *Viruses* **13**; 772 (2021)
[234] Yamamoto M et al. Role of adaptor TRIF in the MyD88-independent toll-like receptor signaling pathway. *Science* **301**; 640-643 (2003)
[235] Yamamoto M et al. The RNA helicase RIG-I has an essential function in double-stranded RNA-induced innate antiviral responses. *Nat Immunol* **5**; 730-737 (2004)
[236] Yanai H et al. Revisiting the role of IRF3 in inflammation and immunity by conditional and specifically targeted gene ablation in mice. *PNAS* **115**; 5253-5258 (2018)
[237] Ye L, Schnepf D, Staeheli P. Interferon-λ orchestrates innate and adaptive mucosal immune responses. *Nat Rev Immunol* **19**; 614-625 (2019)
[238] Yoneyama M et al. Direct triggering of the type I interferon system by virus infection: activation of a transcription factor complex containing IRF-3 and CBP/p300. *EMBO J* **17**; 1087-1095 (1998)
[239] Yoneyama M et al. Viral RNA detection by RIG-I-like receptors. *Curr Opin Immunol* **32**; 48-53 (2015)
[240] Yu XJ et al. Fever with thrombocytopenia associated with a novel bunyavirus in China. *N Engl J Med* **364**; 1523-1532 (2011)
[241] Zhang LK et al. Quantitative Proteomic Analysis Reveals Unfolded-Protein Response Involved in Severe Fever with Thrombocytopenia Syndrome Virus Infection. *J Virol* **93**; e00308-19 (2019)
[242] Zhang M et al. HSV-2 immediate-early protein US1 inhibits IFN-β production by suppressing association of IRF-3 with IFN-β promoter. *J Immunol* **194**; 3102-3115 (2015)
[243] Zhang Z et al. Human bocavirus NP1 inhibits IFN-β production by blocking association of IFN regulatory factor 3 with IFNB promoter. *J Immunol* **189**; 1144-1153 (2012)
[244] Zhou Z et al. Type III interferon (IFN) induces a type I IFN-like response in a restricted subset of cells through signaling pathways involving both the Jak-STAT pathway and the mitogen-activated protein kinases. *J Virol* **81**; 7749-7758 (2007)
[245] Zhu M et al. Bipartite Nuclear Localization Signal Controls Nuclear Import and DNA-Binding Activity of IFN Regulatory Factor 3. *J Immunol* **195**; 289-297 (2015)
[246] Zhu PJ et al. Activation of the ISR mediates the behavioral and neurophysiological abnormalities in Down syndrome. *Science* **366**; 843-849 (2019)
[247] Zyryanova AF et al. Binding of ISRIB reveals a regulatory site in the nucleotide exchange factor eIF2B. *Science* **359**; 1533-1536 (2018)
[248] Zyryanova AF et al. ISRIB Blunts the Integrated Stress Response by Allosterically Antagonising the Inhibitory Effect of Phosphorylated eIF2 on eIF2B. *Mol Cell* **81**; 88-103 (2021)

6 Appendix

a Verzeichnis der akademischen Lehrer

Meine akademischen Lehrer an der Rheinischen Friedrich-Wilhems-Universität in Bonn waren die Damen und Herren Aretz, Bajorath, Barchet, Baur, Betz, Bierbaum, Brötz-Oesterhelt, Bruchhausen, Brüstle, Büttner, de Braganca, Cichon, Drexler, Drosten, Eckhardt, Edenhofer, Eis-Hübinger, Enzmann, Famulok, Faulde, Filippou, Fimmers, Fleischmann, Forsbach, Franz, Fuchs, Galinski, Gieselmann, Gütschow, Haas, Häberlein, Hartmann D, Hartmann G, Heinemann, Heinrichs, Hoch, Höhfeld, Hörauf, Hoppe, Hormes, Hornung, Horré, Hübner, Keller, Kirfel, Klockgether, Knolle, Koch, Kolanus, Kolter, Kümmerer, Kurts, Limmer, Magin, Mayer, Merkelbach-Bruse, Mohr, Molitor, Müller, Nöthen, Piel, Pfeifer, Racké, Rottländer, Runkel, Sahl, Sauer, Schildgen, Schildhaus, Schilling, Schlee, Schlicker, Schorle, Schott, Schultze, Schumacher, Spengler, Tüting, Walter, Weber, Wild, Willecke, van Kügelgen, Zimmer

b Acknowledgement & Danksagung

First and foremost, I want to thank **Friedemann Weber**. Thank you for your mentoring – first, for always being available for listening, giving valuable advice, and discussion; more importantly, for your respect for and trust in my scientific ability, for the high degree of freedom to follow my own ideas and test or develop new projects, the countless opportunities to attend workshops and conferences, take the lead in collaboration projects, and contribute to the writing of review/preview articles and peer-reviewing. I consider all of it invaluable for both my scientific and personal development and shaping the scientist I am today.

I also want to thank **Michaela Gerlach**, **Florian Zielecki**, and **Larissa von Mach** for their warm welcome and thorough introduction to the lab and institute upon my arrival in Marburg, as well as Florian Zielecki and **Markus Kainulainen** for the practical introduction to laboratory work in the BSL-3 facility, **Julia Wulle** for great technical support, and **Daniela Haase-Jüngst** for administrative support, advice, and all of our long conversations.

In Gießen, I thank **Babsi Bank-Wolf** – as well as the diagnostics team of VetViro – for the kind welcome and the open and supportive atmosphere, as well as our collaborative work. I especially want to thank **Anna Zitzlaff** for our long conversations and advice far beyond administrative matters, **Sibylle Herzog** for our extensive conversations and friendship, and **Andreas Schön** for endlessly talking science, experiments, methods, new ideas, and life in general, and always being able to rely on each other. Dear **Besim Berisha**, thank you for your technical support – but more importantly, our friendship. I greatly miss working in a close-knit team together with you!

Although our stays in the Weber lab did not overlap, I am grateful to **Matthias Habjan** for generating the recombinant chimeric virus panel and samples for interactome study, which laid the foundation for projects described in this and other PhD theses, and his enthusiasm and curiosity for the findings of the next generation of PhD students. I also want to thank our collaborators **Andreas Pichlmair** and **Giulio Superti-Furga**, as well as **Katja Becker**, **Stefan Rahlfs**, and **Marie Sorg**. I want to thank **Michael Schoof**, **Lan Wang**, and **Peter Walter** for taking on SFSV NSs and elucidating its effect on eIF2B with advanced structural and biochemical methods, stimulating discussions about the regulation of protein synthesis and diverse molecular tools, as well as insights into their confident way of dealing with the publication process.

I am also grateful to my past supervisors and mentors, especially **Beatrix Schumak**, **Kim Schmidt**, **Veit Hornung**, **Eva Bartok**, and **Jonathan Schmid-Burgk** for all they have taught me about science along the way. On the other hand, I want to thank the students I supervised for everything I learned about teaching and mentoring and the privilege of closely following your personal development for a little while. Dear **Xiaobing He**, while I was to teach you molecular virology, you not only gave me an insight into your cultural background but also valuable lessons for being a better supervisor. **Xiaobing** and **Besim**, you greatly influenced the supervisor I am today and what kind of leader I aspire to be - and I will be forever grateful to you for that.

Liebe **Familie**, vielen Dank für eure grenzenlose Unterstützung, jedes Päckchen und jeden Rat – besonders aber für das nicht immer einfache Verständnis für meine viel zu häufige Abwesenheit wegen diesem oder jenem Experiment oder der einen oder anderen Konferenz!

Liebe **Amelie**, du bist eine Inspiration und es ist ein wahres Privileg, Teil deiner Entwicklung zu sein!

Liebe **Mama**, es gibt keine Worte, die dir genug danken für Alles, was du mir, mitunter unter Opfern deinerseits, gegeben und ermöglicht hast!

Cher **Damien**, merci beaucoup pour tout – notre passé, présent et avenir.